SPATIO-TEMPORAL MECHANISTIC MODELING OF HYDRODYNAMIC, TRANSPORT, AND PHOSPHORUS CYCLING PROCESSES IN LARGE-SCALE CONSTRUCTED TREATMENT WETLANDS

By

RAJENDRA PAUDEL

A DISSERTATION PRESENTED TO THE GRADUATE SCHOOL
OF THE UNIVERSITY OF FLORIDA IN PARTIAL FULFILLMENT
OF THE REQUIREMENTS FOR THE DEGREE OF
DOCTOR OF PHILOSOPHY

UNIVERSITY OF FLORIDA

2011

To my family

ACKNOWLEDGMENTS

Firstly, I thank to my advisor Dr. James W. Jawitz for his patience, creativity and encouraging attitude through the critical stages of my research. I would not have come this far without his unwavering support and encouragement. His ability to bring out the best in each student at all levels is truly inspirational.

My sincere gratitude goes to the members of my committee; Drs. K.R. Reddy, M.D. Annable, H.C. Fitz, and M.J. Cohen for providing me professional as well as technical supports. I thank to Dr. Andrew I. James for the help to setup the transport and reaction model. I sincerely appreciate the time and energy he invested in guiding my research at early stages. Very special thanks to Drs. Zaki Moustafa, Naiming Wang, and Michael Chimney of South Florida Water Management District, who provided me spatial input data for the model and valuable suggestions at different levels of model development phase. I am also grateful to Kevin A. Grace for providing me hydro-ecological information of Stormwater Treatment Areas.

I am deeply indebted to my wife for her affection, support, faith, and mostly patience. I am grateful to my family for providing encouragement for all of my endeavors. I would not be the person I am today without their love, sacrifice, and support.

Finally, I am grateful for the funding agencies that supported my research at different stages: United States Geological Survey, South Florida Water Management District, University of Florida, and the DB Environmental Inc.

TABLE OF CONTENTS

page

LIST OF TABLES

LIST OF FIGURES

Abstract of Dissertation Presented to the Graduate School
of the University of Florida in Partial Fulfillment of the
Requirements for the Degree of Doctor of Philosophy

SPATIO-TEMPORAL MECHANISTIC MODELING OF HYDRODYNAMIC, TRANSPORT, AND PHOSPHORUS CYCLING PROCESSES IN LARGE-SCALE CONSTRUCTED TREATMENT WETLANDS

By

Rajendra Paudel

May 2011

Chair: James W. Jawitz
Major: Soil and Water Science

Human intervention in the Florida Everglades during the last century has caused the disruption of the historical hydrologic regime and nutrient status. These two factors have been attributed as the most fundamental causes of major environmental threats to the Everglades. Specifically, agricultural drainage waters discharged into the northern Everglades have been enriched in phosphorus compared to the historic rainfall–driven inputs, which poses a significant threat to the structure and function of the Everglades ecosystem. To reduce the phosphorus concentrations in the agricultural runoff before entering the Everglades, the 1994 Everglades Forever Act mandated the South Florida Water Management District (SFWMD) to create a network of large-scale constructed treatment wetlands. Optimizing the phosphorus removal performance of these wetlands and sustaining their effectiveness has considerable significance for protecting the downstream Everglades.

This study used spatially distributed transport-biogeochemical model that was coupled with a physically based hydrologic model. The integrated model simulated the combined hydrologic and phosphorus biogeochemical processes operating within the

Stormwater Treatment Areas (STAs). The Hydrologic Simulation Engine of Regional Simulation Model (RSM), developed by SFWMD was used as a basic modeling framework to simulate coupled overland and groundwater flow, hydraulic structures, and levee seepage. To simulate phosphorus transport and transformation processes, a novel water quality model, Regional Simulation Model Water Quality (RSMWQ) was used. The models were demonstrated in the STA 1 West (STA-1W)—formerly known as the Everglades Nutrient Removal Project, and STA-2 Cell 2 (STA2C2) to address various research and management questions.

A two-dimensional phosphorus biogeochemical model of a submerged aquatic vegetation dominated treatment wetland (Cell 4 of STA-1W) was developed, and the model was used to assess the effects of a suite of feasible management alternatives on the long-term ability of the wetland to sustain total phosphorus (TP) removal. The spatial and temporal dynamics of TP retention were simulated under historical (1995-2000) conditions, and under assumptions of removal of short-circuiting channels and ditches, changes in external hydraulic and TP loading, and long-term (> 20 years) impacts on soil and water column TP dynamics under current and reduced load conditions. Result showed that under simulated conditions of preferential channels eliminated, average annual TP treatment effectiveness increased by 25%. When inflow TP loads were assumed to be eliminated after 6 years of loading, the release of accumulated soil TP sustained predicted annual average outlet concentrations above 6.7 μg L^{-1} for 18 years.

A set of phosphorus biogeochemical models for Cell 4, STA1-W were developed with varying levels of process-complexity (i.e., from low to high level of mechanistic explanation of phosphorus cycling processes) to investigate the relationship among

levels of model complexity (modeling cost and effort), prediction performance, and explanatory depth of the model. The flexibility of RSMWQ model platform provided the opportunity to incorporate a wide range of process descriptions in a different complexity levels. Given the field data, and models under consideration, results revealed that the most complex phosphorus biogeochemical model of a treatment wetland (Cell 4 of STA-1W) was not necessarily the most effective model to simulate the TP dynamics.

A spatially distributed, flow, solute transport and phosphorus dynamic model of a more complex system (cell-network treatment wetland, STA-1W) in terms of geometry of the wetland, flow control structures, and spatial heterogeneity was developed. Habitat-specific TP cycling parameters were simultaneously calibrated against spatio-temporal field measured TP concentrations in the water column, and the cumulative TP removal from the water column using mass balance approach for each treatment cell. The calibrated model was applied to simulate the TP accumulation pattern for 10 years under the existing vegetation conditions, and the modification of the vegetation pattern in a sequential treatment trains. Also, investigated questions were the large-scale burning effects of emergent macrophytes for thinning or replacing by another plant species on the internal flow regime of STA2C2 by using a spatially distributed model with relatively fine-resolution spatial inputs. Model results indicate that burning emergent macrophytes to minimize extended periods of water depths greater than 4 feet (1.2 m) within STA2C2 may not be an effective management approach. This study also provided deeper insights about formulating effective vegetation management strategies in the STAs to minimize deep water conditions through reduction in the hydraulic resistance.

Overall, this study provided a deeper understanding of coupled flow and phosphorus behavior in spatial and temporal scales. The mechanistic models developed in this study can be further used to assess additional management scenarios for a given modeling objective. Moreover, results of this study demonstrate that such modeling efforts can be effective as a management tool to predict the responses of alternative approaches in developing effective management techniques and therefore optimizing the phosphorus removal performance of the STAs.

CHAPTER 1
INTRODUCTION

Background

The Florida Everglades is a large oligotrophic freshwater wetland ecosystem that historically extended from the upper basin of the Kissimmee River to Florida Bay. However, this unique wetland area that dominated the landscape of South Florida has been degraded by more than a century of human interventions. The present Everglades ecosystem consists of 1.2 million ha, also referred to as Everglades Protection Area (EPA) that includes Water Conservation Areas (WCAs) and the Everglades National Park (ENP) (Meyers and Fitzpatrick, 2001). Over the last several decades, several changes have been observed on the structure and function of the Everglades ecosystem because of anthropogenic activities such as land reclamation, urban development, and extensive agricultural activities that have led to disruption in the hydrologic conditions and nutrient status (McCormick et al., 2002; Grunwald, 2006). Major changes in the Everglades ecosystem have been attributed to hydrologic modifications and enrichment in phosphorus, which was historically very low (Davis, 1994). In addition, these two factors have been considered the most fundamental causes of major environmental issues in the Everglades (Newman and Lynch, 2001). As a consequence of high phosphorus concentrations exported from the upstream watershed in flowing water, a significant threat has been posed to the community biodiversity, function, and stability in the Everglades (McCormick et al., 2000; Chimney and Goforth, 2001). In general, phosphorus is one of the major limiting nutrients for biological growth in freshwater wetland ecosystems, thus the introduction of small amounts of this element into waters can have profound effects on the structure and

function of aquatic ecosystems (Hecky and Kilham, 1988; Kadlec and Wallace, 2008). The Everglades is particularly phosphorus limited and sensitive to phosphorus enrichment (Noe et. al., 2001; Porter and Porter, 2002). Several authors have indicated that the high level of phosphorus in surface waters flowing into the southern Everglades have negatively affected the water quality and changed the distribution of plant communities, encouraging the over-growth of non-native species (McCormick et al., 2000; Davis, 1991; Noe and Childers, 2007). Koch and Reddy (1992) identified phosphorus as most responsible nutrient for periphyton and plant community composition changes in the EPA.

The southern Everglades primarily receives stormwater runoff from the adjacent Everglades Agricultural Area (EAA), which is the major contributor of the phosphorus-enriched runoff. In 1994, Everglades Forever Act (EFA) was enacted to provide comprehensive efforts to restore the Everglades and provided direction and funding to the South Florida Water Management District (SFWMD) to improve the phosphorus water quality. As a part of the restoration efforts, the EFA adopted a plan to implement Best Management Practices (BMPs) in the EAA and established a mechanism to create a network of large-scale constructed wetlands to remove phosphorus from agricultural drainage waters before entering the Everglades (Chimney and Goforth, 2001). These constructed wetlands, known as Everglades Construction Project Stormwater Treatment Areas (STAs) comprise the world's largest treatment wetlands (Pietro et al., 2009). STAs use physical and biogeochemical processes to reduce the level of phosphorus through vegetation growth. STAs in conjunction with BMPs are intended to achieve interim and long-term Everglades water quality goals mandated by the EFA. The interim

goal consists of the effluent total phosphorus (TP) concentrations of 50 parts per billion (ppb), and a long-term target of 10 ppb on an average basis before the stormwater runoff discharges from the STAs (Chimney et al., 2000).

Six STAs with a total effective treatment area of about 18200 ha (45000 acres) were in operation as of 2010 (Pietro et al., 2010). It has been reported that these STAs appear to be effective in lowering phosphorus concentrations well below the interim standard (Pietro et al., 2009). Since the operation began in 1994, the STAs have retained more than 1400 metric tons of TP; this amount would have potentially entered the EPA if the STAs had not built (Germain and Pietro, 2011). The TP loads were reduced by 74 percent and concentrations from an overall annual TP flow-weighted mean (FWM) concentration of 145 to 40 ppb (Germain and Pietro, 2011). While these results are promising, keeping the performance of the STAs at optimal levels for a long period of time is a challenging task. Generally, the performance of treatment wetlands to reduce phosphorus is largely affected by natural conditions, vegetation growth and distribution, soil conditions, and other numerous complex biogeochemical mechanisms. STAs are large in scale, and such treatment wetlands have never been used before, thus the operation and management of these STAs have become a process of learning and research for the further improvement of water quality. The EFA also mandated SFWMD to initiate research and monitoring programs to achieve optimal phosphorus removal performance of the STAs (Chimney et al., 2000). STAs are the key components of the Everglades restoration; thus, long-term sustainability of these wetlands is critical to help reduce the TP loads to the Everglades (Pietro et al., 2009). Monitoring and synthesizing the field data, and predicting the phosphorus dynamics in

response to the changes in environmental and management conditions are vital approaches to sustain the effectiveness or optimize the performance of the STAs. Predicting alternate management scenarios (i.e., what if analyses) also helps support the decision-making process.

Rationale for Spatio-Temporal Modeling of Flow and Phosphorus Dynamics in Stormwater Treatment Areas

The desire to manage the STAs for optimization of phosphorus removal has generated the need for numerical models that are capable of predicting the performance of treatment wetlands in spatio-temporal scale. Mathematical models often provide a valuable tool to integrate the observational data and existing knowledge, and predict the responses of variety of environmental perturbations and management considerations. Such models may form the scientific basis to make management decisions by providing the predicting link between management actions and the responses of the system (Arhonditsis et al., 2006). Since the STAs were first designed, significant efforts have been made in applying numerical models especially to simulate the transport and transformation of phosphorus in order to calculate the removal performance; however, most of them are simple compartmental models which are not capable of describing spatially varying inputs and parameters (Walker 1995; Chimney et al., 2000). Although transient simulation approaches have been adopted, they are limited in representing topographic variation, and location of structures (Walker and Kadlec, 2005). During recent years, with the advances in increased computing capabilities and knowledge of the system, the focus has been shifted towards developing spatially explicit, coupled hydrologic and biogeochemical models which can embrace both temporal and spatial heterogeneity in treatment wetlands (Jawitz et al., 2008). Particularly, flow-integrated

models in a spatially distributed structure have rarely been applied to simulate coupled flow and phosphorus dynamics in large stormwater treatment wetlands (Min, 2007).

Spatially distributed flow-integrated dynamics models can be used by STA scientists and managers to help understand or predict hydrological or biogeochemical changes over various time scales. In the STAs, many management decisions require spatial and temporal information, for example, identifying high phosphorus accumulation areas for potential cattail expansion, spatial water depth to identify the suitability for desired plant communities, changes in topographic features (e.g., channels/ditches, mounds), vegetation pattern, and other structural modifications to effectively formulate management strategies. Additionally, aquatic systems such as the STAs respond to phosphorus cycling processes, and strongly to spatio-temporal changes in hydrodynamic variables (i.e., water depth, residence time and velocity). Therefore, integrating flow and reactive transport models enables testing of critical management and research questions through both hind- and forecasting scenarios (Min et al., 2010). To obtain meaningful simulations or prediction results, a robust, spatially-explicit flow dynamic model has great potential value in modeling water quality parameters in treatment wetlands such as STAs.

The Role of Model Complexity for Explanation and Prediction

The process of developing a model of a complex dynamic system, as in the case of treatment wetlands, requires a robust way to evaluate the model by comparing its output to observations, as well as an equally robust way to compare model performance across differing levels of model complexity. While research on evaluating the model complexity either for explanation or prediction is promising, it has been hindered by the lack of efficient and rigorous quantitative analysis of model complexity elements. For

wetland scientists, developing or selecting an appropriate level of model complexity that adequately represents the biogeochemical cycling mechanisms and provides a reliable prediction for a specific modeling objective is a fundamental challenge.

While simulation tools exist to address hydro-ecological management needs of the STAs (e.g., Walker and Kadlec, 2005), the inherent complexity of these systems requires a comprehensive modeling tool with greater flexibility for a wide range of management options, and the ability to integrate multiple disciplines into one model, such as hydrology, hydrodynamics, hydraulics, water quality, and ecology. As computer technology has advanced, it has become easier to make sophisticated computations with higher computational power, in a relatively flexible model structure. Recently, Jawitz et al. (2008) and James et al. (2009) developed a novel, spatially-distributed mechanistic water-quality model, Regional Simulation Model Water Quality (RSMWQ), which was designed to be very flexible in how components and reactions are treated. Such an approach facilitates a sound and versatile environment to construct a wide range of model structures with various user-specified process descriptions. Because of its flexibility platform, various levels of model structure of a system can be constructed with less effort; therefore the quality of the model structure can be directly compared. This helps identify the appropriate level of model complexity (i.e., level of details in the model) of a particular system that is required for the given modeling goal and data.

A wide range of phosphorus water quality models were reviewed and classified to their wide range of complexity in flow as well as in phosphorus cycling (Table 1-1; Min et al., 2011). Many of them have been developed and applied particularly in Everglades wetlands to simulate flow and phosphorus dynamics to address varying objectives

(Kadlec and Newman, 1992; Walker, 1995; Walker and Kadlec, 1996; HydroQual, 1997; Walker and Kadlec, 2005; Jawitz et. al., 2008; Min, 2007). While these models are promising tools to simulate phosphorus dynamics in the STAs, lacking is a set of models to predict current and future conditions as well as provide relevant knowledge/information about the system dynamics in different levels of model complexity. There is a need to systematically develop model evaluation criteria that will guide in constructing or selecting a suitable model structure of the STA environments.

Hydrodynamic/Flow Modeling in Wetlands

Hydrology is considered as one of the most important determinants of the establishment and maintenance of specific types of wetlands and wetland processes (Mitsch and Gosselink, 2000). Many wetland researchers have referred to 'wetland hydrology' as one of the most significant components, sustaining the structure and function of the wetland ecosystem (Mitsch and Gosselink, 2000; Erwin, 1990; Kusler and Kentula, 1990). Small changes in hydrologic conditions can significantly affect the biogeochemical characteristics of a wetland (Mitsch and Gosselink, 2000), because flow is the primary pathway for nutrient transportation in and out of the system, and storage volume is the determinant of the residence time of water which provides the information about the time available for the interaction between biota and pollutants (Kadlec and Knight, 1996). It is critical to understand the hydrologic factors such as water depth, flow velocity, and residence time to maintain the desired plant species for the effective removal of pollutants. Thus, the ability to describe hydrodynamic behavior in wetlands, in a realistic and comprehensive way, is important to understand and predict the phosphorus removal processes in wetland systems.

A variety of wetland hydraulic, hydrologic, or hydrodynamic models have been used to simulate flow/transport in wetlands. Kadlec (1994) suggested reactor models to model water and tracer movement in surface flow wetlands, which are based on the assumptions that the wetlands behave with either plug or well-mixed flow. The plug flow was the simplest analytical approach to modeling a flow through treatment wetland. However, the ideal plug flow condition is rarely observed in the real field because of system heterogeneity, which causes dispersive flow (Worman and Kronnas, 2005); as such assumptions are not appropriate in short-circuiting wetlands where the tracer peak concentration reaches the outlet well before the nominal hydraulic residence time (Kadlec, 1994; Persson et al., 1999; Werner and Kadlec, 2000; Martinez and Wise, 2003a, 2003b; Dierberg et al., 2005). The flow model was extended based on the conceptual compartmentalization of wetland into a series of equal-sized, well-mixed regions. This approach was known as tank in series (TIS) model which treated an individual compartment as a fully mixed tank, each characterized with a distinct flow rate. Although TIS model considers for longitudinal dispersion within a wetland, the model assumes one-dimensional single flowpath between the inflow and outflow. The measurements of internal concentrations reveal that the TIS model is not adequate to model flow as it travels through a real wetland (Kadlec, 1994).

Reactor models are limited to describe physical processes of wetlands because these models do not have mechanistic relevance and the potential to describe heterogeneity of the system. Other investigators presented physically based model with diffusion flow assumptions which combines continuity equations and some forms of momentum equations (Feng and Molz, 1997; Restrepo et. al., 1998; Guardo and

Tomasello, 1995; SFWMD, 2005a, 2005b; Lal et al., 2005). The local acceleration terms of momentum equations have been ignored, and demonstrated that the diffusion-based equation are appropriate to simulate overland flow in low-gradient topography (Hammer and Kadlec, 1986; Feng and Molz, 1997; SFWMD, 2007). Hammer and Kadlec (1986) developed one-dimensional diffusion-type model, coupled groundwater and surface water to simulate the hydrologic responses of natural or constructed wetlands. Walton et al. (1996) developed a Wetlands Dynamic Water Budget Model, which incorporated and linked three modules, e.g., surface water, vertical flow, and horizontal groundwater flow. A non-linear diffusion equation was employed to simulate one dimensional surface water flow, and the model was demonstrated in the riparian wetland of Cache River in Arkansas. Arnold et al. (2001) modified the Soil and Water Assessment Tool (SWAT) algorithms to simulate the interactions between ponded water and soil/shallow aquifer below the ground. This model was used to assess impacts of storm flow and baseflow on the bottomland wetland ecosystem.

Wide ranges of physically based, spatially distributed models that are capable of simulating the governing equations of flow in grid-based system have been demonstrated in wetland environments. Swain et al. (2004) developed and tested a two-dimensional hydrodynamic/transport model in southeastern Everglades National Park. They underscored that a sophisticated, reliable flow model is necessary to simulate water quality constituents in a hydrodynamically complex wetland system. A two-dimensional (2-D), depth-averaged model was successfully applied and compared with observed velocities in Monash university research wetland, Australia (Somes et al., 1999) based on the framework of MIKE 21. A fully distributed MIKE SHE model was

coupled with one-dimensional MIKE11 model (Thompson et al., 2004) and successfully applied in Elmley Marshes, southeast England to demonstrate the suitability of the coupled modeling for wetland hydrologic applications. Guardo and Tomasello (1995) applied the SHEET2D model, a two-dimensional, depth-averaged hydrodynamic model to simulate the hydrodynamics of shallow water moving across the treatment cells of the Everglades Nutrient Removal Project (ENRP)—a prototype STA. The model employed grid-based system for the solution of the Saint Venant equations and used to simulate sheet-flow within the wetland. The model predicted water levels within the treatment cells for various steady state flow conditions. However, all simulations were performed under steady-state flow conditions in a large computational grid (50,530 m^2). In south Florida, regional hydrologic conditions have been simulated by the South Florida Water Management Model (SFWMM) for many years (SFWMD, 2005a). SFWMM was a fully distributed, 2-D, and grid-based model, which was developed with a relatively course grid size (3.2 km x 3.2 km). SFWMM has undergone numerous improvements since its inception, and gradually became more complex, difficult to understand, and difficult to expand for further details, which inspired development of the next generation models, such as RSM (SFWMD, 2005b; Lal et al., 2005). Both SFWMM and RSM used diffusion-based equation to simulate overland flow that neglects inertial forces.

Phosphorus Modeling in Wetlands

A wide variety of phosphorus water quality models have been developed and used in conjunction with hydrologic/hydrodynamic models to evaluate the transport, removal and fate of phosphorus in freshwater wetlands (Table 1-1). Vollenweider (1975) presented an elementary nutrient mass balance and export model to describe the eutrophication in lakes as caused by nitrogen and phosphorus. An analogous empirical

mass balance approach, based on input-output analysis has been generally used to describe the phosphorus retention in various wetland systems (Kadlec and Newman, 1992; Kadlec and Knight, 1996). The first-order settling rate was invoked to represent the net result of mechanisms, reflected by the long-term average phosphorus budget in multiple wetland systems (Table 1-1). The first-order settling model, referred to as "*k-C** model" or Vollenweider-typed model has been the most frequently used to explain exponential decrease of phosphorus along the flow direction, under assumptions that the phosphorus removal is a function of phosphorus concentration at a given location and the first-order kinetic constant, *k*, called net uptake coefficient or settling velocity, which lumps all phosphorus retention processes occurring in wetlands (Kadlec, 1997). This model assumes a non-dispersive and unidirectional plug flow to describe the flow/transport of phosphorus from inlet to outlet of the wetland. Some investigators coupled the plug flow model with first-order removal process to predict the retention of water quality parameters (e.g., TP, total nitrogen, total suspended solids, and biogeochemical oxygen demand) in wastewater treatment wetlands (Mitsch et al., 1995; Reed et. al, 1995; Wong and Geiger, 1997).

Walker (1995) presented a similar approach, a simple predictive model of phosphorus retention, which was used as a design model to estimate the area needed for effective phosphorus removal by the STAs. The model was based on a mass-balance approach that presumed steady-state, ideal plug flow and a first-order removal of phosphorus (Walker, 1995). This model was calibrated and tested against peat and water-column monitoring data from Water Conservation Area 2A (WCA- 2A), and successfully applied in designing emergent macrophyte STAs to achieve average

outflow TP concentration of 50 ppb or less. This simple predictive model employed a coupled water-balance and phosphorus mass-balance equations. The model assumed the steady-state system and sheet-flow conditions, and employed simple empirical relationships to determine the flow profile, phosphorous concentrations in water column, and peat accretion in the sediment. Everglades Phosphorous Gradient Model (EPGM) was developed as an expansion to the STA design model that includes mass balances between water column and surface soil (Walker and Kadlec, 1996). EPGM used coupled differential equations with an additional soil-column mass-balance component beyond that of the STA design model (Walker, 1995). EPGM is capable of predicting downstream steady-state flow, water column concentrations, soil phosphorous levels, and peat accretion rate along the horizontal gradient. The model presumes that the soil accretion is the only long-term, sustainable mechanism for phosphorous removal. Although these models are the promising STA modeling tools, and have been widely applied for the design and long-term management purpose, application of plug flow model reveals that these models may not be able to predict performance of the treatment wetlands under varied conditions such as altered flow and vegetation type/density (Kadlec, 2000). The ideal plug flow assumption may not be justified because large variations in flow velocity have been observed in most of the treatment wetlands (DBEL, 2000; Lightbody et al., 2008), due to several characteristics, such as topographic variation, irregular inflow/outflow locations, and variation in vegetation type/density. Wong et al. (2006) modified the *k*-*C** model using continuously stirred tank reactors in a series, instead of plug flow to somehow account the variability in the flow. The model was successfully tested in diverse stormwater treatment systems (e.g.,

wetlands, ponds etc.) to predict the removal of water quality constituents. Nevertheless, all these steady-state models cannot simulate transient conditions to account the variation in flows, loads, and other event-driven behaviors, and generally constrained to predict only a long-term average removal performance.

A wide range of mechanistic wetland phosphorus models have been developed to simulate phosphorus cycling processes linked with hydrologic sub-models (Kadlec and Hammer, 1988; Mitsch and Reeder, 1991; Christensen et al., 1994; Wang and Mitsch, 2000). Mitsch and Reeder (1991) developed a semi-mechanistic, wetland compartment model to predict the fate and retention of phosphorus in a wetland area adjacent to Lake Erie. The phosphorus sub-model was coupled with both the hydrology and primary productivity sub-models and included two components (water column and sediment), which were linked with abiotic linear pathways—sedimentation and resuspension. Also, phosphorus uptake by macrophyte vegetation was assumed to occur in sediments. A single component (i.e., state variable) in the hydrologic model was the volume of water in the marsh, which was controlled by water budget components. Wang and Mitsch (2000) used a similar approach with the addition of a sediment sub-model to simulate phosphorus dynamics in four constructed riparian wetlands at Des Plaines River, northern Illinois. The phosphorus sub-model had four compartments, including water column TP, bottom detritus TP, active sediment layer TP, and deep sediment layer TP. This ‘detailed ecosystem model’ was calibrated and validated against the two-year (1989–1991) field observations. In this approach, the hydrology was described by simple mass-balance of water budget, but biogeochemistry was described by complex physical and biogeochemical processes.

Some phosphorus models have adopted an integrated approach coupling simple phosphorus models with fairly complex hydrodynamic models. For example, Tsanis et al. (1998) developed 2-D, depth-averaged hydrodynamic and transport model using a single parameter sedimentation rate to simulate phosphorus retention in Cootes Paradise marsh, Canada. Raghunathan et al. (2001) used a spatially distributed (grid-based), regional-scale hydrologic flow and transport model coupled with a single kinetic parameter phosphorus model to describe the transport of this element in the Everglades landscape. Similarly, Kazezyilmaz-Alhan et al. (2007) used a semi-distributed hydrodynamic model that was coupled with a transport as well as water quality model, and used to simulate TP removal in wetlands by considering the first-order removal process. Although these models were capable of simulating the complex hydrodynamics of a given system; biogeochemical models were too simple to describe the complexity of phosphorus cycling processes, particularly in a heterogeneous wetland.

A spatially distributed, mechanistic model that predicts the movement and distribution of phosphorus across the south Florida landscape, Everglades Landscape Model (ELM), was developed (Fitz and Sklar, 1999; Fitz et al., 2004; Fitz and Trimble, 2006). The landscape model was primarily designed to evaluate the ecosystem responses to alternative water and nutrient management scenarios, and has been applied in the Everglades restoration efforts. ELM dynamically integrates hydrology, water quality, soils, periphyton, and vegetation, and simulates the hydro-ecological processes at scales suitable for regional assessment. In addition to the horizontal (2-D) transport of water and constituents, the vertical solutions of the landscape simulation

(different ecological processes based on landscape pattern) are calculated in each homogeneous grid cell, known as “unit” General Ecosystem Model (Fitz et al., 1996). ELM does not simulate the flow at hydraulic structures, thus it imports boundary condition hydrologic data from the SFWMM. The general limitations of this model are high computational demand and extensive data requirement in support of the model development, testing and application.

Phosphorus Models of Stormwater Treatment Areas

In the STAs, several models have been applied to primarily simulate flow and phosphorus dynamics to explore a variety of research and management questions. The STA design model and the *k-C** model are the simplest phosphorus models applied for the design of the STAs and to predict phosphorus removal performance, respectively (Walker 1995; Chimney et al., 2000). Expanding on these models, the DMSTA (Walker and Kadlec, 2005) was the widely used dynamic model in the STAs that simulated transient flow conditions to account for the event-driven performance. DMSTA was developed to facilitate the design of the STAs to achieve long-term outflow TP concentrations of 10 ppb in the discharges. DMSTA calculates daily water and mass balances in a user-defined series of treatment cells with phosphorus cycling parameters. A maximum of six treatment cells can be linked in series or parallel compartments, and each cell is further divided in a series of continuous tank reactors to reflect the residence time distribution. DMSTA considers the biomass component, which is primarily the wetland vegetation and includes three classes: emergent macrophytes, submerged aquatic vegetation, and periphyton. Phosphorus cycling model parameters that account the uptake and release from biomass and burial of stable phosphorus residuals were obtained from several wetland systems in the Everglades. Juston and

DeBusk (2011) calibrated the *k-C** and DMSTA models against the outflow TP profiles at monthly time scale in Cell 2 of Stormwater Treatment Area 2, a longest-running and best-performing STA submerged aquatic vegetation (SAV) cell. The authors pointed out that DMSTA model was ineffective to reproduce the measured outlet TP time series at near-background concentrations (16 µg L^{-1}).

A spatially distributed transient model, the Wetland Water Quality Model (WWQM), was developed based on the mass transport and kinetic equations of nutrients (primarily phosphorus) in water, sediment, and emergent vegetation to simulate phosphorus cycling processes (HydroQual, Inc., 1997; Meyers and Fitzpatrick, 2001). WWQM simulates the hydrodynamics followed by water quality constituents. The biogeochemical model component comprised of four submodels: eutrophication, carbonate system equilibrium, sediment diagenesis-nutrient flux, and emergent vegetation sub-models. The model was calibrated against the field data of phosphorus from the prototype STA (i.e., ENRP) and WCAs (Meyers and Fitzpatrick, 2001). The structure of the water quality model consisted of four stationary compartments: macrophyte, periphyton, aerobic sediment, and anaerobic sediment. The complexity of the biogeochemical processes included in this model (over 200 parameters) translated difficulty in the calibration; therefore, the model has not been adopted for management purposes. Similarly, Min (2007) developed flow and phosphorus dynamics model of STA-5 to simulate spatial and temporal variation of phosphorus species using a MIKE 21 hydrodynamic model coupled with ECO Lab (modeling framework for phosphorus cycling processes) The flow integrated model employed detailed phosphorus cycling components and links (12 state variables, 34 processes and 56 constants).

Research Objectives

Developing a numerical model of the STAs holds a considerable importance in order to synthesize field data, test hypotheses, predict present and future conditions, and provide a reliable tool for the scientific research or management evaluation. The overall performance of a treatment wetland depends on a number of factors, such as size, location of hydraulic structures, seasonal effects, soil characteristics, predominant vegetation type, previous land use, and water/nutrient loading. In order to optimize the phosphorus removal performance of the STAs, water managers need to be able to test physical experiments, and simulate alternative, operational and management scenarios (e.g., changes in vegetation pattern, topographic conditions, flow regime, and external loadings).and assess the short- and long-term impacts. Therefore, a comprehensive modeling tool that is capable of addressing a wide range of hydrological, transport, and biogeochemical research and management needs, is crucial for the sustainability of the STAs. For this, a model that integrates multiple disciplines into one model, such as hydrology/hydrodynamics, biogeochemistry, and ecology will provide a promising decision-making tool for the STAs.

The overall goal of this study was to develop spatially distributed, multi-scale, coupled hydrodynamic, transport, and biogeochemical models of the STAs to simulate spatio-temporal flow and phosphorus dynamics, and investigate the effects of different management considerations on internal hydrology and fate and transport of phosphorus. To deepen our understanding of hydrological and phosphorus biogeochemical functioning of constructed treatment wetlands and support the optimization planning efforts, the specific research objectives of this study were to:

1. Develop a flow-integrated, spatio-temporal phosphorus transport and cycling model of a large-scale submerged aquatic vegetation (SAV) dominated treatment wetland to evaluate short and long-term management scenarios (Chapter 3).

2. Assess mechanistic biogeochemical model complexity to describe phosphorus dynamics in a SAV-dominated wetland using a pre-calibrated hydrodynamic model (Chapter 4).

3. Simulate spatial flow dynamics and solute transport processes in a cell-network treatment wetland (Chapter 5).

4. Predict long-term spatio-temporal phosphorus accumulation pattern in response to the changes in vegetation patterns (cattail-SAV treatment trains) in a large-scale cell-network treatment wetland using a coupled hydrodynamic and reactive-transport model (Chapter 6).

5. Assess potential effects of prescribed burning of emergent macrophytes on internal flow dynamics within a cattail-dominated constructed treatment wetland using a spatially distributed hydrologic model (Chapter 7).

Besides achieving the above-mentioned objectives, this research contributed explicitly or implicitly to answering numerous broader questions, such as:

1. What are the phosphorus concentrations profiles of each modeled component and at a specific location within the wetland, or at hydraulic structures?

2. What are the potential cattail expansion areas that exceed a certain threshold of soil phosphorus levels?

3. What are the sensitive model inputs/parameters that have significant impacts on the variable of interest?

4. What level of model complexity could be suitable to be used in support of optimization of the STAs performance, given the available data?

5. Do we need a more complex, mechanistic phosphorus biogeochemical model structure that produce comparable or better results than a simple one and provide adequate information for the given modeling objective?

6. Is there a benefit of increasing modeling cost and efforts (i.e., the level of details in the model; model complexity) in relation to the prediction performance and additional knowledge/information gain about the system components and processes?

7. How long does it take to achieve a certain level of phosphorus concentrations at the outlet structure under reduced external loadings?

Table 1-1. Wetland phosphorus model classification in terms of level of complexity on flow and phosphorus dynamics.

Flow	Phosphorus dynamics	
	More empirical	More mechanistic
Fully assumed	Empirical mass balance approach	Ditch
	Kadlec and Newman (1992)	
	Kadlec and Wallace (2008)	Janse (1998)
	First-order kinetic or Vollenweider type approach	River marginal wetlands
	Kadlec (1994)	
	Mitsch et al. (1995)	van der Peijl and Verhoeven (1999)
	Reed et al. (1995)	Everglades
	Walker (1995)	
	Kadlec and Wallace (2008)	Walker and Kadlec (1996; EPGM)
	Wong and Geiger (1997)	Noe and Childers (2007; phosphorus budget)
	Chimney et al. (2000)	
	Kadlec (2000)	
	Carleton et al. (2001)	
	Black and Wise (2003)	
	Wang and Jawitz (2006)	
	Chavan and Dennett (2008)	
Fully considered	Watershed model-based approach	Lake wetland
	Huber and Dickinson (1988; SWMM)	
	Arnold et al. (1994; SWAT)	Kadlec and Hammer (1988)
	Refsgaard and Storm (1995; MIKE SHE)	Mitsch and Reeder (1991)
	Bicknell et al. (1997; HSPF)	River marginal wetlands
	SWET, Inc. (2006; WAM)	
	Bingner and Theurer (2009; AnnAGNPS)	Wang and Mitsch (2000)
	Hydrodynamic model-based approach	Everglades
	Tsanis et al. (1998)	
	Raghunathan et al. (2001)	HydroQual (1997; WWQM)
	Kazezyilmaz-Alhan et al. (2007)	Fitz and Sklar (1999; ELM)
		Chen and Sheng (2005; Lake Okeechobee)
		Walker and Kadlec (2005; DMSTA2)
		Min (2007; MIKE 21)
		Jawitz et al. (2008; RSMWQ)

CHAPTER 2
MODELING FRAMEWORK

Hydrologic Model Description

Background

A physically based, spatially distributed hydrologic model, Regional Simulation Model (RSM), was used as a basic modeling framework to simulate the flow dynamics. The Hydrologic Simulation Engine (HSE) was developed to provide more flexibility within the RSM (SFWMD, 2005b). HSE simulates a coupled movement and distribution of overland and groundwater flow. In addition, HSE also simulates hydraulic structures, canal networks, well pumping, levee seepage, and other operational rules and conditions unique to the Everglades treatment wetlands. In HSE, governing equations that describe the physical processes of fluid flow are based on the depth-averaged Saint-Venant equation. The acceleration terms of the momentum equations are neglected for the diffusion flow assumption, which has been successfully applied for regional conditions in South Florida (Lal, 1998; Lal, 2000). In HSE, the weighted implicit finite volume method of the diffusive-wave approximation of the Saint-Venant equation was employed, in which the continuity equation is expressed in integral form over an arbitrary control volume that satisfies strict mass balance because of conservative properties (Lal, 1998). A number of test cases used to verify the numerical accuracy of the model can be found in Lal (1998). Earlier studies have demonstrated the potential application of HSE for the shallow flow conditions across south Florida at the basin scale (approximately 104 km^2, Lal et al., 2005), a relatively small area of ridge and slough landscape in central Water Conservation Area 3A (6 km^2, Min et al., 2010), and stormwater treatment wetland, Cell 4 of Stormwater Treatment Area 1 West (1.44 km^2,

Paudel et al., 2010). For detailed description of RSM, the reader is referred to SFWMD (2005b, 2005c).

Governing Equations

The governing equations of flow are based on the depth-averaged, Saint-Venant equations. The two-dimensional (2-D), continuity equation for shallow water bodies is expressed as:

$$s_c \frac{\partial h}{\partial t} + \frac{\partial (uh)}{\partial x} + \frac{\partial (vh)}{\partial y} - R_{rchg} + W = 0 \quad (2\text{-}1)$$

where u and v are the flow velocities in x and y directions, respectively; h is the water depth; R_{rchg} is the net recharge; W is the source or sink term; and s_c is the storage coefficient, which is 1 for the overland flow.

The momentum equations used in the x and y directions are expressed as (SFWMD, 2005b):

$$\left[\frac{\partial (hu)}{\partial t} + \frac{\partial (u^2 h)}{\partial x} + \frac{\partial (uvh)}{\partial y} \right] + hg \frac{\partial (h+z)}{\partial x} + ghS_{fx} = 0 \quad (2\text{-}2)$$

$$\left[\frac{\partial (hv)}{\partial t} + \frac{\partial (v^2 h)}{\partial y} + \frac{\partial (uvh)}{\partial x} \right] + hg \frac{\partial (h+z)}{\partial y} + ghS_{fy} = 0 \quad (2\text{-}3)$$

where g is the acceleration due to gravity; S_{fx} and S_{fy} are the components of frictional slope in x and y directions, respectively; z is the ground elevation. The first term in Equations 2-2 and 2-3 is the local acceleration and the second term is the convective acceleration terms, which are responsible for the inertial effects; therefore the first term is neglected for diffusion flow assumptions in sheet-flow conditions (e.g., slowly varying flow), typically in a low-gradient environment (Feng and Molz, 1997; Bolster and Saiers,

2002). It should be noted that the diffusion flow assumptions can be violated where steep gradients exist (e.g., deep channels) (SFWMD, 2005b).

Under diffusion flow assumptions, these momentum equations are described by using Darcy's law and can be expressed as:

$$v = -\frac{T(H)}{h}\frac{\partial H}{\partial y} \tag{2-4}$$

$$u = -\frac{T(H)}{h}\frac{\partial H}{\partial x} \tag{2-5}$$

For overland flow, $T(H) = C(H)\,|S_n|^{c-1}$ where, the function of *C(H)* is defined as the conveyance, S_n is the magnitude of the maximum water surface slope (approximately equal to the frictional slope), and *c* is an empirical constant. *T(H)* can also be expressed for Manning's equation to describe the overland flow. For groundwater flow in an unconfined aquifer, $T(H) = k_h(H - z_b)$ where, z_b is the elevation of the aquifer bottom; k_h is the hydraulic conductivity of the aquifer. The reason to use *C(H)*, and *T(H)* are to maintain generic functions when used object-oriented design methods (Lal et al., 2005).

A general form of Manning's equation can be expressed as:

$$V = \frac{1}{n_b}h^a S_f^c \tag{2-6}$$

Then the expression *T(H)*:

$$T(H) = \frac{1}{n_b}(H - z)^{a+1}\left|S_n\right|^{c-1} \tag{2-7}$$

where $S_n = max(S_n, d_n)$ when $a < 1$ to avoid division by zero at $S_n = 0$ and $H > z$. A value of d_n (approximately 10^{-13} to 10^{-7}) has been found useful for low-relief topography

in most South Florida applications (SFWMD, 2005b). This equation can be used in wetlands by selecting the parameters as suggested by Kadlec and Wallace (2008).

Numerical Scheme

The implicit finite volume method was employed for the solution of the diffusion flow equation, assuming a continuous medium in which the medium is discretized into finite number of points in space and solved at discrete points in time. HSE use PETSC software to solve the computational matrix (SFWMD, 2005b). The model is implemented with two basic abstractions—“waterbodies” and “watermovers”, which are used to represent the state within a control volume and the flux between the volumes, respectively (SFWMD, 2007). This allows multi-dimensional calculation of the storage in various waterbodies (overland, subsurface, canal and lake) and the flow between two waterbodies. The detailed description about finite volume formulations to simulate 2-D diffusion flow can be found in Lal (1998).

Boundary Conditions

Boundary conditions are necessary at the physical boundaries of the model domain to solve the diffusion flow equations (SFWMD, 2005b). In HSE, several types of boundary conditions can be applied that include prescribed head, prescribed flow rate, general head, no-flow, lookup tables and point discharge (well) boundary conditions for the solution of hydraulic head and flow of finite volume formulation at discrete water bodies in the system (SFWMD, 2005c). Specific cells are specified with head or flows along model boundary lines for cell boundary conditions. Wall-based boundary conditions are applied along a line or section defined over consecutive nodes of the mesh, which include no-flow, prescribed head, general head and uniform flow across the wall segment. A constant value or time series data can be used to specify boundary

conditions. The appropriate type of the boundary condition often depends on the type of the problem, and data availability; however, available data primarily influences the decision in selecting a type of boundary condition (SFWMD, 2005b).

Hydrologic Process Module

Hydrologic Process Modules (HPMs) are a component of the HSE, and were designed to simulate the local surface-water hydrology for each mesh element (or group of elements) in the model domain (SFWMD, 2005b; Flaig et al., 2005). HPMs have been developed for different land-use type, such as agricultural, urban, and natural systems. It provides a surface boundary condition for the regional solution. The HPMs are solved at the beginning of each model time step and the results are provided as known flows to the upper boundary condition of the regional implicit finite volume flow model. The incorporation of HPMs in the HSE accounts for small-scale (i.e., local) hydrologic processes and heterogeneity in the land-use, without having to use a fine mesh in the large-scale (regional) model that would make computations impractical (Flaig et al., 2005). HPMs are also used to process rainfall and potential evapotranspiration (PET) to provide the net recharge to each mesh cell of the model domain. A “layer1nsm” HPM type was reported suitable for the wetland system dominated by the overland flow (Flaig et al., 2005). The detail information about HPMs can be found in SFWMD (2005b), and Flaig et al. (2005).

Transport and Reaction Simulation Model Description

Model Background

The transport and reaction model, Regional Simulation Model Water Quality (RSMWQ) was designed to simulate water quality conditions (primarily phosphorus) and ecosystem responses to hydrologic and water management changes in wetland

environments (Jawitz et al., 2008; James et al., 2009). The model algorithm of RSMWQ was internally embedded with HSE that provides hydrologic information (e.g., flow, depth, and velocity fields) needed for water quality constituents modeling. RSMWQ is comprised of two basic modules: (1) transport (e.g., advection and dispersion) of solutes and particulates and (2) flexible biogeochemical module that simulates storage and transfer of phosphorus between model components. The transport module simulates the advective and dispersive movement of mobile nutrients (solutes) and particulates in a variable-depth water bodies. The advective term describes the bulk conveyance of mobile constituents into the downstream direction, and dispersion term describes mixing due to differential velocity fields. The biogeochemical module allows the simulation of a wide range of user-selectable components (e.g., water, soil, macrophyte, and plankton) and test diverse sets of process reactions. RSMWQ was designed to be very flexible in how components and reactions are treated, using a flexible input platform (XML file) to provide inputs and describe reactions between components using differential equations in the structured XML file.

RSMWQ numerically solves the advection-dispersion-reaction equation (ADRE) using the time-split Godunov-Mixed Finite Element method, where advective, dispersive, and reactive parts of the equation can be separated and solved independently by applying different approximating techniques to the component parts (James et al., 2009). The advective part of the ADRE is approximated by an explicit finite volume technique; whereas, the dispersive part of ADRE is approximated by using a hybridized mixed finite element method (James and Jawitz, 2007). The reactive component is modeled either using a simple backward Euler approximation or can

easily be replaced with more sophisticated ordinary differential equation solvers such as second-order/fourth-order Runge-Kutta methods.

RSMWQ can be applied to problems with irregular boundary geometries as it solves a finite element problem on an unstructured triangular mesh of a spatial domain, in which each mesh element has a unique response function. The accuracy of the model was determined by comparing analytical solutions with simulations in one and two-dimensions with non-reactive and reactive transport (James and Jawitz, 2007). For detailed information about RSMWQ discretization, boundary conditions, and numerical solution algorithms, the reader is referred to James and Jawitz (2007) and James et al. (2009).

Governing Equations

The governing partial differential equation for transport of nutrients (solutes) in a 2-D domain, with variable-depth can be expressed as (James and Jawitz, 2007; James et al., 2009):

$$\frac{\partial(\varphi hc)}{\partial t}+\frac{\partial}{\partial x}\left(huc-hD^{*}.\frac{\partial c}{\partial x}\right)+\frac{\partial}{\partial y}\left(hvc-hD^{*}.\frac{\partial c}{\partial y}\right)$$

$$+\sum_{i=1}^{p}hf_{i}(c)-\sum_{j=1}^{q}hg_{j}(s)=\sum_{k=1}^{r}hf_{k}c_{f_{k}} \qquad (2\text{-}9)$$

where t = time [T]; x and y = spatial coordinate [L]; c = mobile component concentration [ML^{-3}]; ϕ = porosity of the medium; h = water depth [L]; u and v = specific discharge (water velocity) [LT^{-1}]; D^* = dispersive tensor [L^2T^{-1}]; $f_i(c)$ = mobile components, or reactions that act on a single component (e.g. first-order decay) [$ML^{-3}T^{-1}$]; $g_j(s)$ = non-mobile components, or reactions that act on a single component (e.g. first-order decay)

[$ML^{-3}T^{-1}$]; c_{fk} = source concentration [ML^{-3}]. The velocity and dispersion tensor are introduced as:

$$u(x,t) = \frac{u(x,t)}{\varphi} \tag{2-10}$$

$$D^* = D^*(u(x,t)) \tag{2-11}$$

$$D^* = \varphi D_m + \alpha_T |u| + (\alpha_L - \alpha_T)\frac{u.u}{|u|} \tag{2-12}$$

where D_m = coefficient of molecular diffusion [L^2T^{-1}]; $|u|$ = magnitude of specific discharge (water velocity) [LT^{-1}]; α_L and α_T = longitudinal and transverse dispersivities [L].

Information about topography, mesh, starting time, ending time, and run time step is controlled by the HSE; therefore, these control parameters are provided to the HSE through an XML input file. The transport/reaction algorithm utilizes its functionality to provide these model information including water depth and velocity through a linked library (i.e. interface). In RSMWQ application, the inflow concentration boundaries must coincide with hydrodynamic inflow boundaries (James et al., 2009).

.

CHAPTER 3
MODEL APPLICATION TO SUBMERGED AQUATIC VEGETATION DOMINATED TREATMENT WETLAND TO EVALUATE MANAGEMENT SCENARIOS

Over the past several decades, the Florida Everglades have been adversely impacted due to altered hydrologic regimes and elevated nutrient conditions. Specifically, agricultural drainage waters discharged into the northern Everglades have been enriched in phosphorus compared to the historic rainfall–driven inputs, which has contributed to eutrophication and posed a significant threat to biodiversity and function in the Everglades (Chimney and Goforth, 2001; McCormick et al., 2002). To reduce the phosphorus in agricultural runoff before entering the Everglades, the 1994 Everglades Forever Act (EFA) (Section 373.4592, Florida Statutes) provided direction to the South Florida Water Management District (SFWMD) to construct six large-scale treatment wetlands, known as Stormwater Treatment Areas (STAs). These STAs now comprise 18,200 ha and have been effectively maintaining discharge concentrations of TP well below the current legally mandated standard of 50 µg L^{-1} (Pietro et al., 2009).

Because the phosphorus removal performance of treatment wetlands is affected by a combination of management and natural conditions, including vegetation type/distribution, soil conditions, and water chemistry (Kadlec and Wallace, 2008), it is often challenging to maintain or optimize the effectiveness of these wetlands indefinitely. A wide variety of models have been developed to help wetland managers understand these interactions and to predict their effects on fate and removal of phosphorus in wetland environments. An empirical mass balance approach based on input-output analysis is the simplest model used to describe phosphorus retention in various wetland systems (Kadlec and Newman, 1992; Walker 1995; Wong and Geiger, 1997; Moustafa, 1998; Black and Wise, 2003; Kadlec and Wallace, 2008). This

approach has been often used to estimate the size and predict the performance of the treatment wetland by modeling them as plug flow reactors in which nutrient load undergoes first-order removal under steady-state conditions. Models of these types assume non-dispersive, unidirectional, steady-state plug flow. Real wetlands do not behave as ideal plug flow reactors but exhibit conditions of dispersive flow caused by the presence of heterogeneous vegetation (Worman and Kronnas, 2005), and also are often subject to transient, non-steady inputs. Therefore, these models may not be adequate to predict wetland performance for conditions such as varying flow regime and altered vegetation type/density because the removal rate constant is not independent of model input conditions such as mass loading rate and residence time distribution (Kadlec, 2000; Wang and Jawitz, 2006). Walker and Kadlec (2005) developed a dynamic model for the STAs (DMSTA) to simulate transient flow conditions and event-driven performance in treatment wetlands. DMSTA simulates daily water and mass balances in a user-defined series of treatment cells, each with specified hydrodynamics and phosphorus cycling parameters, which were determined from several wetland systems in Everglades. A maximum of six treatment cells can be linked in series or parallel compartments, and each cell is further divided in a series of continuous tank reactors to reflect the residence time distribution.

Alternatively, mechanistic, compartmental models which include interacting sub models for hydrology and phosphorus have been adopted by several researchers (e.g., Mitsch and Reeder, 1991; Christensen et al., 1994; Wang and Mitsch, 2000). However, in these models surface-water flow through the wetland is described as simply a water mass balance, and thus predicting the effects of spatial variability arising from irregular

locations of flow structures, irregular geometry, and heterogeneity in the system is limited. In addition, simplified phosphorus dynamics (described by a single settling rate coefficient) have been linked to wetland-scale two-dimensional (2-D) dynamic flow models (Tsanis et al., 1998; Raghunathan et al., 2001) to simulate water column total phosphorus (TP) behavior. Some attempts have been made to develop spatially explicit, mechanistic phosphorus models coupled with hydrodynamic models within the context of Everglades restoration (HydroQual, Inc., 1997; Fitz and Sklar, 1999). For example, a spatially distributed, transient Wetland Water Quality Model (WWQM) was developed based on mass transport and kinetic equations of nutrients in water, sediment, and emergent vegetation to simulate the phosphorus removal processes, particularly in the STAs (HydroQual, Inc., 1997). The complexity of the biological-chemical processes included in this model (over 200 parameters) resulted in calibration difficulty and the model has not been adopted for management purposes.

The spatial variability in wetland plant communities, bottom elevation, and location of flow structures can influence the spatial distribution of phosphorus uptake and release within the wetland. Also, phosphorus transport and cycling processes are strong functions of inflow loadings, which are often dynamic in a hydrologically managed system such as the STAs. Many management decisions may require spatial and temporal information, such as identifying high-phosphorus accumulation areas for potential cattail expansion, spatial depth regime to identify the suitability for desired plant communities, long-term predictions to evaluate sustainability of wetlands. The utility of a model for management support to optimize phosphorus removal potential in a STA may largely depend on the ability to predict the spatio-temporal response of the

system to changes in internal characteristics as well as external loads. Thus, there is a need to develop a spatially distributed model with the capability to integrate high resolution spatial input data and predict the dynamic response of the system under a variety of management conditions.

A recently proposed approach for treatment wetland modeling is based on coupling flow and transport models that can embrace both temporal and spatial heterogeneity with flexible reaction algorithms (Jawitz et al., 2008). This paper describes the application of an integrated hydrologic, transport/reaction model to simulate spatial and temporal variation of TP dynamics in response to the variety of forcing functions in a stormwater treatment wetland of the northern Everglades. The coupled movement of overland flow and groundwater flow are simulated using the 2-D, Regional Simulation Model (RSM), originally designed to simulate regional flows across south Florida (SFWMD, 2005b). The transport/reaction model, Regional Simulation Model Water Quality (RSMWQ, James and Jawitz, 2007) is internally coupled with RSM to provide hydrologic information (i.e., depth, velocity field) needed to accurately simulate the transport processes. RSMWQ uses flexible, user-defined reaction algorithms so that the modeler can incorporate physically-based descriptions of biogeochemical cycling in aquatic systems. The paper first describes the model development, calibration and validation with extensive field data from Cell 4 of STA 1 West (STA-1W), one of the most-studied treatment wetlands in the Everglades (Dierberg et al., 2005; Reddy et al., 2006). Then, the model is implemented to investigate the short- and long-term effects on spatio-temporal TP behavior in soil and

the water column under various feasible management alternatives such as removing short-circuiting channels/ditches, and changes in external hydraulic and TP loadings.

Study Site

Cell 4 is one of the treatment cells of STA-1W, formerly known as the Everglades Nutrient Removal Project (ENRP), located in central Palm Beach County, along the northwestern boundary of Water Conservation Area 1 (WCA-1) and on the eastern boundary of the Everglades Agricultural Area (EAA) in south Florida (26°38'N, 80°25'W, Figure 3-1). Cell 4 is a 147-ha marsh dominated by submerged aquatic vegetation (SAV), and had proven to be the most effective of the four large ENRP cells for phosphorus removal (DBEL, 2002). Cell 4 was flooded during the study period (1995–2000); thus the dominant mechanism for flow and transport was overland flow. The primary inflow to Cell 4 consisted of surface-water from Cell 2 through G254 (5 culverts), with outflow to Cell 3 through G256 (5 culverts) (Figure 3-1). A seepage return canal adjacent to the western levee was used to collect the groundwater seepage (approximately 11% of outflow discharge, Nungesser and Chimney, 2006) from the wetland. As the STA1-W was built on former agricultural land, abandoned agricultural ditches and borrow canals remained in the wetland (Guardo and Tomasello, 1995; Dierberg et al., 2005). The open-water, borrow canals oriented parallel to flow direction along the levees were up to 1.2 m deeper than the average Cell 4 ground elevation, creating preferential flow conditions (Dierberg et al., 2005).

The study area was actively maintained with SAV and periphyton community dominated by coontail (*Ceratophyllum demersum*) and southern naiad (*Najas quadalupensis*) with less abundant pondweed (*Potamogeton illinoensis*), and cattail

(*Typha sp*.) in small patches along the east-west canal at the middle of the wetland and near the outlet structure (Chimney et al., 2000, Figure 3-1). Although there was temporal variation in the vegetation community during the model application period (1995 to 2000), *Najas* remained the dominant vegetation, followed by *Ceratophyllum*, usually found in the inflow zone (DBEL, 2002). For detailed information about Cell 4 characteristics and operational histories, the reader is referred to Chimney et al. (2000) and Chimney and Goforth (2006).

Methods

Modeling Framework

RSM and RSMWQ models described in Chapter 2 were used as a basic modeling framework for this study.

Phosphorus Cycling Model

The phosphorus cycling model implemented here was based on the primary mechanisms regulating TP behavior in soil and water column, and all TP removal processes were lumped as soil-water uptake and release to describe the exchange of TP between soil and water column.

$$\frac{dS_{TP}}{dt} = k_u d\theta_{sw} C_{TP}^{SW} - k_r S_{TP} \quad (3\text{-}1)$$

$$\frac{dC_{TP}^{SW}}{dt} = -k_u C_{TP}^{SW} + \frac{k_r}{d\theta_{sw}} S_{TP} \quad (3\text{-}2)$$

where S_{TP} = soil TP [ML^{-2}]; C_{TP}^{SW} = water column TP [ML^{-3}]; k_u = first-order uptake rate constant [T^{-1}]; k_r = first-order release rate constant [T^{-1}]; d = depth of water column [L]; θ_{sw} = water content in water column (i.e., reduced volume due to vegetation) [L^3L^{-3}].

The uptake/release terms are represented by volumetric first-order reaction rate constants which reflect the net effects of several combined physical and biochemical processes of phosphorus removal (Equations. 3-1 and 3-2). More detailed description of phosphorus cycling processes could include phosphorus forms such as soluble reactive phosphorus (SRP), particulate phosphorus (PP) and dissolved organic phosphorus (DOP). However, accurate simulation of processes associated with these state variables requires more types of data than are available for the STAs. Therefore, a simple phosphorus cycling model was selected with processes that were particularly supported with available data, in contrast to the more mechanistic approaches such as those of HydroQual, Inc. (1997) and Wang and Mitsch (2000). Further, by representing both uptake and release of phosphorus, we extend previous STA models that employed a single, net settling rate coefficient (Walker, 1995; Kadlec and Wallace, 2008).

Data Sources

The bulk of the field measurement data (i.e., hydrological, meteorological and water quality) employed in this study were collected by SFWMD personnel and are publicly available on their online environmental database, DBHYDRO (http://my.sfwmd.gov/dbhydroplsql/show_dbkey_info.main_menu). Flow data were typically available as a daily average for each flow control structure. Chloride concentrations at internal monitoring stations (Figure 3-1) were sampled bi-weekly/monthly using grab samples. Similarly, TP concentrations at inflow and outflow structures were collected weekly from time-proportioned composite samples using autosamplers. Spatial data for topography, vegetation, and soil TP were provided by SFWMD personnel. Rhodamine-WT tracer concentration data from Dierberg et al. (2005) were used to calibrate the hydrologic and transport components of the model.

Wet deposition of TP, 10 µg L^{-1}, was based on the earlier study conducted at STA-1W site (Ahn and James, 2001).

Hydrologic and Transport Model Simulations

The wetland (Cell 4) was represented by a 2-D finite element mesh of 298 unstructured triangular elements (average area: 5,100 m^2) and 192 nodes, generated in Groundwater Modeling System (GMS) v6.0. The mesh density was further refined in some specific areas to better represent the location of flow structures. The bathymetry was generated using inverse distance weighting from the topographic survey data. The bottom elevation in Cell 4 ranged from approximately 2.7 to 3.2 m (NGVD 29) (Figure 3-2a). The internal hydrology and transport processes calibration period of December 16, 1999 to January 15, 2000 (31 days) was selected based on the concurrent tracer test of Dierberg et al. (2005). The validation period was January 10, 1995 through December 31, 2000 for outlet discharge, and from January 10, 1995 through December 31, 1999 for chloride concentrations. Chloride was assumed to be conservative tracer that provided a basis for further testing of water balance and transport processes.

Depth-dependent hydraulic resistance was simulated with a power function of the following form (SFWMD, 2005a, 2005b):

$$n = Ad^B; \text{ for } d > d_t \quad (3\text{-}3)$$

where n = Manning's flow resistance factor [$TM^{-1/3}$]; A, and B are empirical constants, usually determined through model calibration; and d_t is detention depth [L] which was assigned 0.01 m throughout the model domain. The values of A and B primarily depend on the wetland habitat (vegetation type) or vegetation density. The model area was divided into three primary habitats: SAV, cattail, and open water/sparse submerged

vegetation. The channels and ditches parallel to the flow direction along the levee were represented by open water/sparse submerged vegetation (Dierberg et al., 2005). Calibration was used to determine final *A* values for these three zones. Previous work found *B* = -0.77 to be appropriate for most Everglades wetland plant communities (SFWMD, 2005a) and this value was used here for all vegetation types. The groundwater flow resistance was described by the hydraulic conductivity (k = 3.5 x 10^{-4} m s^{-1}, Harvey et al., 2000) which was assigned spatially constant throughout the model.

To simulate the tracer test of Dierberg et al. (2005), a constant flow-weighted tracer concentration (6.78 mg L^{-1}) was assigned in all five inflow culverts for 35 minutes on 16 December 1999. The average stage (3.48 m) measured immediately upstream of G-256 culvert was used as a constant head boundary to simulate flow at the outlet structure. The initial water surface elevation was set to 3.64 m throughout the domain. In Cell 4, there was a significant difference in stage between the wetland and the adjacent seepage return canal along the western boundary; therefore, the flow in the surficial aquifer was driven towards the canal from the wetland. Nungesser and Chimney (2006), in studies of ENRP hydrology for the period from January 13, 1995 to June 20, 1999, found that the seepage from the wetland to the canal across the western levee was about 11% of outflow discharge. However, groundwater inflow was believed to be a minor component of the water budget (Chimney et al., 2000) because the head difference between Cell 4 and adjacent treatment cells was relatively small. Therefore, seepage inflow was not modeled here, whereas the seepage outflow was modeled using the cell head boundary condition which was based on the difference in stage between the wetland and the seepage return canal. The value of seepage coefficient

(K_s) that controls the rate of flow through the western boundary wall was estimated based on the residual term of water budget to make seepage close to the mass balance in the Cell 4 for the period of January 1995 through December 2000 (Table 3-1). Precipitation and potential evapotranspiration were assigned spatially constant values.

The hydrologic and transport parameters such as flow resistance coefficient (A), vegetation reference crop PET correction coefficient (K_{veg}), longitudinal dispersion (α_L), and transverse dispersion (α_T), were estimated through model calibration. These parameters were adjusted by trial and error over reasonable ranges to minimize the Root Mean Square Error (RMSE) and Mean Absolute Error (MAE) between observed and simulated tracer concentrations. The calibrated model was subsequently validated against two independent data sets: (1) outflow daily discharge at G-256 structure for the time period of 1995 to 2000; and (2) chloride concentrations at two internal monitoring stations (i.e., ENR401, and ENR402) for the time period of 1995 to 1999.

Phosphorus Cycling Model Simulations

Weekly composite data monitored at inlet structures G-254B and G-254D were used as a source boundary condition. The spatially constant water column TP concentration (40 µg L^{-1}) was set as the initial condition, which was the mean observed value from monitoring stations ENR401 and ENR402 at the beginning date of the simulation. An average wet atmospheric TP deposition of 10 µg L^{-1} (Ahn and James, 2001), estimated at the ENRP site, was assigned to the entire model domain. Initial soil TP content was based on sampling conducted by SFWMD throughout the STA-1W on 20 January 1995. Four sampling stations (4-2E, 4-2W, 4-1W, and 4-1E) were within Cell 4 (Figure 3-1). In the STAs and the Everglades region, a 0-10 cm upper soil layer was generally used to describe the soil TP concentrations (DeBusk et al., 2001; Pietro et al.,

2009). Therefore, soil TP in the upper 10 cm soil layer for the STA-1W (i.e., ENRP) was estimated from these data using a kriging interpolation scheme, and the estimates for Cell 4 were extracted for this study. The mean soil TP was 8.56 g m^{-2} which was consistent with the average TP in the upper 10 cm (8.3 g m^{-2}) reported for soil collected prior to construction of the STA-1W (Reddy and Graetz, 1991). Peat accretion was monitored from mid-1995 to mid-1999 using feldspar horizon markers throughout the STA-1W (Chimney et al., 2000). Soil TP measured in samples collected at 4-1E and 4-2W on November 12, 1998 and October 20, 1999 were compared to model simulated predictions of soil TP.

Spatially non-uniform values of k_u were assigned to characterize the variable uptake by different vegetation types. Since the channelized zone contained less vegetation, TP removal was set to be less effective than the remaining more dense SAV area (Dierberg et al., 2005). A much lower k_r was assigned constant over the entire wetland. The final values of these parameters were determined through calibration (Table 3-1). To ensure numerical stability, the model was run in a relatively short time step (1 hour). Phosphorus cycling processes were characterized by linear kinetics in ordinary differential form, and these equations were solved by fourth-order Runge-Kutta numerical integration method.

Model calibration was performed against the long-term outlet TP concentrations of Cell 4 for the period from January 10, 1995 through December 31, 1998. During calibration, the dominant parameters k_u and k_r were adjusted by trial and error to minimize RMSE and MAE. For k_u, we attempted to vary our parameters within the range of reported settling parameter from relevant past studies (Dierberg et al., 2002; Dierberg

et al., 2005; Walker and Kadlec, 2005). However, the release coefficient, k_r was not available from previous studies; therefore, we tested the model for a wide range of k_r values during calibration. Validation was performed using the two-year data from 1999 and 2000 without changing calibrated parameters.

Simulation Scenarios Design

The following scenarios were designed to evaluate the effects of changes in management conditions on the spatial and temporal behavior of TP retention in Cell 4. The baseline scenario (S0) was designed to emulate the system operations and management applied from 1995 through 2000. The next scenario (S1) evaluated the effect of removing short-circuiting pathways on TP removal by changing the open water/sparse SAV areas to dense SAV. Changes in TP loads were studied by decreasing TP inflow concentrations by 25%, 50% and 75% as scenarios S2a, S2b, and S2c, respectively. Similarly, flow input was decreased by 50%, and increased by 50% and 100%, as simulation scenarios S3a, S3b, and S3c, respectively. These scenarios are relevant to specified load limits of TP in discharges from the EAA using agricultural Best Management Practices (BMPs) (Horn et al., 2007) that are required to achieve annual-average TP load reduction of at least 25% compared to pre-BMP period (i.e., before 1996). However, even greater reduction has been achieved than that specified in the 1994 EFA. For example, TP reductions of 73% and 59% were achieved in the EAA in 2001 and 2005, respectively (Horn et al., 2007).

Two basic hypothetical scenarios were designed to simulate the long-term response of the wetland starting from 1995: continuation of operational management adapted during the period 1995-2000 for an additional 18 years (S4), and complete elimination of inflow TP after 2000 (S5). In S4, the 1995-2000 input data (e.g., rainfall,

ET, hydrologic and TP loads) used for the baseline were sequentially repeated for remaining period of January 2001 through December 2018, assuming that Cell 4 would have future water and TP loadings similar to the historic one. Similarly, for S5 the 6-year historic hydrologic loading was sequentially repeated but the TP inflow concentrations were set zero after the year 2001. It was assumed that the biological and chemical conditions within Cell 4 remained similar during the projection period to that of the period of the baseline. The scenarios listed in Table 3-2 were used to calculate TP dynamics in soil and water column.

Results and Discussion

Hydrodynamics and Transport

The calibrated model fit for the Rhodamine-WT tracer concentrations at the outlet structure showed an excellent agreement to the observed concentrations (Figure 3-3, RMSE = 1.9 μg L^{-1}; MAE = 1.3 μg L^{-1}). The simulated spatial distribution of the tracer is compared in Figure 3-4a and 4b to maps based on aerial photographs collected by Dierberg et al. (2005) at tracer elapsed time of 7, 27, and 51 hours. The simulated and observed patterns of tracer evolution are similar, with the clearly visible short-circuiting along east and west levees of the Cell 4. Although the mesh resolution was not sufficient to capture the local effects of narrow channels seen in the photograph in Kadlec and Wallace (2008), the integrated solute transport through the system, as reflected in the tracer breakthrough curve (Figure 3-3) was well matched by the model. The simulated flow rate across the transect BB' (Figure 3-1) shows that 70% of the inflow water is channelized through the zones adjacent to the levees (Figure 3-4c).

The outflow discharge and chloride concentrations simulated during model validation also closely matched the observed data (Figure 3-5). These results suggest

that the 2-D hydrologic/transport model successfully simulated the spatial and temporal variation of internal hydrology and solute transport processes of the wetland during the calibration and validation periods.

The set of calibrated parameters, which provided the best-fit between simulations and observations of tracer data, are summarized in the Table 3-1. The Manning's *n* values for the open water/sparse submerged vegetation and SAV dominated areas were approximated using their respective mean water depths to be 0.056 s $m^{-1/3}$ and 1.0 s $m^{-1/3}$. These *n*-values were somewhat higher than those used in previous STA modeling studies. For example, DBEL (2000) applied $n = 0.07$ and 0.6 for open water/canal and SAV areas in Cell 4, respectively. Similarly, Sutron Corp. (2005) estimated $n = 0.038$ s $m^{-1/3}$ for canals, and depth-varying *n* values for SAV of 0.3 to 1.0 s $m^{-1/3}$ for corresponding water depths of 0.9 to 0.15 m in STA-1W Cell 5. The difference in these estimated *n*-values can be explained by the difference in vegetation density, bed slopes, and other hydraulic characteristics such as discharge, inlet/outlet locations, and shape of the wetland.

The α_L and α_T values of 35 m and 3 m compare favorably with the values reported from tracer experiments conducted in the ridge and slough area of the Everglades marsh (Ho et al., 2009). They reported longitudinal dispersion coefficients of 0.037 and 0.26 m^2 s^{-1} for corresponding mean velocities of 1.5×10^{-3} and 8.0×10^{-4} m s^{-1}, for the first and last three days of experiments, respectively. The equivalent α_L would be within the range of 25 to 325 m. Similarly, the transverse dispersion coefficient of 0.012 m^2 s^{-1} reported for the entire experiment period suggested $\alpha_T = 11$ m for the mean velocity of 1.1×10^{-3} m s^{-1}. However, a relatively low α_L was reported based on the particle tracer

experiments in surface-water field flumes located in the Everglades (Saiers et al., 2003; Huang et al., 2008). The spatial scale of the experiment is one of the primary reasons for the difference in dispersion rate (Ho et al., 2008) because of wide range of local velocities due to heterogeneities in landscape and vegetation pattern (Variano et al., 2009) in a large scale experiment like Cell 4.

Calibration and Validation of Total Phosphorus

The overall agreement between simulated and observed outlet TP concentrations during the calibration period was moderate, and a similar prediction accuracy was observed during the validation period (Figure 3-6). During periods of relatively steady conditions, such as May 1997 through September 1999, the model simulations closely tracked the observed data. However, during period of dynamic conditions, such as January 1995 through April 1997, the model substantially under-predicted outlet TP concentrations (Figure 3-6). In contrast, the model over-predicted the outlet TP concentrations from January 1999 through August 2000 of validation period. During the calibration period (1995-1998), simulated cumulative TP removed from the water column showed excellent agreement with the observed data; however the model slightly under-predicted during validation period (Figure 3-7). As indicated above, limited data were available to compare soil TP changes in Cell 4. In location 4-1E, the model was generally able to capture the overall trend of the observed soil TP, but somewhat underestimated the data at station 4-2W (Figure 3-8). Overall, the model was able to reproduce the spatio-temporal variations of soil TP content over a 5-year period; and predicted the integral effect of TP accumulation in the soil.

Given the complexity of internal hydrology and phosphorus biogeochemical processes, the simple phosphorus cycling model calibration and validation results are

encouraging. Although outflow concentration simulations show moderate RMSE and MAE values, the model generally captures the trends and temporal variations of the outlet TP concentrations. The discrepancies are the most noticeable for the first six months of the calibration period (January 1995 to June 1995), where the model fails to capture the observed TP concentrations (Figure 3-6). We suspect that these variances may be caused by the biological changes that occurred during the adaptation (i.e., start-up) period of the wetland, which were primarily dictated by antecedent soil conditions (Kadlec and Wallace, 2008). The lack of establishment of complete coverage of vegetation would have contributed less removal of phosphorus through vegetation during the first few months of 1995, as the flow through operation at STA-1W was started in August 1994 (Chimney and Goforth, 2006). During the validation period, the model over-predicted the observed outflow TP concentrations, particularly on two instances (Figure 3-6). This may have been due to the wide disparity between inflow and outflow TP concentrations during the calibration and validation periods, with higher inflow TP concentrations during the validation period. Also, the calibration parameters might have been impacted by the start-up period of the wetland. Other factors such as model spatial resolution, uncertainties in observed data, and model simplification could also affect the predicted results. In treatment wetlands, many phosphorus cycling processes involve feedbacks or processes that are also not discernible in linear representations.

Phosphorus Cycling Parameters

The best-fit volumetric TP uptake rate coefficient for the SAV-dominated interior marsh (k_u = 0.4 d^{-1}) was double that for the channelized zone (k_u = 0.2 d^{-1}). These values are consistent with those of Dierberg et al. (2005), who estimated k_u = 0.5 d^{-1} for

SAV-occupied areas and 0.24 d^{-1} for short-circuiting channels. Because it is also common in the treatment wetlands literature to report first-order uptake coefficient on an areal basis, the volumetric uptake rate constants were multiplied by the mean water depth and water column porosity to obtain areal values (Kadlec and Wallace, 2008): 90 m yr^{-1} for SAV/cattail and 45 m yr^{-1} for channelized zones. A cell-average areal k_u = 59 m yr^{-1} was estimated by flow-weighting these values, based on 70% flow through the channelized zone (Figure 3-4c). This value is consistent with the range for net TP settling rate coefficient of 43 to 64 m yr^{-1} estimated by Walker and Kadlec (2005) using DMSTA for SAV treatment cells of STAs. Also, for SAV-dominated mesocosms, the areal uptake rate constant was estimated in the range of 63 to 132 m yr^{-1} (Dierberg et al., 2002). Cell 4 had a lower k_u value than the mesocosms because the mesocosms received higher concentrations of labile phosphorus (i.e., SRP) in its inflows compared to Cell 4 inflows (Dierberg et al., 2002). In Cell 4 inflows, the labile phosphorus species were partially treated by upstream cells (Buffer Cell and Cell 2). Thus, higher concentrations of more recalcitrant DOP and PP forms (less labile phosphorus species) accounted, in part, for the lower k_u value for Cell 4 than the mesocosms. Walker (1995) estimated the 90% confidence interval for settling rate coefficients in WCA-2A in the range of 8.9 to 11.6 m yr^{-1} based on soils data and 11.3 to 14.8 m yr^{-1} based on water column data during the period of continuous inundation. The higher uptake rates for Cell 4 are attributed to the SAV community, which is highly effective in phosphorus removal from wetlands. The TP release rate constant from soil to overlying water (k_r) was found to be 1.97 x 10^{-4} d^{-1}. While net phosphorus uptake rate constants are widely reported in the literature, no published release rates were available for comparison.

The values of k_u and k_r primarily depend on phosphorus equilibrium relationships between soil and the water column. Factors that affect this relationship include the amount of labile phosphorus stored in the soil, inflow TP concentration, new soil accretion rate and phosphorus concentration therein, and rate and extent of organic matter mineralization. The variability in these factors may affect uptake and release parameters, and increase uncertainty of predicting future TP dynamics in soil and the water column. To reduce uncertainty in future predictions, as with all other models, continued refinement of these parameters is suggested as process understanding and data become more available.

Sensitivity Analysis

The sensitivity of outflow discharge and outlet TP concentration to variations in selected input parameters and initial/boundary conditions was evaluated to help identify the inputs that contribute most to output uncertainty. The sensitivity of a state variable (*x)* to the changes in parameter (*p*) was evaluated using the sensitivity coefficient,

$$S_p = \frac{\Delta x / x}{\Delta p / p} \tag{3-4}$$

A positive sensitivity coefficient of *p* indicates an increase in *x* when *p* is increased. For example, a sensitivity coefficient of 0.3 indicates that a 10% increase in parameter would increase *x* by 3%. The sensitivity test results are summarized in Table 3-3 to changes in initial/boundary conditions and process parameters within a reasonable range from the baseline data of Cell 4 (Table 3-3). Absolute changes in water level and outlet boundary head were evaluated (± 20 cm and ± 10 cm respectively), and percent change (± 30%) was used for the other parameters. Outflow discharge was primarily influenced by the seepage coefficient (K_s), and outlet boundary head. The TP outflow

was relatively insensitive to uncertainty (30%) in transport parameters α_L and α_T, but was most sensitive to TP cycling parameters (k_u and k_r) and initial soil TP content. An increase of 30% in soil TP content could increase the annual average outlet TP concentrations by about 7%. Such a high sensitivity of initial soil TP emphasizes the importance of spatial soil TP data. The high sensitivity of TP outflow to the uptake and release parameters indicates the importance of accurately calibrating these parameters.

Effects of Management Alternatives on Treatment Effectiveness

The simulated effect of removal of preferential flow paths (S1) was to increase cumulative TP removal by 52% (Figure 3-7), and average annual TP removal by 25% (Table 3-4), suggesting that removing preferential flow paths through vegetation manipulation within the treatment cell could be a good management alternative to improve the phosphorus removal performance. These results also highlight how assumptions of uniform flow might be a poor approximation to flow through the wetland, and could substantially limit the ability to accurately model the phosphorus transport and cycling processes, especially to those wetlands with highly heterogeneous topographical features or vegetative communities (Wang and Jawitz, 2006; Min and Wise, 2009).

Table 3-4 summarizes the simulation results of changes in inflow TP concentrations and hydraulic loading rates (S2-S3) for Cell 4. A 75% reduction in inflow TP concentration resulted in predicted six-year (1995–2000) average outlet TP concentration of 8.9 μg L^{-1}, which is less than the EFA long-term goal of the target TP concentration of 10 μg L^{-1} in STA discharges. Percent removal, or removal effectiveness, is directly related to inflow TP concentration. Thus, reduction/increase of TP concentrations in inflow water results in a decrease/increase in removal

effectiveness (Table 3-4). Low-flow conditions correspond to higher retention time, which leads to higher TP removal effectiveness, consistent with observations in south Florida Boney Marsh (Moustafa et al., 1998). In addition, sensitivity in simulation results for ± 30% uncertainty in k_u and k_r values were estimated (Table 3-4). For all scenarios, sensitivity in outlet TP concentrations were found to be more dominated by uncertainties in k_u compared to k_r. Sensitivity in the percent TP removal was inversely related to the inflow TP concentrations to both ± 30% uncertainty in k_u and k_r; however there was not much difference among varying inflow conditions (Table 3-4).

Long-term Simulations of Current and Reduced Load

Under conditions of no significant long-term management actions or load changes (S4), predicted outflow TP concentration gradually increased to 41.0 µg L^{-1} after 18 years of operation (Figure 3-10a). The gradual increase of TP concentrations over time results from release from TP accumulated in the soil. It should be noted that a saturation level of TP uptake was not considered in the model. Temporal changes in soil TP along longitudinal transect AA' (Figure 3-1) are shown in Figure 3-9 under the assumption (S4) of continuation of operational management adapted during the period 1995–2000. The largest decrease in soil TP was in the upstream portion of the wetland (within 500 m of the inlet structures), with relatively stable soil TP content beyond 500 m downstream. The sharp change of soil TP content after 500m is likely due to the transition in the topography and initial soil TP content.

Under reduced external phosphorus loading conditions, wetland soils may act as a source, releasing accumulated phosphorus to the overlying water column, contributing to eutrophication even after the external load has been eliminated (Reddy, 1991, Fisher and Reddy, 2001; Pant and Reddy, 2003). Under S5, the predicted mean annual outlet

TP concentrations was still 6.7 μg L^{-1} 18 years after elimination of external loading that occurred during the 6-year period 1995-2000 (Figure 3-10b). The simulated soil TP distribution under S5 at the end of the year 2000 and 2018 is shown in Figure 3-11a and b, respectively. Results indicated that the accumulated soil phosphorus slowly releases from Cell 4 and would require many years to approach natural Everglades background concentrations of ≤ 500 mg/kg (DeBusk et al., 2001) under the calibrated parameters and assumptions imposed in our model.

Model Limitations

Although the model reasonably reproduced measured outflow TP concentrations and successfully simulated the integrated effects of soil TP accumulation, it has a number of limitations. Therefore, scenario simulation results have to be interpreted with caution when used in the management context. A major limitation is that the phosphorus uptake and release coefficients represent the combined effect of all biogeochemical processes between water column and soil. Therefore, the model cannot segregate the effects of individual processes that affect TP dynamics in the wetland. For example, this model cannot independently specify individual processes such as diffusion due to concentration gradient between water column and soil, resuspension of sediment TP, chemical precipitation, or particulate matter deposition. Another limitation is that spatially explicit models are computationally intensive and thus constrain the use of formalized parameter estimation and uncertainty analysis techniques. A further limitation is that field data were not available to calibrate and verify the model for a wide range of conditions, for example, relaxation of the wetland after significant reduction in

inflow TP concentrations, re-flooding after drying, high and low inflow/outflow TP concentrations, and time-series soil TP content under these varied conditions.

Summary

This study described the development of a flow-coupled, spatially distributed TP transport and cycling model, and investigated the effects of various management alternatives on spatial and temporal dynamics of TP in a stormwater treatment wetland. The model reasonably predicted the response of the wetland to alternate management conditions, and provided consistent information of spatial TP evolution over time in both soil and water column. Considerations that could improve the model predictions include higher resolution spatial data to better describe the complexity of the wetland, finer resolution mesh elements that could better capture narrow channels and ditches, temporally varying (e.g., seasonal) uptake and release parameters, and a more complex representation of wetland phosphorus cycling. However, we simplified our spatial and process complexity based on data availability, computation time, reasonable calibration and ease of use. This approach demonstrated a good match of overall trends including hydrodynamics, multi-year cumulative TP removal, and multi-year changes in soil TP.

The outlet TP concentrations were highly sensitive to TP cycling parameters, and moderately sensitive to initial soil TP content and overland flow resistance parameter (A). It was found that removing preferential flow paths would remarkably improve TP removal effectiveness of the wetland (i.e. annual average increased by 25%); suggesting the utility of accurately modeling short-circuiting flow for predicting treatment wetland performance. Furthermore, if inflow TP loads were eliminated after several years of historic loadings, substantial water column TP concentrations were maintained

from release of accumulated soil TP. The TP removal performance was also highly sensitive to both hydraulic and TP loads. These simulations indicate that outlet TP concentrations could be reduced by either eliminating short-circuiting pathways within the wetland (e.g., replacing channels, open water with dense SAV vegetation which can improve internal flow distribution and biological uptake) or controlling TP concentrations at inlet sources.

The modeling approach presented here is flexible, in which algorithms can be easily modified or added to accommodate additional internal processes. Ultimately, the model can be used as a management tool to assess the impacts of different management conditions. Such estimates are important in designing and developing operational strategies to maximize the phosphorus removal performance of STAs.

Table 3-1. Primary model parameters/inputs, descriptions, values and sources.

Symbol	Description	Value	Sources
Initial conditions			
-	Water level, m	3.64	DBHYDRO
C_{TP}^{SW}	Water column TP concentration, µg L^{-1}	40	DBHYDRO
S_{TP}	Soil TP, g m^{-2}	Varies	Unpublished data, SFWMD
Parameters			
-	Outlet boundary head, m	3.48	DBHYDRO
A	Empirical constant of flow resistance, unitless		
	SAV	0.72	Calibrated
	Cattail	1.28	Calibrated
	Open water/ sparse submerged vegetation	0.065	Calibrated
B	Empirical constant of flow resistance, unitless	-0.77	SFWMD (2005a)
K_{veg}	Vegetation reference crop potential ET correction coefficient, unitless (0-1)	0.64	Calibrated
k	Hydraulic conductivity, m s^{-1}	3.5×10^{-4}	Harvey et al. (2000)
K_S	Seepage coefficient, m^2 s^{-1}	0.0092	Estimated from water budget (1995-2000)
α_L	Longitudinal dispersivity, m	35	Calibrated
α_T	Transverse dispersivity, m	3	Calibrated
D_m	Molecular diffusion, m^2 d^{-1}	7.3×10^{-5}	Kadlec and Wallace (2008)
k_{up}	Uptake rate constant, d^{-1}		
	SAV and cattail	0.4	Calibrated
	Open water/ sparse submerged vegetation	0.2	Calibrated
k_r	Release rate constant, d^{-1}	1.97×10^{-4}	Calibrated

Table 3-2. Scenarios designed to evaluate management conditions on spatial and temporal dynamics of total phosphorus in the water column and soil.

Scenario	Description	Questions to be answered
S0	Evaluate current conditions using data from 1995-2000	
Internal characteristics		
S1	Identify short-circuiting locations and change vegetation pattern to improve performance	Vegetation effects of channels/ditches on TP removal efficiency of Cell 4
External loadings from 1995 to 2000		
S2a	Original TP concentrations x 0.75	Impacts of loading on outlet TP concentrations and wetland removal performance
S2b	Original TP concentrations x 0.50	
S2c	Original TP concentrations x 0.25	
S3a	Original flow x 0.5	
S3b	Original flow x 1.5	
S3c	Original flow x 2	
Long-term simulations(1995-2018)		
S4	Repeat 6-year (1995-2000) input data and run for additional 18 years	Temporal evolution of long-term performance (TP outflow and accumulation in soil)
S5	No inflow TP concentrations applied after 2001, repeat hydrologic inputs through 2018	Release of TP from accumulated solids (i.e., internal load)

Table 3-3. Model sensitivity analysis for Cell 4 of Stormwater Treatment Area 1 West.

Input parameters and variables	Change	$S_{P,\ V}$	$S_{P,\ C}$
Initial/boundary conditions			
Water level	+20 cm	-0.013	0.019
	-20 cm	-0.013	-0.012
Outlet boundary head	+10 cm	-0.149	-1.616
	-10 cm	-0.076	-1.180
C_{TP}^{SW}	+30%	0.000	0.002
	-30%	0.000	0.002
S_{TP}	+30%	0.000	0.244
	-30%	0.000	0.244
Parameters			
A	+30%	-0.012	-0.141
	-30%	-0.014	-0.178
K_{veg}^{*}	+30%	-0.012	0.010
	-30%	-0.013	0.004
k	+30%	0.000	0.001
	-30%	0.001	-0.001
K_S	+30%	-0.090	-0.007
	-30%	-0.091	-0.015
α_L	+30%	0.000	0.006
	-30%	0.000	0.005
α_T	+30%	0.000	-0.019
	-30%	0.000	-0.023
k_{up}	+30%	0.000	-0.588
	-30%	0.000	-0.852
k_r	+30%	0.000	0.325
	-30%	0.000	0.341

The parameters are changed from the baseline data of Cell 4 (Table 1). The selected response variables are the total volume of water discharge from outlet structure (V), and mean annual TP outflow concentrations (C) for the period of simulation (1995-2000).
* To test the sensitivity of the model to changes in ET, we modified the vegetation reference crop potential ET correction coefficient (K_{veg}).

Table 3-4. Simulated average annual total phosphorus retention from water column, and predicted outlet total phosphorus concentration for Cell 4.

Simulations	Flow ($m\ yr^{-1}$)	TP-inflow ($g\ m^{-2}\ yr^{-1}$)	TP-inflow conc. ($\mu g\ L^{-1}$)	Predicted TP outlet conc. ($\mu g\ L^{-1}$)	Total TP-input ($g\ m^{-2}\ yr^{-1}$)*	Total TP-output ($g\ m^{-2}\ yr^{-1}$)+	TP-removal ($g\ m^{-2}\ yr^{-1}$)	TP- removal (%)++
S0	51.7	2.41	48.1	20.3 (0.17)	2.42	1.27 (0.14)	1.15 (0.16)	48 (0.15)
S1	51.7	2.41	48.1	10.9 (0.29)	2.42	0.66 (0.28)	1.76 (0.11)	73 (0.11)
S2a	51.7	1.81	36.1	16.5 (0.17)	1.82	1.00 (0.14)	0.82 (0.18)	45 (0.18)
S2b	51.7	1.20	24.0	12.7 (0.17)	1.21	0.74 (0.15)	0.47 (0.24)	39 (0.24)
S2c	51.7	0.60	12.0	8.9 (0.19)	0.61	0.48 (0.16)	0.13 (0.62)	21 (0.60)
S3a	25.7	1.19	48.1	15.9 (0.26)	1.20	0.55 (0.21)	0.65 (0.19)	54 (0.19)
S3b	77.7	3.62	48.1	22.9 (0.14)	3.63	2.08 (0.12)	1.55 (0.16)	42 (0.17)
S3c	103.8	4.84	48.1	25.0 (0.13)	4.85	2.96 (0.11)	1.89 (0.17)	39 (0.18)

Simulated values are based on calibrated parameters (k_u and k_r). Shown in parentheses are the coefficient of variation (standard deviation divided by the mean) of four simulations using calibrated k_u and k_r ± 30%.

*Total TP-input includes wet TP deposition (10 $\mu g\ L^{-1}$)

+Total TP-output includes seepage loss

++Percent TP removed calculated relative to the amount of TP that entered in to Cell 4

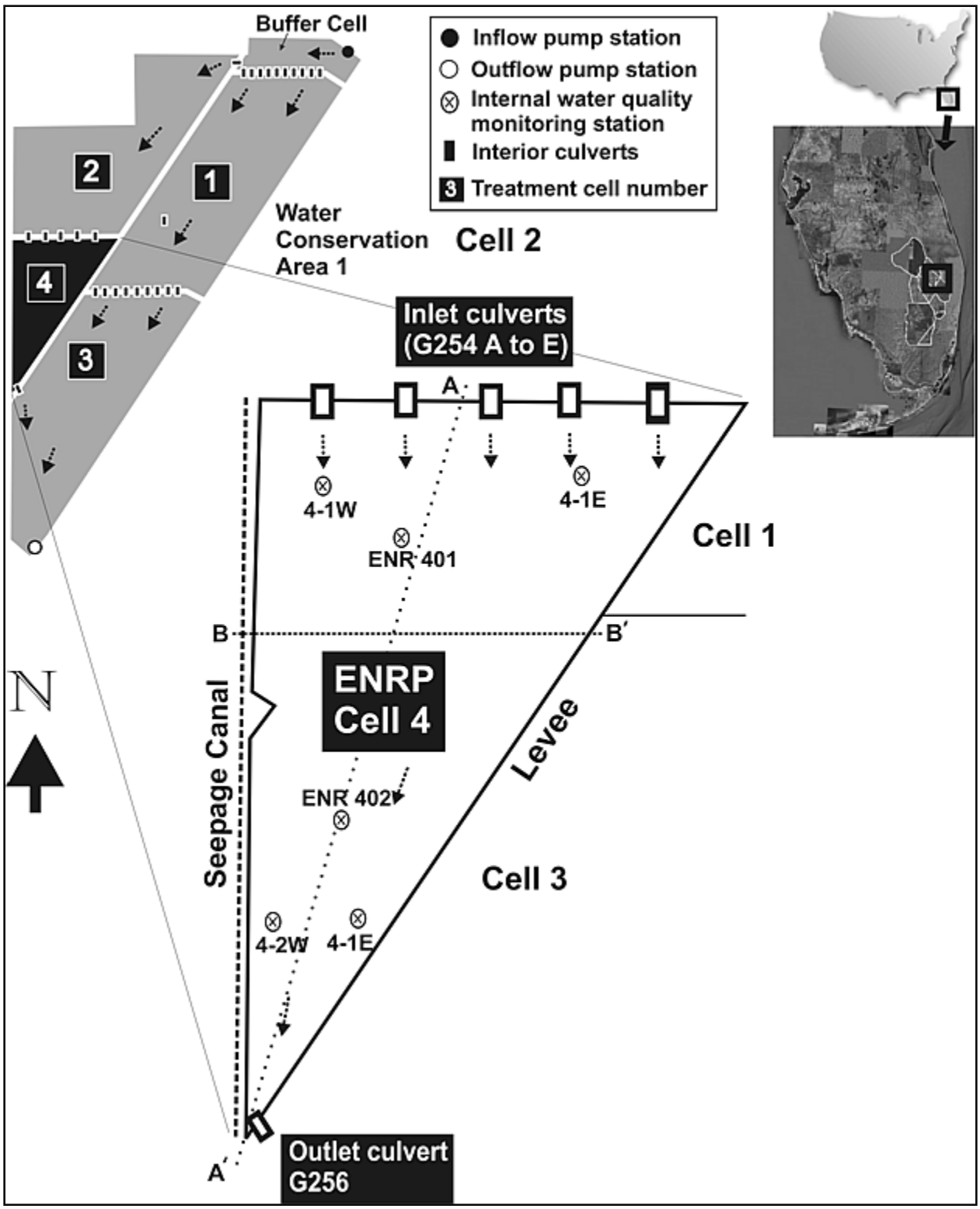

Figure 3-1. Location and plan view of study area, Cell 4 of Stormwater Treatment Area 1 West.

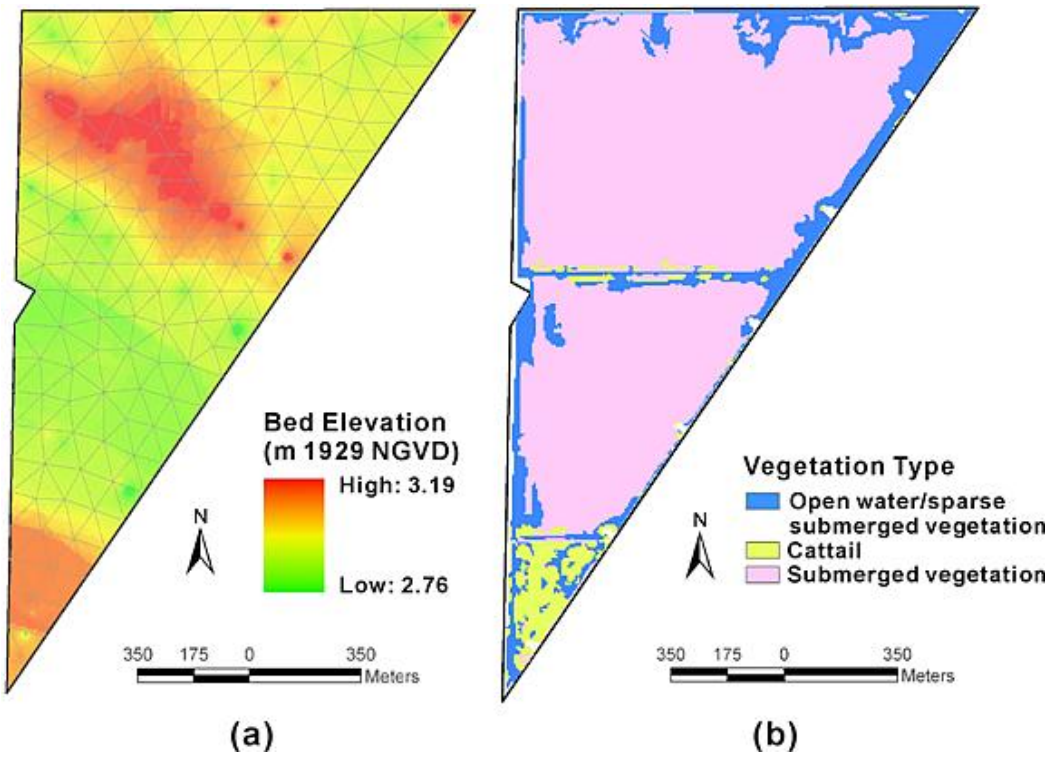

Figure 3-2. Spatial maps of Cell 4,Stormwater Treatment Area 1 West: (a) model mesh and bathymetry and (b) vegetation type and coverage. The mean bed elevation of raster cells within each mesh element were considered in the model.

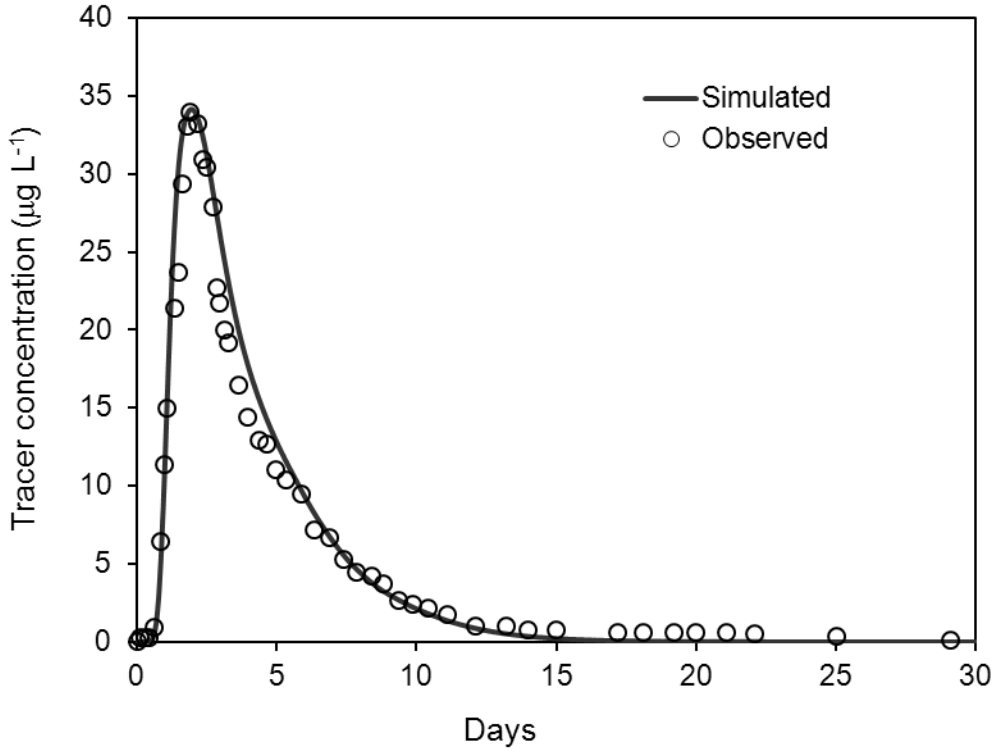

Figure 3-3. Observed and simulated tracer concentrations at outflow structure (G-256) of Cell 4. The Rhodamine WT dye was applied to Cell 4 on December 16, 1999 (Dierberg et al., 2005).

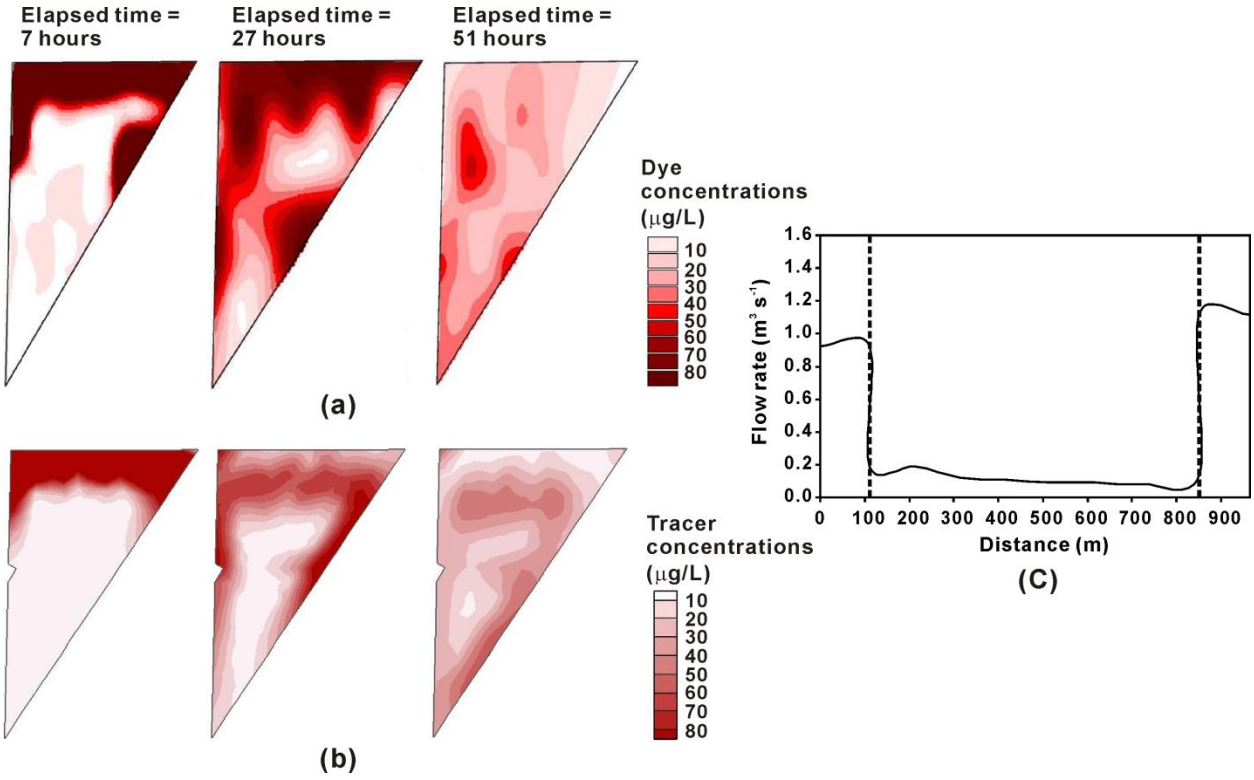

Figure 3-4. Comparison between observed and simulated two-dimensional progression of Rhodamine WT dye plume, and simulated flow rate across the transect BB' (Figure 1) at Cell 4: (a) observed dye plumes at elapsed time (7, 27, and 51 hours); (b) simulated dye plume at elapsed time (7, 27, and 51 hours); (c) average simulated flow rate during tracer test period. The observed spatial map of dye was estimated by Dierberg et al (2005).

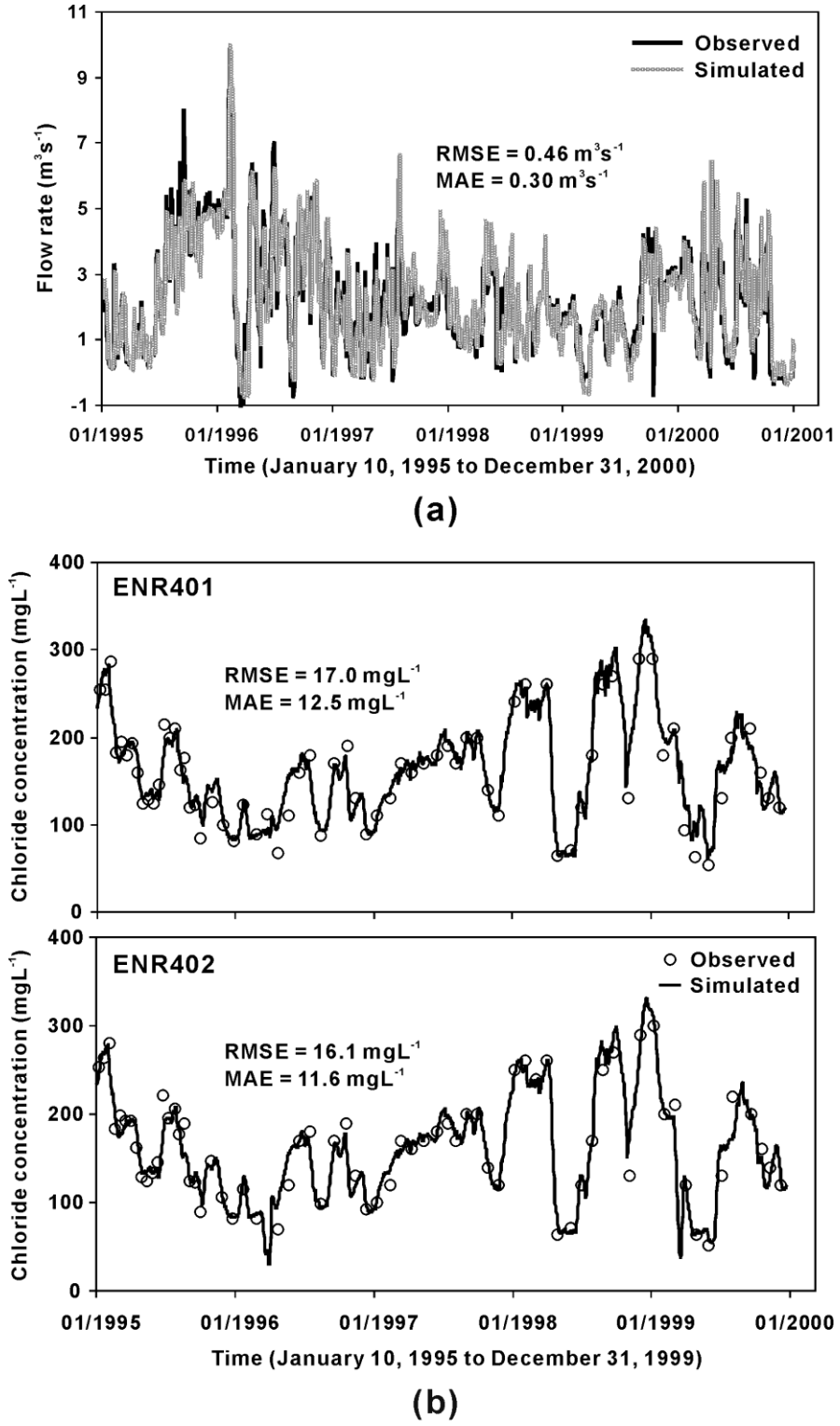

Figure 3-5. Comparison between observed data and model predictions: (a) outflow discharge at outlet structure (G-256), (b) chloride concentrations at internal monitoring stations (ENR401 and ENR402).

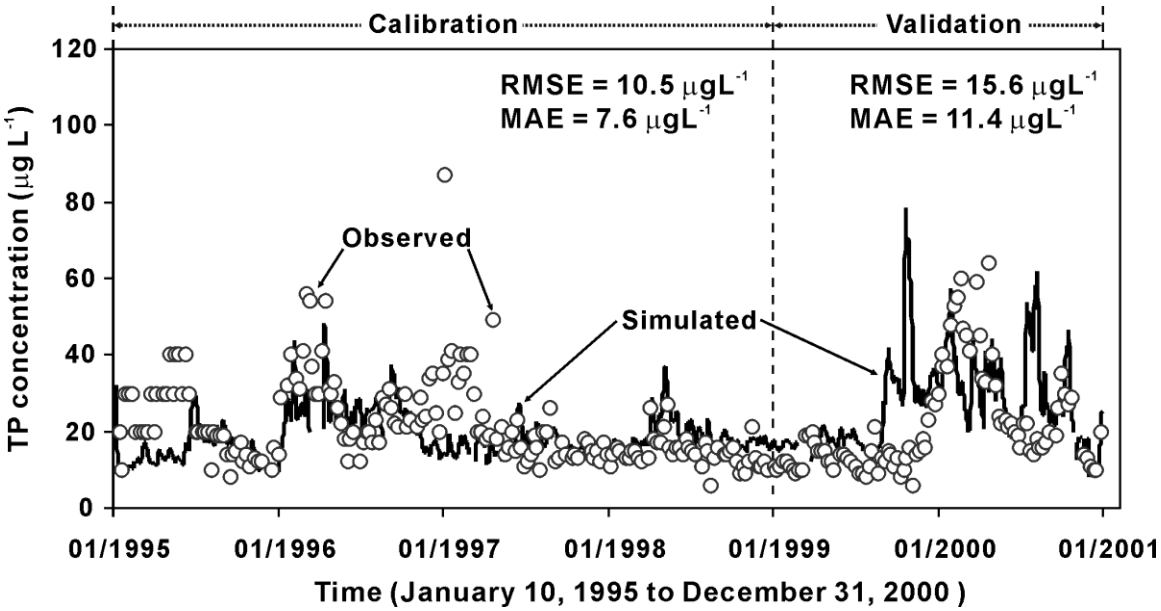

Figure 3-6. Observed and simulated total phosphorus concentrations at the outflow structure (G-256) of Cell 4 for the model calibration period (January 10, 1995 to December 31, 1998) and validation period (January 1, 1999 to December 31, 2000).

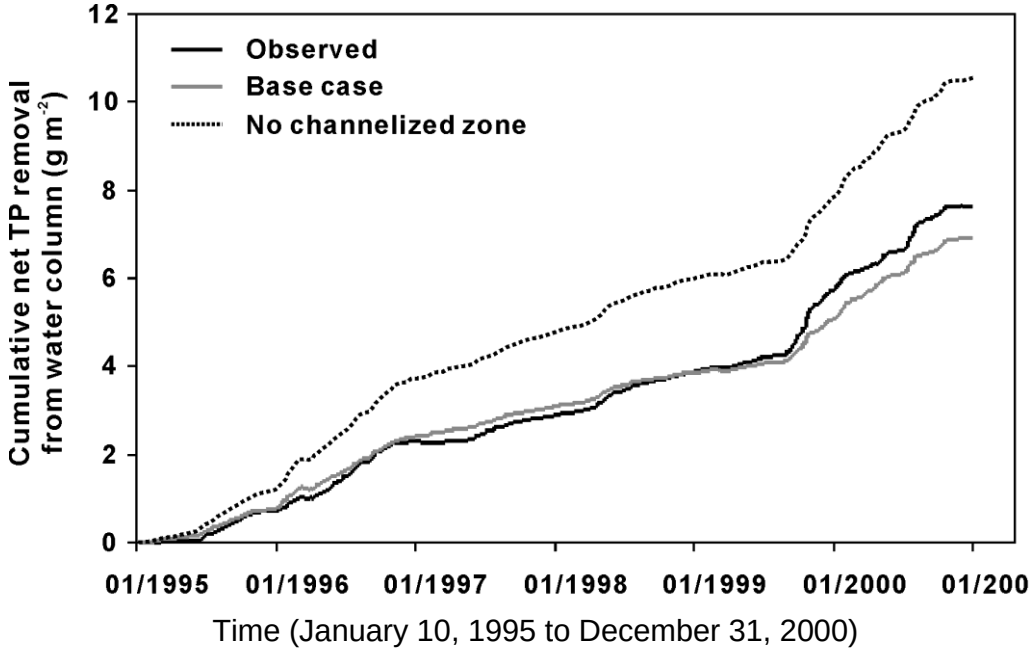

Figure 3-7. Predicted cumulative total phosphorus removal from water column based on the mass balance calculations from measured data and model predictive scenarios (S0 and S1).

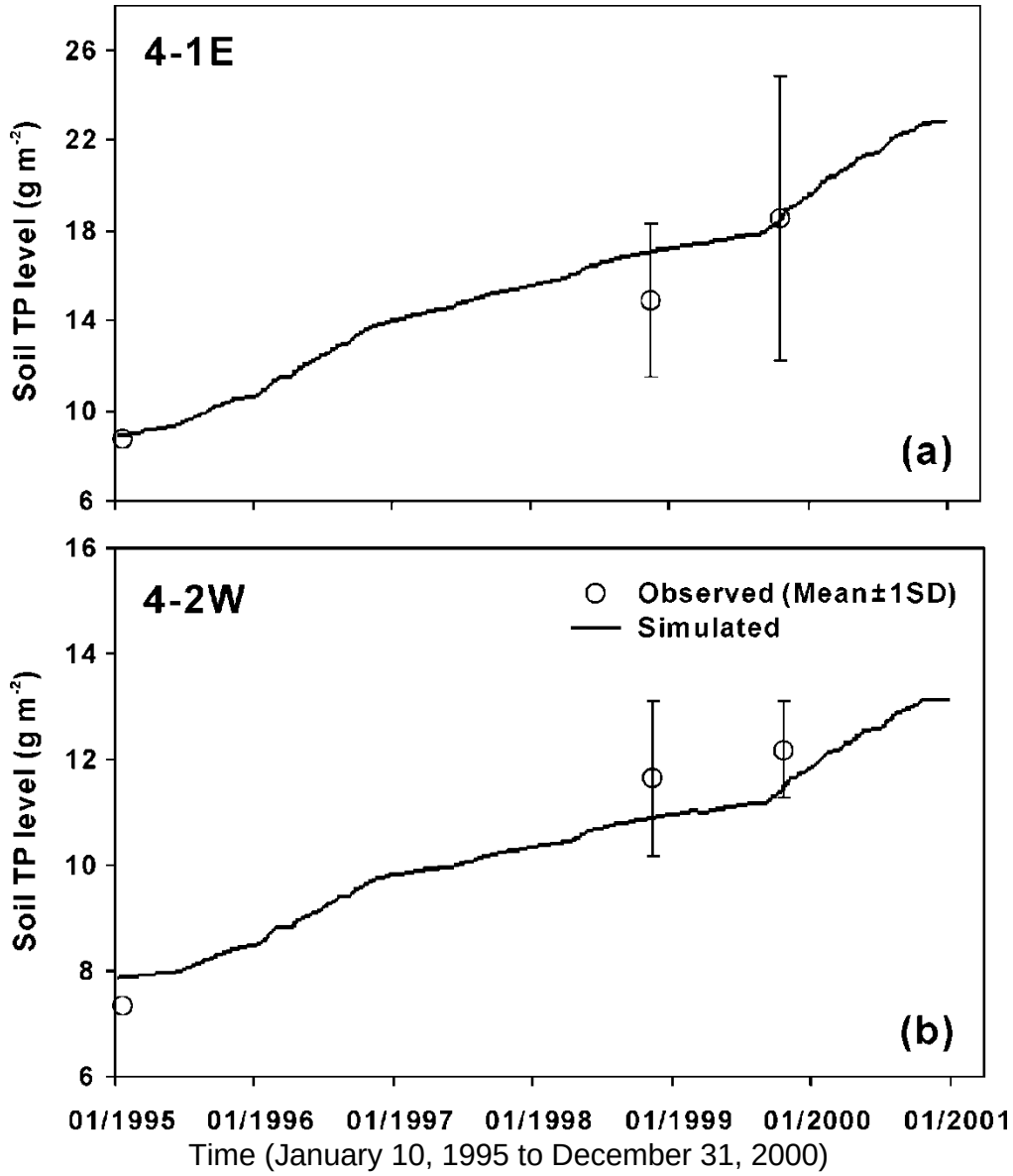

Figure 3-8. Observed and predicted soil total phosphorus content at two locations within Cell 4 for the upper 10 cm of the soil profile: (a) upstream area, 4-1E and (b) downstream area, 4-2W.

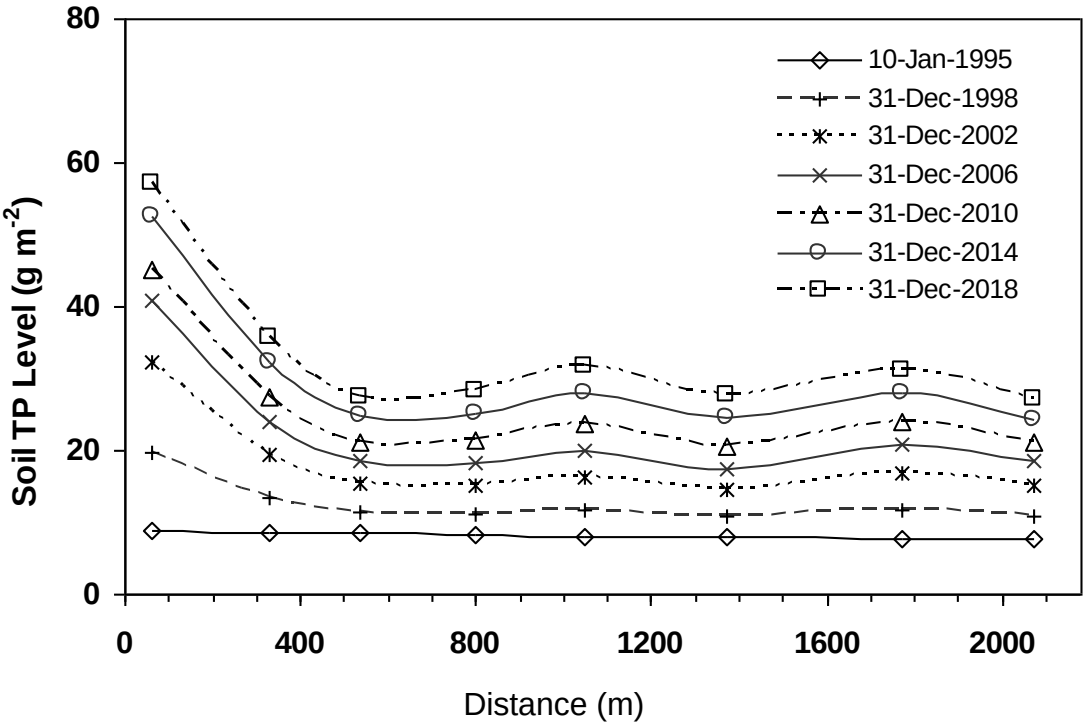

Figure 3-9. Predicted soil total phosphorus content along the transect AA' for the upper 10 cm of the soil profile (from inflow to outflow culverts) under S4 from January 10, 1995 to December 31, 2018.

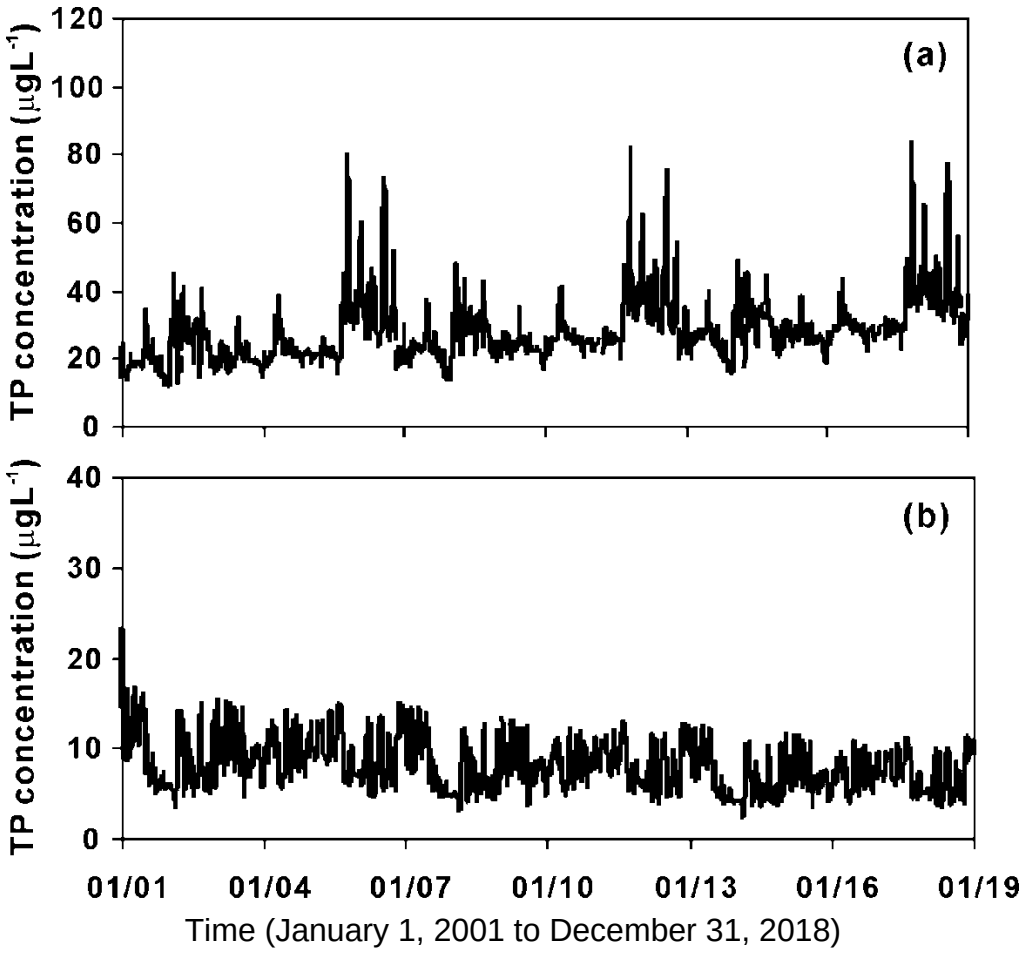

Figure 3-10. Predicted outlet total phosphorus concentrations for (a) S4 and (b) S5.

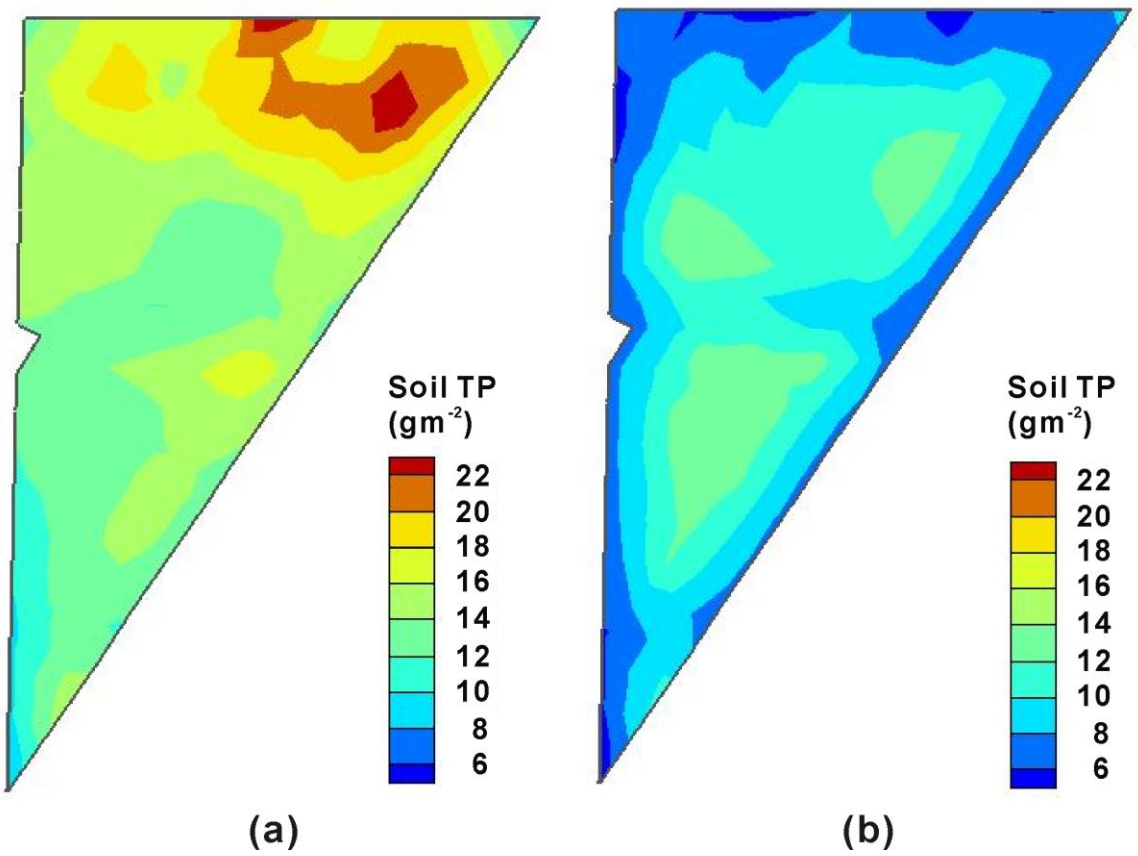

Figure 3-11. Snapshots of soil total phosphorus pattern predicted under S5 for the upper 10 cm of the soil profile on (a) December 31, 2000 and (b) December 31, 2018.

CHAPTER 4
ASSESSING MECHANISTIC BIOGEOCHEMICAL MODEL COMPLEXITY TO DESCRIBE PHOSPHORUS DYNAMICS IN A STORMWATER TREATMENT WETLAND

Mechanistic biogeochemical models are becoming critical tools for predicting nutrient behavior in constructed treatment wetlands to address a wide range of management and research questions. However, there is a continuing challenge of constructing or selecting an appropriate model structure that adequately represents the nutrient cycling mechanisms and establishes a rigorous link to the measured field data to provide reliable predictions. This is primarily because a model is the physical representation of governing processes; and the nutrient cycling processes in wetland systems are mainly governed by complex, heterogeneous, micro-scale, physical, chemical and biological processes, which are often hard to discern and characterize. Given the inherent complexity of wetlands, models developed with simplistic assumptions do not adequately represent the reality of a dynamic system, losing physical meaning to make numerically reliable predictions (Kadlec, 2000; Fulton et al., 2003; Haws et al., 2006). Therefore, overly simplistic models will likely fail under different field conditions that are beyond the bounds of the calibration data (Martin and McCutcheon, 1999). These failures are attributable to the simplifications in the model formulation that do not sufficiently account for complex interactions among various wetland components, such as water, soil, biota, and dissolved and particulate constituents. Conversely, if the model has too many parameters that surpass the type of data needed, calibration to measured data can be non-unique (no particular parameter combination that represents the solution) (Martin and McCutcheon, 1999), and we may not be able to discern the underlying causes of system behaviors.

When formulating a model structure of an aquatic ecosystem (such as a treatment wetland), a common misconception is that if one model structure fails to reasonably predict the data or experimental scenario, increasing the level of complexity (i.e., greater process descriptions) will improve model performance. However, a review of 153 aquatic biogeochemical models published from 1990 to 2002 failed to support this commonly held notion (Arhonditsis and Brett, 2004). These authors found that adding complexity to an aquatic biogeochemical model did not guarantee improved prediction accuracy. A similar finding was presented by Min et al. (2011) in the context of Everglades wetlands. Complex biogeochemical models usually have simple and fewer restricting assumptions and exhibit more flexibility (Snowling and Kramer, 2001); however, increasing the level of model complexity leads to an increased sensitivity of the output to the input (Snowling and Krammer, 2001; Lindenschmidt, 2006). This is primarily because large uncertainties may arise due to the increased number of interactions between state variables and unconstrained parameters (Robson et al., 2008). Conversely, Fulton et al. (2003) underscored the need to better delineate and represent complex mechanisms and processes in an ecosystem model because simple models with too few details cannot produce realistic behavior, and tend to be of less use as more detailed aspects of the system behavior are not addressed (Murray, 2007). However, there remain practical limitations to incorporate comprehensive representations of biogeochemical processes and their effects into models. For example, mechanistic biogeochemical models require large amounts of data (Robson et al., 2008), which may be relatively scarce. If the model is not constrained by the available field data, the cost associated with fitting noise could lead to diminished

performance (Friedrichs et al., 2006). Complex models also need huge human and computer resources (Jorgensen et al., 2002); therefore, increasing model complexity by incorporating more state variables and processes may not be cost effective, because the majority of the modeling resources may then be devoted to developing and maintaining the model, rather than its application (Fulton et al., 2003). In addition, the computational cost of adding more detail may effectively inhibit the utility of the model. As a consequence, there is a conflict between the desire to constrain the model complexity and to incorporate more processes mechanistically.

Costanza and Sklar (1985) showed that model accuracy (based on the quantitative goodness-of-fit of models) decreased monotonically as a function of model complexity in their review of several published freshwater wetland models. They measured complexity by ‘articulation’ which incorporated the size of the model in terms of components (number of state variables), and spatial and temporal resolutions. Model performance was measured by ‘effectiveness’ (a quantity used to represent the trade-off between complexity and prediction accuracy). These authors found that the maximum effectiveness was for models of moderate complexity. Fulton et al. (2001) presented a similar finding in the context of the published literature on marine ecosystem models.

In south Florida, large-scale constructed wetlands were designed to protect the Everglades ecosystems, where eutrophication has become a serious environmental concern. To reduce the phosphorus concentrations in agricultural drainage waters before entering the Everglades, a state water management agency (South Florida Water Management District, SFWMD) constructed large-scale treatment wetlands (over 18,000 ha), known as Stormwater Treatment Areas (STAs). Given the difficulty and cost

associated with physical experiments, building a predictive model in these treatment wetlands has considerable importance, because models facilitate the study of interactions of several simultaneous processes in a single experiment, and predict future scenarios that cannot be physically tested in the present. In this respect, developing models of these wetlands has great implications in operating as well as optimizing the phosphorus removal performance in order to protect the downstream Everglades ecosystem.

Simple empirical mass balance models (based on input-output analysis), and first-order kinetic models, referred to as a *k-C**, frequently have been used in designing and predicting phosphorus removal in STAs (Kadlec and Newman, 1992; Walker, 1995; Chimney et al., 2000). The first-order kinetic constant, *k*, called net uptake coefficient or settling velocity aggregates all phosphorus retention processes occurring in the wetland (Kadlec, 1997). Mechanistic approaches to describe phosphorus biogeochemical cycling processes have also been investigated in a wide range of model complexity (HydroQual, 1997; Walker and Kadlec, 2005; Min, 2007; Paudel et al., 2010). Generally, simple models (i.e., linear, first-order) provide a valuable hands-on tool to interpret field data and make predictions in poorly characterized systems. In recent years, complex models have been increasingly pursued in these systems. However, field data are often scarce, and it is always not possible to characterize the detailed aspects of the system characteristics (e.g., components and links) in the model. In such a case, many parameters in the model cannot be independently determined using the field data; although such a model may produce superior goodness-of-fit, this invariably the result

of increase in the degrees of freedom rather than the more mechanistic representation of underlying phenomena.

When developing a biogeochemical model of a treatment wetland for a specific modeling purpose—such as synthesizing the data/knowledge, testing hypotheses, assessing management strategies, and forecasting future outcomes—a critical question is: how complex should the model structure be to produce the most reliable numerical predictions that balance the tradeoffs between undesirable details and unjustified simplifications (Flynn, 2005). As a rule of thumb, an appropriate model for a given condition is minimally parameterized with adequate representation of the available data, also referred to as the 'principle of parsimony' (Box and Jenkins, 1970), so that the model can be tested more comprehensively, given the intrinsic limitations of the available data (Kirchner, 2006). As wetland ecosystem structures are intrinsically complex, the task of formulating an appropriate level of model complexity remains a critical and challenging one. This issue needs to be properly addressed in wetland modeling to minimize cost and effort, as well as lead to a maximum knowledge gain about system behavior. Generally, while formulating the model structure, judgments (which are often implicit) are made about the level of details that need to be considered (Cox et al., 2006). However, consideration of some standard qualitative as well as quantitative model evaluation criteria is essential to assess the suitable structure for any specific purpose.

Selecting or developing a suitable model requires comparative assessment of different criteria with respect to complexity. McDonald and Urban (2010) used Akaike's Information Criterion (AIC) for selecting the most suitable mechanistic aquatic

biogeochemical model by evaluating a set of one-dimensional algal dynamics models in a low to high complexity spectrum. Recently, this technique has been applied to mechanistic models in ecological studies (Cox et al., 2006; Bouletreau et al., 2008) to identify the most suitable model. However, Myung et al. (2009) used other model criteria, including explanatory adequacy, interpretability, complexity or simplicity, descriptive adequacy, and generalizability. Costanza and Sklar (1985) used articulation and descriptive accuracy to derive model effectiveness scores for freshwater wetland models. Here, we used following model properties to compare a candidate set of phosphorus biogeochemical models: a) modeling cost and effort; which is basically the level of model complexity (Haraldsson and Svedrup, 2004), b) descriptive adequacy (whether the model describes the existing knowledge and field data of the system); c) predictive adequacy (whether the model predicts the behavior of a system or data outside the existing boundaries); and d) explanatory depth (whether the model describes more underlying phenomenon to provide the knowledge/information about the system structure). Even though each of these criteria describes a property (i.e., element) of a model that can be evaluated on its own, they are closely related to each other. We suggest that concomitant consideration of all four criteria is essential to fully evaluate the suitability (i.e., effectiveness) of a model.

While some researchers have assessed model complexity particularly in ecological and marine biogeochemical studies (Costanza and Sklar, 1985; Friedrichs et al., 2006; McDonald and Urban, 2010), little quantitative knowledge is yet available about the role of model complexity for simulating phosphorus dynamics in treatment wetlands. Here, we quantitatively analyzed six candidate phosphorus biogeochemical

models of a large-scale constructed treatment wetland, Cell 4 of the Stormwater Treatment Area 1 West (STA-1W) of northern Everglades, particularly to identify the relative effectiveness of models in simulating the total phosphorus (TP) dynamics given the available data. Subsequently, the most effective model was identified, which was simultaneously optimal for understanding and predicting the phosphorus dynamics, while balancing the benefits of increased performance in relation to the modeling cost and effort (model complexity).

This chapter begins with a review of applications of the model properties evaluated here, with an emphasis on environmental and ecological studies. This is followed by the formulation of six phosphorus cycling model structures applied in Cell 4, with hierarchal level of process complexity (from low to high level of mechanistic descriptions). All six models were coupled with a pre-calibrated two-dimensional (2-D) hydrodynamic model of Cell 4, STA-1W (Paudel et al., 2010). We then systematically evaluated the properties of model effectiveness (suitability). In addition, we applied multi-model selection technique (i.e., AIC) to identify the best fit model that optimized trade-offs between model complexity and goodness-of-fit. Finally, we discussed future biogeochemical modeling needs of the STAs.

Approaches to Evaluating Model Effectiveness

While research on evaluating the elements of model complexity is promising, it has been hindered by the lack of efficient and rigorous quantitative analysis. The process of developing a model of a complex and dynamic system, as in the case of wetlands, requires a robust way to evaluate the model predictions relative to observations, as well as an equally robust way to compare across differing model complexity. Many modeling studies in environmental science have primarily focused on the goodness-of-fit at the

expense of evaluating the effects of model complexity (modeling cost and effort) on the performance, but often ignored the capacity of a model to provide more relevant information towards understanding future system behaviors. The purpose of this section is to systematically define and describe key model properties (i.e., evaluation criteria) that are critical in constructing or selecting a suitable model structure of wetland environments.

Model Complexity (Modeling Cost and Effort)

As knowledge of wetland ecosystem structure has grown in recent years, the models developed in wetland systems are correspondingly becoming more complex. While the study of model complexity has been rapidly growing; a unique well-accepted definition of either level of details or model complexity is lacking (Brooks and Tobias, 1996). In the general sense, the term, model complexity or modeling cost and effort are intuitive concepts because they are related to a variety of factors, and as yet there has been no formal definition of these model properties. Conceptually, complexity gives the measure of intrinsic difficulty and efforts of developing and applying the model. In this respect, modeling effort and cost is directly correlated with the model complexity, and often used interchangeably in the literature (e.g., Haraldsson and Sverdrup; 2005). We have used interchangeably in this study as well.

There are wide ranges of conceptions about model complexity depending on the type of difficulty focused on, and the type of formulations desired for any specific goal (Edmonds, 2000). Defining the complexity level of a model is confounded by the diverse nature of the problems, modeling purpose, assumptions, and limitations. In an extensive review of literature, Wagenet and Rao (1990) categorized models into three basic groups as: (a) research models (more complex), (b) management models (less

complex), and (c) screening models (analytical solutions used only for relative comparisons). Snowling and Krammer (2001) related model complexity to its structure and the level of details in the processes (i.e., number of parameters, state variables, and the sophistication of the mathematical relationships that explain the modeling processes). Other studies have measured the complexity level only in proportion to the number of optimized parameters (Gan, et al., 1997; Perrin et al., 2001). That is, the greater the number of optimized parameters, the greater the complexity of the model. In this study, we categorized the complexity level of each model structure by assessing the number of process-specific parameters from all model components: hydrodynamics, transport, and phosphorus biogeochemistry.

Descriptive Adequacy

To evaluate the robustness of a model, it is obvious that the simulated results need to be compared with observations. In general, the term ‘descriptive’ refers to models that describe an existing knowledge and a known behavior of the system (Costanza and Sklar, 1985). The degree of adequacy with which a particular model describes existing structures and behaviors can be measured a number of ways. Frequently, a residual (misfit) is used to characterize model performance that evaluates whether the model is capable of producing a particular data set that is used in the calibration exercise (Friedrichs et al., 2006). Perhaps, the consideration of misfit between the model and data is one of the best approaches to evaluate the (relative) descriptive adequacy of a set of models. Myung et al. (2009) considers this is a critical part of evidence in favor of the model adequacy. In this study, we used mean squared error (MSE), also referred to as a ‘general error function’ (E_k) to measure the misfit between the measured variables (O_{jk}) and predicted variables (P_{jk}). E_k can be

expressed as a sum of residual squares divided by the number of observations of each variable, *k*:

$$MSE(E_k) = \frac{1}{r}\sum_{j=1}^{r}[O_{jk} - P_{jk}]^2 \quad (4\text{-}1)$$

where *r* is the number of sampling points in space and time for which simulated values correspond to the available observations of each variable *k.* In order to make a dimensionless index, E_k was normalized by the maximum E_k of all complexity levels. This is represented by misfit error index ($E_{I,k}$) and can be expressed as:

$$E_{I,k} = \frac{E_k}{max[E_k]} \quad (4\text{-}2)$$

where $max[E_k]$ is the maximum error function of each variable *k*, among all complexity levels for which observations are available to compare with model predicted values. The descriptive accuracy index (*DAI*) of each candidate model was then expressed:

$$DAI_k = 1 - E_{I,k} \quad (4\text{-}3)$$

Predictive Adequacy

Descriptive adequacy describes the performance of the model during calibration for a specific data set, but it is essential to test the model against the data that are beyond the calibration boundaries (Friedrichs et al., 2006). The term ‘predictive adequacy’ refers to the ability of a calibrated model to produce the replications of structural characteristics or behavior of a system outside the existing data boundaries. A validation exercise is just a robust approach to evaluate the predictive adequacy of a model. The best model should be consistently good when extending the simulations across different conditions. Hence, we employed ‘prediction adequacy’ as one of the model performance elements. This was quantified by extending model simulations to a

new, unassimilated data set that was not used in the calibration. In some literature, predictive adequacy is also referred to as ‘generalizability’, and it has been described as one of the best measures to compare competing models (Pitt and Myung, 2002; Myung et al., 2009). The predictive accuracy index (*PAI*) was determined in the same manner as the *DAI* for validation data:

$$PAI_k = 1 - E_{I,k} \tag{4-4}$$

Model Performance Index

The overall performance of each candidate model was represented by a model performance index (*MPI*). The *MPI* incorporates both descriptive and predictive accuracy indices. *MPI* is the relative index that ranges between 0 to 1; 1 indicates the perfect accuracy and 0 indicates accuracy of the worst performing model.

$$MPI = \frac{1}{n_k}\sum_{i=1}^{n_k}\left(W_k DAI_k\right) + \frac{1}{n_k}\sum_{i=1}^{n_k}\left(W_k PAI_k\right) \tag{4-5}$$

where n_k is number of variables for which the measured data were available for the comparison; W_k is the weight given to each variable k, if more than one variable is available for comparisons. The value of W_k is the arbitrary, subjectively chosen by considering the importance and availability of spatio-temporal field measured data to make comparisons with simulated results. In this study, an equal weight was given to both *DAI* and *PAI* based on the assumption that both descriptive and predictive adequacy are equally important.

Explanatory Depth

General goals of modeling environmental systems include not just future forecasting, but also testing and analyzing hypotheses, and gaining deeper understanding of system behaviors, which enable us to identify cause-effect

relationships of system structures. For these latter cases, models that can explain diverse phenomena are more generally applicable than simple ones. We suggest that models that describe system behavior with greater detail should be weighted more heavily than simple models. However, this assumption does not account whether the complex models are overly parameterized and diminish their effectiveness (suitability).

Generally, the ability of a model to describe more processes can be related to the amount of details it provides about system components (i.e., state variables), and processes. A model is an abstraction of a real system; hence it will not reflect all of the reality (Wainwright and Mulligan, 2004). It is the simplification or approximation of underlying behaviors of a dynamic system. Given the complexity of a dynamic system, models developed with higher levels of abstraction generally explain more features of a system structure, not only in principle but also in practice (Beven, 2001). Generally, most modelers are exhaustively focused on just the model performance for the phenomena being predicted and believe that the predictive accomplishments are simply an indication of the most suitable model; they are not willing to consider the explanatory capacity of a model as an important property. If the model was not for explanation, an equally predictive empirical model would always be the best model because of its parsimony (Wainwright and Mulligan, 2004). In this respect, we attempted to assess the ‘explanatory depth’ of each candidate model to account for their capability in simulating more underlying phenomena.

The term ‘explanatory depth’ is generally based on an intuitive idea (Beven, 2001). For example, a complex-structured model can predict many components as well as individual processes, but the simple model can only predict few. Since explanatory

depth is a more qualitative concept, it is often difficult to assess objectively (Beven, 2001). Here, to decrease the subjectivity, we accounted number of relative process-parameters of each candidate model and generated an index that aimed to reflect the level of details in the description of processes. The explanatory depth index (χ_m) for model *m* can be expressed as:

$$\chi_m = \frac{\left[exp\left(c\Delta_P\right)\right]}{\sum_{i=1}^{m}\left[exp\left(c\Delta_P\right)\right]} \tag{4-6}$$

$$\Delta_P = \left(P_m - P_f\right) \tag{4-7}$$

where P_m, and P_f are the number of process-specific parameters for each model *m*, and the model that consists of fewest parameters among the set of models, respectively; c is the exponential scale factor that determines the shape of the explanatory depth curve in relation to the complexity index (Figure 4-1). The shape of the curve reflects how well the added processes in each model provide the more relevant information with respect to the modeling questions. To some extent, the choice of the exponential factor involves subjectivity. The explanatory depth index of each set of model considered in this study is depicted in Table 4-1.

Model Effectiveness

Comparison of model effectiveness and complexity has been a long-term interest in the ecological sciences (Costanza and Sklar, 1985). Parsimony (the smallest possible number of parameters for adequate representation of the data) has become a guiding principle for multi-model inference (Burnham and Anderson, 2002). A parsimonious model is the one with the greatest explanation and/or predictive performance in relation to the least process complexity (Wainwright and Mulligan, 2004). As a first principle, the

best model is the one that is most parsimonious in state variables and parameters, while satisfying the modeling objective. We suggest that the 'best' model (also referred to as 'most effective' model) is the one that optimizes the benefits of increased performance in relation to the cost and effort needed in developing and maintaining the model, as well knowledge/information gain by the modeling work (Figure 4-1). As previously noted, a complex model needs large amounts of data, and significant effort and time to develop the model and adjust unconstrained parameters (Friedrichs et al., 2006). Even if a given complex model produces better model performance, extensive time invested during the model developing process makes the model less effective.

Here, we developed an index to evaluate the effectiveness of each model, represented as a "coefficient of effectiveness". The weighted resultant of performance (*MPI*) and explanatory depth (χ_m) was normalized by the modeling cost and effort index (*CI*) for model *m* to calculate coefficient of effectiveness (φ_m), and can be expressed as:

$$\varphi_m = \frac{\sqrt{\frac{\left(K_p MPI_m^2 + K_e \chi_m^2\right)}{\left(K_p + K_e\right)}}}{CI_m} x100 \qquad (4\text{-}8)$$

where K_p, and K_e are the weighting constants for *MPI* and χ_m, respectively. If both elements are equally valued, K_p, = K_e = 1. The values of φ_m are relative, and can be used only to compare models within the same study.

Akaike's Information Criterion

Akaike (1973) derived an information criterion, based on Kullback-Leibler (K-L) information, which is known as Akaike's Information Criterion (AIC). It has become a fundamental basis for selecting the best model from a set of candidate models (Burnham and Anderson, 2002), and has been broadly used in the fields of information

science and statistics (Cox et al., 2006). AIC evaluates the likelihood of each candidate in a set of models taking into account the goodness-of-fit and number of estimated parameters in the model. Even if all models are very poor in the performance, AIC will still select the one estimated to be the best; therefore, this criterion is particularly useful in selecting a best performing model structure, where models use same data set. AIC is often used as a decision tool for choosing between competing models (Burnham and Anderson, 2001).

In this study, we applied the AIC to phosphorus biogeochemical models of Cell 4 to examine the results provided by effectiveness index. Although AIC is commonly used in linear regression models in the ecological sciences, it is not commonly applied to mechanistic models. Nevertheless, more recently, AIC has been used to evaluate a set of mechanistic models to identify the best model structure to simulate a specific variable of interest in environmental and ecological studies (Poeter and Anderson, 2005; Cox et al., 2006; Bouletreau et al., 2008; McDonald and Urban, 2010). In this approach, we viewed mechanistic biogeochemical models as a probabilistic model of a dynamic system (Ljung, 1987; McDonald and Urban, 2010), in which each model describes the probability distribution of the data, given the model parameters and a particular model structure. Residuals are assumed to be normally distributed with a constant variance, σ^2. Generally, when the ratio of the number of data points to the number of optimized parameters (n/k) is small (roughly <40), often in the wetland biogeochemical modeling study, a bias adjustment term is added to AIC (Hurvich and Tsai, 1989).The value of k must be considered from the highest-dimensioned model. The bias corrected AIC can be expressed as:

$$AIC_c = -2ln\left(L\left(\hat{\theta}\right)\right) + 2k + \frac{2k(k+1)}{n-k-1} \quad (4\text{-}9)$$

where n is the number of points; k is the number of optimized parameter; $L(\hat{\theta})$is the maximum likelihood function of the parameter vector θ.

The maximum likelihood function for the univariate case is:

$$L\left(\hat{\theta}\right) = \left[\frac{1}{\sqrt{2\pi\sigma}}\right]^n e^{-\frac{1}{2}n} \quad (4\text{-}10)$$

and the maximized log-likelihood is therefore

$$\ln L\left(\hat{\theta}\right) = -\frac{1}{2}\ln\left(\sigma^2\right) - \frac{n}{2}\ln\left(2\pi\right) - \frac{n}{2} \quad (4\text{-}11)$$

The second and third terms in Equation 4-11 are the additive constants, and can be omitted from the log-likelihood function while using identical data for a set of candidate models (Burnham and Anderson, 2002). Details about the likelihood function and AIC metric can be found in Burnham and Anderson (2002) or elsewhere.

AIC is the relative value over the candidate set of models considered. The least AIC value corresponds to the best model structure that most likely emulates the underlying phenomena, based on the goodness-of-fit and degrees of freedom with respect to the data (McDonald and Urban, 2010). As the parameters are increased in the model, performance improves (bias reduced) and uncertainties increase (variance increased). AIC_c selects models with a trade-off between accuracy and uncertainty (bias versus variance); this is the principle of parsimony (Poeter and Anderson, 2005).

Relationship among Model Performance, Explanatory Depth, and Complexity

Models of complex environmental systems are designed to answer many questions; thus modeling can be costly when the problem involves many questions

(Haraldsson and Sverdrup, 2004). A robust model that answers the desired questions is not necessarily a complex model because such models are relatively costly and prone to higher uncertainties in the structure and modeled processes. Even if the model performs better, the performance must be compromised with costs and efforts required to develop the model. Increasing the complexity in the model contributes to the performance; however, the contribution to the performance may not be necessarily effective in relation to the added complexity (Figure 4-1). Our general hypothesis states that the phosphorus biogeochemical model performance in a treatment wetland is generally increased, as the modeled process-complexity increases; however, the benefits of marginal increase in accuracy compared to the added complexity (cost and efforts) are insignificant. Ideally, there is an optimal level of model complexity (a point that corresponds to the highest effectiveness scores) for a given system and a modeling question, which may be met at certain point of a low to high complexity spectrum (Figure 4-1). At this level, complexity matches with model performance as well as leads to maximal knowledge gain about the modeled system (Joergensen, 1992).

As a scientific product, developing biogeochemical models are regarded from two basic perspectives: future forecasting, and understanding behaviors or test hypotheses. The latter often desires the detailed representation of system components, which eventually enhance the understanding about the system dynamics. A complex model entails deeper explanation ability and provides cause-effect relationships at various levels. In this respect, increased complexity will increase the descriptive capacity of a model exponentially with model complexity (Figure 4-1). Thus, developing a model

requires a holistic perspective among degree of complexity, performance, explanation depth and a modeling objective.

The Case Study: Cell 4 of Stormwater Treatment Area 1 West

Biogeochemical Models

Our goal was to develop a set of phosphorus biogeochemical models using Regional Simulation Model Water Quality (RSMWQ) to simulate phosphorus dynamics in Cell 4 of STA-1W (the study site was described in Chapter 3). Based on the available data, resources, and knowledge about the system, we formulated six model structures. The Hydrologic Simulation Engine (HSE) and RSMWQ, discussed in Chapter 3 were used as a basic modeling framework for this study. To include the coupled effects of hydrodynamics, all six models were internally embedded with a hydrodynamic model of Cell 4 (Paudel et al., 2010). The level of details in the model was increased by adding physical processes, components in a sequence of relevance to increase the level of process-complexity. All these phosphorus biogeochemical model structures were formulated in terms of “stores” and “flow” model. Conceptually, phosphorus cycling in a wetland is the transfer of this element in various forms between different stores, often referred to as ‘variables’ (e.g., water column, macrophyte, soil, pore water, suspended solids, and biofilm). Each component is considered in terms of phosphorus storage, and the flow is considered as a transfer of phosphorus from one store to another. Transfer processes include growth, senescence, settling, release, diffusion, and so forth, which are described by linear (e.g., first-order) or nonlinear (typically second-order, and Monod types of transformations). Models differ with respect to the detailed physical representations used to describe the phosphorus cycling processes, and formulated with an increasing level of process complexity, that ranges from a simple first-order

phosphorus removal model (low-level mechanistic descriptions) to more complex phosphorus limited vegetation growth dynamics (high-level mechanistic descriptions).

Predicting the phosphorus behavior of STA systems is often challenging and uncertain, since they involve analyzing the system made up of many components and parts that are interconnected, and interact in a nonlinear ways with many feedback loops. Ideally, all properties of natural systems would be deducible from fundamental physics (Alridge et al., 2006). However, as a result of the complexity that is inherent within dynamic systems, it is difficult to set an appropriate level of abstraction in the model. Here, we particularly formulated model structures using instantiated processes that were selected on the basis of experience from previous wetland models, available field data, and existing knowledge about the system (Kadlec, 1997; DBEL, 2000; DBEL, 2002; Dierberg et al; 2005; Walker and Kadlec, 2005; Kadlec and Wallace, 2008); however, the sequence in which the processes/parameters were added was arbitrary. All models were forced with same physical fields, flow and biogeochemical data; therefore, they directly compared the quality of model structures. Process diagrams of all model structures are depicted in Figure 4-3.

Model 1

The simplest complexity model represents the net uptake of TP from the water column. In this model, all phosphorus removal processes are ‘lumped’ together to result in a single state variable and a single equation. Net removal of TP was represented with a simplified ‘lumped rate’ coefficient, known as volumetric first-order rate constant. Given the location of the model domain, TP is presumed to be removed in proportion to the water column phosphorus concentrations. The model consists of one state variable (C_{tp}) and one calibration parameter (k_{st1}).

$$\frac{dC_{tp}}{dt} = -k_{st1}C_{tp} \quad (4\text{-}12)$$

Model 2

In this model, all phosphorus reactions are lumped as soil-water uptake and release, represented by the volumetric first-order reaction rate constants. These constants reflect the effects of one or combination of several physical and biochemical processes between the water column and the soil. The model tracks storage of the soil TP and simulates the release of TP from soil to the water column. Conceptually, the modeled exchange between the two components is a simple settling (or uptake) and release, where settling refers to the transfer from water column to the soil, and release is in the opposite direction. Soil TP release mechanisms (e.g., resuspension, diffusion, and so forth) were aggregated together and modeled as a single release mechanism. Particularly, under reduced external phosphorus loading conditions, wetland soils may act as a source and release accumulated soil phosphorus to the overlying water column (Reddy, 1991; Pant and Reddy, 2003), likely maintaining high level of phosphorus in the water column. Thus, Model 1 was extended with an additional parameter (i.e. release rate coefficient). Water column TP was considered as a mobile component, which was essentially transported by water or other mechanisms, whereas soil TP and macrophyte TP were assigned to be stabile (stationary).

$$\frac{dC_{tp}}{dt} = -k_{st2}C_{tp} + \frac{k_{rs2}}{z_d\theta_{wc}}S_{tp} \quad (4\text{-}13)$$

$$\frac{dS_{tp}}{dt} = k_{st2}z_d\theta_{wc}C_{tp} - k_{rs2}S_{tp} \quad (4\text{-}14)$$

where S_{tp} is the soil TP storage (g m^{-2}); k_{st2} is the TP uptake rate (d^{-1}); k_{rs2} is the TP release rate (d^{-1}); z_d is the water column depth (m); and θ_{WC} is the water column porosity; k_{st2} and k_{rs2} are the calibration parameters.

Model 3

At this complexity, we simulated the exchange of TP between water column, soil, and an additional vegetation (macrophyte) component. Macrophytes primarily include submerged aquatic vegetation (SAV) and other emergent vegetation. Model 3 consisted of 3 components (state variables), 4 kinetic processes, and 4 first-order rate constants. All processes were represented by linear relationships (typically first-order kinetics) that account for a single process or an aggregation of multiple physical and biogeochemical processes (Equations 4-15, 4-16, and 4-17).

$$\frac{dC_{tp}}{dt} = -k_{st3}C_{tp} + \frac{k_{rs3}}{z_d\theta_{wc}}S_{tp} - k_{up\_mf3}C_{tp} \quad (4\text{-}15)$$

$$\frac{dM_{tp}}{dt} = k_{up\_mf3}C_{tp}z_d\theta_{wc} - k_{b3}M_{tp} \quad (4\text{-}16)$$

$$\frac{dS_{tp}}{dt} = k_{st3}z_d\theta_{wc}C_{tp} - k_{rs3}S_{tp} + k_{b3}M_{tp} \quad (4\text{-}17)$$

where M_{tp} denotes the macrophyte TP storage per unit area (g m^{-2}); k_{st3} is the water column TP settling rate (d^{-1}); k_{rs3} is the soil TP release rate (d^{-1}); k_{up_mf3} is the macrophyte foliage TP uptake rate (d^{-1}); and k_{b3} is the macrophyte TP burial rate (d^{-1}).

Model 4

At this complexity, two processes (i.e., macrophyte TP recycle, and macrophyte root uptake) were added to increase the complexity level. Model 4 consists of 3 state variables, 6 kinetic processes, and 6 first-order rate constants. All processes were

represented by linear relationships (typically first-order kinetics) (Equations 4-18, 4-19, and 4-20).

$$\frac{dC_{tp}}{dt} = -k_{st4}C_{tp} + \frac{k_{rs4}}{z_d\theta_{wc}}S_{tp} + \frac{k_{rc4}}{z_d\theta_{wc}}M_{tp} - k_{up\_mf4}C_{tp} \quad (4\text{-}18)$$

$$\frac{dM_{tp}}{dt} = k_{up\_mf4}C_{tp}z_d\theta_{wc} - k_{rc4}M_{tp} - k_{b4}M_{tp} + k_{up\_mr4}S_{tp} \quad (4\text{-}19)$$

$$\frac{dS_{tp}}{dt} = k_{st4}z_d\theta_{wc}C_{tp} - k_{rs4}S_{tp} + k_{b4}M_{tp} - k_{up\_mr4}S_{tp} \quad (4\text{-}20)$$

where k_{st4} is the water column TP settling rate (d^{-1}); k_{rs4} is the soil TP release rate (d^{-1}); k_{rc4} is the macrophyte TP recycle rate (d^{-1}); k_{up_mf4} is the macrophyte foliage TP uptake rate (d^{-1}); k_{b4} is the macrophyte TP burial rate (d^{-1}); k_{up_mr4} is the macrophyte root TP uptake rate (d^{-1}).

Model 5

At this complexity, periphyton TP was employed as an additional component than that of Model 4. As in the case of macrophyte TP, a linear (first-order) expression was used to all governing processes of periphyton TP variable. TP uptake by periphyton was assumed to be the proportional with water column TP concentrations. In order to increase the mechanistic relevance, it was presumed that TP losses from macrophyte and periphyton primarily occur during senescence and decay; therefore, TP loss from these components was represented by first-order decay rate constants. Also, it was presumed that a fraction of both macrophyte and periphyton TP loss was recycled back into the water column, while the remaining TP fraction was buried and assimilated with soil TP. This complexity consists of 4 state variables, 9 processes, and 9 calibration parameters.

$$\frac{dC_{tp}}{dt} = -k_{st5}C_{tp} + \frac{k_{rs5}}{z_d\theta_{wc}}S_{tp} + \frac{k_{d\_m5}\alpha M_{tp}}{z_d\theta_{wc}} + \frac{k_{d\_p5}\beta P_{tp}}{z_d\theta_{wc}} - k_{up\_mf5}C_{tp} - k_{up\_p5}C_{tp} \quad (4\text{-}21)$$

$$\frac{dM_{tp}}{dt} = k_{up\_mf5}C_{tp}z_d\theta_{wc} - k_{d\_m5}M_{tp} + k_{up\_mr5}S_{tp} \quad (4\text{-}22)$$

$$\frac{dP_{tp}}{dt} = k_{up\_p5}C_{tp}z_d\theta_{wc} - k_{d\_p5}P_{tp} \quad (4\text{-}23)$$

$$\frac{dS_{tp}}{dt} = k_{st5}z_d\theta_{wc}C_{tp} - k_{rs5}S_{tp} + k_{d\_m5}M_{tp}(1-\alpha) + k_{d\_p5}P_{tp}(1-\beta) - k_{up\_mr5}S_{tp} \quad (4\text{-}24)$$

where P_{tp} denotes the periphyton TP storage per unit area (g m^{-2}); k_{d_m5} and k_{d_p5} are the TP decay rate resulting from senescence and root respiration of macrophyte and periphyton (d^{-1}); k_{st5} is the settling rate constant of water column TP (d^{-1}); k_{rs5} is the release rate of soil TP (d^{-1}); α and β are the fraction of macrophyte and periphyton TP recycled back to the water column, respectively.

Model 6

The model complexity was further increased by adding parameters in some specific processes, such as linking vegetation TP uptake (both macrophyte and periphyton) to the growth dynamics by considering the influence of TP concentrations in the water column. Theoretically, the vegetation growth can be a function of its own density, with sub-maximal rates achieved under limiting conditions. STA-1W was reported as a phosphorus-limited system (Pietro et al., 2006b, Chimney et al., 2000). Therefore, we simulated vegetation TP based on the vegetation growth dynamics using Michaelis-Menton type kinetics (Equation 4-25), i.e., that the demand for phosphorus would reach a maximum growth rate at phosphorus concentration that saturated all cellular transport sites (Darley, 1982), which is conceptually reasonable. It was presumed that the macrophyte and periphyton senesced/decayed according to the first-

order reaction; hence, the TP in these vegetation types also decayed as the first-order reaction. Macrophyte and periphyton TP were recycled back (turnover) to the water column as second-order kinetics. The settling of stabile residual phosphorus accounted for between 15-25% of the TP removal in Cell 4 (DBEL, 2002), and was implicitly modeled using a second-order settling rate constant. Similarly, release of phosphorus from the soil sediment store is mobilized back to the water column, and was assumed to be linearly proportional to the soil TP storage. This complexity consists of 4 state variables, 9 kinetic processes, and 11 calibration parameters.

The TP dynamics in the water column (C_{tp}), macrophytes (M_{tp}), periphyton (P_{tp}), and soil (S_{tp}) can be expressed as:

$$\frac{dC_{tp}}{dt} = -k_{st6}C_{tp}^2 + \frac{k_{rs6}}{z_d\theta_{wc}}S_{tp} + \frac{k_{rec\_m6}M_{tp}^2}{z_d\theta_{wc}} + \frac{k_{rec\_p6}P_{tp}^2}{z_d\theta_{wc}} - r_m\left(\frac{C_{tp}}{C_{tp}+k_{c\_m}}\right)\frac{M_{tp}}{z_d\theta_{wc}} - r_p\left(\frac{C_{tp}}{C_{tp}+k_{c\_p}}\right)\frac{P_{tp}}{z_d\theta_{wc}} \quad (4\text{-}25)$$

$$\frac{dM_{tp}}{dt} = r_m\left(\frac{C_{tp}}{C_{tp}+k_{c\_m}}\right)\frac{M_{tp}}{z_d\theta_{wc}} - k_{b\_m6}M_{tp} - k_{rec\_m6}M_{tp}^2 + k_{up\_mr6}S_{tp} \quad (4\text{-}26)$$

$$\frac{dP_{tp}}{dt} = r_p\left(\frac{C_{tp}}{C_{tp}+k_{c\_p}}\right)\frac{P_{tp}}{z_d\theta_{wc}} - k_{b\_p6}P_{tp} - k_{rec\_p6}P_{tp}^2 \quad (4\text{-}27)$$

$$\frac{dS_{tp}}{dt} = k_{st6}z_d\theta_{wc}C_{tp} - k_{rs6}S_{tp} + k_{b\_m6}M_{tp} + k_{b\_p6}P_{tp} - k_{up\_mr6}S_{tp} \quad (4\text{-}28)$$

where r_m, and r_p are the intrinsic growth rate of macrophyte and periphyton (d^{-1}), respectively; k_{c_m}, and k_{c_p} are the half-saturation constants for phosphorus-limitation on macrophyte and periphyton phosphorus uptake (µg L^{-1}); k_{st6} is the second-order settling rate constant of water column TP (m^3 g^{-1} d^{-1}); k_{rs6} is the release rate of soil TP (d^{-1});

k_{rec_m6}, and k_{rec_p6} are the second-order recycle rate constants of macrophyte and periphyton TP (m^2 g^{-1} d^{-1}), respectively; k_{b_m6}, and k_{b_p6} are first-order decay rate constants of macrophyte and periphyton TP (d^{-1}), respectively; and k_{up_mr6} is the first-order macrophyte root TP uptake (d^{-1}).

Model Setup

The computational domain of Cell 4 was discretized by unstructured triangular elements (average area: 5,100 m^2) with 192 nodes, generated in Groundwater Modeling System (GMS) V6.0. To ensure the numerical stability of the models, a 10-minute time-step was chosen for all simulations (hydrologic, transport and cycling). Detailed information about setup, calibration, and validation of 2-D hydrodynamic model of Cell 4, which was coupled with all candidate phosphorus biogeochemical models, can be found in Paudel et al. (2010).

All biogeochemical models were forced by weekly auto-sampled composite (time-averaged) TP concentrations, monitored at inlet hydraulic structures (G-254B, G-254D; Figure 4-4). TP inflow concentrations were specified as a source/sink boundary condition. In each simulation, the initial water column TP concentration of 40 µg L^{-1} was specified as a spatially constant value throughout the model domain, which was the average measured value from two sampling locations (ENR401 and ENR402) at the beginning date of simulation. A spatially distributed soil TP level for the upper 10 cm soil layer was used to initialize the model, which was based on sampling conducted by SFWMD throughout the STA-1W on 20 January 1995. Four sampling stations (4-2E, 4-2W, 4-1W, and 4-1E; see locations in Figure 4-2) were within Cell 4. Soil TP in the upper 10 cm soil layer for Cell 4 was estimated from these data (Paudel et al., 2010). Peat accretion was monitored from mid-1995 to mid-1999 using feldspar horizon

markers throughout the STA-1W (Chimney et al., 2000). Soil TP measured in samples collected at 4-1E and 4-2W on November 12, 1998 and October 20, 1999 were compared to model simulated soil TP levels. A spatially constant wet deposition of TP, 10 μg L^{-1}, was applied over the entire domain. Macrophyte and periphyton TP profiles were not available; however, initial value of macrophyte TP was based on the study conducted by DB Environmental Inc. (DBEL, 2004) at outlet zone of Cell 4, where *Najas*- and *Ceratophyllum* vegetation species were dominant. These vegetation species were considered the representative SAV biomass for the entire Cell 4 (DBEL, 2000; Dierberg et al., 2005) and dominated for the most of the simulation periods. Simulated profiles of macrophyte and periphyton TP were maintained close to a dynamic equilibrium condition during calibration.

In all model structures, phosphorus cycling processes were characterized by linear/non-linear kinetics in ordinary differential equations, and these equations were solved by fourth-order Runge-Kutta numerical integration method. Initial values of kinetic rate constants and other parameters in most pathways were based on the previous models of STAs, available knowledge, and literature of similar type of treatment wetlands. Final values of parameters were determined through model calibration (Table 4-3). As spatial phosphorus biogeochemical data were limited, parameters were specified as spatially constant values throughout the model domain. This consideration facilitated the consistency in comparing model performance across all levels of model complexity.

Calibration and Validation

Calibration includes adjusting unconstrained parameters that is aimed to produce an adequate fit between model results and field observations (Robson et al., 2008).

Frequently, goodness-of-fit and/or error metrics are used to statistically evaluate the misfit between model results and measured data. In practice, mechanistic biogeochemical model parameters are generally calibrated by trial and error (Robson et al., 2008). The level of expertise (understanding about the system dynamics, model structures and field data) of a modeler often dictates ability to produce best fit with near optimal parameters. Here, we adopted a trial and error approach to calibrate the model by adjusting individual parameters within literature ranges because spatially explicit models, as in our case, are computationally intensive and prohibited the use of formal calibration techniques. The long-term measurements of TP concentrations over four-year period (1/10/1995–12/31/1998) at the wetland outlet hydraulic structure (G-256) was primarily used for the model calibration exercise. In addition, spatial soil/sediment TP over five-year period (1995–1999) at two monitoring sites (4-1E and 4-2W), were used to optimize the model parameters. Calibration runs were continuously performed until the optimal or near optimal fit was obtained, with lowest statistical metrics (MSE) of each variable for which observations were available. Similarly, all models were validated against unassimilated field data of outlet TP concentrations for approximately three-year period (1/1/1999–10/31/2001). We re-initialized the model inputs and performed simulations without any modifications in the calibrated parameters during the validation.

Results

Predictive Performance of Biogeochemical Models

The simulated and measured outflow TP time series in Cell 4 during the model calibration and validation are presented in Figure 4-5. During the validation period, the model predicted TP concentrations were off in time from the measured TP, particularly on two instances of peak concentrations (Figure 4-5). The possible reason could be the

existence of unknown mechanisms or operations that helped reduce the peak inflow TP concentrations during those instantaneous events. Nevertheless, the model was able to reproduce the outlet TP concentration profiles except few discrepancies (Figure 4-5). Several sources of errors might have influenced these simulated results that inhibited the better fit, such as limited field data, uncertainties in observations, mesh resolution, and computational constraints. The most complex model that represents greatest modeling cost and effort (i.e., Model 6) resulted relatively lower misfit error (MSE = 90) than other competing models. Conversely, the simplest model (i.e., Model 1) yielded the highest misfit error (MSE = 142).This is primarily because the simplest model structure was not capable of incorporating adequate mechanisms to reproduce the key features of the outlet TP concentration profile. However, the introduction of the soil TP as a state variable including release of soil TP, greatly improved the model performance (Table 4-2). The gain in *DAI* by adding periphyton TP component in Model 5, however, is clearly much less pronounced comparing to the gain in *DAI* by adding soil and macrophyte TP components in Model 2 and Model 3, respectively.

In addition, we compared simulated soil TP profile to the available field data. Both outlet TP and soil TP data set were used simultaneously to constrain the model parameters. Optimized model parameters are depicted in Table 4-3. Soil TP data at two locations within Cell 4 (4-1E, and 4-2W) for three sampling events (1/20/1995, 11/12/1998, and 10/20/1999) were used for the calibration. Results show that all models successfully reproduced the spatio-temporal variation in soil TP over a five-year period (Figure 4-6). Although the short-term variability in outlet TP profile was not fully captured, a good prediction of the integral effects of TP accumulation in the soil was

found, which illustrates that models also corresponded well to the overall trend of outlet TP profile. As the level of details in the model increased, there was a slight improvement in the model fit against the data from 4-1E station; however, the improvement was less pronounced for the 4-2W station (Figure 4-6).

In order to evaluate the predictive accuracy performance of the calibrated models, all model simulations were extended for about three-year period (1/1/1999–10/15/2001). Simulated outlet TP concentration profiles were compared against observations; similar trends have been observed, as in the case of the calibration (Figure 4-5). The misfit error was the highest for the Model 1 (MSE = 474) and lowest for the Model 6 (MSE = 140). As the complexity level was further increased, *PAI* increased rapidly at the beginning (low complexity level); whereas the *PAI* increased monotonically at the end (high complexity level), with a diminished rate of improvement in the performance (Table 4-2). These results highlight that the influence of increasing level of complexity on the predictive accuracy is significant at lower level of complexity spectrum.

Results showed that there was a variable influence of phosphorus biogeochemical model structures on the accuracy for both outlet TP concentrations and soil TP level; every free parameter did not contribute equally to the ability of the model to fit the observations, as indicated by the varying rate of improvement in *DAI* over *CI* (*ΔDAI/ΔCI*), and *PAI* over *CI* (*ΔPAI/ΔCI*) (Table 4-2). As model complexity was further increased, a diminished rate of improvement in the performance was found (Figure 4-7).

The overall model performance was evaluated in terms of *MPI*, that combines both calibration and validation performances for all state variables for which observations were available. Results revealed that the overall performance was rapidly gained from

Model 1 to Model 2, as shown by steep *MPI* curve (Figure 4-8). The curve appeared to flatten, most notably from Model 5 to Model 6; this indicates that the increasing the level of details in the model at this complexity level was not best supported by the available field data. Figure 4-8 shows the plot of coefficient of effectiveness as a function of modeling cost and efforts (i.e., model complexity). Results revealed that the model effectiveness (y-axis) followed a 'right skewed hump' curve in relation to the modeling cost and efforts (x-axis) (Figure 4-8) with highest effectiveness scores with Model 4. It is interesting to note that the maximum effectiveness was not with the most complex model (Model 6).

Akaike's Information Criteria

As a further evaluation of model complexity, a multi-model selection technique, AIC_c, which accounts the trade-off between goodness-of-fit and complexity, was used to rank the set of phosphorus biogeochemical models. The inflection point of AIC_c was identified at intermediate complexity, as indicated by the minimum value with Model 4 (AIC_c = 1353). AIC_c decreased from Model 1 through Model 4, but it increased again from Model 4 through Model 6 (Table 4-2). Due to the large number of parameters and uncertainties in the structure and components in the complex model, the miss-fit error due to variance outweighed the miss-fit error due to bias; hence, the AIC_c increased again. Although Model 6 represents the more physical phenomena, Model 4 yielded the best model, given data and the models considered. Using AIC_c needs common data set to fit all competing models (Burnham and Anderson, 2002). As time-series field data were not available for other variables (e.g., macrophyte and periphyton TP), and with a very limited soil TP data, we only considered the univariate case. The univariate AIC_c result does not apply to the multivariate setting (Burnham and Anderson, 2002;

McDonald and Urban, 2010). Therefore, it should be noted that the consideration in multivariate setting could result differently.

Discussion

Influence of Complexity Level (Modeling Cost and Effort) on Model Performance

Simulation results of six mechanistic phosphorus biogeochemical models of a stormwater treatment wetland showed a better performance in a sequence, as the level of detail (modeling cost and efforts) increased in the model. This implies that adding each physical process in the model (assumed that they are added in the order of relevance) contributed to the performance. The highest accuracy was observed when soil TP was added as a state variable from Model 1 to Model 2, which illustrates that adding an additional component in Model 1 plays a critical role in representing biogeochemical transformations in the wetland. Although a model performance was achieved in a sequence with increasing levels of model complexity, the rate of improvement in the performance differed significantly across the complexity spectrum (Figure 4-7). Increasing the last few levels of complexity caused a small improvement in the performance. Accuracy improvement rate consistently decreased as the complexity was further increased. These results indicate that complex models were not best supported by the available field data in response to each additional component and unconstrained parameters (Friedrichs et al., 2006). However, at this point, it is unclear that at what point the model would end up being poorer in the performance than a simple one as further complexity is added. Still, the most complex model (Model 6) does not explicitly account the short-term phosphorus removal processes, such as sorption by variety of substrates, and chemical precipitation. Further adding the model complexity by incorporating phosphorus speciation (PP, SRP, DOP) as a state variable

and associated cycling processes, and considering the flocculent detrital organic matter layer (floc-layer) as a separate compartment could have provided much better analyses about the suitability of the model. However, due to lack of field measured data, and limited resources, this study did not consider the complexity levels further than the Model 6.

Model Effectiveness

Quantitatively assessing the elements of model complexity is not straightforward, and often involves subjectivity (Friedrichs et al., 2006). Nevertheless, we attempted to objectively evaluate key model elements that are relevant and critical for the evaluation of effectiveness among wetland phosphorus biogeochemical models. The effectiveness scores were generated as a function of four elements: (a) how much cost and effort was invested to develop each model; (b) how well each model described the existing field data (descriptive adequacy); (c) how well each model simulated the features outside the calibration boundaries (predictive adequacy); and (d) how much knowledge/information each model provided about underlying phenomena. Results showed an interesting pattern of effectiveness in relation to the modeling cost and effort, as indicated by a 'humped' curvilinear relationship. This indicates that there exists an optimal level of model complexity corresponding to the maximum effectiveness (Figure 4-9). More interestingly, Model 6 (the most complex model) was not the "effective" model to simulate TP dynamics in Cell 4; even though it produced the best field observations with highest accuracy. It should be noted that the interpretation was solely dependent on the set of models under consideration and the perspective of the model effectiveness, as defined previously.

Reconciling the trade-offs in the level of model complexity is still a significant challenge in mechanistic biogeochemical modeling (Min et al., 2011). There is an ongoing debate about the appropriate level of model complexity in simulating the TP behavior in wetlands. Some researchers advocate simple models (low-level mechanistic detail in the model description) as practical tools (Raghunathan et al., 2001; Walker and Kadlec, 2005; Kadlec and Wallace, 2008), with the notion that, no simulation models of natural systems will replicate the complexity of the nature and be able to explain the underlying phenomenon (Reckhow, 1999). They argue that significant uncertainties can be introduced in estimating a large number of model parameters. Conversely, other researchers highlight the need of using relatively complex mechanistic models that have robust theoretical basis and are able to mimic the complexities of wetland ecosystems (Fitz et al., 2004; Min, 2007; Jawitz et al., 2008). Oreskes (2000) presented the view of using a complex model:

> increased complexity in models is often interpreted as evidence of closer approximation to reality.

However Janssen (1998) presented the opposite view of model complexity as:

> a model should be made no more complex than can be supported by the available brains, computers and data.

As environmental systems are inherently complex and given that no models can explain their complexities, as in the case of treatment wetlands, the choice of an appropriate level of complexity is often not clear. The critical question is how complex of a model is needed to simulate the behavior of these systems. In wetland modeling, the best-fit models are often regarded as the most robust and appropriate models, assuming that these models potentially replicate the system behaviors more accurately. This perspective likely claims the Model 6 is the most suitable model to simulate TP

dynamics because of its higher accuracy. Note that the appropriate model is not just a function of accuracy. It can be related with several other factors, such as model developing process, definitions, available resources, and data. In some cases, a poorly performed model can still adhere to the principles of a good model, and may be sufficient to address modeling questions (Haraldsson and Sverdrup, 2004). For the meaningful evaluation of a set of models under similar circumstances, one should not only account the goodness-of-fit. Generally, a complex model is expected to be more accurate (Brooks and Tobias, 1996); but, the modeling requires additional resources and becomes expensive. Although comparison of modeling cost and effort among the set of models is a difficult task, an approximate relationship can be assessed to make a choice of an effective model.

Here, we have argued that we need to include explanatory depth, a property of a model complexity while evaluating the model effectiveness. More than two decades of research have provided the strong evidence that the structure of wetland ecosystem involves large biogeochemical complexities, with various components and links, as in the case of other types of complex systems (Hannah et al., 2010). If the objective of the model is to provide an understanding about the system dynamics, a simple model may not be effective because it cannot address complex functionalities of a treatment wetland. For example, Model 6 is capable of modeling the dynamics of four variables, such as TP at macrophyte, periphyton, soil, and the water column, whereas Model 1 can only model a single variable (water column TP). Simplicity in the model inhibits the general application of a model in many respects. It is suggested that a holistic approach

that measures the key properties of model complexity and model performance is critical to evaluate the model effectiveness while satisfying the modeling goal.

The principle of parsimony (sometimes referred to as Occam's razor) provides a philosophical basis for selecting the appropriate model complexity. This criterion has been frequently used as a basic guiding principle to select a suitable model, particularly in ecological studies (Burnham and Anderson, 2001). Based on this principle, the most effective model for a given condition uses as few as possible unspecified parameters to describe the model outcomes of interest with reasonable accuracy, so that the model is not overly parameterized (Haws et al., 2006). As Haws et al. (2006) pointed that the use of parsimonious model will minimize the likelihood of non-uniqueness in parameters (no particular parameter combination that represents the solution), and increase the likelihood of parameter values that can explain the reality of the system dynamics more appropriately. In this study, Model 4 was found the most parsimonious model, based on the AIC_c. This finding is consistent with the model effectiveness scores (Table 4-2). As AIC_c only accounts the goodness-of-fit and the complexity (as reflected by the number of estimated parameters), Model 4 compromised the accuracy with the model complexity; that means the Model 4 was best supported by the calibration data with least possible number of parameters. In a statistical sense, Model 4 balanced the bias (goodness-of-fit) and variance (uncertainties in estimated parameters) of the misfit error. Model 5 and Model 6 were penalized for the inclusion of the additional parameters in relation to the accuracy. Although both approaches identified the same model (Model 4) as one of the best models, AIC_c technique may not be adequate if the modeling goal is

to provide understanding about the system dynamics because it does not account for the explanatory depth which may limit the scope in wetland biogeochemical modeling.

While we rigorously evaluated the important properties of model complexity and performance of a set of phosphorus biogeochemical models of Cell 4, there are still other attributes not included in this study, such as quality and availability of field/laboratory data, uncertainties in model parameters, plausibility, understandability, modeling goal, available resources, and the ability and experience of a modeler. Total objectivity in all these model attributes is a mere illusion. As noted by Pitt and Myung (2002):

> objectively comparing competing models is no easier or less subjective than choosing between competing theories.

Hence, the approach used here should be viewed as a tool to deepen the understanding about the assessment of wetland models under consideration.

In future, other wetland phosphorus cycling models can be employed into this setting and evaluate the model effectiveness. For example, the phosphorus cycling algorithm of the DMSTA model (a widely used model in STAs) can be incorporated into the existing setting and compare with models of this study. However, different models developed in a different setting cannot be fitted into this analysis.

Caveats and Future Directions for Stormwater Treatment Areas Phosphorus Biogeochemical Modeling

Phosphorus biogeochemical cycling in a treatment wetland is primarily governed by complex mechanisms and feedbacks (Kadlec and Wallace, 2008); therefore, models of these systems need to describe numerous interconnected components and links between broad characteristics of sciences: hydrological, biological, and geochemical. Constructing or selecting an effective phosphorus biogeochemical model of the STAs is

typically a difficult undertaking. An important question is what level of complexity is justified to provide a reasonable representation of an ecosystem structure and address the modeling questions? To address this question, first, we need to have a clear modeling goal, for example, whether the model is intended to use as a management or a scientific research tool? Often, a modeling question or the issue under investigation defines the level of details in the model (Haraldsson and Sverdrup, 2004). For example, what specific area has higher accumulated soil TP than a threshold level in order to classify the potential cattail expansion zones? Or, how long does it take to achieve a certain level of outlet TP concentration, such as 10 ppb? Or, how do topographic features (e.g., channels/ditches, mounds), changes in vegetation pattern, and other structural modifications affect the flow and phosphorus dynamics?

To address above mentioned questions, different type of models may be suitable depending on the definition of a problem and the type of desired answers for given data sets. If the models were intended to use for the design purpose, a simple empirical model, such as the STA design model (Walker, 1995) would satisfy the modeling needs. Choosing such a simple model entails relatively low modeling cost and effort. The widely used STA model (DMSTA2; Walker and Kadlec, 2005) may serve as a hands-on tool in predicting TP concentrations at the outlet hydraulic structure, and evaluating the wetland performance The computational cost of DMSTA2 is low compared to the distributed model (Paudel et al., 2010). However, the model is limited in representing the location of hydraulic structures, and variable topography. If the model was intended to use as a scientific research tool or address a broad aspect of problems, a relatively complex model, such as ecosystem model (ELM; Fitz and Trimble, 2006), or detailed

phosphorus speciation model (STA-5, Northern Flow-Way; Min, 2007), or an integrated water quality model (STA-1W; HydroQual, 1997; Meyers and Fitzpatrick, 2001) could serve the greater applicability.

In a different facet, if the modeling questions are related to the spatial characteristics (e.g., changes in vegetation pattern, cattail expansion area), a spatially distributed model may provide greater utility because such model can represent and predict local variability within the wetland. In this situation, either a simple biogeochemical model in a spatially-explicit domain (e.g., Raghunathan et al., 2001; Paudel et al., 2010), or a complex biogeochemical model in a spatially-simplified domain (Meyers and Fitzpatrick, 2001) can be developed. The choice of one over another primarily depends on the modeling questions and availability of measured data. If the modeling questions were to explore detailed aspects of phosphorus biogeochemical transport, and transformation in various components/links, then the model with high-dimensioned kinetic structures can be more effective (Meyers and Fitzpatrick, 2001). Simple models are less flexible during calibration (Snowling and Krammer, 2001). In Model 2, for example, vegetation TP cycling processes were implicitly aggregated together into first-order uptake and release mechanisms between soil and the water column. This assumption prohibited the application of Model 2 in simulating any aspects of vegetation TP dynamics. If our interest were to predict or understand the dynamics of TP in vegetation, we certainly need the complex model structure that can explicitly simulate vegetation TP as a state variable (e.g., Model 5 and Model 6).

Building a simulation model of a complex and dynamic environmental system is a long process if the models are required to answer many questions (Haraldsson and Sverdrup, 2004). In such a case, developing a sub-model for each question (or a group of questions), and coupling those individual sub-models into an 'integrated' model can be the best approach (Meyers and Fitzpatrick, 2001). Within each model or a sub-model, connections between components and parts can be described either by empirically or mechanistically (Reckhow and Chapra, 1999). Min et al. (2011) suggested a 'hybrid type model', a model structure, in which some elements are empirically aggregated and others are mechanistically described. This is reasonable because it is often difficult to obtain field data to describe many individual processes. Thus, processes those are not supported by the field measured data processes may be aggregated together and simulated as a combined mechanism (Reckhow and Chapra, 1999; Robson et al., 2008). However, appropriate degrees of process aggregation pose significant challenges in a complex and dynamic system (Fulton et al., 2003). A rigorous testing of a model with diverse combination of process aggregations would help identify the processes that can be grouped together without losing accuracy. One approach is to start from simplest model representations and test whether they produce observations reasonably (Min et al., 2011), and add additional components/links if the model still provides the desired accuracy and obtains adequate information, given the resources, data, and modeling questions. Such approaches help identify the potential convergence to an optimal level of model complexity, where the data are fully exploited with adequate information, as well as the model complexity is minimized (Schoups and Hopmans, 2006). Nevertheless, a great care must be exercised to identify the 'effective' level of

complexity. This analysis showed that the Model 4 was the most effective phosphorus cycling model that balances the benefit of adding complexity level with accuracy, and the explanatory depth.

Summary

A set of six phosphorus biogeochemical models with hierarchal level of process-complexity were constructed and tested against the long-term field measured data of a large-scale constructed treatment wetland, Cell 4 of STA-1W. All six models were coupled with a pre-calibrated hydrodynamic/transport model of Cell 4 (Paudel et al., 2010). Then, this study discussed the influence of the modeling cost and effort, or model complexity (as reflected by the number of process-specific parameters) on the performance and effectiveness of the model. We attempted to identify the most suitable model structure to simulate TP cycling processes in a treatment wetland, given the observations, scale, and wetland conditions.

Four key model evaluation criteria (modeling cost and effort, descriptive adequacy, predictive adequacy, and explanatory depth) were used to calculate the effectiveness index of each candidate model. All models were calibrated against the long-term TP concentration profile measured at the outlet hydraulic structure, and soil TP level at two locations, and subsequently validated against three-year outlet TP concentration profile. Simulation results were used to generate indices of descriptive and predictive adequacy. As the level of complexity in the model increased, an increased accuracy was observed; however, the rate of improvement was diminished. The model performance rapidly increased at the beginning of the complexity spectrum, but monotonically increased at the end. More interestingly, the maximum effectiveness was with the Model 4, which illustrates that the most complex model (Model 6) was not

necessarily the most ‘effective’ model to simulate the TP dynamics in STA-1W. Results of the Akaike’s Information Criterion also supported the evidence that the Model 4 was the most effective model among the set of models considered.

Further investigation of our current findings would help identify whether there is a limit (stopping point); so that the complex model would end up being poorer in performance than a simple one. A high-dimensioned phosphorus biogeochemical model structures (more complex than Model 6) would answer this question. However, at this point, this study was generally limited with field measured data, knowledge about the system and computer resources. Nevertheless, the findings of this study have remarkable implications to future modeling strategies either selecting or developing an appropriate mechanistic phosphorus biogeochemical model of a constructed treatment wetland. We believe that this study provides a promising approach for future model evaluation efforts and applications.

Table 4-1. Explanatory depth index (χ_m) of a set of candidate phosphorus cycling models.

Models	P_m†	Δ_P	χ_m
Model 1	11	0	0.00
Model 2	12	1	0.12
Model 3	14	3	0.15
Model 4	16	5	0.18
Model 5	19	8	0.25
Model 6	21	10	0.30

†P_m represents the total number of process-specific parameters in each model m.
χ_m increases exponentially as the number of process-specific parameters are increased.

Table 4.2. Mean squared error (*MSE*), descriptive accuracy index (*DAI*), predictive accuracy index (*PAI*), model performance index (*MPI*), explanatory depth index (χ_m), model effectiveness scores (φ_m), and AIC_c scores using outlet TP data for the calibration period (n=179). The best values of each factor are shown in bold. Modeling efforts and cost index, or model complexity index (CI_m) is equal to the number of optimized parameters. Minimum AIC_c represents the best balance between goodness-of-fit and uncertainty in estimating parameters.

Model	CI_m	Calibration (descriptive accuracy)						Validation (predictive accuracy)			*MPI*	χ_m	φ_m	AIC_c
		Outlet TP concentrations			Soil TP			Outlet TP concentrations						
		MSE (E_k)	$E_{I,k}$	DAI_k	MSE (E_k)	$E_{I,k}$	DAI_k	MSE (E_k)	$E_{I,k}$	PAI_k				
Model 1	11	142.0	1.00	0.00	0.00	0.00	0.00	474.0	1.00	0.00	0.00	0.00	0.00	1395
Model 2	12	107.0	0.75	0.25	3.78	1.00	0.00	241.0	0.51	0.49	0.55	0.12	3.34	1370
Model 3	14	99.0	0.69	0.30	2.90	0.77	0.23	190.0	0.40	0.60	0.73	0.15	3.78	1360
Model 4	16	92.0	0.65	0.35	2.48	0.66	0.34	159.0	0.34	0.66	0.84	0.18	**3.79**	**1353**
Model 5	19	91.0	0.64	0.36	2.11	0.56	0.44	141.0	0.30	0.70	0.90	0.25	3.48	1358
Model 6	21	90.0	0.63	0.37	1.94	0.51	0.49	140.0	0.29	0.71	**0.92**	0.30	3.25	1360

Results are based on the spatially distributed modeling framework.

Table 4-3. Parameters used in phosphorus cycling models in a spatially distributed modeling framework. The subscript at the end of each parameter corresponds to the level of complexity models (Model 1 through Model 6).

Parameter	Definition	Units	Value
k_{st1}	TP settling rate	d^{-1}	0.1425
k_{st2}	TP settling rate	d^{-1}	0.2678
k_{rs2}	TP release rate as a function of soil TP	d^{-1}	1.97×10^{-4}
k_{st3}	TP settling rate	d^{-1}	0.19
k_{rs3}	TP release rate as a function of soil TP	d^{-1}	1.97×10^{-4}
k_{up_mf3}	Macrophyte foliage TP uptake rate as a function of water column TP	d^{-1}	0.1
k_{b3}	Macrophyte TP burial rate	d^{-1}	2.70×10^{-3}
k_{st4}	TP settling rate	d^{-1}	0.22
k_{rs4}	TP release rate as a function of soil TP	d^{-1}	1.97×10^{-4}
k_{up_mf4}	Macrophyte foliage TP uptake rate as a function of water column TP	d^{-1}	0.21
k_{b4}	Macrophyte TP burial rate	d^{-1}	2.70×10^{-3}
k_{up_mr4}	Macrophyte root TP uptake rate as a function of soil TP	d^{-1}	2.20×10^{-5}
k_{rc4}	Macrophyte TP recycle rate	d^{-1}	3.50×10^{-3}
k_{st5}	TP settling rate	d^{-1}	0.18
k_{rs5}	TP release rate as a function of soil TP	d^{-1}	1.97×10^{-4}
k_{up_mf5}	Macrophyte foliage TP uptake rate	d^{-1}	0.3
k_{up_p5}	Periphyton foliage TP uptake rate	d^{-1}	0.03
k_{up_mr5}	Macrophyte root TP uptake rate	d^{-1}	2.20×10^{-5}
k_{d_m5}	Decay rate of macrophyte TP	d^{-1}	9.00×10^{-3}
k_{d_p5}	Decay rate of periphyton TP	d^{-1}	0.01
α	Recycled fraction of macrophyte TP	-	0.56
β	Recycled fraction of periphyton TP	-	0.50
k_{st6}	TP settling rate	$m^3\ mg^{-1}\ d^{-1}$	0.01036
k_{rs6}	TP release rate	d^{-1}	1.97×10^{-4}
r_m	Macrophyte intrinsic growth rate	d^{-1}	4.00×10^{-3}
r_p	Periphyton intrinsic growth rate	d^{-1}	7.00×10^{-3}
k_{c_m}	Half saturation constant for phosphorus as limiting nutrient in macrophyte growth	$g\ m^{-3}$	0.01
k_{c_p}	Half saturation constant for phosphorus as limiting nutrient in periphyton growth	$g\ m^{-3}$	0.015
k_{up_mr6}	Macrophyte root TP uptake	d^{-1}	2.20×10^{-5}
k_{b_m6}	Macrophyte TP burial rate	d^{-1}	2.70×10^{-3}
k_{b_p6}	Periphyton TP burial rate	d^{-1}	4.80×10^{-3}
k_{rec_m6}	Macrophyte TP recycle rate	$m^2\ g^{-1}\ d^{-1}$	3.11×10^{-3}
k_{rec_p6}	Periphyton TP recycle rate	$m^2\ g^{-1}\ d^{-1}$	3.45×10^{-3}

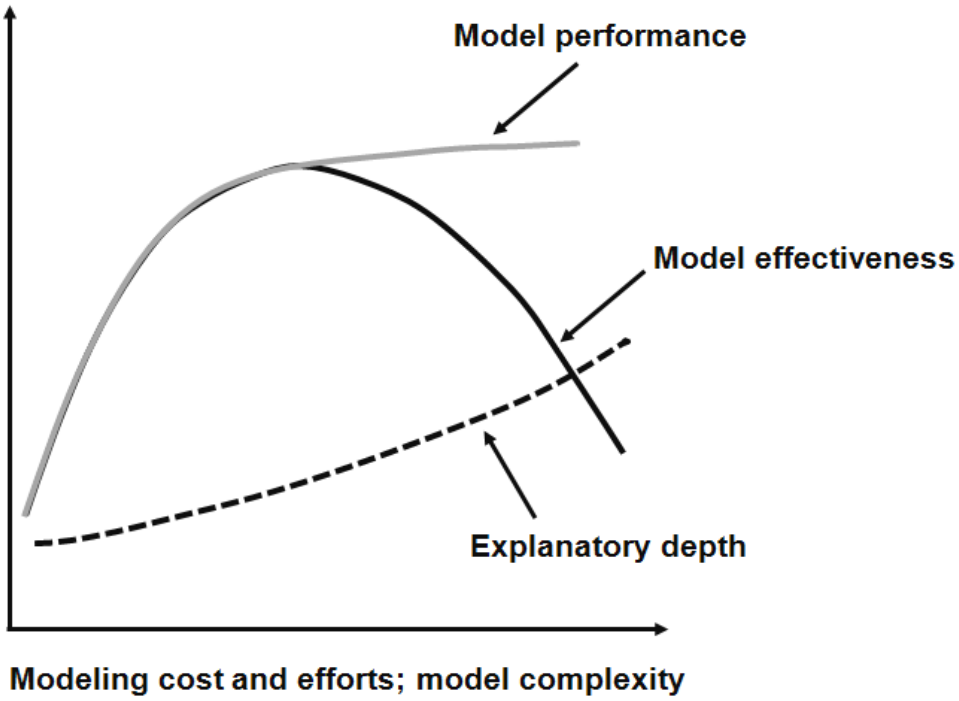

Figure 4-1. Conceptual schematization of relationship between model performance and explanatory depth as a function of modeling efforts and cost (i.e., model complexity). The model performance (light solid line) is the weighted value of descriptive and predictive accuracy, in which a larger value indicates a better performance. The model effectiveness (dark solid line) is the estimate of the maximum possible effectiveness as a function of modeling cost and efforts for the set of biogeochemical models. Explanatory depth curve (dashed line), which follows an exponential function.

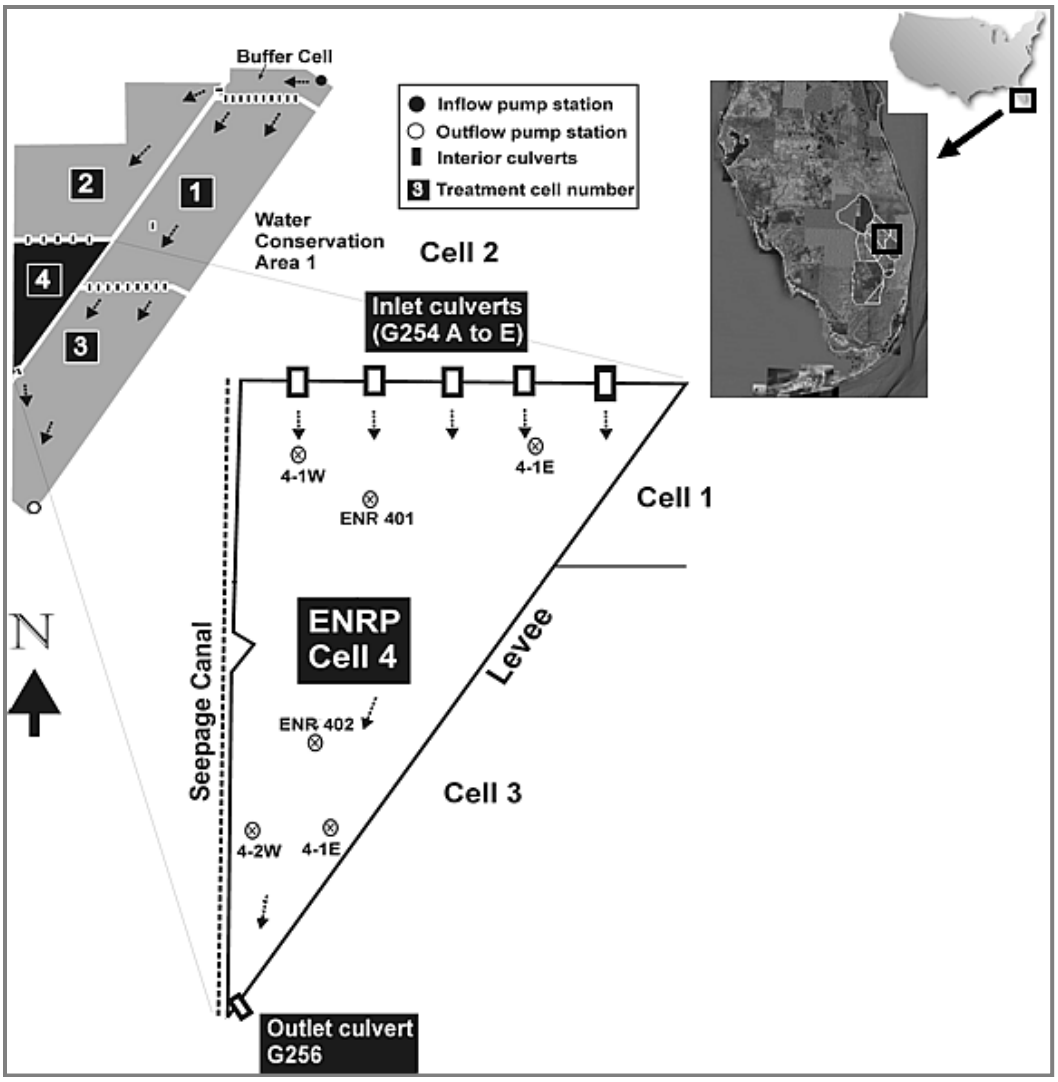

Figure 4-2. Location and plan view of study area, Cell 4 of Stormwater Treatment Area 1 West with inlet and outlet hydraulic structures (G-254 A to E, G-256), water level and soil TP monitoring sites.

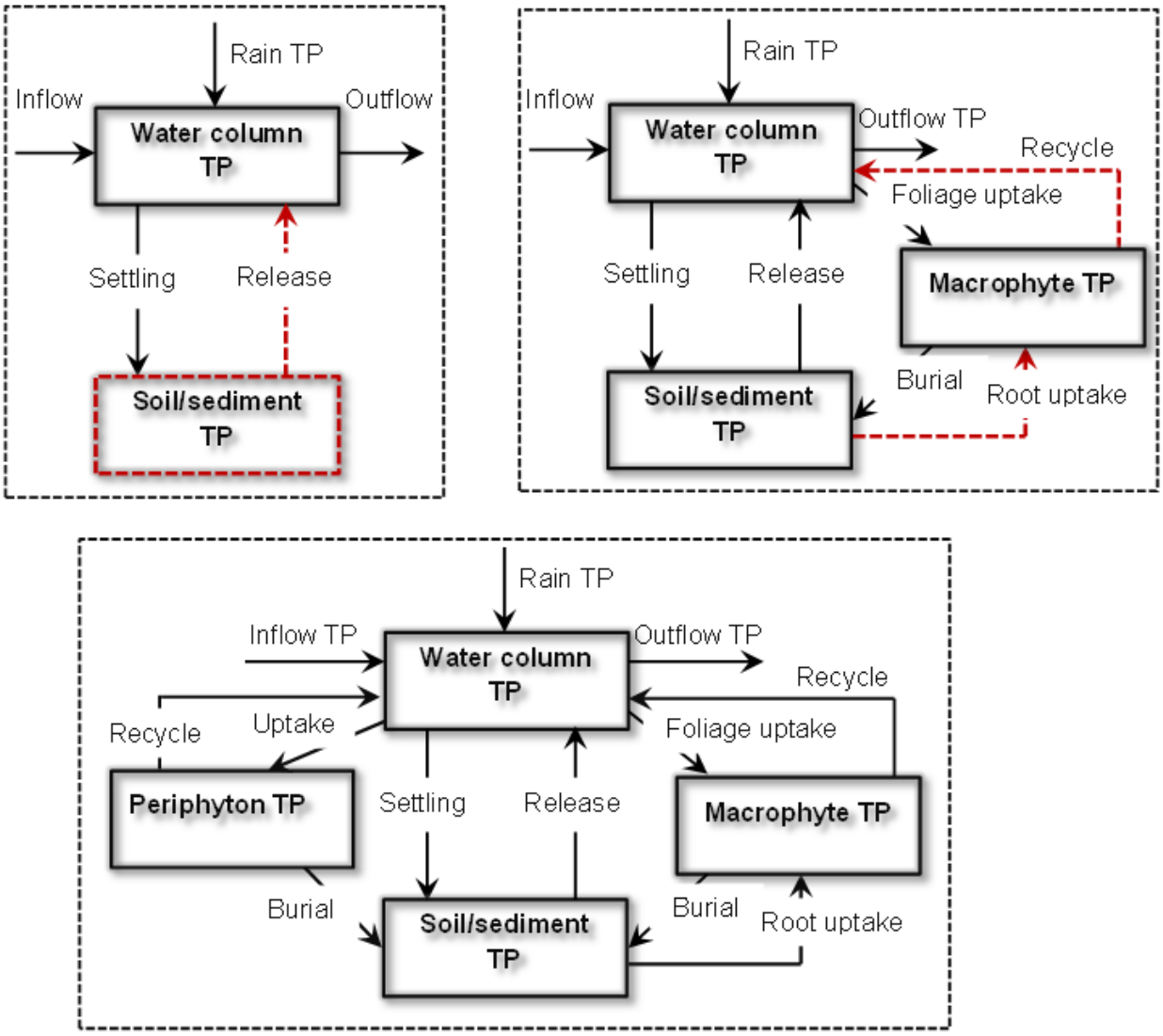

Figure 4-3. Conceptual process diagram for the candidate set of phosphorus biogeochemical models. Each rectangle represents the component (i.e., state variable), and the arrow represents the process. (a) Model 1 and Model 2: Model 1 considers only the water column TP component and settling (black rectangle and arrows), but Model 2 considers both water column and soil TP variables; (b) Model 3 and Model 4: Model 3 does not consider macrophyte TP recycle, and root uptake (shown in red lines) but Model 4 considers all components and processes shown in the figure; (c) Model 5 and Model 6: Both models have the same number of components; however, Model 6 simulates periphyton and macrophyte TP uptake with considering P-limited Monod transformation equation. Additional model parameters make Model 6 more complex than Model 5.

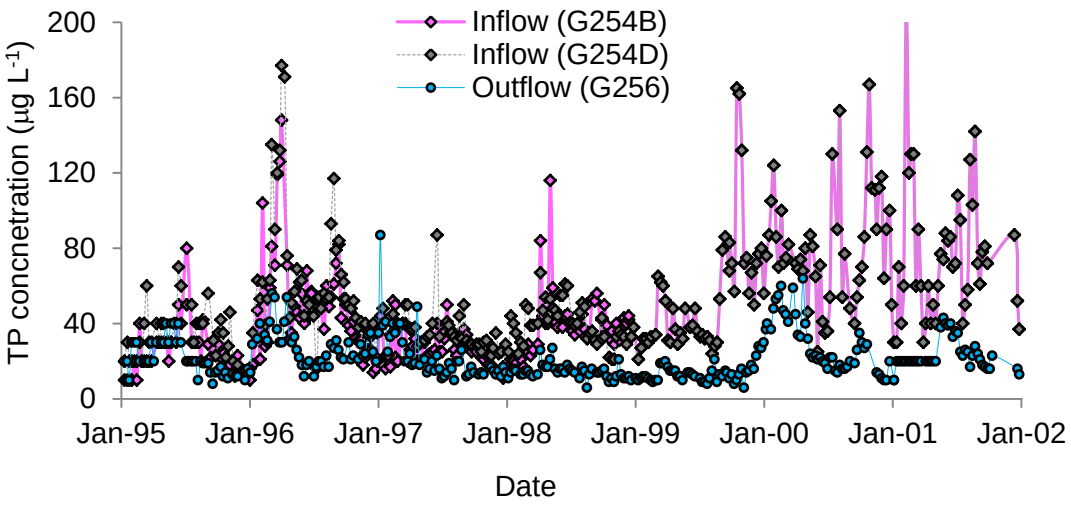

Figure 4-4. Inflow and outflow total phosphorus concentrations used in the model. Inflow TP data at G-254B structure were only available up to 12/15/1998; therefore data for the G-254D were used for all inflow hydraulic structures for the remaining period (12/16/1998 – 10/15/2001).

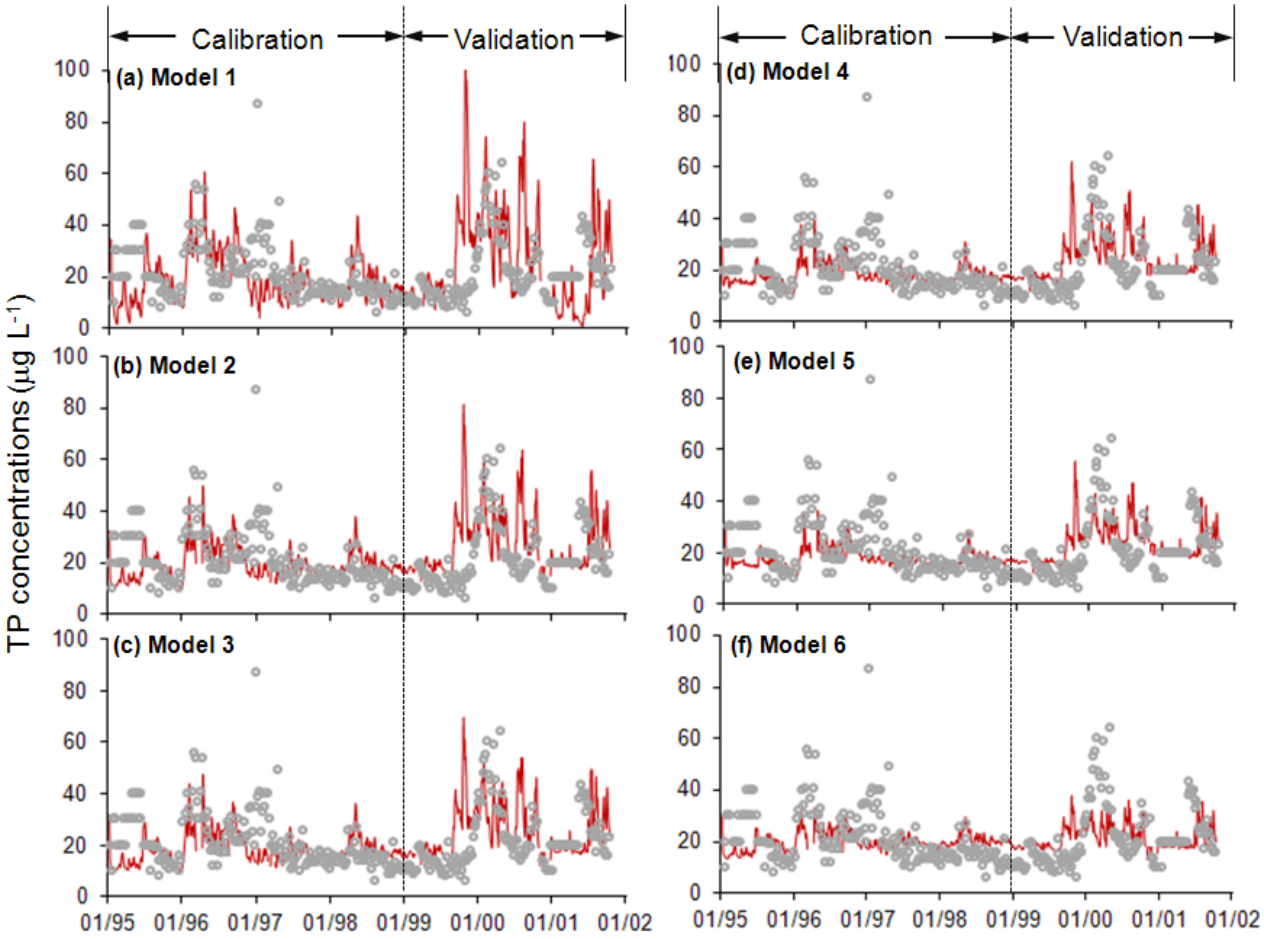

Figure 4-5. Observed (gray symbols) and modeled (red lines) for the outlet total phosphorus concentrations during calibration (1/10/1995 – 12/31/1998), and validation (1/1/1999 – 10/15/2001) periods.

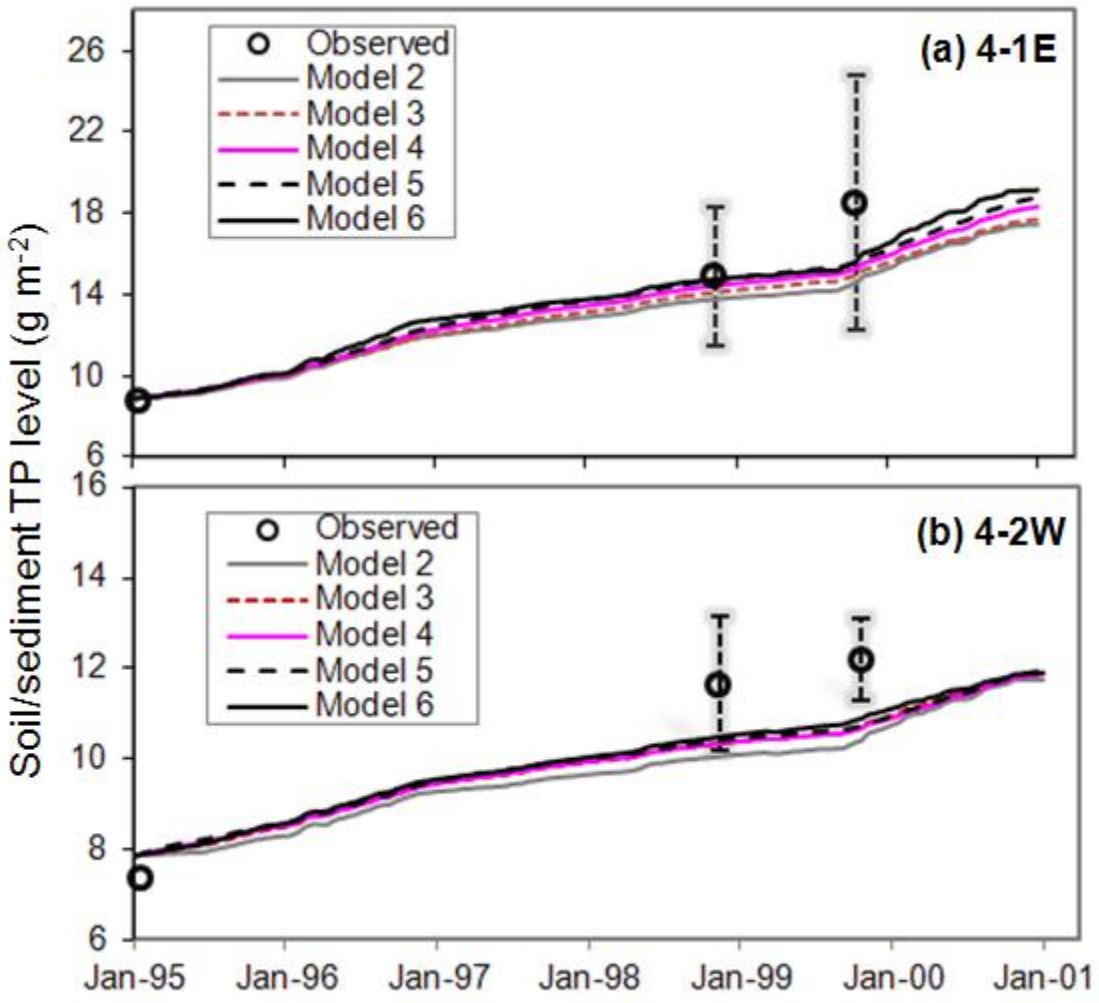

Figure 4-6. Simulated and observed soil total phosphorus content at two locations within Cell 4 for the upper 10 cm of the soil profile: (a) upstream area, 4-1E and (b) downstream area, 4-2W. Observed values are shown as Mean ± 1SD. Simulated results are derived from spatially distributed models.

(a)

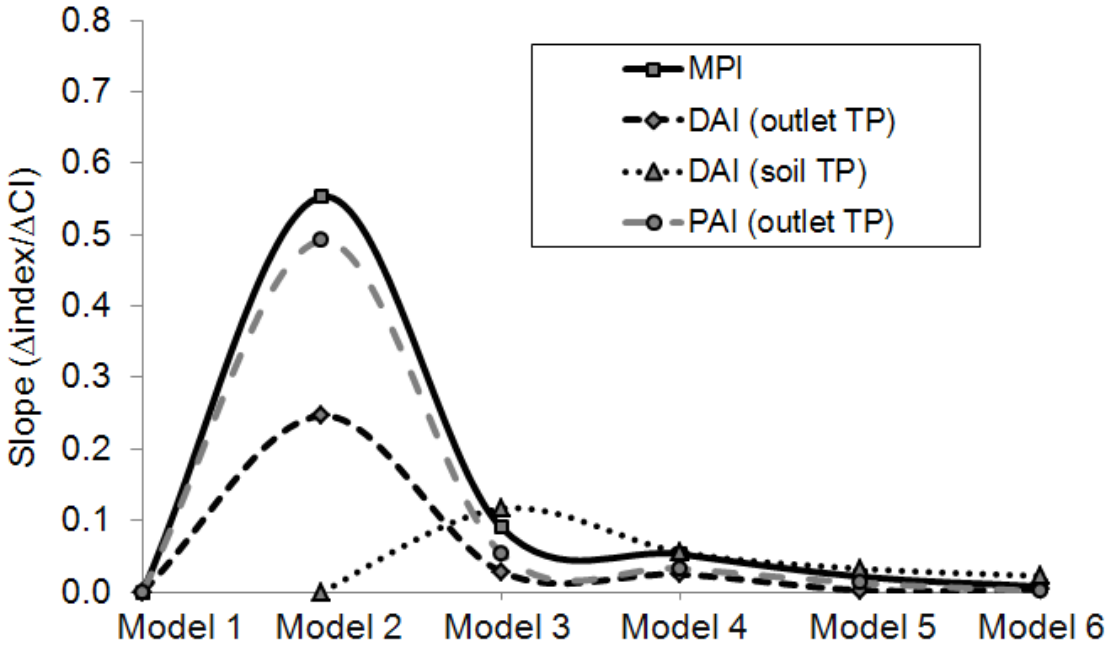

Figure 4-7. Slope of each model properties over modeling cost and efforts index (*CI*) for different variables. For example, slope of model performance (*MPI*) is the $\Delta MPI/\Delta CI$.

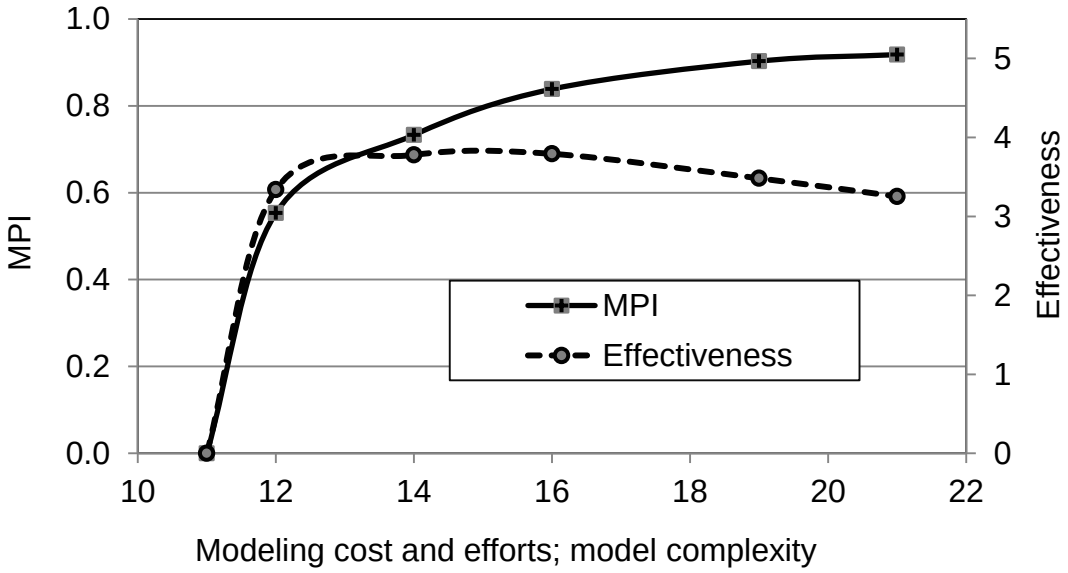

Figure 4-8. Model performance (left y-axis) and model effectiveness (right y-axis) as a function of modeling cost and efforts (model complexity) from six phosphorus biogeochemical models of Cell 4.

CHAPTER 5
MODELING SPATIAL FLOW DYNAMICS AND SOLUTE TRANSPORT PROCESSES IN A CELL-NETWORK TREATMENT WETLAND

In recent years, treatment wetlands have become an emerging technology to treat wastewaters from various sources, including municipal and industrial wastewater, stormwater, agricultural runoff, and other waste streams (Knight et al., 1994; ITRC, 2003; Kadlec and Wallace, 2008). While many treatment wetlands are of single treatment-cell structure (i.e., one hydraulic unit) others consist of multiple treatment cells connected by hydraulic structures, which is often referred to as a "cell-network wetland" (Wang and Jawitz, 2006). In a cell-network wetland, treatment cells are separated by earthen berms (i.e., levees) and connected by hydraulic structures to control quantity, timing and distribution of flows in upstream cells. Cell-network wetlands with multiple treatment cells offer a wide range of benefits over single treatment-cell wetland that have been discussed in Wang and Jawitz (2006).

Of all the factors that influence wetland characteristics, hydrology is considered to be the critical determinant of the establishment and maintenance of specific types of wetlands and wetland processes (Mitsch and Gosselink, 2000). Several studies have emphasized a need for an improved understanding of wetland hydrology as an important component for supporting a variety of management and research objectives (Kusler and Kentula, 1990; Kadlec and Wallace, 2008; Hughes et al., 1998). Water flow is the main pathways for pollutant transport, thus hydrodynamic factors, such as water depth, mean flow velocity and velocity variability (dispersion) are known to affect the ability of the wetland to treat pollutants. Generally, seasonal variability in hydrologic inputs as well as spatial variability in wetland characteristics makes it difficult to accurately describe the flow dynamics quantitatively (Wetzel, 1994). Also, the available

data are usually inadequate for dynamic wetland conditions (e.g., drying, flooding, relaxation after flooding) to get accurate results. In many cases, it is infeasible to obtain field data in a large spatio-temporal scale, and evaluate management alternatives (e.g., structural modification, vegetation pattern changes) physically at the field scale. Numerical models are therefore valuable tools that can be used to assess a variety of management options, and test hypotheses in evaluating the role of different wetland processes (Mitsch and Reeder, 1991).

Over the past several decades, hydrologic alteration and eutrophication resulting from phosphorus-rich stormwater runoff have been designated as major environmental issues in the Florida Everglades—a sensitive aquatic ecosystem (Chimney and Goforth, 2001). Agricultural development has led to an enriched phosphorus concentration in surface waters that enter into the wetlands of the greater Everglades, including Everglades National Park, resulting in an impaired water quality. To address this issue, South Florida Water Management District (SFWMD) built and operates six large-scale constructed treatment wetlands, known as Stormwater Treatment Areas (STAs), which are used to reduce phosphorus levels in surface runoff through physical, chemical and biological processes before entering the Everglades. STAs are typically composed of multiple treatment cells that are hydraulically connected through networked structures which allow sequencing of flows through various types of aquatic plants, and facilitate control of water depths and flow patterns within the treatment cell. Therefore, it is critical to integrate understanding of the coupled effects of hydrologic and biogeochemical processes in support of Everglades restoration. Models are valuable tools that can help

such integration of process behaviors, design of complex engineered systems, and assess a variety of management alternatives that are infeasible to physically test.

Previous STA Hydrodynamic Modeling Efforts

Hydraulic/hydrodynamic models developed to support design and management decision-making of south Florida treatment wetlands have recently expanded in scope and complexity. Existing models are widely varied in degree of complexity; most them are two-dimensional (2-D) models for steady-state flow conditions (Guardo and Tomasello, 1995; Burns and Mcdonnell, 2000; von Zweck et al., 2000; SFWMD, 2001; Piccone, 2003). Even though these models are quite useful for design and use as a diagnostic tool to facilitate interpretation of field-data, the utility is limited in the application for dynamic wetland conditions. Previous studies illustrated that STA flows exhibited unsteady flow patterns (Chimney et al., 2000; Nungesser and Chimney, 2006; Min and Wise, 2010), the reason could be the extensive control of inflows/outflows using gated culverts, pump stations, weirs and gated spillways; therefore the assumption of steady-state flow in these models is unrealistic. As an early effort to simulate spatial hydrodynamics in the STAs, Guardo and Tomasello (1995) applied the SHEET2D model to simulate hydraulic structures between treatment cells and 2-D hydrodynamics of the sheet-flow moving across the buffer and four treatment cells of the Everglades Nutrient Removal Project (ENRP), and obtained stages at specified grids. However, all simulations were performed under steady-state flow conditions in a large computational grid (50,530 m^2). Also, physical model parameters were assumed rather obtaining explicitly through calibration or using field data. The persistent demand for greater accuracy and finer spatio-temporal resolution led to an extensive modeling effort in the STAs that included more detailed, spatially-explicit models. Moustafa and

Hamrick (2000) developed a depth-integrated, 2-D model of the ENRP (a portion of the STA-1W), was calibrated against time-variant water depths and validated against measured chloride concentrations at 4 internal monitoring sites. Although the model adequately reproduced measured water depths and chloride concentrations, it has not been applied to assess management options. On the other hand, Sutron Corp. (2005) developed a 2-D, linked-cell hydraulic model of STA-1W to simulate surface water flows using a finite element mesh. However, in this study, rainfall, evapotranspiration (ET) and groundwater seepage flows were considered negligible. Nungesser and Chimney (2006) estimated the combined ET and groundwater outflow budget to be 33% of the STA-1W outflow volume during the period from August 18, 1994 to July 31, 1999, which justifies the significance of these components to the STA-1W water budget. Also, the model was calibrated against field measured flow and stage data of a relatively short period (11 days) that could potentially impose uncertainty in simulating long-term dynamic flow conditions. More recently, Min and Wise (2010) developed a hydrodynamic and solute transport model of STA-5 and simulated depth-averaged flow and solute transport processes within the northern flow-way (two cells). In this study, inflows/outflows through hydraulic structures were modeled as a source/sink option.

Rationale of the Research

Beyond proper design and construction of STAs, the critical factors to optimizing the treatment performance include optimal operation and maintenance by sustaining ideal hydrodynamic conditions (e.g., hydraulic residence times, velocities, and water depths), and avoiding dry-out conditions (Smith and Hornung, 2005). In addition to more obvious performance-related factors, such as inflow nutrient loads and vegetation health, these hydrodynamic variables including hydraulic loading rates are thought to

have the greatest influence on the STA performance (Chimney and Moustafa, 1999). To ensure the sustainability of desired vegetation, it is also critical to control these hydrodynamic factors as well as sustain hydraulic loadings within design and operational guidelines. From over a decade of STAs operation, it has been recognized that excessive water depths have adverse impacts on emergent vegetation communities. For example, a significant amount (approximately 40%) of the cattail standing crop died in the west flow-way (Cell 2) between May 1997 and November 1998, presumably due to the high water levels in the western flow-way (Chimney and Moustafa, 1999). Such remarkable cattail mortality highlights the need of well-informed hydraulic operations to effectively manage vegetation communities and therefore enhance the treatment performance of STAs.

Generally, it is presumed that more even distribution of flows within the treatment cell can improve treatment performance. Full-scale tracer tests have demonstrated non-ideal flow characteristics in most treatment wetlands (DBEL, 2000; DBEL and MSA, 2006; Kadlec and Wallace, 2008); therefore they are being designed with specific features to maintain an evenly distributed influent across the entire width of the wetland (von Zweck et al., 2000). However, STAs are usually characterized by stagnant water areas, preferential flow paths, and internal dispersion due to uneven topographical features, heterogeneity in vegetation communities (e.g., clumped nature of vegetation), and location of hydraulic structures (Piccone, 2003; Dierberg et al., 2005; Kadlec and Wallace, 2008). The importance of heterogeneity in topography and vegetation for understanding wetland hydraulic behaviors has been well documented (Dierberg et al., 2005; Min and Wise, 2009; Paudel et al., 2010). Preferential flow paths (i.e., short-

circuiting flows) cause short residence of inflow water, and therefore reduces the interaction time between inflow water and the bulk of the wetland system (e.g., biota, sediments), and possibly results in poor treatment (Kadlec and Wallace, 2008). Short-circuiting flow has been shown to be one of the main causes that undermine the ability of STAs to effectively remove phosphorus from stormwater runoff (Dierberg et al., 2005; Paudel et al., 2010) because most of these wetlands are constructed on former agricultural lands with widespread remnant farm ditches (Chimney et al., 2000).

Over the past few years, SFWMD has considered several construction and/or restoration activities as part of the Long-Term Plan project to optimize the phosphorus removal performance of these wetlands (Pietro et al., 2009). Some of these activities include construction and/or modification of levees/hydraulic structures to promote uniform flow distribution and maintain low velocities to minimize erosion and sediment re-suspension, and establish uniform vegetation to minimize short-circuiting. Despite considering these actions, the effects on the flow patterns within a wetland cell through changes in management options, are still not fully understood. Previous detailed modeling studies (e.g., Guardo and Tomasello, 1995; Moustafa and Hamrick, 2000; Min and Wise, 2010) have not fully considered the impacts of such management options on flow behavior. Modeling studies have yet to assess the impacts of adopting different operations (e.g., structural modifications, and changes in vegetation pattern for various flow regimes) in cell-network wetlands such as the STAs. Here, we developed an integrated hydrologic and transport model for four treatment cells of STA-1W, and performed simulations of various scenarios to understand and predict how the system responds. Such simulations are important because the benefits of adopting an

alternative are only observable after they are constructed or modified–often not viable and may entail an enormous cost to evaluate in the field level. Therefore, there is a need of spatially-explicit, transient, hydrodynamic model that can integrate high resolution spatial input data/parameters, and simulate the dynamic response of the wetland that might result from operation and management options; the ability to accurately predict spatio-temporal flow dynamics is a vital step to optimizing the phosphorus removal performance of STAs.

Study Objectives

The overall goal of this study was to develop and apply a 2-D, physically based flow and transport simulation model of a cell-network treatment wetland of south Florida to explore the distribution of flow regimes under different 'what-if' scenarios, aimed to improve the phosphorus removal effectiveness in the STAs in relation to more uniform flow distribution across the space. STAs exhibit significant velocity variation and mixing (Dierberg et al., 2005; Paudel et al., 2010); therefore, the transport model was additionally tested by simulating advection and dispersion processes for the transport of chloride, assumed to act as a conservative tracer. Moreover, our objective was to determine the values (or range) of physical parameters for the STA-1W through the calibration of the spatially distributed flow and transport model that can provide valuable insights into future modeling efforts of treatment wetlands.

Study Site

The STA-1W (formerly known as the ENRP) is a constructed freshwater wetland designed to remove phosphorus from agricultural drainage waters before entering the Arthur R. Marshall Loxahatchee National Wildlife Refuge, also known as Water Conservation Area 1 (WCA-1). STA-1W is located in the central Palm Beach County

along the northwestern boundary of WCA-1 and on the eastern boundary of the Everglades Agricultural Area (EAA) in south Florida (26^{o}38'N, 80^{o}25'W, Figure 4-1). This STA is approximately 2700 ha in size. A portion of STA-1W was operated as the ENRP (1544 ha) from August 1994 through April 1999 (Chimney et al., 2000). STA-1W consists of three flow-ways: east flow-way (Cells 1 and 3), west flow-way (Cells 2 and 4), and north flow-way (Cells 5A and 5B).

The major source of inflow water to STA-1W was the S-5A basin, which drained the northeastern portion of the EAA runoff. Water was delivered into the STA-1W from West Palm Beach Canal (C-51), and through a supply canal to the inflow pump station (G-250).The primary inflow consisted of surface water pumped into the Buffer Cell at the north end of the wetland (Figure 4-2). From the Buffer Cell, the flow was distributed via gravity flow into east flow-way (Cells 1 and 3) through G-252A-J (10 culverts) and west flow-way (Cells 2 and 4) through G255A-E (i.e., collectively G-255) that were separated by an interior levee. Cells were connected by pipe culverts that had inlet risers with flashboards to regulate upstream water depths (Nungesser and Chimney, 2006). Both flow-ways emptied into a common channel from which the pump delivered treated water into the adjacent WCA-1. During the study period, the STA-1W always remained flooded (Guardo, 1999); thus the dominant mechanism for flow and transport was overland flow. The general direction of groundwater flow was from east to west because higher water levels were maintained in WCA-1 relative to the STA-1W (Rohrer, 1999). The average stage difference between WCA-1 and the east flow-way (average over Cells 1 and 3) was approximately 1.4 m (NGVD 29); therefore, the seepage flow into the STA-1W emerged to the surface along the toe of L-7 levee at eastern boundary

(Rohrer, 1999). To the west of the STA-1W was the EAA where the stages were relatively lower than the STA-1W, which contributed the seepage flow from the STA-1W to the seepage canal. The bottom topography of the STA-1W was relatively flat. However, topographic survey data indicated a downward slope in surface elevation from east to west (Figure 5-4). The surficial aquifer system underlying the STA-1W was reported to be approximately 60 m thick, composed of sand, sandstone, silty marl, and limestone (Rohrer, 1999).

Several vegetation types were identified in the STA-1W during the vegetation monitoring program conducted in pursuant to the requirements of Florida Department of Environmental Protection (Chimney et al., 2000). Cattail (*Typha sp*.) was found to be the relatively dominant emergent vegetation in Buffer Cell, and Treatment Cells 1 and 2. Cell 3 consisted of a mixture of various plant species and is therefore referred to as a "mixed-marsh" (Chimney et al., 2000). These major species included arrowhead (*Sagittaria latifolia),* Spikerush *(Eleocharis interstincta)*, maidencane (*Panicum hemitomon*), pickerelweed (*Pontederia cordata*), and sawgrass (*Cladium jamaicense*). Cell 4 was maintained with submerged macrophyte/periphyton community dominated by coontail (*Ceratophyllum demersum*), and southern naiad (*Najas quadalupensis*) with less abundant pondweed (*Potamogeton illinoensis*). In the eastern boundary of Cells 1 and 3, sawgrass was found to be the dominant vegetation type. The areal coverage of major vegetation groups in treatment cells are summarized in Table 5-1.

As the ENRP was built to gather scientific information and operational data that could be used in the design and construction of larger STAs; it was one of the most well-studied stormwater treatment wetlands in the world, but with a particular emphasis

on Everglades restoration (Dierberg et.al; 2005; Reddy et al., 2006). The ENRP generated a large quantity of spatial and temporal data, which are often necessary to develop and test a flow-integrated, spatially distributed model. Most of the flow and chloride data for the ENRP were available from August 1994 to April 1999 because the project ceased to exist as a separate entity on April 1999 including several modifications of water control structures (Chimney et al., 2000). More complete descriptions of layout, history and operational management can be found in Chimney and Moustafa (1999), Chimney et al. (2000), Chimney and Goforth (2006), and Nungesser and Chimney (2006).

Modeling Approach

The Regional Simulation Model (RSM) and Regional Simulation Model Water Quality (RSMWQ), discussed in Chapter 2 were used as a basic modeling framework for this study.

Data Sources

The bulk of the hydrological field measurement data employed in this study were collected by SFWMD personnel and are publicly available on their online environmental database, DBHYDRO. These data include daily mean water levels, flow rates, and daily rainfall and evapotranspiration (ET) depths. Daily mean water level data were available at several monitoring sites, and daily mean flow rates were available at all water control structures shown in Figure 4-2. Precipitation collected at 7 monitoring stations located throughout the STA-1W were spatially averaged over the entire area using Thiessen-weighted coefficients developed for each gauge station to estimate a mean rainfall depth (Abtew and Downey, 1998). The areal average ET depth (available in DBHYDRO) for the STA-1W was based on the continuous daily data measured at

automated lysimeters installed in cattail, open water/algae system, and mixed marsh and/or predicted using calibrated ET models based on the meteorological conditions (Abtew and Obeysekera, 1995; Abtew, 1996).

Chloride concentrations at internal monitoring stations (Figure 4-2) were sampled bi-weekly/monthly using grab samples. Bi-weekly chloride concentrations measured at ENR004 were used to estimate chloride that enters from WCA-1 to the STA-1W by seepage flow. Spatial input data such as topographic survey points with bottom surface elevation and vegetation coverage maps were provided by SFWMD personnel. Wet deposition of chloride, 2 mg L^{-1}, was based on the earlier study conducted at the ENRP site (Chimney et al., 2000).

Model Construction

Spatial and Temporal Discretization

The portion of STA-1W (ENRP) was represented by a two-dimensional, variable size finite element mesh of 920 unstructured triangular elements (average area: 17,560 m^2) and 507 nodes, generated in Groundwater Modeling System (GMS) v6.0. The mesh density was further refined in some specific areas to better represent the location of flow control structures. The mesh resolution was particularly chosen to trade-off simulation time with a reasonable representation of spatial data (e.g., topography, vegetation, and soil total phosphorus), and location of inflow/outflow structures because spatially distributed models are computationally intensive. Horizontal coordinates of the model domain were in NAD 83 HARN, State Plane, Florida East Zone and elevations were in NGVD 29. Although the model mesh includes the Buffer Cell, it was not included in this study. All boundaries of the Buffer Cell were specified as no-flow (both surface water and groundwater) to eliminate the effects of the Buffer Cell on Treatment Cells 1

through 4. This is because the topographic data (survey points) were not available for the Buffer Cell. As the Buffer Cell allows independent water delivery to east and west flow-ways in a disproportionate amount through hydraulic structures G-252 (10 culverts, approximately equally spaced across 1450 m levee), and G-255 (5 culverts, spaced across approximately 40 m levee). However, 56.5% of total outflow of the Buffer Cell was passed through G-255 into the western flow-way, and 37.6% of total outflow of the Buffer Cell, was passed through G-252 into the eastern flow-way, calculated by using the data from 8/18/1994 to 4/30/1999 (Chimney et al., 2000). In this condition, the precise bathymetry holds a significant importance to correctly simulate the flow through these structures. Otherwise, the error generated in simulating flows through these structures due to incorrect bathymetry of Buffer Cell would propagate through all treatment cells.

The hydrologic model calibration and validation periods were chosen from January 15, 1995 to July 15, 1997 (2.5 years), and March 1, 1998 to February 28, 1999 (1 year), respectively. The transport model calibration period was chosen to be concurrent with the hydrologic model calibration period. The eastern-flow way was closed by blocking the G-252 culverts during the adjustments to the north and south banks of test cells from July 17, 1997 to February 4, 1998 and February 17 to 30, 1998; then the project ceased to exist as a separate entity on April 1999 (Chimney et al., 2000). Therefore, the time period from July 16, 1997 to February 28, 1998 was excluded from model simulations. In order to maintain the Courant-Friedrichs-Lewy stability requirements for all elements in the mesh, a relatively small time step (1 hour) was used for model simulations.

Model Bathymetry

The model bathymetry was constructed using a kriging interpolation scheme from more than 500 points surveyed along parallel transects in Treatment Cells 1, 2, 3 and 4 provided by SFWMD. A mean surface elevation of all raster cells (20 m x 20 m) within each computational mesh element was assigned in the model. Initial survey data included extreme elevations at the top of levees, structures, and bottom of the ditches. However, these points were excluded in order to eliminate the effects of such extreme high and low elevation areas. Also, some of the points along the eastern boundary were higher than the average bottom elevation of Treatment Cells 1 and 2, which posed a numerical stability problem in the model run; thus, these higher elevation data along eastern boundary were adjusted to maintain model run stability. The bottom elevation in the ENRP ranged from approximately 2.1 to 4.0 m (NGVD 29) (Figure 5-4) with most nodal elevations ranging from 2.5 to 3.2 m (NGVD 29). As indicated by the ground surface elevation, the treatment cells in the west flow-way were relatively deeper than the treatment cells in the east flow-way.

Hydrologic Model Setup

The hydrologic model was forced by measured daily inflows, rainfall, ET, and initial water levels. The east and west flow-ways received water from the Buffer Cell through G-252A-J (10 circular culverts), and G-255 (5 circular culverts), respectively. Inflows to both east and west flow-ways were represented by source and/or sink terms, and assigned to a specific mesh element that corresponded to the location of each culvert discharge. The outflow pump (G-251) was modeled as a constant wall-head boundary condition; an average value of historic stages recorded at ENR012 (i.e., immediately upstream of the outflow pump) was specified at the outlet boundary. At the northern

boundaries of Cell 2, no-flow boundary condition was used for both surface water and groundwater, as reported by previous hydrologic monitoring studies of the ENRP (Guardo, 1999; Chimney et al., 2000; Nungesser and Chimney, 2006). All interior levees were assigned as a no-flow boundary condition for overland flow. Seepage flow across the eastern and western boundaries was modeled using a cell general head boundary condition, which determined the seepage flow as a function of stage difference between the STA-1W and boundary areas (i.e., WCA-1 and EAA). The HPM of RSM (SFWMD, 2005b; Flaig et al., 2005) was used to process rainfall and potential ET (PET) values that provided net recharge to mesh cells of the model domain. A "layer1nsm" HPM type was reported suitable for the wetland system dominated by overland flow (Flaig et al., 2005). Available daily ET values in DBHYDRO were spatially averaged ET depth over the ENRP estimated using ET models (Abtew, 1996), thus, the maximum PET correction coefficient for open water, and vegetation reference PET correction coefficient (K_{veg}) of "layer1nsm" HPM type (SFWMD, 2005b) were set to one.

Measured water levels on the simulation starting date (January 15, 1995) at 18 monitoring stations were used to generate a spatial map using a kriging interpolation method, and set as the initial head for each mesh element. Seepage was one of the key components of the water budget in the ENRP, which was most complex and difficult to evaluate (Guardo, 1999; Choi and Harvey, 2000). Stages in WCA-1 were maintained higher than the east flow-way stages (an average difference of 1.4 m NGVD29), and stages in the EAA at western boundary were lower than the west flow-way stages (an average difference of 1.2 m NGVD 29); therefore, the flow in the surficial aquifer was driven towards the west by higher stages in WCA-1. Estimates of seepage from WCA-1

to the STA-1W were based on the stage difference between the L-7 canal and the mesh elements adjacent to the eastern boundary. Similarly, seepage flow across the perimeter levee at western boundary was simulated as a function of stage difference between seepage return canal and mesh elements adjacent to western boundary. It was assumed that the stage in the canal was equal to the head in the levee (i.e. boundary of the model domain) for boundary condition applications. The expression used for the general head boundary in the form:

$$Q_s = K_s\left(H_B - H_i\right) \tag{5-1}$$

where Q_S is the seepage flow across the wall boundary ($m^3\ s^{-1}$), H_i is the water level at the *i* mesh element adjacent to the wall boundary (m), H_B is the water level on wall boundary (m), and K_s is the seepage flow coefficient ($m^2\ s^{-1}$). Daily historical stages of the L-7 canal measured at ENR004 station were used to establish the head (H_B) at the eastern wall boundary. Similarly, daily historical stages of seepage canal at ENR006 station were used to establish the head at the western boundary.

In the ENRP, treatment cells were hydraulically connected by water control structures (a group of pipe culverts) across interior levees to regulate depths and flow regimes in upstream treatment cells (Figure 5-2). These flow structures (i.e., G-254A-E, G-256, and G-253A-J) were modeled as a conceptual water mover, in which water flow is computed with generic equation to represent the actual structure. The flow equation in the generic form (SFWMD, 2005c) is:

$$Q_c = C_d L\left(H_u - z_c\right)^a\left(H_u - H_d\right)^b \tag{5-2}$$

where Q_c is the discharge through the culvert ($m^3\ s^{-1}$), H_u is the water level at the mesh element that corresponds headwater location of the culvert (m), H_d is the water level at

the mesh element that corresponds to the tailwater location of the culvert (m), z_c is the crest elevation (m), L is the crest length (m), C_d is the flow coefficient (s^{-1}), and a, and b are the user specified coefficients. C_d, a, and b were calibrated against daily measured discharges at G-253A-J, G-254A-E, and G-256 culverts for the period of 15 January, 1995 to 15 July, 1997.

Hydraulic Parameters

In treatment wetlands, the resistance to surface flow primarily depends on the drag exerted by plant communities and a water depth; therefore, a depth-dependent hydraulic resistance was simulated with a power function of the following form (SFWMD, 2005a, 2005b):

$$N = Ad^B; \text{ for } d > d_t \quad (5\text{-}3)$$

where N = hydraulic resistance factor; A, and B are empirical constants, usually determined through model calibration; and d_t is detention depth (m) which was assigned 0.01 m throughout the model domain to characterize the flooding and dry conditions. d_t refers to the depth of ponding within a mesh element below which no transfer of water from one mesh cell to the next is allowed even if a hydraulic gradient exists between adjacent cells. When stage is low in the treatment cell, flow can be impeded due to varying topography; as water level rises sheet-flow starts to dominate and flow becomes more uniform function vegetation cover. The values of A and B primarily depend on the wetland habitat (i.e., vegetation type) and/or vegetation density. Here, the entire vegetation coverage was reclassified into 5 major vegetation groups (Figure 5-5a) in order to simplify the calibration of A. The initial value of A was approximated based on the reported Manning's n from previous studies (DBEL, 2000; Sutron Corp., 2005; Min

and Wise, 2010) and a mean water depth of the treatment cell. Because the field measured *n*-values or velocity data for specific habitat type/density were not available in the STA-1W, calibration was used to determine the final values of *A* for these 5 vegetation groups (Figure 5-5b). During the calibration process, *A* was carefully adjusted manually over a reasonable range to best-fit the spatio-temporal water levels, because this parameter was the most sensitive to the water level variation. Previous work found *B* = -0.77 to be appropriate for most Everglades wetland plant communities (SFWMD, 2005a) and this value was used here for all vegetation types. The groundwater flow resistance was described by the hydraulic conductivity (k = 3.5 x 10^{-4} m s^{-1}, Harvey et al., 2000) which was considered isotropic and homogeneous for a single layer of 60 m thick surficial unconfined aquifer beneath the STA-1W (Rohrer, 1999).

Transport Model Setup

A mass conservative approach was used to simulate 2-D advective and dispersive processes. Chloride was assumed to act as a conservative tracer, and used to calibrate key transport parameters. Since the transport model was coupled with a hydrologic model, information about hydrodynamic state variables (i.e., water depth, and velocity field) that are required for transport simulations were internally used by the transport model from hydrologic model outputs. For model initialization, chloride concentration data from 18 internal monitoring stations on the simulation start date were used to develop a 2-D spatial map using kriging interpolation scheme. Time series measured chloride concentrations obtained from bi-weekly grab samples at G255 were specified as a source boundary condition for the west flow-way. Concentration of a specific sample date was applied to the subsequent daily flows until the next sample date.

Similarly, chloride concentrations measured at G-252C and G-252G were specified for the east flow-way. Since the concentration data were only available for these two stations, G-252C concentrations were assigned for G-252A-E (five culverts) and G-252G concentrations were assigned for G-252F-J (five culverts). Bi-weekly chloride concentrations measured at ENR004 station were used for seepage flow across L-7 levee (from WCA-1 to STA-1W). Initial values of model parameters, such as longitudinal and transverse dispersivities (α_L and α_T) were specified as suggested by previous studies of Everglades wetlands (Ho et al., 2009; Variano et al., 2009; Paudel et al., 2010) and subsequently calibrated against measured chloride concentrations at internal monitoring stations from January 15, 1995 to July 15, 1997. A relatively short time step (1 minute) was used for transport modeling to ensure the numerical solution stability.

Model Assessment Criteria

Model performance during calibration and validation were evaluated through qualitative and quantitative measures using both graphical comparisons and statistical tests. The quantitative measures (i.e., statistical tests) involve the assessment error and/or goodness-of-fit metrics between observations and simulations. In this application, model performance was evaluated using established statistical measures of error and goodness-of-fit. The goodness-of-fit metrics, coefficient of determination (R^2) and coefficient of efficiency (CE), which are frequently used in hydrologic modeling studies (Legates and McCabe, 1999; Dawson et al., 2007), were used to evaluate the model performance. R^2 is a dimensionless term that varies from 0 to 1, with 1 representing a perfect agreement between the model and the observed data. CE ranges from minus infinity to 1, with higher values indicating better agreement. Legates

and McCabe (1999) suggested using an error term such as the RMSE in addition to goodness-of-fit measures.

$$\text{RMSE} = \sqrt{\frac{\sum_{i=1}^{n}\left(S_i - O_i\right)^2}{n}} \tag{5-4}$$

$$\text{R}^2 = \frac{\sum_{i=1}^{n}\left(O_i - \bar{O}\right)\left(S_i - \bar{S}\right)}{\left[\sum_{i=1}^{n}\left(O_i - \bar{O}\right)^2\right]^{0.5}\left[\sum_{i=1}^{n}\left(S_i - \bar{S}\right)^2\right]^{0.5}} \tag{5-5}$$

$$\text{CE} = 1 - \frac{\sum_{i=1}^{n}\left(O_i - S_i\right)^2}{\sum_{i=1}^{n}\left(O_i - \bar{O}\right)^2} \tag{5-6}$$

where S_i and O_i are the simulated and measured data at a time step i, respectively, and n is the number of observations for the simulation period, $\bar{O}$ is the mean value of observed data.

Model Calibration and Validation

In the hydrologic model, the flow resistance coefficient (A) was calibrated to best-fit historical stages at 4 internal monitoring stations (ENR101, ENR301, ENR204, and ENR401; Figure 5-2) for the period from January 15, 1995 to July 15, 1997 (2.5 years) until the discrepancies between model generated values and those measured in the field, as quantified by RMSE, were minimized. Similarly, α_L and α_T were calibrated against bi-weekly measured chloride concentrations at 6 internal monitoring stations (ENR102, ENR204, ENR305, G-253C, G-254D, and G-256; Figure 5-2) for the period of 15 January 1995 to 15 July 1997. These parameters were carefully adjusted over a reasonable range and final values were determined that minimized the average RMSE between simulated and measured chloride concentrations at all 6 stations. The calibrated model was subsequently validated without any adjustment of calibrated

parameters against independent data (daily water levels) for the period from March 1, 1998 to February 28, 1999 (1year). To perform validation simulations, the model was re-initialized with new hydrologic conditions.

Sensitivity Analysis

The sensitivity of a state variable (*x)* to the changes in parameter (*p*) was evaluated using the sensitivity coefficient,

$$S_p = \frac{\Delta x / x}{\Delta p / p}. \quad (5\text{-}7)$$

A positive sensitivity coefficient for *p* indicates an increase in *x* when *p* is increased. For example, a sensitivity coefficient of 0.3 indicates that a 10% increase in parameter would increase *x* by 3%. Subjective criteria were used to specify a reasonable range of parameter values for sensitivity analyses. The values of A, K_s, and K_{veg} were varied by ± 30%, so this range was used to test these parameters. Then, for each simulation, the variation in water levels as result of changing parameter values was evaluated. A sensitivity analysis of chloride concentrations at internal monitoring stations (stations used for calibration) was performed by varying calibrated α_L and α_T to double and half (i.e., multiplying and dividing by a factor 2).

Water Budget

The governing water budget equation that applies to the ENRP treatment cells consists of the following components:

$$\frac{\Delta V}{\Delta t} = P + S_i - ET - S_o \pm GW_f + R \quad (5\text{-}8)$$

where ΔV is the change in system storage during a time interval ($V(t) - V(t\text{-}1)$), phosphorus is precipitation, S_i and S_o are surface inflow and outflow, GW_f is net

groundwater seepage flow, R is the water budget error, and Δt is the time interval. The change in storage for a specific treatment cell was based on the daily mean water depth of that cell. Culverts G258 and G259 were rarely operated during the simulation period (Nungesser and Chimney, 2006); therefore, the surface flow through these culverts were assumed negligible components of the water budget. In the STA-1W, all water budget components were well monitored except groundwater flow. The unknowns in the system are net groundwater inflow/outflow and error terms. Abtew and Mullen (1997), in the study of STA-1W water budget analysis, estimated the net groundwater seepage using the remainders from the water budget. Remainders may include measurement errors in water budget components and/or unmeasured sources of water (Abtew and Mullen, 1997). Chimney et al (2000) and Nungesser and Chimney (2006) estimated the net surficial and deep groundwater seepage for each treatment cell using regression equations driven by stage differences. However, these estimated seepage values were affected by measurement errors and/or undocumented flows, as indicated by large water budget residuals.

In this study, daily net groundwater seepage flow (GW_f) across the levees was estimated by setting the water budget error zero (Equation 5-8). Then, seepage flow coefficients were calibrated to best fit the daily cumulative flow volume of net groundwater seepage for each treatment cell. The direction of flow (inflow or outflow) was determined based on the stage difference between the STA-1W and boundary areas (i.e., WCA-1 and EAA). The simulated water budget was of the general form:

$$\frac{\Delta V}{\Delta t} = \bar{P} + \overline{S_i} + \overline{G_i} - \overline{ET} - \bar{S}_o - \bar{G}_o + R_s \qquad (5\text{-}9)$$

where overbars denote simulated flows, G_i overbar is the simulated groundwater inflow, G_o overbar is the simulated groundwater outflow, and R_s is the simulated water budget residual.

Results and Discussion

Water Level Simulations

Simulated and field-measured water levels at 4 monitoring sites (ENR101, ENR203, ENR301, ENR401; Figure 5-2) for the model calibration period are presented in Figure 5-9. Although measured daily water level data were available at several monitoring stations, only the results at these 4 stations were selected for illustration of model comparisons; these stations represent approximately the center of each treatment cell. During the calibration process, *A* was found to be the most influential parameter for the STA-1W hydrodynamic modeling. This parameter was adjusted until the simulated results reasonably matched observed water levels. After several adjustments, *A*-values were finalized for 5 vegetation groups to provide the lowest average RMSE between daily observed and simulated values of all 4 monitoring stations. The K_s that controls the seepage flow was adjusted by fitting the cumulative residual term of the water budget to make seepage close to the mass balance in each treatment cell for the calibration period. Final K_s-values ranged from 0.006–0.036 m^2/s, with the highest value for Cell 2 at the western wall boundary, and lowest for both Cell 1 and Cell 3 at eastern wall boundaries.

As indicated by performance statistics, the model generally reproduced the temporal fluctuations in daily observed water levels at all monitoring sites (Figure 5-9). However, the east flow-way water levels were better simulated compared to the west flow-way. Overall, the model simulated spatio-temporal water levels reasonably well, as

indicated by mean calibration metrics (RMSE = 0.09 m; R^2 = 0.73; CE = 0.49) of all 4 monitoring stations. In the west flow-way, the model slightly overestimated water levels, especially during the period from July 1995 to May 1996, which is likely due to the seepage simulation technique because the seepage was modeled using the residual term of the water budget (Equation 5-8) to best-fit the total cumulative residual volume, so the temporal fluctuation in the seepage flow might not be well-captured by the model.

The model was validated against 1 year (March 1, 1998 to February 28, 1999) water level data at 4 monitoring sites used for calibration. In contrast to the calibration results, the model produced observed water levels much better in the west flow-way compared to the east flow-way during validation. The model tended to capture low stage-events in the west-flow way during calibration suggesting that the seepage might have been underestimated, or there may have been other unrecorded outflows, especially at the time of high-stage events. Overall, the simulated water levels were in good agreement with observed values as indicated by mean statistics (RMSE = 0.08 m; R^2 = 0.64; and CE = 0.45) of all 4 monitoring stations during the validation period (Figure 5-10). In the east flow-way, the model reproduced measured daily water levels well during calibration; however, observed water levels were slightly underestimated in both stations of the east flow-way during the validation period (Figure 5-10). Although there were few anomalies during this relatively short period of time, the model predicted reasonable water levels in a spatio-temporal scale, which illustrates the ability of the model to simulate real flow dynamics in STA-1W east and west flow-ways.

Discharge Simulations

Simulating water control structures is of considerable importance in a cell-network treatment wetland because these structures control quantity, timing and distribution of

flow in the upstream treatment cell. In this study, flow through the structures was governed by the difference in the head between mesh elements that represent headwater and tailwater locations of a culvert. Figure 5-11 compares the measured and model simulated daily averaged flow rates at culverts G-253A-J, G-254A-E, and G-256 for the calibration period, showing that the culvert discharges were well reproduced by the model. This indicates that the model is capable of simulating culvert flow in a realistic manner by using a generic equation of a conceptual water mover, resulting in high accuracy for both low- and high-flow events (Figure 5-11). The best set of flow parameters, C_d (1.0), *a* (1.5), and *b* (0.5) were determined by adjusting initial values manually until the average value of RMSE between simulated and observed daily flow rates of all culverts was minimized. Note that the culverts in the STA-1W were circular, but the flow equations in RSM are based on rectangular structures. Explicit representation of circular pipe algorithms would improve the simulation results.

The model performance in simulating outflow pump discharge was satisfactory, as the measured daily discharge and cumulative volume were well reproduced (Figure 5-12). This indicates that the specified wall-head boundary can be used to simulate G251 pump outflow, which is often highly managed with significant temporal fluctuations (Figure 5-12).

Hydraulic Parameters

Resistance to flow (i.e., frictional resistance) is one of the most important flow-controlling terms in hydrodynamic models of wetland systems (von Zweck et al., 2000; Swain et al., 2004). Vegetation type/density strongly influences the movement of water in wetlands, providing a resistance to surface flow commonly represented by the Manning's coefficient of roughness, *n* (Kadlec and Wallace, 2008).The drag exerted by

plant stems and litter reduces the mean flow and leads to an increase in water depth and residence time (Nepf, 1999; Lee et al., 2004); therefore, understanding of vegetation type/density and spatial distribution is of considerable importance to wetland hydrodynamics. Manning's equation, which was originally formulated for the turbulent flow regime in an open channel, is the most common and frequently used model of frictional resistance to wetland surface water flow (Sutron Corp., 2005; Min and Wise, 2009, 2010). Kadlec and Wallace (2008) suggested a power law model which they found more suitable for wetlands because the flow regime in wetland nearly always remains laminar or transition. It has been well-documented that the Manning's *n*-value decreases with depth of water in studies of south Florida wetlands (Piccone, 2003; Sutron Corp., 2005; SFWMD, 2005a). When thick vegetation is present, the *n*-value can be large for shallow flow, but decreases significantly with flow depth. Recent studies of STAs (Piccone, 2003; Sutron Corp., 2005; Paudel et al., 2010) indicate that a depth-dependent resistance is more applicable for STAs than the use of the constant Manning's *n*. In this study, depth-dependent resistance, also referred to as effective roughness (*N*) (SFWMD, 2005b) was calculated as a function of habitat type, and water depth.

The optimal set of flow resistance parameters (*A*), which provided the best-fit between simulated and measured water levels at 4 monitoring sites, are summarized in Table 5-2. Sensitivity analyses indicated that *A* was the most influential parameter on predicted water levels; therefore the range of *A*-values was initially determined for 5 major vegetation types as suggested by previous relevant studies (DBEL, 2000; SFWMD, 2005a; Sutron Corp., 2005) and final values were estimated by calibration.

The calibrated values of *A*, and computed *N* (modified Manning's *n*) for a specific water depth (i.e., average water depth) for 5 major vegetation groups of the STA-1W are presented in Table 5-2. The Manning's *n*-values for cattail and algae/macrophyte complex (i.e., SAV) were somewhat lower than those applied in previous STA1-W studies (Sutron Corp., 2005). The anomalies in these *n*-values are likely due to modifications in hydraulic characteristics, such as levees, inlet/outlet locations of treatment cells, and changes in the vegetation pattern within the system. These factors may have significant impacts on the surface flow resistance across treatment cells. DBEL (2000) used relatively higher *n*-value (0.6 s $m^{-1/3}$) for SAV-dominated areas, but used slightly lower value (0.07 s $m^{-1/3}$) for open-water areas of STA1-W Cell 4. However, the estimated *n*-value for SAV was higher than those used by Min and Wise (2010) for SAV areas of the STA-5 northern flow-way (0.12 – 0.15 s $m^{-1/3}$). But they reported a slightly higher range for emergent aquatic vegetation (EAV) dominated areas (0.67 – 1.0 s $m^{-1/3}$) than those determined for the cattail and other emergent vegetation in this study. The difference in Manning's *n*-values in these studies (Table 5-3), is possibly due to the difference in several wetland characteristics, such as vegetation density, bed slopes, inlet/outlet locations, discharge, and shape of the wetland.

Water Budget

A water budget was determined for each treatment cell (Cells 1 through 4) of the STA-1W from the hydrologic simulations, using mean values for the calibration period (Table 5-4). Surface inflow and outflow were the dominant water budget components in all treatment cells. In Cells 1, 2, 3 and 4, the surface inflow contributed approximately 85%, 95%, 87%, and 97% of the total inflow to each cell, whereas the groundwater inflow contributed only 6%, 0%, 6% and 0.2% of Inflow, respectively. Similarly,

groundwater outflow contributed approximately 0.2%, 10%, 5%, and 6% of total outflow of each cell in Cells 1, 2, 3, and 4, respectively. The STA-1W water budget was highly influenced by inflow/outflow management decisions (Nungesser and Chimney, 2006) rather than precipitation and ET (<10% of the water budget); therefore, temporal variations in water levels did not correspond to the pattern of local precipitation and ET.

Sensitivity Analysis

Sensitivity analyses are often performed to identify the response of a model to variations in input parameter values and initial/boundary conditions, which helps identify the input errors that may contribute the most to output uncertainty (Swain et al., 2004). It is important to perform a sensitivity analysis to determine the relative magnitude of model response to changes in selected parameters prior to accepting the final set of calibrated parameters. The sensitivity of the model to changes in *A* shows that the simulated water levels are the most sensitive to the variation in *A* (Table 5-5). For example, a 30% increase in *A*-value increased average water level at station ENR203 by 6.9%. The range of sensitivity coefficient to ± 30% uncertainty of *A* confirms that the calibrated *A*-values for the major vegetation groups of the STA-1W are reasonable (Table 5-5). Simulation results (water levels) were relatively insensitive to ± 30% uncertainty in K_{veg} for all the treatment cells. ET contributed less than 10% of the outflow volume for all treatment cells; therefore its effect of ET on the water level was low. Similarly, K_s was slightly more sensitive to the variation in water level than K_{veg} for ± 30% uncertainty. In addition, sensitivity of predicted water levels to neglecting the seepage flow was evaluated in terms of RMSE. The RMSE for the simulations without seepage flow were higher than the RMSE for the existing condition simulations, with an increase in RMSE for sites ENR101, ENR203, ENR301, and ENR401 of 0.00, 0.13,

0.01, and 0.16 m, respectively. This indicates that modeling seepage in the west flow-way is critical compared to the east flow-way, as indicated by larger errors in water level predictions resulting from neglecting the seepage in the model. Results show that consideration of seepage losses has an obvious impact on the water levels of west flow-way and therefore it would likely underestimate the values of *A* without considering seepage.

Transport Simulations

The coupled hydrologic and transport model was used to simulate chloride concentrations for additional verification of the hydrologic simulations as wells as to estimate critical transport parameters for the STA-1W. The information about hydrodynamic state variables (i.e., velocity field, and depth) was acquired internally from the hydrologic model. Simulated chloride concentrations were in close agreement with field measured values for all stations (Figure 5-13). The average RMSE, R^2, and CE between observed and simulated concentrations of 6 monitoring stations were 25.6 mg L^{-1}, 0.70, and 0.68, respectively. These results demonstrate that the model is capable of simulating important hydrologic and transport processes in the STA-1W. Chloride input concentrations, measured bi-weekly for 2.5 years (1/15/1995–7/15/1997) at inflow hydraulic structures of both flow-ways, were poorly correlated to the data at corresponding monitoring stations of each flow-ways. The R^2 values between G255 inputs and the data at ENR204, G-254D, and G-256 sites (west flow-way) were 0.24, 0.36, and 0.28, respectively. Similarly, R^2 between G-252 inputs and the data at ENR102, G-253C, and ENR305 sites (east flow-way) were 0.49, 0.18, and 0.04, respectively. This indicates that the hydrodynamic model was essential to obtain a good match between observations and simulated results (Figure 5-13).

Based on the chloride simulations, the best α_L and α_T values were estimated to be 625 m and 160 m, respectively. It should be noted that dispersivity coefficients were assumed to be spatially uniform throughout the study area. This approximation is justified by noting that the model reproduced measured chloride concentrations well at all sites, despite different vegetation types and density (Figure 5-13). The parameters α_L and α_T were calibrated by fitting simulated values with bi-weekly measured chloride concentrations from January 15, 1995 to July 15, 1997, and final values were determined that resulted in the lowest mean RMSE for 6 monitoring sites. The simulated mean velocity for the entire study area was approximately 0.007 m s^{-1}, which yielded the spatially uniform mean longitudinal and transverse dispersion coefficients of 4.3, and 1.1 m^2 s^{-1}, respectively. Dispersion coefficients determined in this study were somewhat higher than that the wetland values in the literature (Martinez and Wise, 2003; Saiers et al., 2003; Keefe et al., 2004; Lightbody and Nepf, 2006; Ho et al., 2009; Huang et al., 2008; Min and Wise, 2010) (Table 5-6). Although these values were relatively higher, they were most comparable to the values reported from tracer experiments conducted in the ridge and slough area of the Everglades marsh (Ho et al., 2009). Model-estimated values of α_L and α_T for the northern flow-way of STA-5 were reported to be 2 and 0.1 m, respectively (Min and Wise, 2010). Similarly, approximately one order magnitude higher values of α_L (36 m) and α_T (3 m) than reported for STA-5 were estimated from a model Cell 4 of STA1-W (Paudel et al., 2010).The difference in dispersion coefficients in these studies is likely due to the scale of the experiment and a wide range of local velocities due to heterogeneity in landscape and vegetation pattern (Variano et al., 2009) in a large-scale, cell-network treatment wetland like the STA-1W.

In addition, irregular locations of water control structures and levees, and shape of the wetland may cause differential velocity with enhanced mixing; therefore higher dispersion coefficients estimated for the STA-1W is consistent with expectations.

Sensitivity to Dispersivity

A sensitivity analysis was performed on dispersivity parameters to better understand the influence of dispersion component on transport processes. The sensitivity of the model to dispersivity variations was assessed by increasing and decreasing α_L and α_T by a factor of 2. When α_L was multiplied and divided by a factor 2, the mean RMSE of 6 monitoring sites increased to 25.65 and 25.92 mg L^{-1}, respectively. These values differ only slightly from the base calibration simulation (mean RMSE = 25.62 mg L^{-1}), indicating that chloride concentration is not sensitive to variations in dispersivity parameters. A non-reactive tracer test would be good measure to estimate dispersivity parameters, as reported by Paudel et al. (2010). Similarly, when α_T was multiplied and divided by a factor 2, the mean RMSE increased to 25.98 and 25.67 mg L^{-1} from calibration simulation, respectively (Table 5-7). However, the best-fit to the chloride data and the sensitivity analyses of upper and lower range (multiplied and divided by a factor 2) provide confidence that estimated α_L and α_T for the STA-1W are reasonable.

Model Applications

The validated coupled hydrologic/transport model was applied to predict and understand hydraulic behaviors and transport mechanisms in response to management alternatives, which are often infeasible to test at the field scale. The model was used to evaluate several “what-if” scenarios as well as to test the model sensitivities resulting from changes in the existing inputs/parameters. The existing condition scenario (S0)

was designed to imitate the system operations and management applied from January 15, 1995 to July 15, 1997. The next S1 scenario evaluated the existing condition, but used design maximum and low inflows instead of historical data, as scenarios S1b, and S1c, respectively. Scenario S2 evaluated the effects of compartmentalization on the flow distribution and water levels. For this, all interior levees within treatment cells were removed, and simulations were performed under historical, design maximum, and low inflows as scenarios S2a, S2b, and S2c, respectively. The final scenario (S3) evaluated the effects of changes in vegetation sequence (EAV treatment cells followed by SAV treatment cells) on water levels and flow distribution. The S3 simulations were also performed under historical, design maximum, and low inflows as scenarios S3a, S3b, and S3c, respectively. All these scenario simulations were performed from January 15, 1995 to July 15, 1997, which is in concurrent with the calibration period. Design maximum flow rate was chosen as constant inflow of 16.9 $m^3 s^{-1}$, which is equivalent to the maximum pumping capacity of G250 inflow pumps (Chimney and Goforth, 2006). This flow was distributed with 9.9 $m^3 s^{-1}$ (59%) for the west flow-way, and 7.0 $m^3 s^{-1}$ (41%) for the east flow-way because the Buffer Cell was not considered in this study. The inflow proportions sent to these treatment trains (i.e., east and west flow-ways) were based on the mean observed inflows recorded at G-255 and G-252 culverts for the simulation period. The low flow condition was chosen as constant inflow of 2.1 $m^3 s^{-1}$ (Guardo and Tomasello, 1995) and distributed 59 and 41% into the west and east flow-ways, respectively.

The results of the S1, S2, and S3 were compared to the results of the existing condition simulations (S0). The predicted mean annual water levels at 4 monitoring sites

for the scenarios are presented in Table 5-8. Mean water levels were generally reduced in both S2a and S3a compared to S0. The water level variation across treatment cells under S1b and S3b was greater compared to S1c and S3c, respectively. However, S2 simulation results illustrated a small variation in spatial water levels for all flow regimes (Table 5-8). This is expected, because, once the levees were removed (no compartmentalization) there would be no control of water levels in individual cells and the entire wetland area would attain a more uniform water level. Change in vegetation pattern within treatment cells did not have much impact on water level variation. Mean water levels for the simulation period, were only slightly decreased as a result of change in vegetation pattern from existing conditions (Table 5-8). This information can have strong implications for managing aquatic vegetation.

In addition, the model was extended to examine whether water levels overtop the existing levee system under design maximum inflows. Results of S1b show that simulated water levels along west and east interior levee ranged from 3.8 to 4.3 m NGVD 29, and 3.6 to 4.0 m NGVD 29, respectively. Predicted maximum water levels at the east and west interior levees were 0.4 and 0.7 m less than the top elevation of the interior levee, 4.7 m NGVD 29 (Guardo and Tomasello, 1995). Similarly, water levels along the interior levee that separated the east and west flow-ways ranged from 3.8 to 4.3 m NGVD 29, for a predicted maximum water level 0.4 m less than the top elevation of the levee. For illustration, a snapshot of predicted water levels for S1b scenario on August 11, 1996 is shown in Figure (5-14). This indicates that design maximum inflows will be contained within the existing levee system.

Comparisons of velocity distribution simulation results between S0, S2a and S3a revealed that there were not significant effects on the velocity distribution as a result of changes in management alternatives. However, under S2a, flows tended to be clustered along the center-line from inlet to outlet compared to S0 and S3a. As an example, snapshots of velocity distributions from these scenario simulations on August 11, 1996 are presented in Figure 5-15. Also, flow distributions were quantitatively evaluated as an additional verification of visual comparison results. The unit flow rate through cross-sections of all treatment cells (along transects AA', BB', CC', DD'; Figure 5-2) are illustrated in Figure 5-16. Although there were some differences in flow rates among these scenarios the general anticipated improvement in flow distribution in S3a compared to S0 simulations, and in S0 compared to S2a simulations were found. It should be noted that the interpretation is made for the steady-state inputs and the scenarios under consideration.

A more thorough analysis could have been performed using a fine-resolution mesh and spatial input data. For the purpose of this study, the model mesh was selected to trade-off computational time with reasonable representation of spatial data; therefore, the mesh was too coarse to delineate narrow ditches, small open areas, and patches of clumped vegetation and therefore precisely predict all internal flow patterns within the wetland. To further explore these particular issues, a finer resolution mesh and spatial input data were used in one of the STA treatment cells, as described in the next chapter.

Summary

This study described the development of a spatially distributed, coupled hydrologic and transport model of a cell-network treatment wetland of south Florida. The model

was tested against available field measured data on water levels, culvert discharges, pump outflows and chloride concentrations. Subsequently, the validated model was applied to explore the effects of different operation and management scenarios potentially aimed for improving wetland treatment performance. In addition, sensitivity analyses were performed by varying key model parameters to evaluate the impacts on major output variables. Results from this study indicate:

- The hydrologic model predicted water levels at 4 monitoring sites (approximately at the center of each treatment cell) were in close agreement with measured values for the model calibration (2.5 years) and validation (1 year) periods. The mean RMSE, R^2, and CE values of all 4 monitoring sites were 0.09 m, 0.73, and 0.49 for the calibration, and 0.08 m, 0.64, and 0.45 for the validation period, respectively.

- The model successfully simulated the daily discharges through all water control structures as well as pump outflow, which are critical components of the STA-1W hydrodynamics.

- The transport model reproduced the field measured chloride concentrations reasonably well. The mean RMSE, R^2, and CE values of all 6 monitoring sites were 25.3 mg L^{-1}, 0.70, and 0.68, respectively. Based on transport simulations, the spatially uniform longitudinal and transverse dispersivities for the STA-1W were determined to be 625 m and 160 m.

- Sensitivity analyses indicated that the flow resistance coefficient (*A*) was the most influential parameter on water level variations. However, chloride concentration was not sensitive to variations in dispersivity parameters.

- Steady-state simulation results indicate that the design maximum inflow will be contained within the existing levee system.

- There was not a quantifiable improvement in the flow distribution across treatment cells—in terms of uniform flow—resulting from the changes in vegetation pattern (EAV treatment cells followed by SAV treatment cells). Also, there was not significant improvement in the internal flow pattern under the existing levee system compared to the interior levee-removal condition.

In summary, the calibration and validation results of the model described here suggest that the model was capable of adequately representing key physical conditions and system responses, and simulating different management alternatives. This

integrated hydrologic/transport model can provide valuable information, facilitate better understanding of the hydraulic and transport behaviors, and assist with optimizing the STA1-W system operations. Also, the model can be extended for the simulation of non-reactive (tracers) as well as reactive (e.g., phosphorus, nitrogen, mercury) transport and transformation within the wetland because the transport model used here also includes a flexible biogeochemical module that allows users to incorporate a wide range of reaction equations as needed for the modeling purpose.

Table 5-1. Areal coverage of major vegetation groups in the east and west flow-ways of Stormwater Treatment Area 1 West.

Major vegetation groups	Cell 1		Cell 2		Cell 3		Cell 4	
	Area (ha)	%	Area (ha)	%	Area (ha)	%	Area (ha)	%
Open water/Submerged vegetation	233.1	44.4	52.6	12.7	58.2	14.3	36.6	25.0
Cattail	184.3	35.1	312.5	75.4	163.9	40.3	5.2	3.5
Floating macrophytes	20.5	3.9	38.9	9.4	6.1	1.5	2.2	1.5
Algae/macrophyte complex	0.0	0.0	0.0	0.0	0.0	0.0	100.4	68.5
Other emergent macrophytes*	87.1	16.6	10.4	2.5	178.5	43.9	2.2	1.5
Totals	525.0	100	414.4	100	406.7	100	146.6	100

*Other emergent macrophytes includes sawgrass, primrose willow, willow, bulrush, fern emergent mix, spikerush, pickerelweed, wild taro, arrowhead, misc. grasses, leather fern, smartweed, shrub mix, misc. spp. mix 1, misc. spp. mix 2, misc. spp. mix 3 (Chimney et al., 2000)
Source: Vegetation coverage map of the ENRP, collected data on May, 1997 (SFWMD, unpublished data).

Table 5-2. Flow resistance coefficients, and computed Manning's *n* values for major vegetation groups in Stormwater Treatment Area 1 West.

Major vegetation groups	Flow resistance coefficient		Ponding depth (m)*	Effective flow resistance *n* ($s/m^{1/3}$)
	A	*B*		
Open water/Submerged vegetation	0.06	-0.77	0.58	0.09
Cattail	0.30	-0.77	0.58	0.46
Floating macrophytes	0.10	-0.77	0.58	0.15
Algae/macrophyte complex	0.20	-0.77	0.58	0.31
Other emergent macrophytes	0.33	-0.77	0.58	0.50

* Average ponding depth was taken from 4 treatment cells (i.e., Cells 1, 2, 3, and 4) for the period of 13 January 1995 to 20 June 1999 (Nungesser and Chimney, 2006).

Table 5-3. Manning's flow resistance coefficient (*n*) from previous studies.

Literature	Vegetation type	Manning's '*n*'	Comments
DBEL (2000)	SAV vegetation Open water areas	0.07 0.6	Cell 4, STA-1W
Min and Wise (2010)	Emergent Submerged	0.67 - 1.0 0.12 - 0.15	STA-5, Northern Flow-way
Paudel et al. (2010)†	Open water SAV	0.056 1.0	Cell 4, STA-1W
Sutron Corp. (2005)	Canals SAV EAV	0.038 0.3 - 1.0 0.8 - 1.3	STA-1W Cell 5

† Manning's *n*-values were derived by using flow resistance coefficients (*A* and *B*) using an average water depth within the Cell 4.

Table 5-4. Water budget for Stormwater Treatment Area 1 West treatment cells (Cells 1 through 4) from 15 January, 1995 to 15 July, 1997.

	Inflow (10^6 m^3)				Outflow (10^6 m^3)					
	S_i	P	G_i	Σ_{in}	S_o	ET	G_o	Σ_{out}	ΔS	R
Cell1	172.7	17.9	12.7	203.3	185.6	18.1	0.4	204.1	-0.8	0.0
Cell2	249.8	13.9	0.0	263.7	223.5	14.1	26.4	264.0	-0.7	-0.4
Cell3	185.6	14.1	12.8	212.5	188.4	14.3	10.1	212.8	-0.2	0.1
Cell4	223.5	4.9	0.5	228.9	210.7	5.0	13.2	228.9	-0.2	-0.2

S_i, surface water inflow; P, precipitation; G_i, groundwater inflow; Σ_{in}, total inflow into the system; S_o, surface water outflow; ET, evapotranspiration; G_o, groundwater outflow; Σ_{out}, total outflow from the system; ΔS, change in storage; R, water budget residual.

Table 5-5. Summary of sensitivity tests (hydrologic parameters).

Water level monitoring sites	Baseline value of water level (m)*	Sensitivity coefficient, $S_{p,h}$					
		+30% of A	-30% of A	+30% of K_s	-30% of K_s	+30% of K_{veg}	-30% of K_{veg}
ENR101	3.60	0.145	0.123	0.005	-0.004	-0.015	-0.022
ENR203	3.69	0.231	0.071	0.069	-0.173	0.067	-0.118
ENR301	3.53	0.135	0.149	-0.003	-0.008	-0.013	-0.017
ENR401	3.62	0.160	0.075	0.045	-0.070	0.063	-0.057

*Baseline value was the average simulated water level for the period from January 15, 1995 to July 15, 1997

A is the flow resistance parameter, K_s is the seepage coefficient, and K_{veg} is the vegetation reference crop potential ET correction coefficient.

Table 5-6. Dispersion coefficients from previous studies.

Literature	Parameter		Mean velocity ($m\ s^{-1}$)	Comments
	D_L ($m^2\ s^{-1}$)	D_T ($m^2\ s^{-1}$)		
Min and Wise (2010)	0.002 - 0.1	1.0×10^{-4} - 5.0×10^{-3}	0.001 - 0.05	STA-5, Northern Flow-way
Paudel et al. (2010)	0.14	0.012	4.0×10^{-3}	Cell 4, STA-1W
Ho et al. (2009)	0.037 - 0.26	0.012	1.5×10^{-3} - 8.0×10^{-4}	Ridge and Slough, Everglades marsh
Martinez and Wise (2003a)	0.157 (0.010 - 0.512)	-	-	OEW(Cell 1-15), Florida
Saiers et al. (2003)	4.4×10^{-5}	4.2×10^{-5}	1.5×10^{-3}	Flume based tracer experiment within Shark River Slough, Everglades National Park
Keefe et al. (2004)	9.9×10^{-3} ($\pm 2.3 \times 10^{-4}$) 2.1×10^{-2} ($\pm 4.0 \times 10^{-4}$) 2.5×10^{-3} ($\pm 7.7 \times 10^{-4}$)	- - -	8.2×10^{-4} 8.9×10^{-4} 2.4×10^{-3}	Tres Rios Wetlands, Phoenix, Arizona in H1, C1, and C2 wetlands
Lightbody and Nepf (2006)	4.0×10^{-4} - 2.7×10^{-3}	-	0.03	*Spartina alterniflora* salt marsh in the Plum Island Estuary in Rowley, Massachusetts
Huang et al. (2008)	3.0×10^{-3} - 4.8×10^{-3}	-	0.029	Flume based particle tracer experiments in Water Conservation Area 3A

D_L and D_T are the longitudinal and transverse dispersion coefficient, respectively.

Table 5-7. Summary of sensitivity tests (transport parameters).

Chloride concentration monitoring sites	Calibration simulation RMSE (mg L^{-1})	RMSE (mg L^{-1})			
		α_L x 2	α_L/2	α_T x 2	α_T/2
East flow-way					
ENR102	29.1	28.5	29.7	29.6	28.7
G-253C	28.8	29.0	28.8	30.8	28.6
ENR305	25.8	26.0	26.2	25.6	26.2
West flow-way					
ENR204	28.4	28.8	28.5	28.0	28.9
G-254D	18.4	18.3	18.7	18.7	18.4
G-256	23.2	23.3	23.6	23.2	23.2
Average	25.62	25.65	25.92	25.98	25.67

α_L is the longitudinal dispersivity, and α_T is the transverse dispersivity.

Table 5-8. Average annual water levels at internal monitoring sites for different model application scenarios in Stormwater Treatment Area 1 West.

Monitoring sites	Existing condition (S0)	Existing condition but varying inflows (S1)		Remove levees (S2)			Change vegetation pattern (S3)		
		S1b	S1c	S2a	S2b	S2c	S3a	S3b	S3c
ENR101	3.60	3.93	3.47	3.55	3.80	3.44	3.58	3.90	3.45
ENR203	3.69	4.22	3.48	3.55	3.80	3.44	3.66	4.19	3.45
ENR301	3.53	3.77	3.44	3.53	3.78	3.43	3.49	3.69	3.41
ENR401	3.62	4.06	3.45	3.54	3.78	3.44	3.58	4.00	3.42

Water levels are in m, NGVD 29

"a" represents the historical inflow; "b" represents the maximum peak inflow; and "c" represents the low inflow condition.

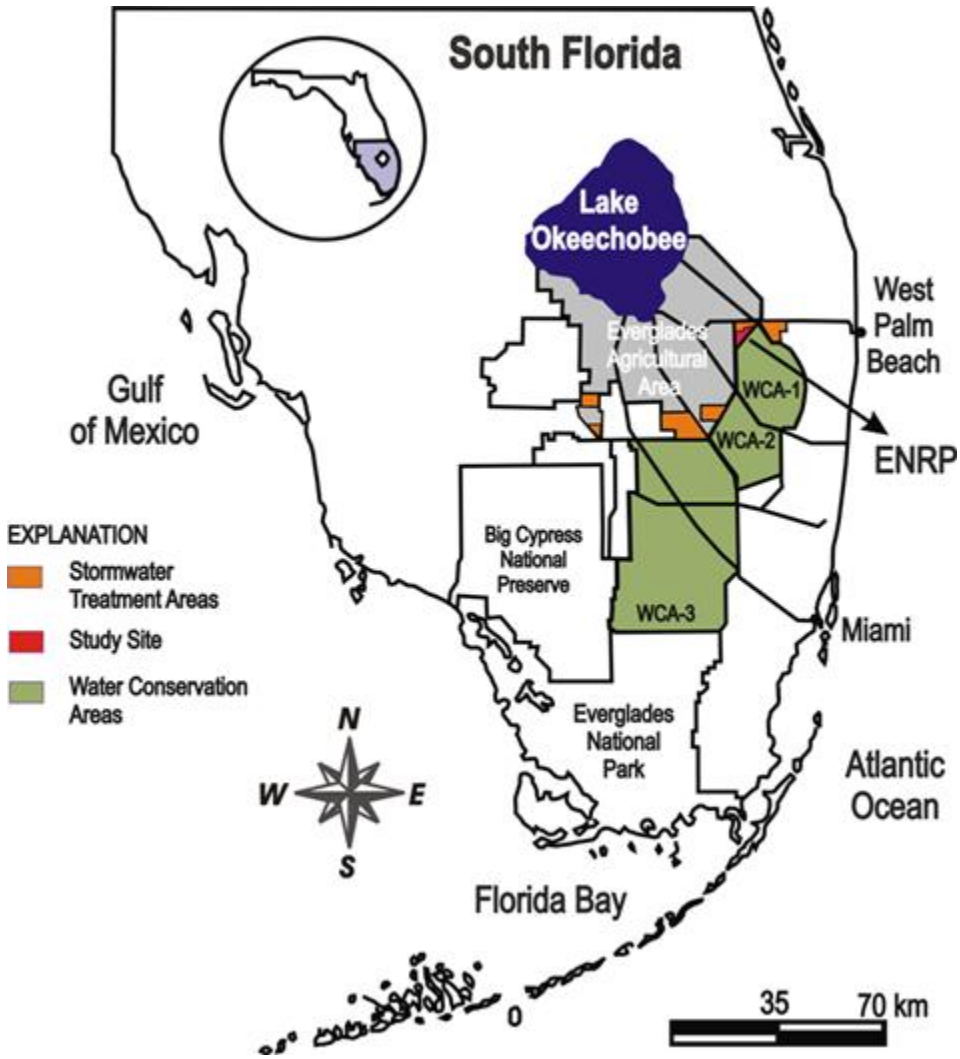

Figure 5-1. Map of South Florida showing location of study area.

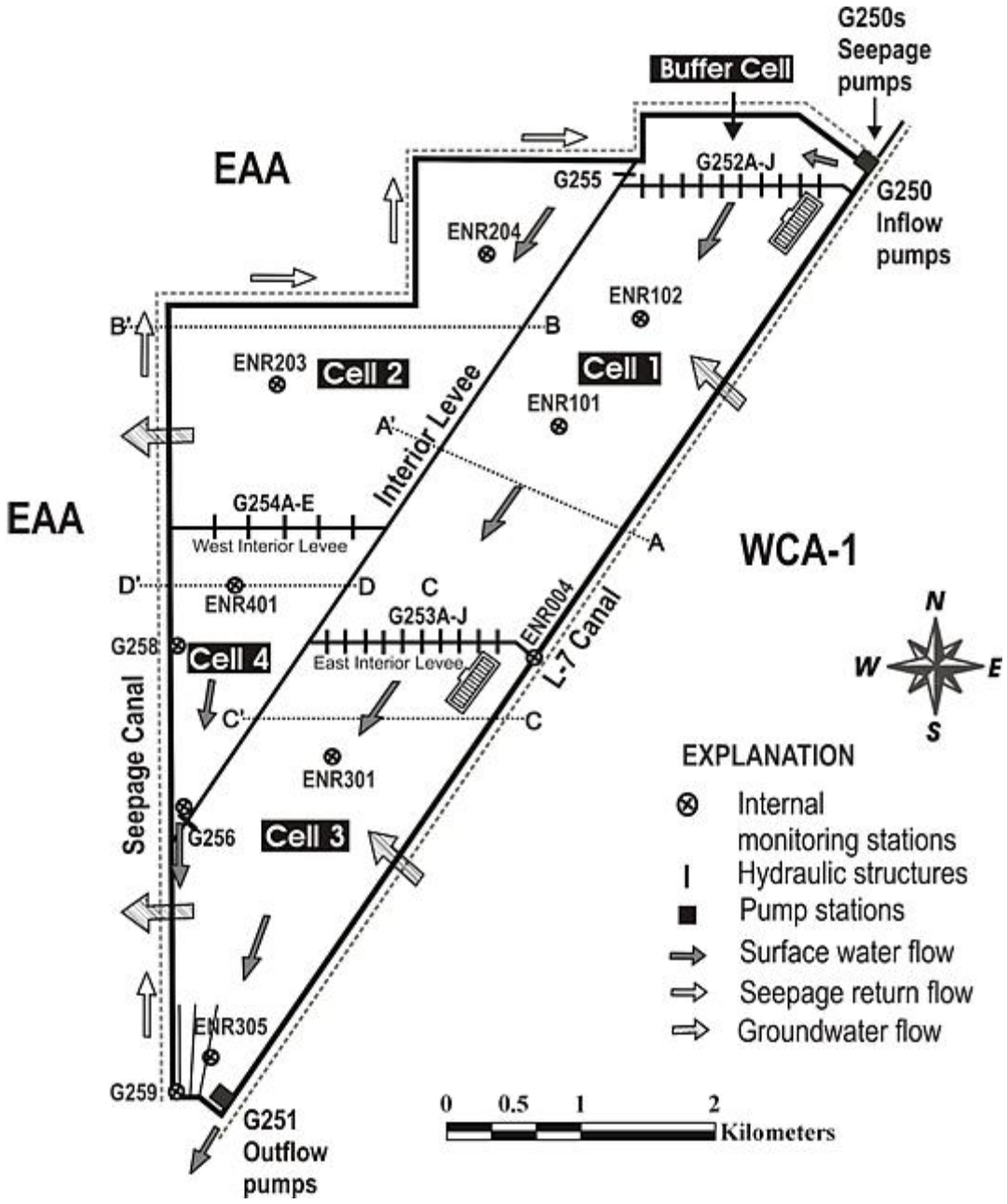

Figure 5-2. Site map of a portion of Stormwater Treatment Area 1 West (Everglades Nutrient Removal Project).

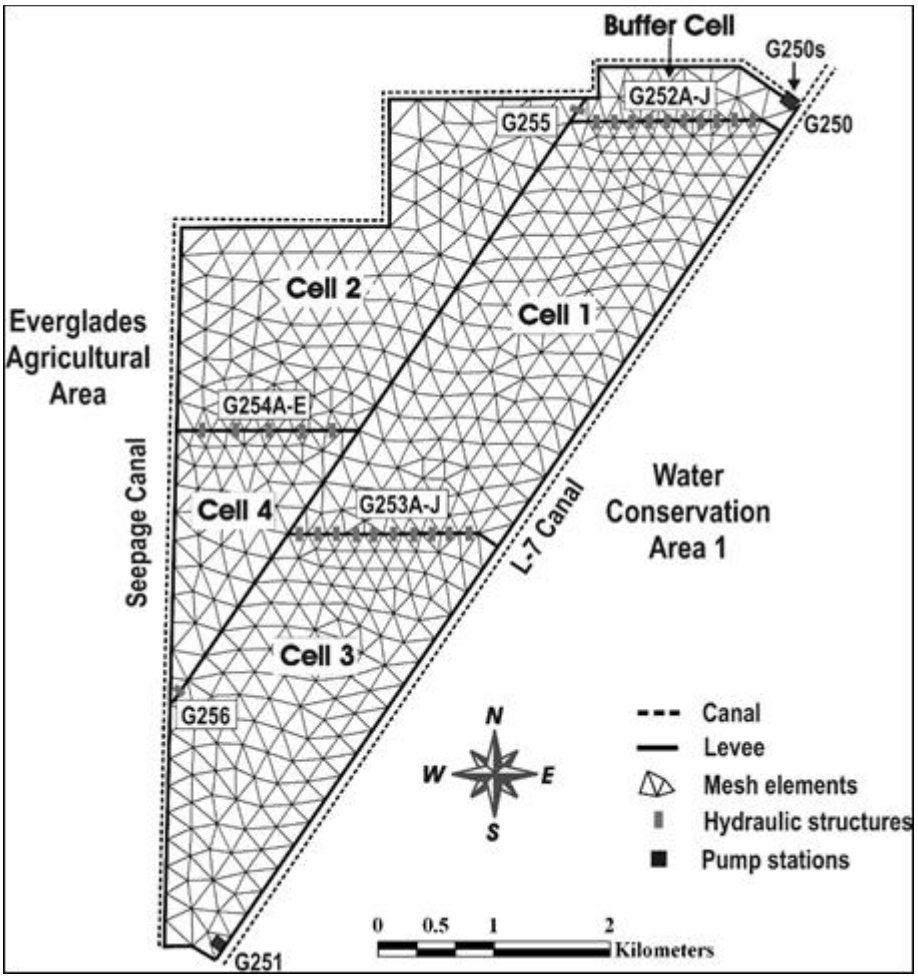

Figure 5-3. Model mesh of Stormwater Treatment Area 1 West (Cells 1 through 4).

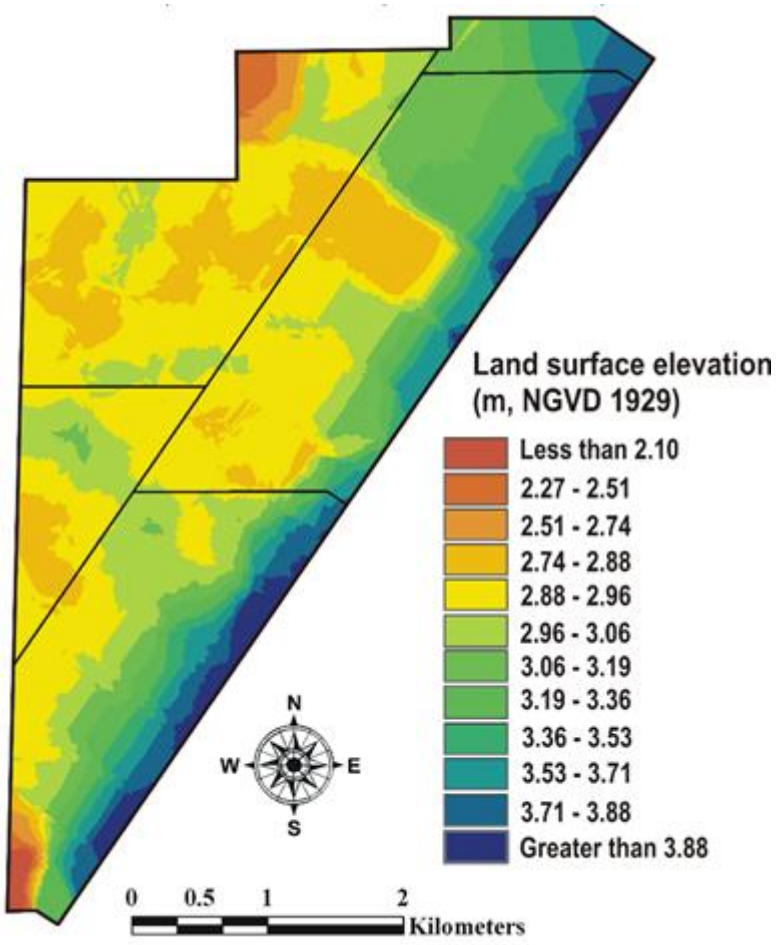

Figure 5-4. Land-surface elevation of Stormwater Treatment Area 1 West (Cells 1 through 4).

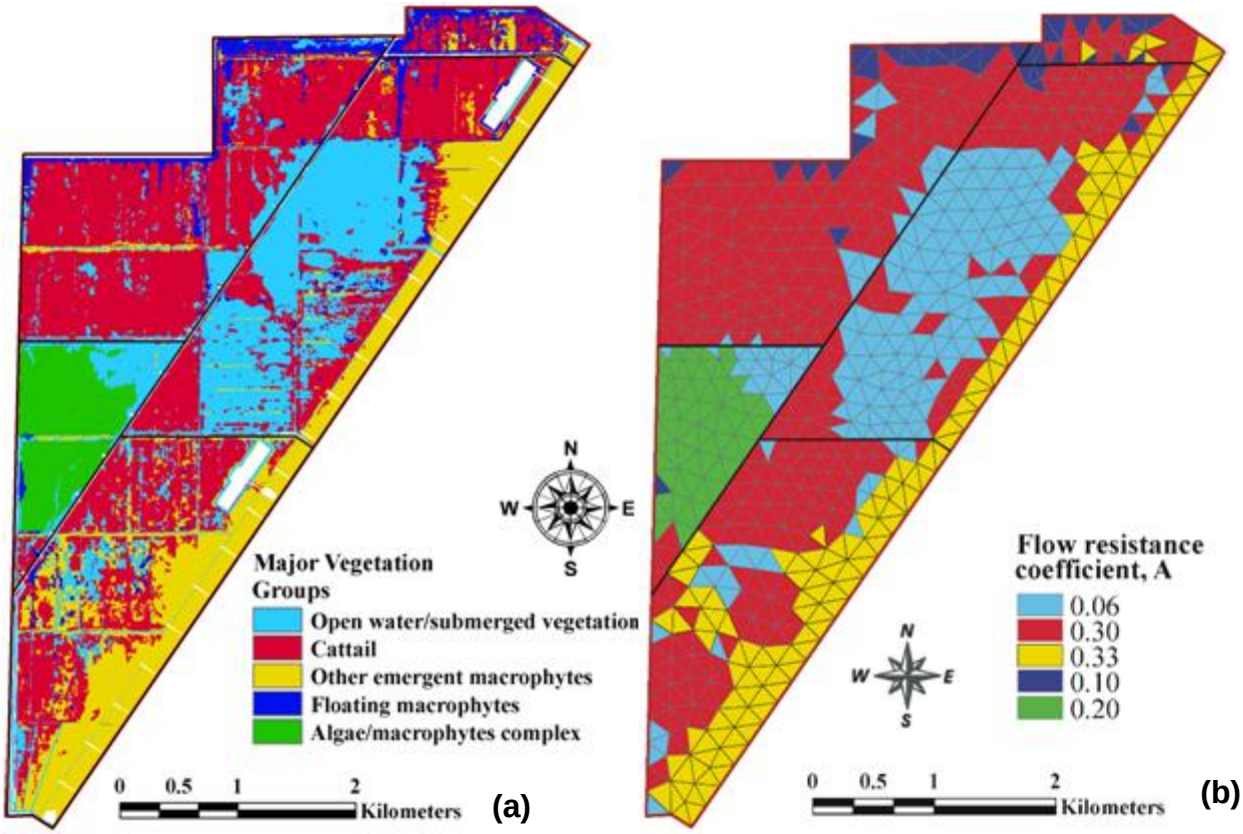

Figure 5-5. Spatial maps of Cells 1 through 4 of Stormwater Treatment Area 1 West: (a) major vegetation features (b) flow resistance coefficient (*A*) in mesh elements.

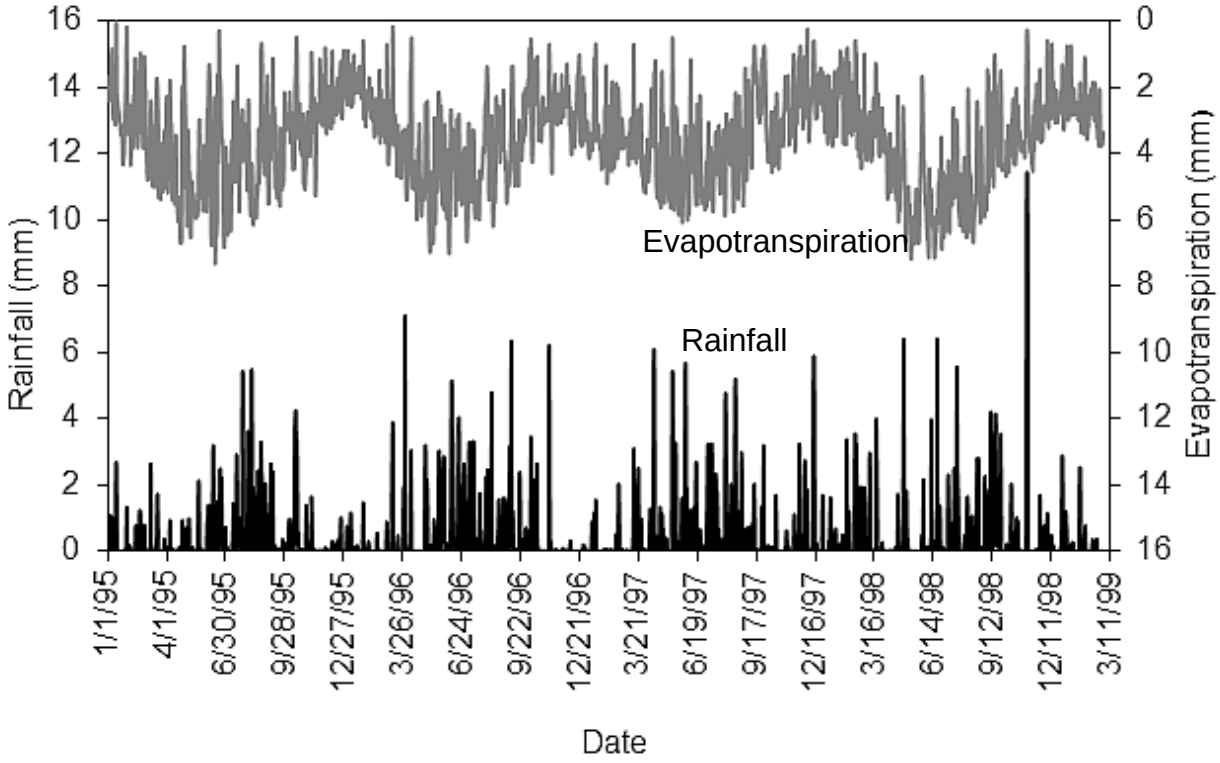

Figure 5-6. Rainfall and evapotranspiration inputs.

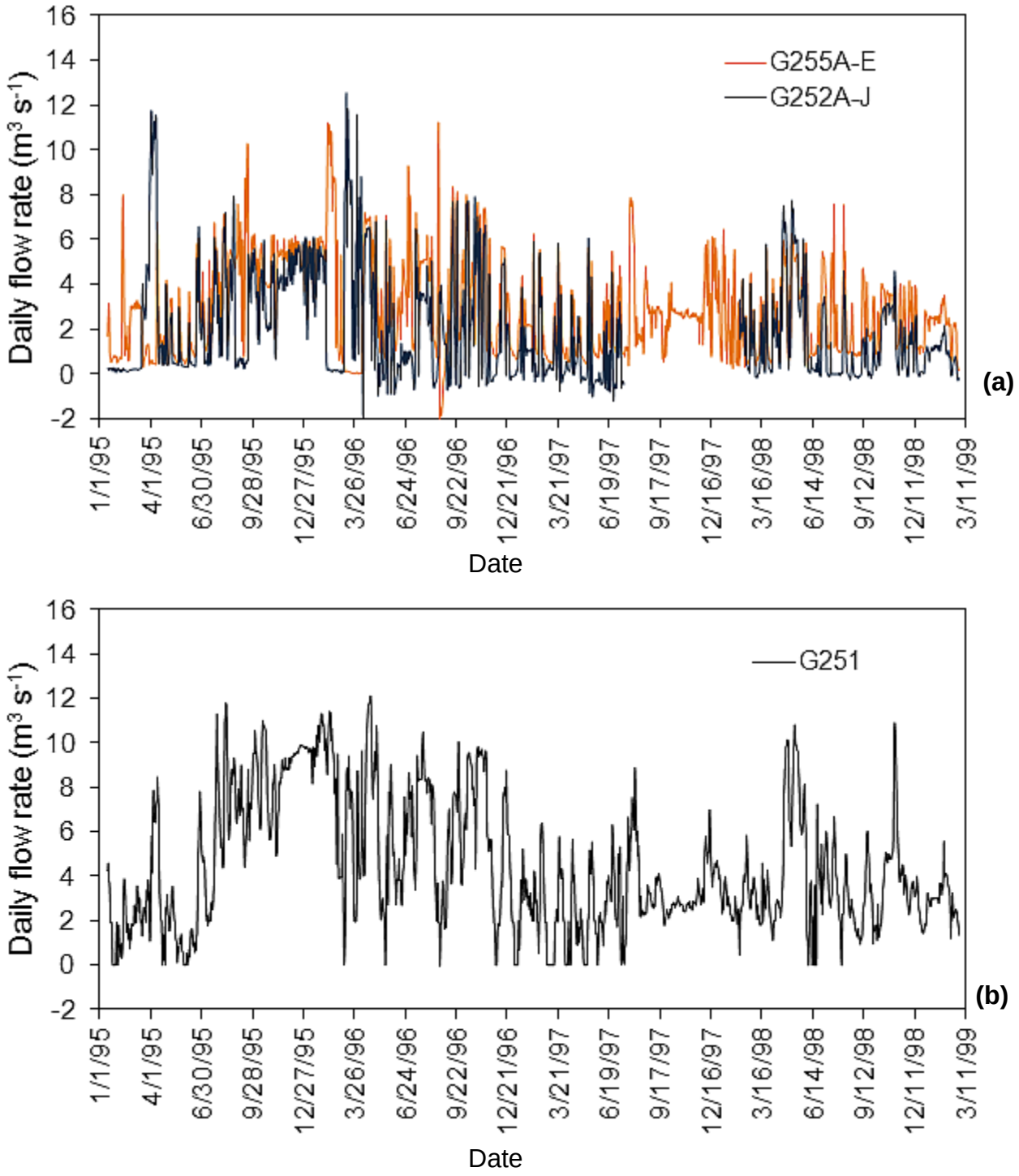

Figure 5-7. Daily flow rates used in the model: (a) inflow through G-252A-E (combined flow from 10 culverts) (b) outflow from G251 pump. The culverts G-252A-J were closed during the period from July 17, 1997 to February 4, 1998 and February 17 to 30, 1998 (Chimney et al., 2000).

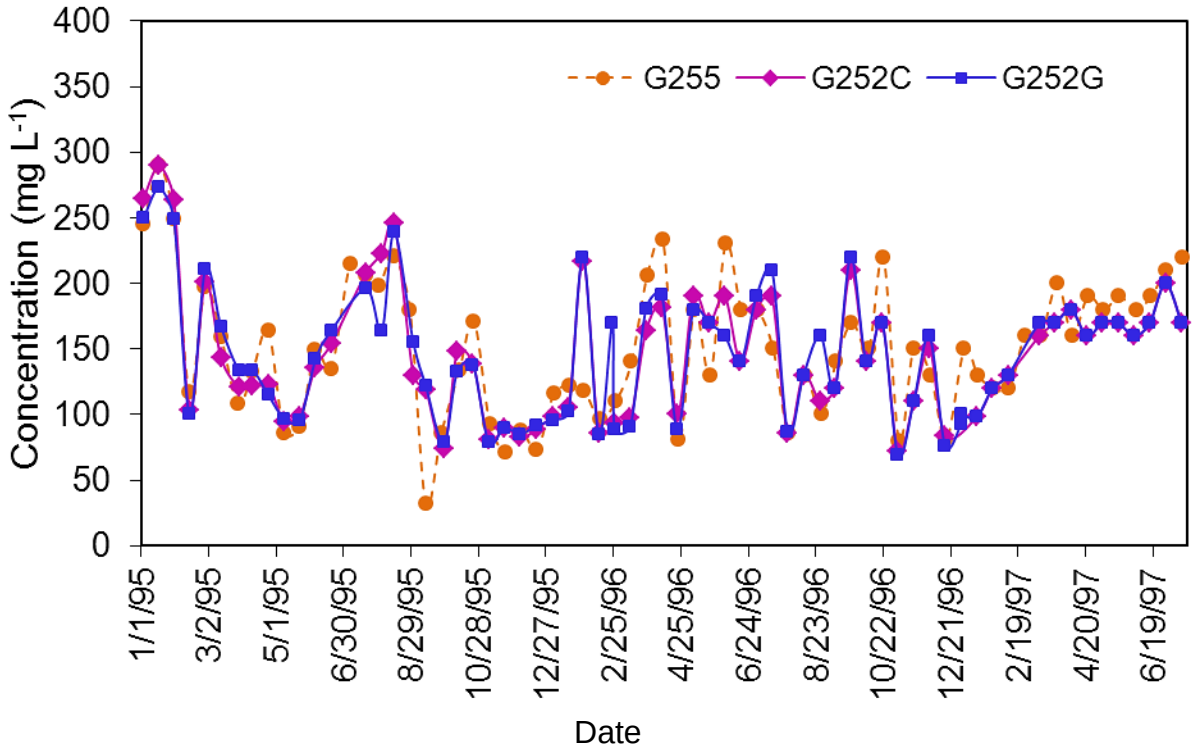

Figure 5-8. Inlet chloride concentration profiles in east and west flow-ways of Stormwater Treatment Area 1 West, used for boundary conditions during the model calibration.

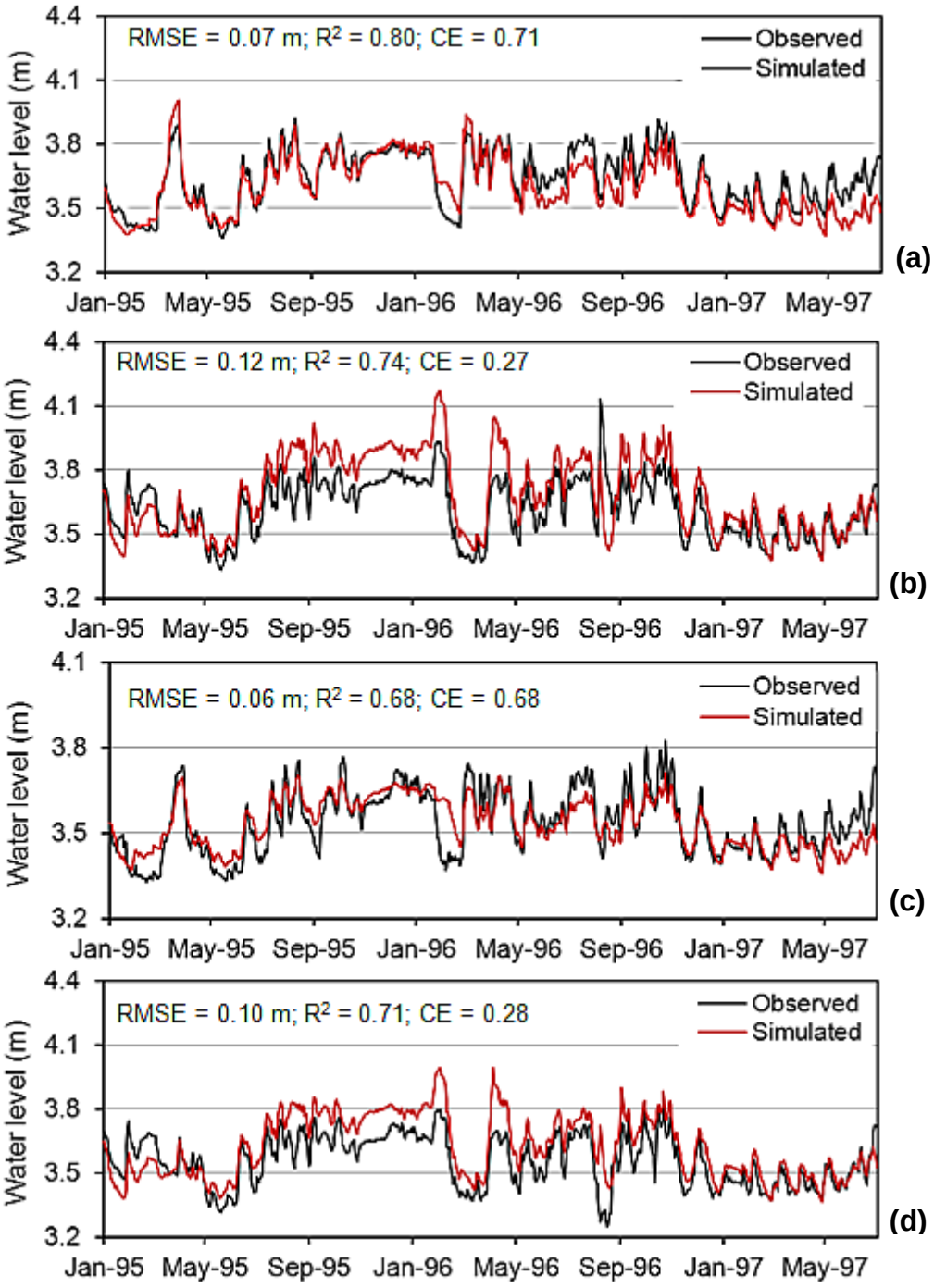

Figure 5-9. Measured and simulated water level for calibration simulation (15 January, 1995 to 15 July, 1997) at monitoring stations: (a) ENR101 (b) ENR203 (c) ENR301 (d) ENR401.

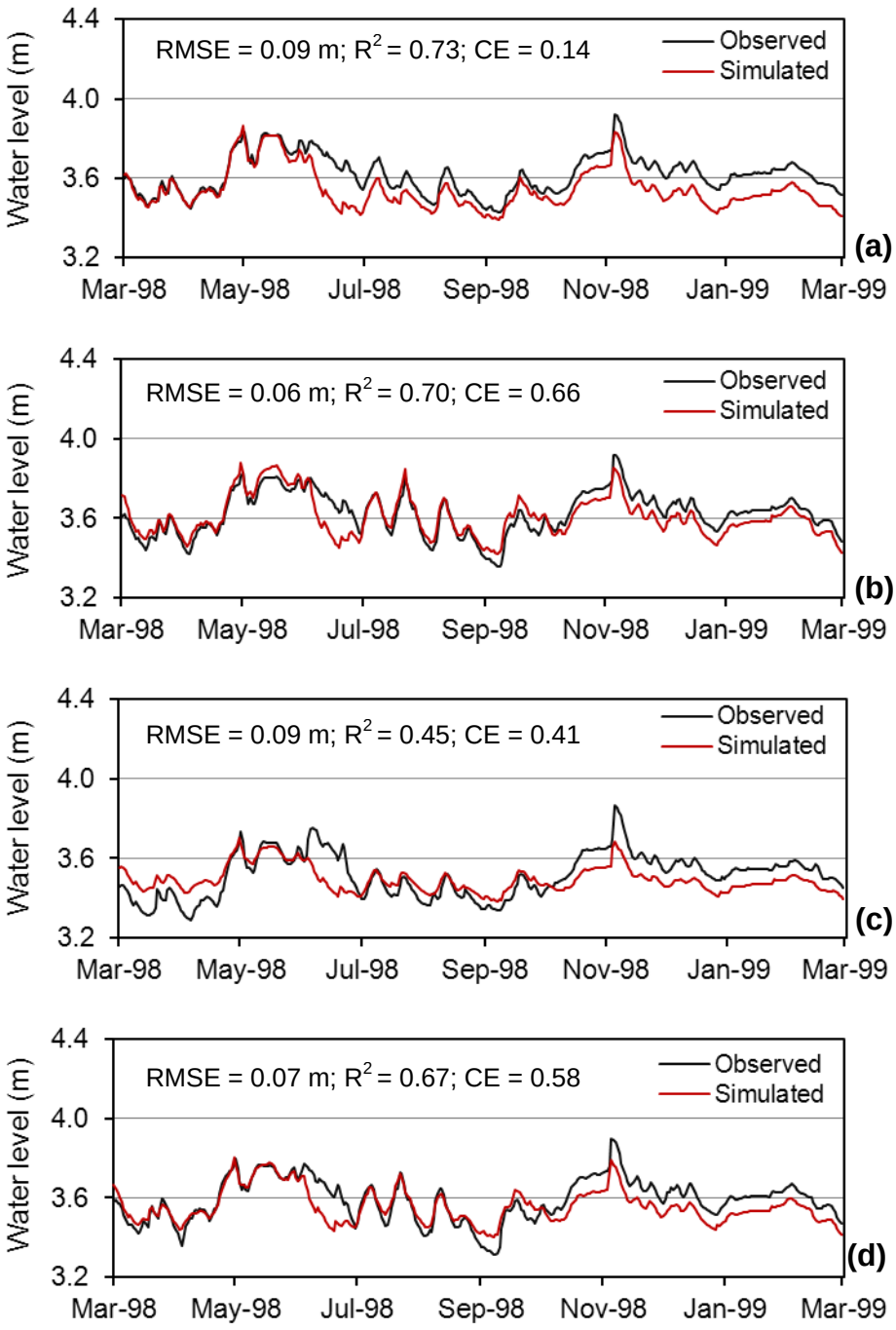

Figure 5-10. Measured and simulated water level for validation simulation (1 March, 1998 to 28 February, 1999) at monitoring stations: (a) ENR101 (b) ENR203 (c) ENR301 (d) ENR401.

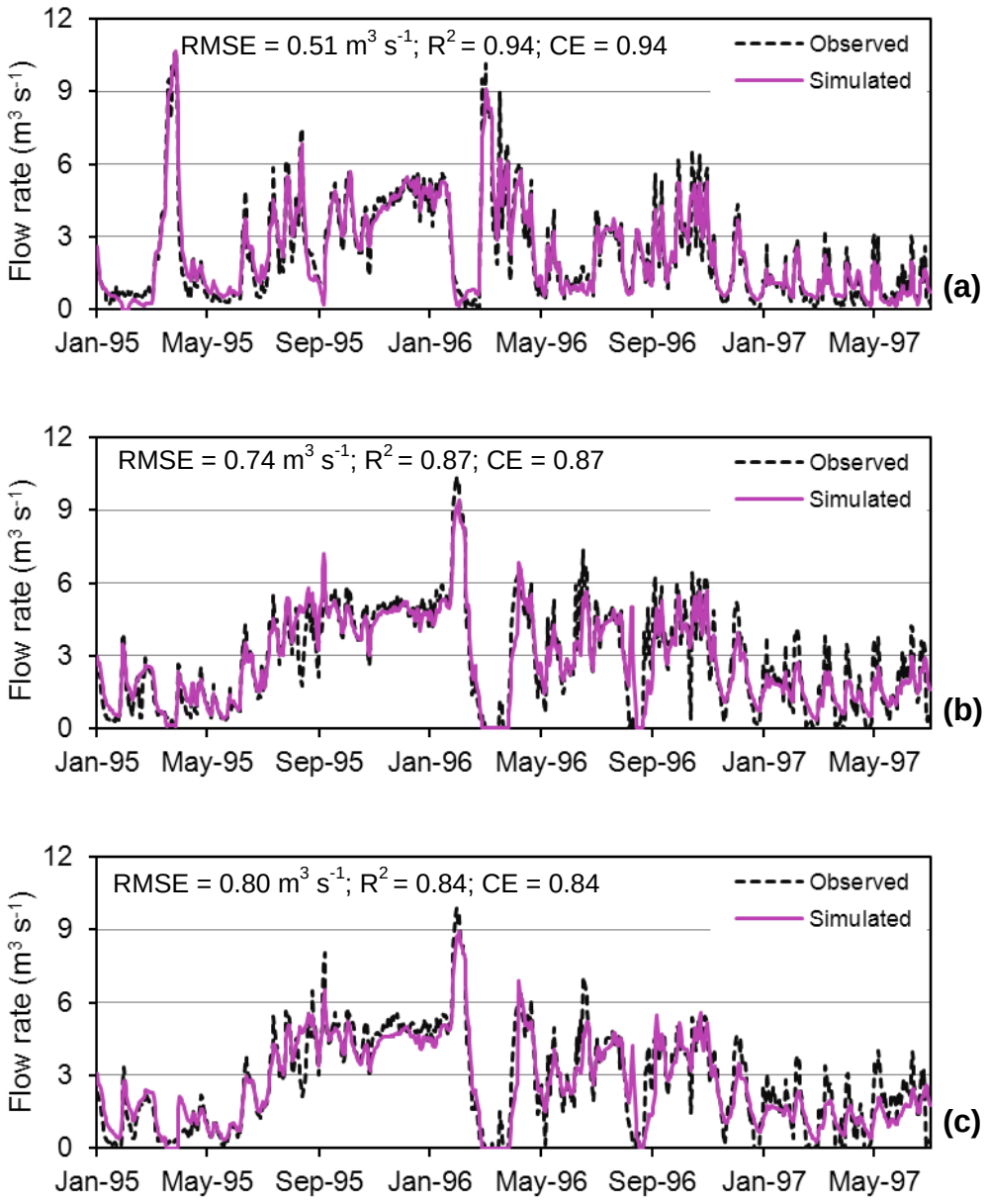

Figure 5-11. Measured and simulated daily flows for calibration simulation (15 January, 1995 to 15 July, 1997) at flow structures: (a) G-253A-J (b) G-254A-E and (c) G-256.

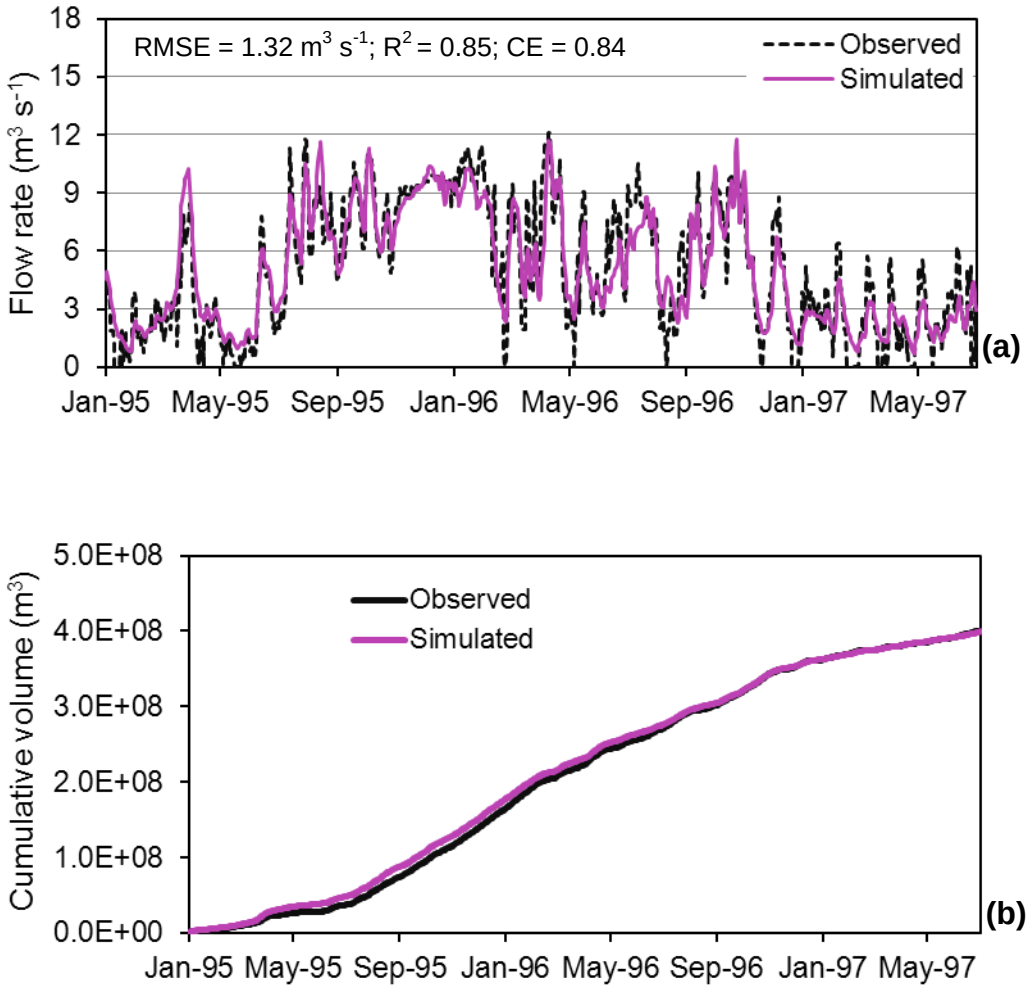

Figure 5-12. Comparison between measured and simulated values at G251 pump station: (a) daily flows, and (b) cumulative volume for the calibration simulation (15 January, 1995 to 15 July, 1997).

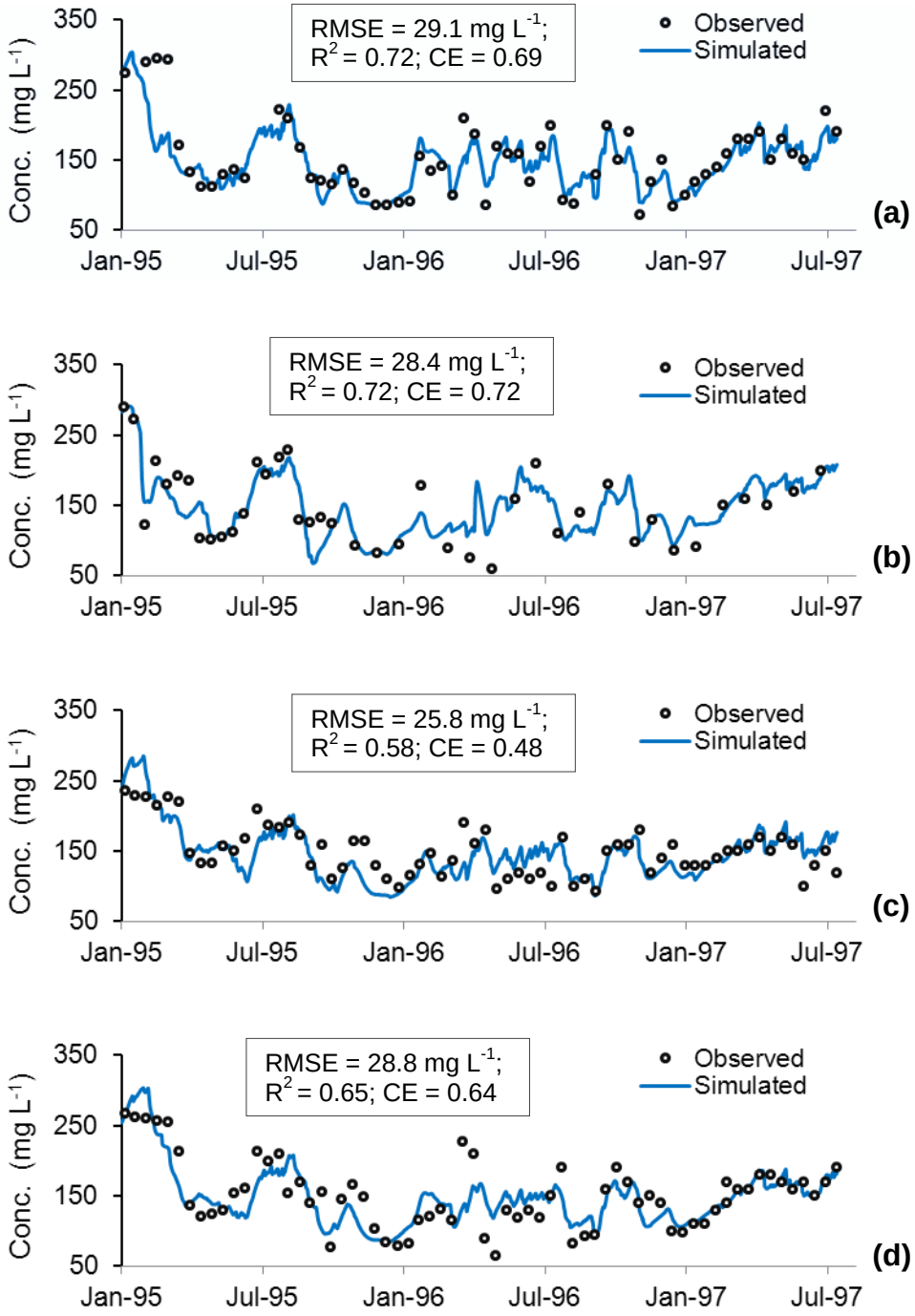

Figure 5-13. Daily simulated and biweekly measured chloride concentrations for calibration simulation (15 January, 1995 to 15 July, 1997) at monitoring sites: (a) ENR102 (b) ENR204 (c) ENR305 (d) G-253C (e) G-254D, and (f) G-256.

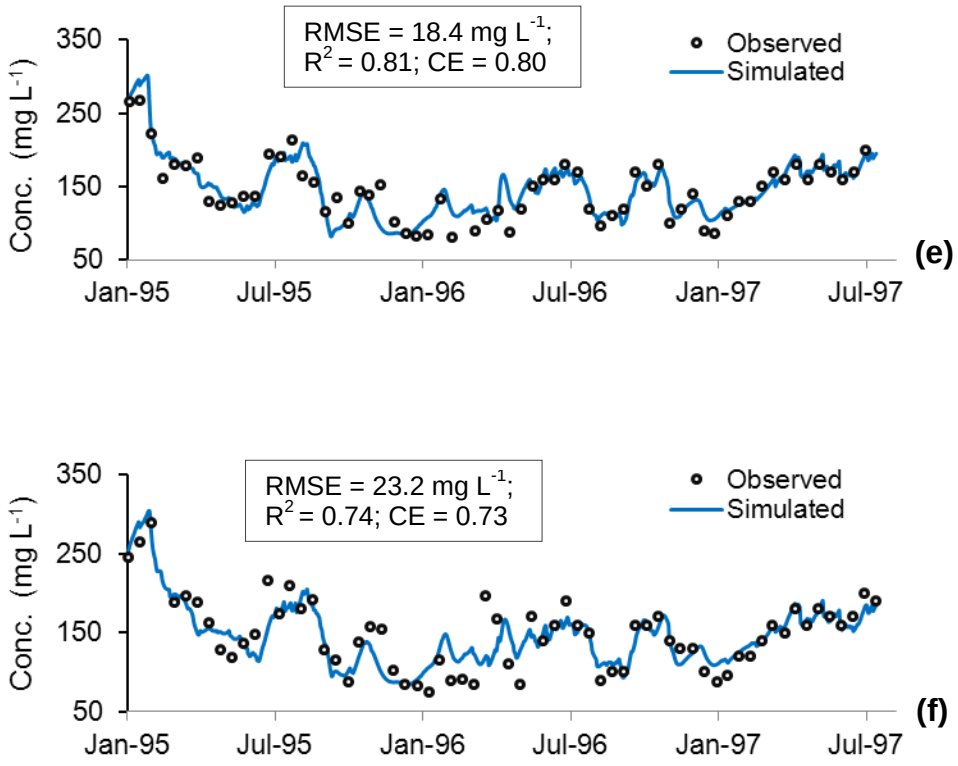

Figure 5-13. Continued.

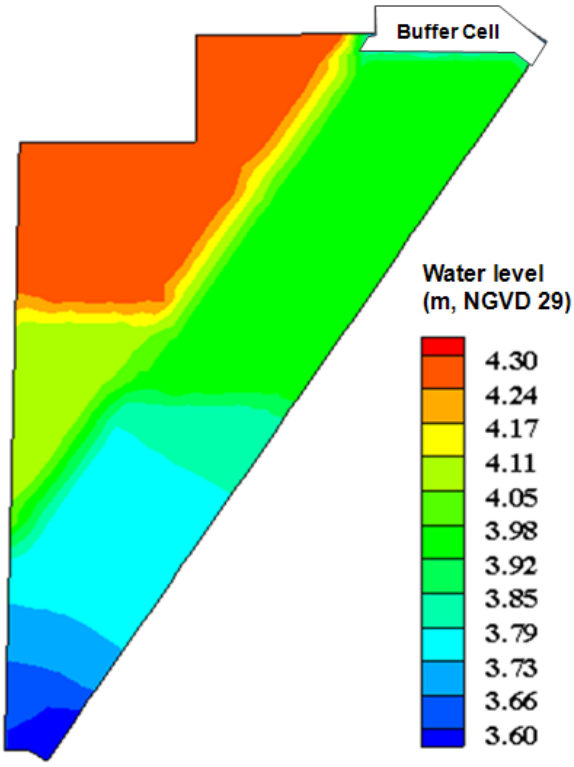

Figure 5-14. Snapshot of computed water levels for S1b scenario on August 11, 1996.

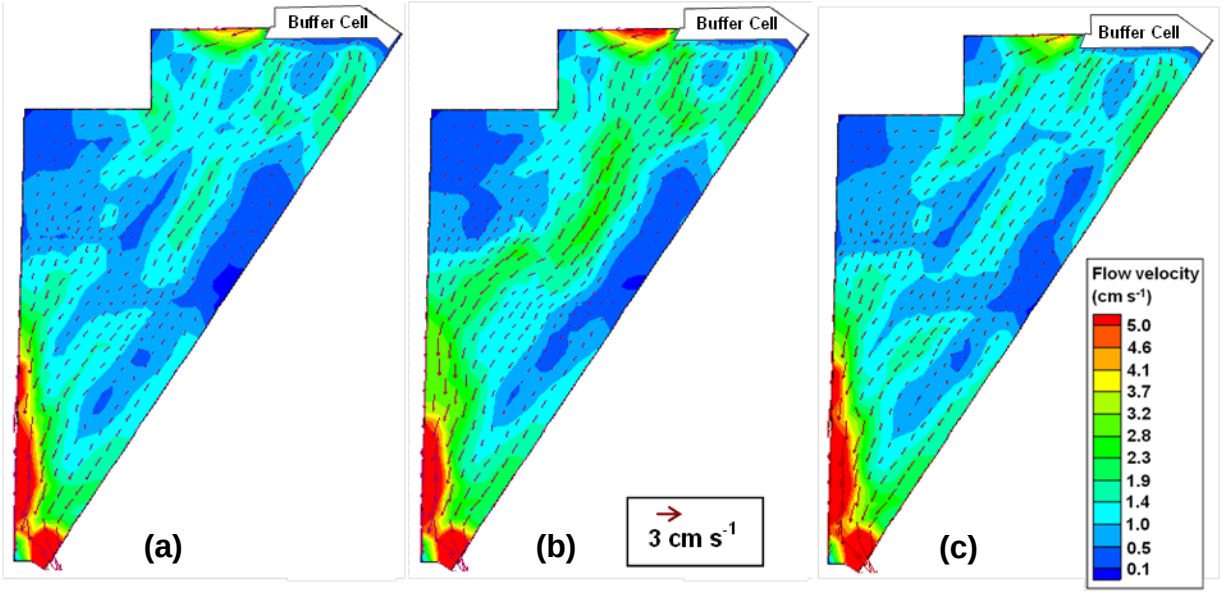

Figure 5-15. Snapshots of computed velocity in the model domain from scenario simulations (August 11, 1996): (a) S0, (b) S2a, and (c) S3a.

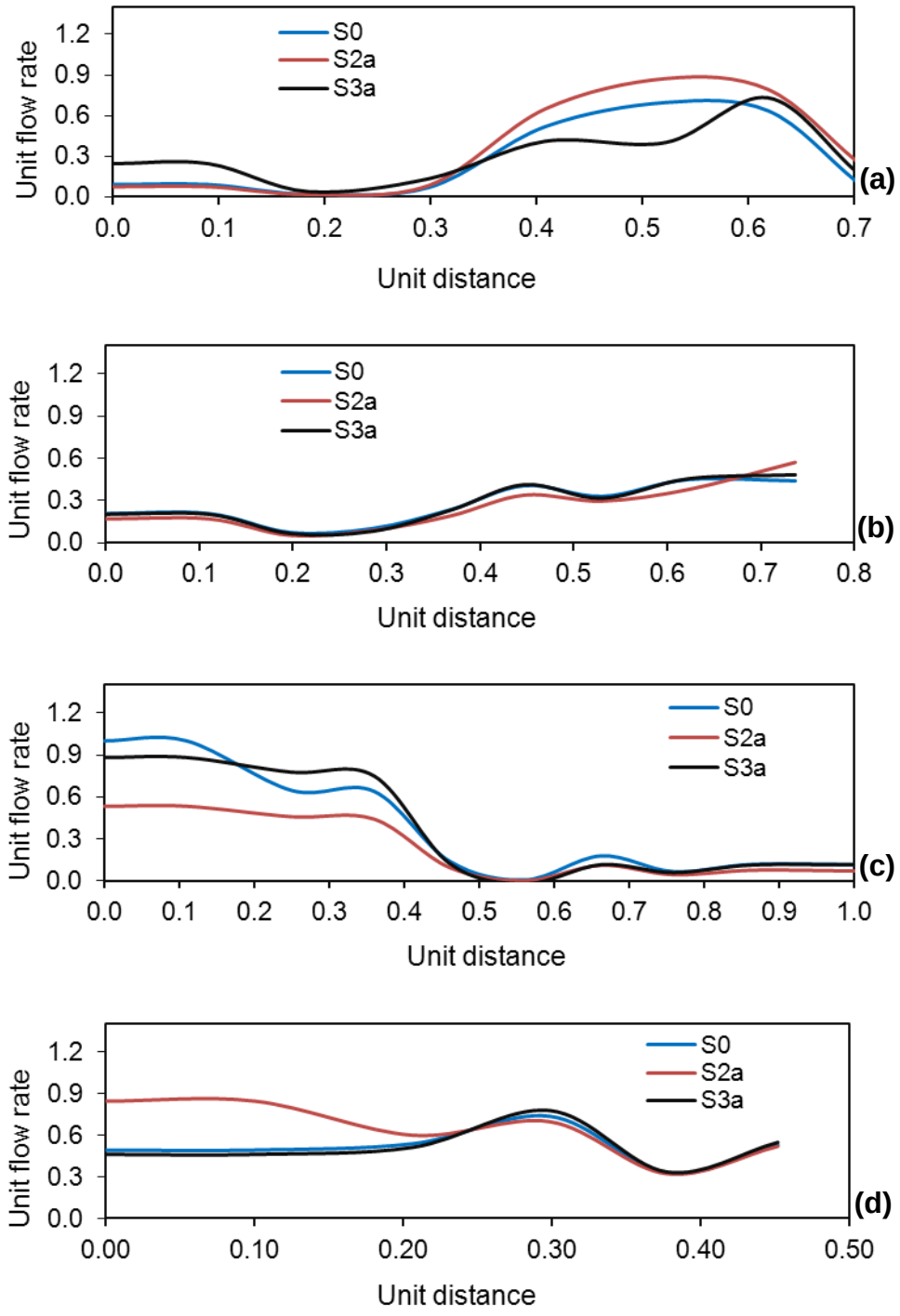

Figure 5-16. Cross-sectional unit flow for three model scenarios across (a) transect AA' of Cell 1 (b) transect BB' of Cell 3 (c) transect CC' of Cell 2, and (d) transect DD' of Cell 4. S0 is the existing condition; S2a is the levee removal and historic inflows; S3a is the change in vegetation pattern in treatment cells and historic inflows.

CHAPTER 6
PREDICTING LONG-TERM SPATIO-TEMPORAL PHOSPHORUS ACCUMULATION PATTERNS IN A CELL-NETWORK TREATMENT WETLAND

Stormwater Treatment Areas (STAs) are recognized for their ability to remove phosphorus in agricultural drainage waters through short- and long-term removal mechanisms (Chimney et al., 2000; Pietro et al., 2010). The short-term removal mechanisms primarily include sorption by variety of substrates, chemical precipitation, and direct uptake by microbes and plant communities, and the only long-term removal mechanism is the continuous peat accretion through burial in the soil/sediment (Chimney et al., 2000). To date, Everglades STAs (i.e., combined all six STAs) have retained over 1400 metric tons of total phosphorus (TP) since 1994; this amount would potentially enter the Everglades Protection Area (EPA) if STAs were not built (Germain and Pietro, 2011). The TP loads were reduced by 74 percent and concentration levels from an overall annual flow-weighted mean (FWM) TP concentration of 145 to 40 ppb (Germain and Pietro, 2011).

Surface soil relatively stores large amount of phosphorus and integrate conditions over longer time scales compared to the water column and plant biomass (Walker and Kadlec, 1996). It is critical to understand the changes in soil phosphorus levels because spatial variations in soil phosphorus levels are related to the changes in the vegetation patterns. Also, short-term mechanisms and dynamics are accountable for the longer term “memory” in the system. Exceeding the threshold level of phosphorus concentrations in the water column and soil are often used as criteria for potential detrimental effects to the marsh ecosystem (Walker and Kadlec, 1996). Determining the progression of phosphorus enrichment in the STAs will have several implications for the long-term management strategies and the sustainability of the wetland.

Over a decade of operation of the STAs, research has shown that the wetland plant communities have considerable influence on the phosphorus removal performance (Dierberg et al., 2002; Gu and Dreschel, 2008). Submerged aquatic vegetation (SAV) cells were found to be more effective in removing phosphorus as a polishing cell (producing effluent concentrations) than conventional emergent-vegetated treatment cells (Chimney et al., 2000; Dierberg et al., 2002; Juston and DeBusk, 2006). In most of the STA flow-ways, emergent-dominated front-end cells were followed by SAV dominated back-end cells (11 of the 19 STA flow paths) (Juston and DeBusk, 2011). Approximately 85% of the current STA system consists of SAV treatment cells producing final stage treatment of the flow paths). Research has been going on to understand why SAV cells are more competitive as a polishing cell. In this regard, vegetation management activities in the STAs have both operational as well as research components (Pietro et al., 2006a). Juston and DeBusk (2011) pointed out the formation of calcium-rich marl sediments by SAV as a possible cause of why SAV communities were more effective in sequestering phosphorus than muck soil under emergent-vegetated beds. Gu and Dreschel (2008) found that cattails were effective in removing DOP (approximately 60% of DOP inflows) and the SRP removal was found to be correlated with the removal of calcium in test cells of the STA 1 West (STA-1W). Also, the physical filtration of the suspended PP by emergent macrophytes could be an important mechanism to effectively remove PP at the front-end cells. Gu (2008) summarized the possible ecological reasons of why SAV communities are more effective than emergent aquatic vegetation (EAV). Author pointed out that the removal of SRP through pH-mediated co-precipitation of calcium carbonate ($CaCO_3$) could

make the SAV cells more competitive as a polishing cell in removing phosphorus from inflow discharges, in which DOP and PP were significantly removed at the front-end EAV cell. In recent years, South Florida Water Management District (SFWMD) has converted some of STAs back-end cell vegetation to SAV to improve the treatment performance of STAs (Pietro et al., 2006a).

The primary research questions of this study were to:

- Assess quantitatively how TP was transported through the heterogeneous cell-network treatment wetland
- Predict soil phosphorus accumulation in response to the changes in vegetation pattern
- Identify the processes that are likely to be dominant for the TP dynamics and the roles of biogeochemical processes in large-scale treatment wetlands

To address above mentioned objectives, the hydrodynamic/transport model described in Chapter 5 was coupled with a phosphorus biogeochemical model of four treatment cells of STA-1W, formerly known as Everglades Nutrient Removal Project (ENRP). Hydrodynamic/transport model provided the water depth and velocity fields to simulate the phosphorus transport mechanisms. As STA-1W was one of the most-studied treatment wetland in the Everglades (Dierberg et al., 2005; Reddy et al., 2006), spatio-temporal field measured data provided a good opportunity to test the model comprehensively. The model was simultaneously calibrated against 2.5-year (January 15, 1995–July 15, 1997) spatio-temporal field measured TP concentrations in the water column, monitored at eight internal locations, and the cumulative TP removal from the water column using mass balance approach for each treatment cell. In addition, simulations were performed to assess long-term (10 years) phosphorus accumulation trends in each treatment cell under: (a) existing vegetation conditions; and (b)

modification of vegetation pattern by managing EAV and SAV communities in a sequence (EAV cells followed by SAV cells). The goal of the future simulation scenarios was to investigate the spatio-temporal pattern of TP accumulation in the soil/sediment in response to the operations in a sequential treatment trains.

Methods

A spatially distributed hydrodynamic model of STA-1W described in Chapter 5 was coupled with a phosphorus biogeochemical model (Model 4; Chapter 4). Model 4 was identified as the most effective phosphorus biogeochemical model structure among a set of models; therefore, we particularly chose this model to simulate phosphorus dynamics in STA-1W. This flow-integrated model simulates the phosphorus transport and transformation mechanisms in a spatially-explicit framework.

Phosphorus Input Data

The phosphorus concentration levels at several monitoring stations were obtained from the DBHYDRO database. The inflow TP concentrations at G-255, G-252C, and G-252G hydraulic structures were the time-proportioned composite samples collected by using autosamplers on a weekly basis. However, composite samples were not available for the entire simulation period, for all locations considered in this study. In those locations, grab samples collected on a weekly/biweekly basis were used. Concentration of a specific sample date was applied to the subsequent daily flows until the next sample date. Wet deposition of TP, 10 μg L^{-1}, was based on the earlier study conducted at ENRP site (Ahn and James, 2001). Figure 6-1 presents the profile of TP concentrations at inlet hydraulic structures (G-255, G-252C, and G-252G; see Figure 5-2 for the location). TP concentrations at location ENR012 were assumed equivalent to the outflow TP concentrations via G-251 pump. Soil TP data were based on sampling

conducted by SFWMD throughout the STA-1W in different time periods. Measured time-series TP data for macrophyte were not available to compare with model simulated values; however, initial values were based on the study conducted by DB Environmental Inc. at various locations within the STA-1W (DBEL, 2004).

Model Configuration

Initialization

The model was initialized with spatial input variables. For water column TP and soil TP, spatial maps were generated using field data. FWM TP concentration data from 20 internal sampling locations at the simulation starting date were used to generate a 2-D map by using kriging interpolation scheme, and specified a unique value for each mesh element of the model domain. Initial soil TP level was based on sampling conducted by SFWMD within the STA-1W on the third-week of January, 1995. Soil TP levels in the upper 10 cm soil layer from 34 sampling locations were used to generate spatial distribution map. In STAs and Everglades region, a 0-10 cm upper soil layer was generally used to describe the soil TP concentrations (DeBusk et al., 2001; Pietro et al., 2009). Initial soil TP levels ranged from 5.5 to 10.6 g m^{-2}. Vegetation-specific TP data were limited; however, macrophyte TP variable was initialized with available spatial TP inputs of abundant vegetation classes, based on the study conducted by DBEL (2004). Vegetation samples were collected at different sampling locations of dominant plant-species beds, such as emergent macrophytes (*Typha* spp.), SAV communities (primarily *Najas guadalupensis*, *Ceratophyllum demersum*, and *Chara* spp.), and floating macrophytes (primarily *Pistia stratiotes* and *Eichhornia crassipes*). We reclassified the model domain into four vegetation classes: open water/sparse SAV, cattail, dense SAV, and mixed emergent vegetation. Floating macrophytes, sawgrass,

shurbs, and other emergent macrophyte plant communities were grouped in to the "mixed emergent vegetation" type. Spatial pattern of macrophyte TP was specified to each group of mesh elements of corresponding vegetation class. TP data for open water/sparse SAV class was not available; thus, we assigned relatively lower representative values (0.71 g m^{-2}). Atmospheric wet deposition was assumed to have a spatially- and temporally- constant concentration of 10 µg L^{-1} (Ahn and James, 2001).

Initial values of model parameters were derived from the literature, previous modeling studies conducted in STAs and Everglades region (e.g., DBEL, 2002; Walker and Kadlec, 2005; Chimney and Pietro, 2006; McCormick et al., 2006; Pietro et al., 2006b; Min, 2007; Jawitz et al., 2008; Paudel et al., 2010). As the field data were not available to empirically derive the parameter values, we used calibration to determine near optimal values. Before calibration, sensitivity analyses of parameters were initially performed in a relatively short time period (3 months) to identify the sensitivity of each parameter to the water column TP. A spatially non-uniform value of key model parameters was assigned to characterize the heterogeneity in plant communities and associated phosphorus cycling processes.

In this study, the water column TP was modeled as a mobile variable, and other two variables (i.e., soil TP and macrophyte TP) were modeled as a stabile. Mobile variables are transported in accordance with the flow dynamics, but the stabiles are not affected by the transport mechanisms. As the phosphorus-cycling processes were characterized by linear kinetics in ordinary differential form, these equations were solved by fourth-order Runge-Kutta numerical integration method. To insure numerical stability, the model was run in a relatively short time step (10-minute).

Boundary conditions

Simulation of phosphorus dynamics requires real-time boundary conditions within the model domain, which is a dynamic driver of the model. FWM TP concentration profiles measured at inlet hydraulic structures (G-255; G-252C, and G252-G) were specified as a source boundary condition. Time-varying concentrations measured at G-252C culvert were specified to culverts G-252A-E. Similarly, TP concentrations measured at G-252G were specified to culverts G-252F-J. In the west flow-way, measured concentration profiles at G-255 were used as a source/sink boundary condition. As TP concentrations were associated with the flows, source/sink boundary conditions were coincided with hydrodynamic inflow boundaries of the model domain.

Model Calibration

The model was simultaneously calibrated against the 2.5-year (January 15, 1995 – July 15, 1997) spatio-temporal field measured TP concentrations in the water column monitored at eight internal locations (ENR102, ENR103; ENR204, ENR303, ENR012, G-254B; G-253C; and G256), and the cumulative TP removal from the water column using mass balance approach for each treatment cell. The model parameters were adjusted through an iterative approach (trial and error) over a reasonable range (within available literature ranges) to produce measured dynamic water column TP concentrations. During the calibration process, the most kinetic-pathway rate constants, such as settling, recycle (turnover), macrophyte root uptake, macrophyte foliage uptake, and burial were characterized spatially non uniform values to represent the heterogeneity in vegetation communities and associated phosphorus cycling processes. Release rate constant was specified a spatially constant value (k_r = 1.97 x 10^{-4} d^{-1}) based on the previous modeling study of the STAs (Paudel et al., 2010). The model

performance was evaluated in terms of RMSE and percent model error (PME), often used in biogeochemical model applications (Robson et al., 2008; Min et al., 2011).

Simulations of Vegetation Management Alternatives

The simulations were performed to assess phosphorus accumulation trends over a 10-year period in each treatment cells under: (a) existing vegetation conditions; and (b) modification of vegetation pattern by managing EAV and SAV communities in a sequence (SAV cells followed by EAV cells). For the simulation experiments, the 10-year (1995–2004) daily measured inflow discharges at G-255 was used, and 5-year (1995-1999) inflow discharges at G-252 hydraulic structures were repeated for 10 years. Similarly, daily measured five-year (1995–1999) stages at boundary canals, rainfall, and computed ET for STA-1W (Abtew, 1996) were repeated for the 10-year simulations. A temporally constant inflow TP concentration, averaged over sixteen-year period (1995–2010) at G-255 and over 4-year period (1995-1999) at G-252 hydraulic structures were used as source boundary conditions of the model domain, which include 110.9, 61.3, and 56.6 μg L^{-1} at G-255, G-252C, and G-252G structures, respectively.

Results and Discussion

Model Performance

The values of vegetation class/group-specific model parameters were determined by the model calibration (Table 6-1). As the macrophyte TP time series data were not available, this component was maintained close to the dynamic equilibrium condition for the simulation period. This calibration approach was based on an assumption that increased TP storage through macrophyte uptake may be compensated with burial and recycle (turnover) on the long-term (Walker and Kadlec, 1996). Spatial parameters were

adjusted iteratively until the overall simulation error (RMSE) on the model fit from eight monitoring location was minimized (Table 6-2). The model results were generally agreed with spatio-temporal variation in TP concentration profiles. Particularly, the model performed poorly at the ENR102, ENR103; and ENR204 locations in terms of RMSE and at the ENR012 location in terms of PME (Table 6-2). The reason of higher PME value with ENR012 station was a smaller range of observed concentrations. In the west flow-way, the model performance was relatively better as indicated by the median statistical measures (RMSE = 23.9 μg L^{-1}; PME = 12.5%) compared to the east flow-way (RMSE = 32.7 μg L^{-1}; PME = 19.9%). For predicting water column TP concentrations within the entire site, the median RMSE and PME values were 28.9 μg L^{-1} and 17.3%, respectively. Results showed that the model was able to capture the mean behavior of the water column TP concentrations, but somewhat failed to capture the peak concentrations. There could be a possibility on the existence of unknown processes, which were not considered in this dynamic modeling study. In addition, random measurement errors in the field measured data could be another possible reason that the model failed to capture TP concentration pulses.

Cumulative TP removal from the water column was calculated using measured and simulated inflow and outflow TP concentrations based on the mass balance approach were closely matched in all treatment cells. This illustrates that the model was able to describe the average temporal trend of the water column concentrations. Given the stochastic behavior of measured TP concentrations in the water column (occasional high pulses; Figure 6-3), it was expected that the cumulative removal based on the mass balance approach could be a better approach to evaluate the model performance,

particularly if the model was intended to predict the long-term accumulation in the system.

Long-term Impacts and Implications of Managing Stormwater Treatment Areas into Parallel Treatment Trains

The simulations were performed to assess long-term phosphorus accumulation trends in each treatment cell under existing management conditions and changes in the vegetation pattern. When emergent-vegetated cell was followed by the SAV cells, higher TP accumulation was observed at front cells in both flow-ways. The possible reason could be the higher settling rate as a result of higher concentrations in the surface water. From the 2.5-year simulations, the annual rate of phosphorus removal was found to be 0.28, 0.81, 0.78, and 0.73 g m^{-2} yr^{-1} for Cell 1, Cell 2, Cell 3, and Cell 4, respectively. Simulation results of a 10-year period showed that soil TP levels rapidly increased at the inlet region of Cell 2 (Figure 6-5). The possible reason could be the lower ground surface elevation with higher water depths as well as higher settling of water column TP because of the higher concentrations in the less treated water at inlet region. Simulation results of a long-term TP accumulation have several implications for the long-term STA management, such as identifying phosphorus-enriched area above a certain threshold level to effectively manage the plant communities in the wetland, and identifying potential high internal loading zones. A less pronounced effect on the soil TP level was observed when treatment cells were managed in a sequential process trains (Figure 6-5). However, changes vegetation communities in a parallel treatment trains, (EAV to SAV at downstream cells) resulted a more uniform distribution of soil TP level in the front-end cells.

Limitations

The discrepancies between measured and simulated TP concentrations in the water column may be influenced by several factors, such as random measurement errors in the observations, lack of good and high intensity inputs, and initial/boundary data, uncertainties in the calibration parameters, and the resolution of the model mesh. In this model, the macrophyte and soil TP dynamics were not fully verified due to the lack of field measurement data; therefore, there was an intrinsic limitation in accurately calibrating the parameters associated with these variables. Most importantly, this study was primarily limited by the computational time, which constrained the detailed investigation of formal calibration, sensitivity and uncertainty analyses techniques. These analyses would increase the utility of the model to predict specific management and research questions.

Summary

A phosphorus cycling model of a cell-network treatment wetland (STA-1W) was developed based on the mass transport and kinetic equations of TP in surface water, soil and macrophyte wetland compartments. The model simulated the spatially distributed habitat-specific parameters of TP cycling processes. The model was simultaneously calibrated against the 2.5-year (January 15, 1995–July 15, 1997) spatio-temporal field measured TP concentrations in the water column monitored at eight internal locations, and the cumulative TP removal from the water column using mass balance approach for each treatment cell. The calibrated model was applied to simulate the TP accumulation pattern for 10 years under the existing vegetation conditions, and the modification of the vegetation pattern in a sequential treatment trains (EAV cells followed by SAV cells). Results show that there was not a significant accumulation of

TP at the back-end SAV cell of both east and west flow-ways as a result of vegetation conversion; however, greater TP accumulation was has been observed at the inlet zone of front-end EAV cells. Overall, this study provided insights about how changes in vegetation pattern influence the distribution of TP accumulation in the STAs.

Table 6-1. Calibrated vegetation-specific model parameters.

Kinetic rate constant	Unit	Vegetation class/group			
		G1	G2	G3	G4
TP settling rate	d^{-1}	0.0173	0.1209	0.1814	0.0346
TP release rate	d^{-1}	1.97×10^{-4}	1.97×10^{-4}	1.97×10^{-4}	1.97×10^{-4}
Macrophyte foliage TP uptake rate	d^{-1}	0.0432	0.2160	0.1037	0.3890
Macrophyte root TP uptake rate	d^{-1}	1.04×10^{-5}	4.32×10^{-4}	2.59×10^{-4}	2.19×10^{-5}
Macrophyte TP burial rate	d^{-1}	1.38×10^{-3}	2.24×10^{-3}	1.98×10^{-3}	2.70×10^{-3}
Macrophyte TP recycle rate (turnover)	d^{-1}	1.73×10^{-3}	2.76×10^{-3}	2.42×10^{-3}	3.50×10^{-3}

G1 = open water and sparse submerged vegetation; G2 = cattail and floating macrophytes; G3 = sawgrass and other emergent macrophytes; G4 = algae/macrophyte complex

Table 6-2. Performance statistics of calibration simulations.

Sampling location	Calibration	
	RMSE ($\mu g\ L^{-1}$)	PME (%)
ENR102	157.9	17.3
ENR103	145.2	12.3
ENR204	147.4	12.5
ENR303	32.7	19.9
ENR012	11.9	23.4
G-253C	25.1	20.1
G-254B	23.9	17.3
G-256	18.9	10.3

PME is defined as the RMSE divided by the range of the observed value, and multiplied by 100 to express in terms of percentage.

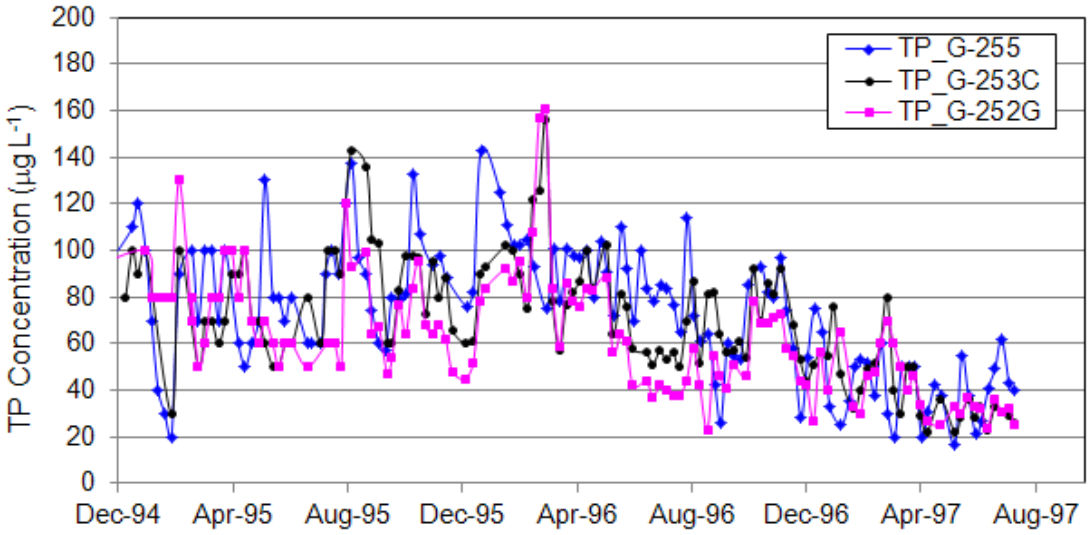

Figure 6-1. Inflow total phosphorus concentrations used in the model. G-255 was the source boundary condition for the west flow-way, and G-253C and G-253G were the source boundary conditions for the east flow-way, respectively.

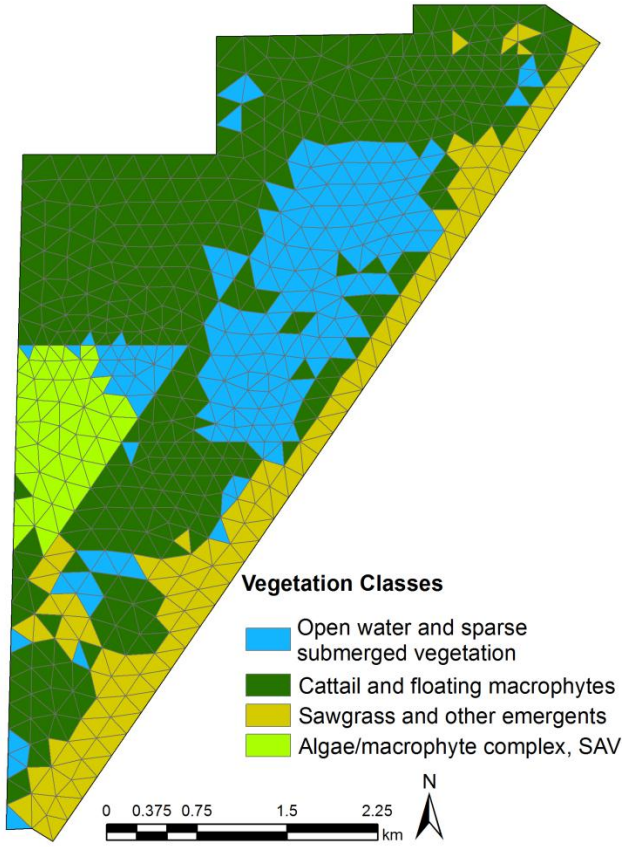

Figure 6-2. Reclassified vegetation types into four major classes and used in the model to specify vegetation class-specific phosphorus cycling parameters to primary kinetic pathways.

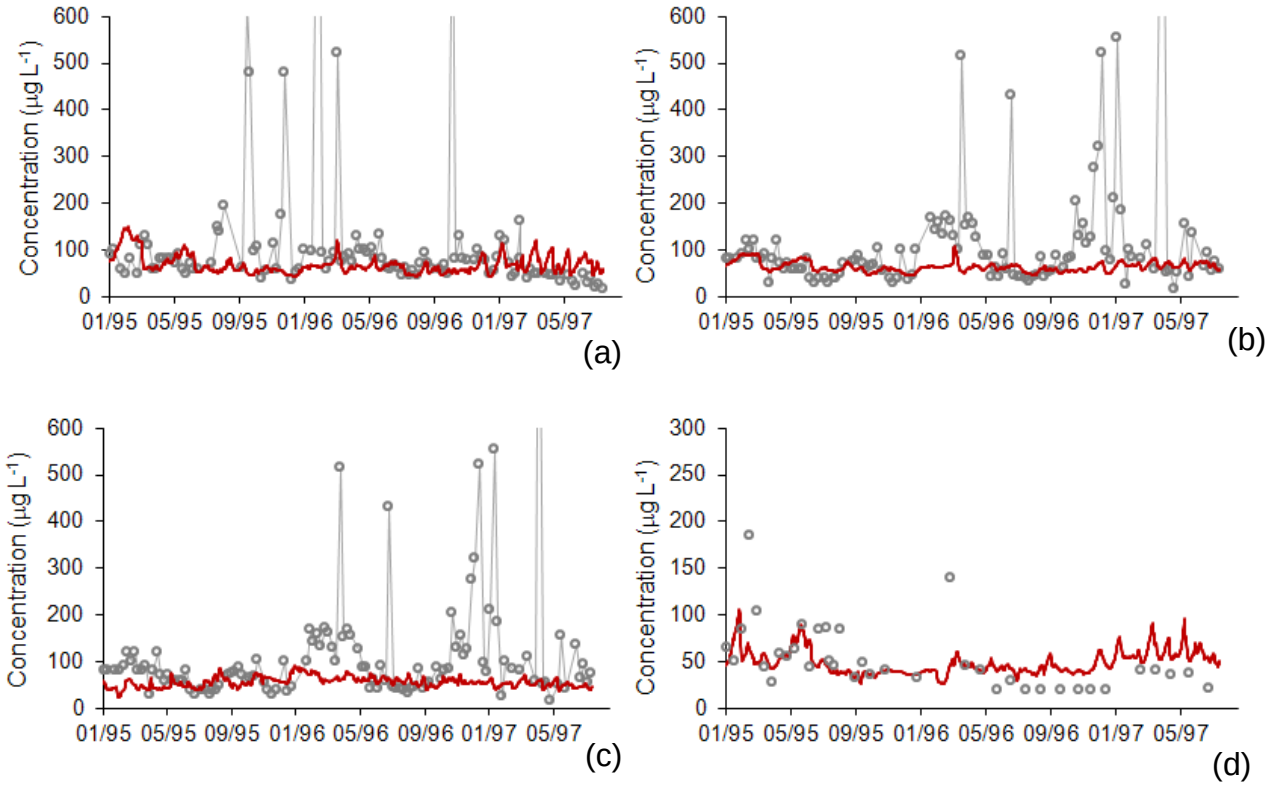

Figure 6-3. Observed weekly/bi-weekly flow-weighted mean total phosphorus concentrations (circles with or without line) and modeled (red lines) total phosphorus concentrations during the calibration period: (a) ENR102, (b) ENR103, (c) ENR204, (d) ENR303, (e) G-253C, (f) G-254B, (g) G-256, and (h) ENR102.

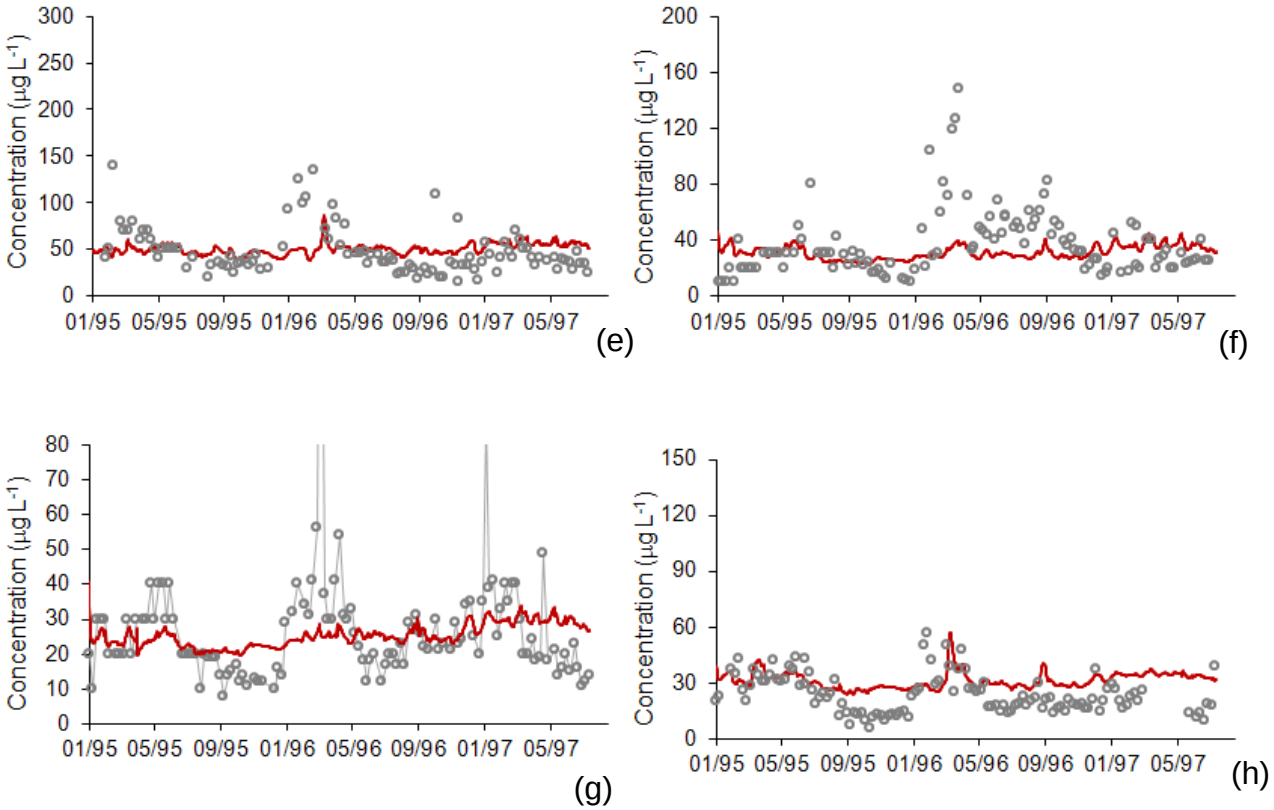

Figure 6-3. Continued.

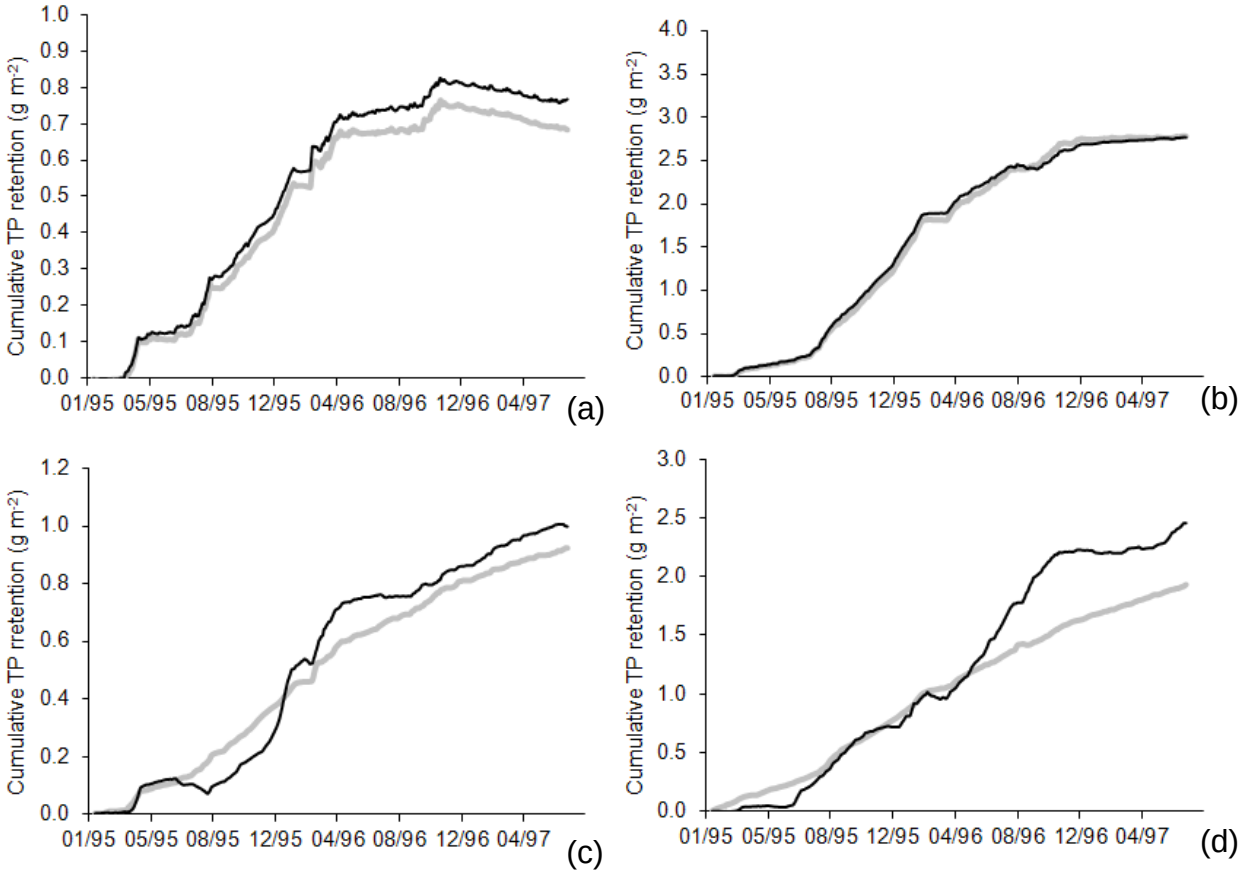

Figure 6-4. Predicted (light color) and measured (dark black) cumulative total phosphorus removal from the water column based on mass balance calculations of measured and predicted values: (a) Cell 1, (b) Cell 2, (c) Cell 3, and (d) Cell 4.

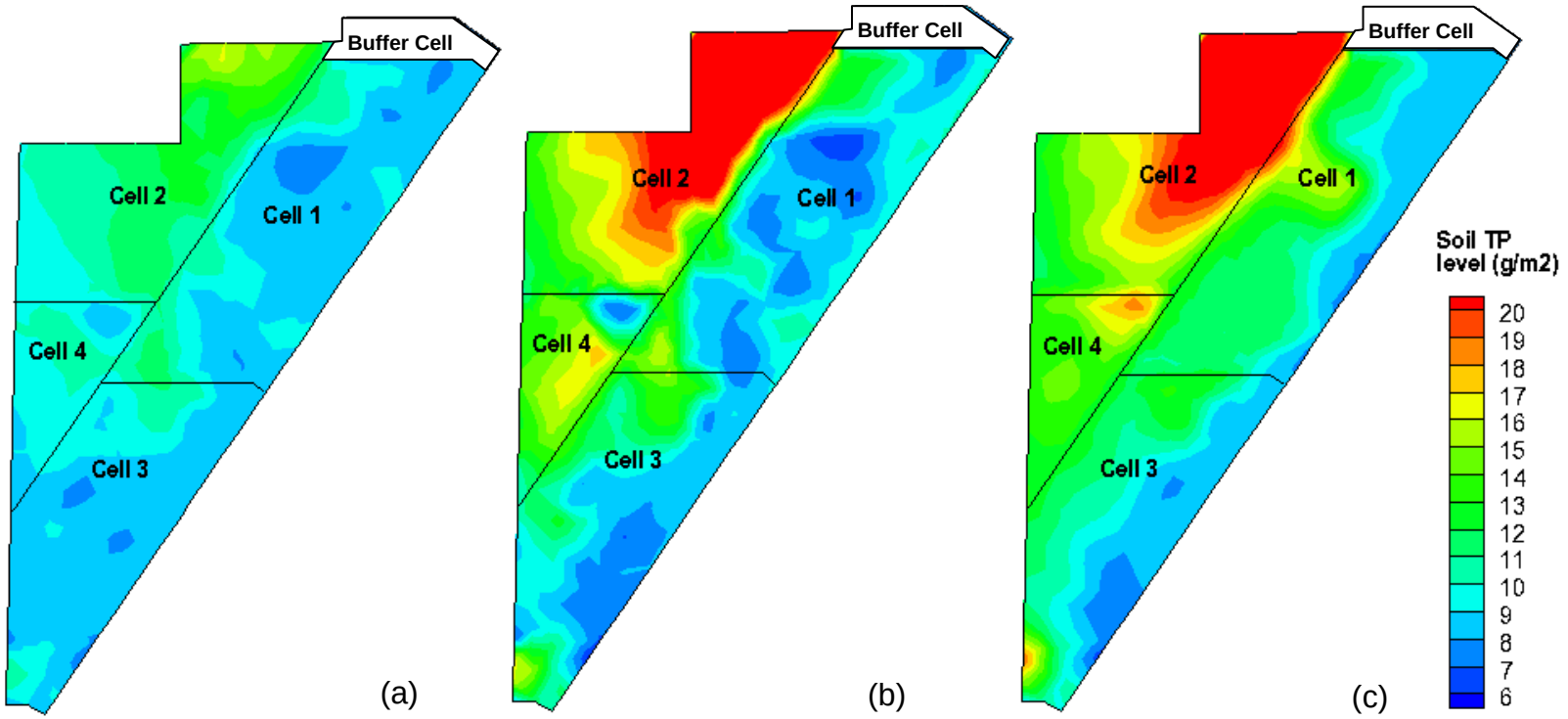

Figure 6-5. Snapshots of soil total phosphorus pattern for the upper 10 cm of the soil profile: (a) at the beginning of the simulation period (January 20, 1995); (b) under existing vegetation condition on December 29, 2004; and (c) under modification of vegetation pattern by managing vegetation communities in a sequential treatment trains (SAV cells followed by EAV cells) on December 29, 2004.

CHAPTER 7
EVALUATING POTENTIAL EFFECTS OF PRESCRIBED BURNING OF EMERGENT MACROPHYTES ON INTERNAL FLOW DYNAMICS WITHIN A STORMWATER TREATMENT WETLAND

This chapter is an illustration of the type of research and management questions that can be addressed by using a spatially distributed modeling tool.

Emergent macrophytes are the dominant form of aquatic plants in treatment wetlands (Kadlec and Wallace, 2008); they are often established in dense stands to reduce contaminants and nutrient concentrations in drainage water through physical, chemical and biological mechanisms (Thullen et al., 2005; Kadlec and Wallace, 2008). Macrophytes physically remove particulate matters through filtration and sedimentation, and other dissolved pollutants through various biogeochemical processes, such as nutrient uptake by foliage and root, adsorption by sediment, and chemical precipitation. Pollutant reduction in a treatment wetland is considerably influenced by the hydraulic features of the wetland (Kusler and Kentula, 1990). Water flow is the main pathways for pollutant transport. Other hydrodynamic factors, such as water depth and velocity affect the vegetation health and conditions and therefore the ability of the wetland to treat pollutants (Kadlec and Wallace, 2008). Flow resistance induced by the macrophyte stem/leaf drag reduces the mean flow velocity and hence increases the water levels and detention times (Jadhav and Buchberger, 1995). During the wet season, inflow rates are generally higher and therefore some parts of the wetland experience prolonged periods of high water depths. In such a case, increased flow resistance would cause several undesirable ecological consequences. Recent studies of surface-flow wetlands indicated that the composition of the emergent macrophyte (typically cattail) is profoundly influenced by the depth of flooding (Grace 1989; Squires and Van der Valk,

1992; Sharma et al., 2008). Extended submergence of emergent stands in deep water causes physiological stress and adversely influences growth, seed germination, and reproduction of vegetation species (Grace 1989; Sharma et al., 2008; Chen et al., 2010); therefore, emergent macrophytes are often constrained to depths less than 1.5 m to minimize negative ecological impacts (Kalff, 2002).

In recent years, constructed treatment wetlands are being increasingly used to treat stormwater runoff (Kadlec, 2005; Kadlec and Wallace, 2008). In South Florida, large-scale constructed treatment wetlands, known as Stormwater Treatment Areas (STAs), were built to reduce phosphorus concentrations in the agricultural runoff before entering the Everglades for the restoration of the phosphorus sensitive Everglades ecosystem (Chimney and Goforth, 2001; Noe et al., 2001; Sklar et al., 2005). The vegetation communities in these systems are primarily dominated by emergent macrophytes; among them, cattail (*Typha domingensis* and *Typha latifolia*) is one of the most abundant emergent macrophyte species, with the greatest areal coverage (Chimney et al., 2000). In order to optimize the phosphorus removal performance, South Florida Water Management District (SFWMD) has been actively engaged in managing vegetation community types and distribution within the wetland (Pietro et al., 2010). For example, emergent and floating macrophytes are frequently removed through periodic and selective use of herbicides and prescribed burning to facilitate the establishment of desired vegetation community types (Pietro et al., 2010). Recent studies have documented that submerged aquatic vegetation (SAV) was more effective in removing the phosphorus at the back-end of the flow-way as a polishing vegetation community (Chimney et al., 2000; Dierberg et al., 2002; Pietro et al., 2010); thus, some

flow-ways of these systems have been reconfigured into the sequence of two vegetation community types, typically emergent aquatic vegetation (EAV) communities are followed by SAV communities (Pietro et al., 2010). Many of the emergent macrophyte-dominated STA-cells now contain dense vegetation stands, consisting of both living and dead plant materials. At high flows, particularly during the wet season, the hydraulic resistance induced by the dense vegetation contributes to greater water depths due to reduced flow cross-sectional area (Jadhav and Buchberger, 1995; Bal et al., 2011), which has been often observed at the front-end of many of the STA flow-ways. From over a decade of the STAs operation, it has been recognized that excessive water depths have adverse impacts on the cattail (Chimney et al., 2000; Pietro et al., 2010). For example, a significant amount (approximately 40%) of the cattail standing crop died in Cell 2 of STA 1 West (STA-1W) between May 1997 and November 1998. The possible cause may be the higher water depths that may have exceeded the tolerance range for the cattail. Most noticeably, frequent high water levels were observed in the west flow-way during that period, which can be correlated with the cattail die-off in Cell 2 (Chimney and Moustafa, 1999). Such remarkable cattail mortality highlights the need for well-informed hydraulic operations to sustain desired plant communities and therefore improve the treatment performance of the STAs. As pointed out by Chen et al. (2010), 1.37 m water depth was sufficient to cause physiological stress on cattail; they presented that this water depth was harmful to both growth and reproduction of clonal cattail species. Although efforts are made to determine the cattail (*Typha domingensis*) tolerance and stress patterns in the STAs as a result of extreme water depths (Pietro et al., 2010), to date, however, the information regarding the cattail sustainability in these

systems remains unknown. Recently, SFWMD has set operating guidelines in compliance with the permit requirements for the STAs in order to reduce the effects of prolonged durations of high water levels on the vegetation health and therefore improve the treatment performance (Brown and Caldwell, 2010). Detailed information about proposed depth-duration thresholds can be found in Brown and Caldwell (2010).

Periodic burning or treating by herbicide for thinning of emergent macrophytes is often instrumental for vegetation management practices in the STAs (Pietro et al., 2010). However, the potential impacts of burning or applying herbicide to the emergent vegetation on subsequent surface-water flow behavior have been rarely investigated in large-scale wetland systems (Schaffranek et al., 2003; Miao et al., 2010). It is known that burning emergent plants can alter the vegetation properties, such as density, volume, and composition and therefore affects the hydrologic regimes in the wetland (Kirkman, 1995). A limited study of the effects of water depths on emergent macrophytes, mostly in cattail, have been investigated through field and laboratory studies (Boers and Zedlers, 2008; Sharma et al., 2008; Chen et al., 2010). However, these studies were merely focused on the species composition, growth, photosynthesis, and rhizome dynamics of cattail in response to the changes in water depths.

Characterizing the changes in hydraulic regimes as a function of flow rate and vegetation community type and condition is crucial for the sustainability of the STA vegetation communities and therefore improving the phosphorus removal performance. The primary aim of this study was to investigate the effects of large-scale vegetation conversion through burning or using herbicides of the STA emergent macrophytes on the changes in internal stage dynamics using a numerical flow model. In addition, the

goal was to explore the influence of peak inflows and outflow structure operations on the variability of water depths at the front-end (inlet region) and the back-end (outlet region) of the STA-2 Cell 2 (STA2C2), respectively. For this, a physically based, spatially distributed dynamic flow model of STA2C2 was developed and applied to wide range of vegetation management and operations using high resolution spatial topographic, vegetation coverage data, as well as spatio-temporal hydraulic data. This modeling study will help understand how the flow behavior varies with vegetation management considerations (i.e., burning dead cattail biomass for thinning; conversion of cattail to SAV) over time in large-scale patches of STAs.

Study Site

STA-2 is a large constructed freshwater wetland designed to remove phosphorus from stormwater and agricultural runoff before entering the Water Conservation Area 2A (WCA-2A). STA-2 is located in southern Palm Beach County along the northwestern boundary of WCA-2A and on the southeastern boundary of the Everglades Agricultural Area (EAA) in south Florida ($26^{o}24$'N, $80^{o}31$'W, Figure 7-1). The SFWMD built this 3372 ha (8332 acres) treatment wetland on former agricultural land and wildlife management areas (Huebner, 2008). The original STA-2 consisted of three parallel treatment flow-ways (Cells 1-3), where the flow-through operation began in 2000. An additional 770 ha (1902 acres) treatment cell was expanded as Cell 4, which became flow-capable before December 2006.

The STA-2 primarily receives stormwater runoff originating from the Hillsboro Canal and Ocean Canal drainage basins upstream of the S-6 pump station and agricultural runoff from EAA through S-6 and G-328 pump stations, respectively (Huebner, 2008). Inflows from these basins enter the supply canal and are conveyed

southward to the inflow canal, which extends across the northern perimeter of STA-2. A series of inflow culverts distributed flows from the inflow canal to the respective treatment cells. STA2C2 is located between Cell 1 and Cell 3, which receives inflows through G331A-G inflow gated culverts (Figure 7-1). Flows then move southward through the treatment cell and discharge into the Discharge Canal through G-332 gated spillway, and eventually exit to the L-6 borrow canal through STA-2 outflow pump station, G-335.

In Cell 2, 22 vegetation coverage types were identified, with cattail (*Typha sp*.), open water with or without submerged aquatic vegetation (SAV), and emergent sawgrass (*Cladium jamaicense*) the dominant types (SFWMD, 2005). Of the total areal coverage, these three vegetation types covered approximately 89% (53% cattail, 19% open water with or without SAV, and 17% emergent sawgrass). In April 2009, Cell 2 vegetation in the southern section was reconfigured, in which emergent aquatic vegetation (EAV) was converted to SAV in approximately 400 acres of land (Figure 7-1) (Germain and Pietro, 2011). Existing cattail was treated with herbicide to allow SAV establishment. As the SAV was not established in the area by the end of 2010 Water Year, a large-scale SAV inoculation was initiated in July 2010 to aid in SAV establishment in the conversion zone (Germain and Pietro, 2011).

Cell 2 was characterized by dense emergent communities, stochastic flows, uneven topography, open canal along southeastern levee, and atypical location of outflow culverts. Such stochastic and heterogeneous wetland features confound the understanding of the hydraulic behaviors within the wetland. To gain deeper understanding about the internal stage dynamics in a response to vegetation

management and flow operations, SFWMD personnel deployed pressure transducers at 8 internal locations, and these instruments are being routinely monitored. In addition, recent topographic data (surveyed in 2010), and fine resolution vegetation coverage maps were obtained from the SFWMD. These data provided excellent dataset to construct the spatially explicit flow dynamics model.

Hydrologic Data

The majority of the hydro-meteorological field measurement data employed in this study were collected by SFWMD personnel, and are publicly available on their online environmental database, DBHYDRO. These data include daily average stages at the location of hydraulic structures, daily average flow rates across culverts and spillway, and daily cumulative rainfall and evapotranspiration (ET) depths. Rainfall data were available at three gauging stations located in the proximity of the STA-2 (EAA5, S6_R, and S7_R). The arithmetic mean rainfall for these three stations was used as a spatially constant value. The ET data used in the model were derived from the data maintained in the DBHYDRO for STA-1W, located at the eastern side of the STA-2 (approximately at 25 km distance); which was considered the highest quality data available for the STA2C2 (Huebner, 2008). The average areal ET depths were based on the continuous daily data measured at automated lysimeters installed in cattail, open water/algae system, and mixed marsh and/or predicted using calibrated ET models based on the meteorological conditions (Abtew and Obeysekera, 1995; Abtew, 1996).Internal stage data were recorded in a 15-minute interval at eight internal monitoring locations within the wetland using pressure transducers

Hydrodynamic Modeling

Model Domain

Hydrologic Simulation Engine (HSE) of Regional Simulation Model (RSM), described in Chapter 2 was used as a basic modeling framework for this study. STA2C2 was represented by a two-dimensional (2-D), variable size finite element mesh of 1135 unstructured triangular elements and 632 nodes, generated in Groundwater Modeling System (GMS) v5.1 (Brigham Young University, 2004) (Figure 7-1). The mesh density was further refined in some specific areas (e.g., along eastern levee, and inlet /outlet zones) to better represent the location of flow control structures, and narrow ditches/channels to capture the local effects. The mesh resolution was particularly chosen to trade-off simulation time with a reasonable representation of spatial data (e.g., topography and vegetation). Horizontal coordinates of the model domain were in NAD83 HARN, State Plane, Florida East Zone and elevations were in NGVD 29.

Bathymetry

The ground surface elevations were estimated using kriging interpolation scheme from 211 points surveyed in 2010, along parallel transects in a north-south direction, were surveyed in 2010 were provided by SFWMD. Each computational mesh element of the model domain requires a single elevation value; therefore, an average surface elevation of raster cells (20 m x 20 m) within each mesh element, was specified in the model. The bottom elevation in marsh areas of the STA2C2 ranged approximately from 2.7 to 3.6 m (NGVD 29), with a spatial mean value of 3.2 m (NGVD 29). As indicated by the ground surface elevation, the outlet and the north-west areas were relatively deeper than the remaining areas of the model domain (Figure 7-2).

Model Configuration

The model was forced by measured daily inflows, initial water levels, rainfall, and ET data. STA2C2 received water from G-331A-G inflow culverts, and discharged to the Discharge Canal through G-332 gated spillway at the south end. Therefore, inflows were specified as a source/sink boundary condition to a specific mesh element that corresponds to the location of each culvert tailwater, and the outflow from the spillway was modeled as a constant wall-head boundary condition. An average value of historic stages recorded at G-332_H station (i.e., headwater stage of the spillway) was initially specified at the outlet boundary, and then calibrated against outflow discharge and internal stage observations. All boundaries of the model domain were specified as a no-flow boundary condition, except the outlet edge of the mesh element that corresponds to the spillway location. The measured stages on simulation starting date (September 23, 2008) at 11 stations (G-331B_T, G-331E_T, G-332_H, B-west, B-east, E-west, E-east, D-3, F-3, G-west, and G-east) were used to generate a 2-D water level map using a kriging interpolation method, and obtained stages for each element of the model to specify the initial water levels.

No direct measurement of seepage was made at STA2C2; therefore, seepage flows across levees were modeled using a cell-general head boundary condition, which determines the seepage flow as a function of stages difference between model domain and surrounding water bodies and the surficial aquifer. Net seepage was estimated using the expression:

$$Q_s = K_s\left(H_B - H_i\right) \qquad (7\text{-}1)$$

where Q_s is the seepage flow across the wall boundary ($m^3\ s^{-1}$), H_i is the water level at the *i* mesh element adjacent to the boundary wall (m), H_B is the water level on wall boundary (m), and K_s is the seepage flow coefficient ($m^2\ s^{-1}$). Daily average historical stages at STA-2 treatment cells 1 and 3 were used to establish the head at the boundary (H_B).

Hydrologic Process Module (HPM) was used to process rainfall and potential ET (PET) values, which provided the net recharge to mesh cells of the model domain (SFWMD, 2005b; Flaig et al., 2005). A "layer1nsm" HPM type was reported the most suitable for the wetland system dominated by the overland flow (Flaig et al., 2005). As ET-values were the computed areal ET, maximum PET correction coefficient for open water, and vegetation reference PET correction coefficient (K_{veg}) of "layer1nsm" HPM type were set to one.

Hydraulic Parameters

A non-linear, depth-dependent effective flow resistance coefficient (modified Manning's *n*) was simulated (for details, see Chapter 3). A geographical information system (GIS) shapefile of STA-2 vegetation coverage was obtained from the GIS data catalogue of the SFWMD (SFWMD, 2005d). The classification of vegetation community types was derived using 1:6000 CIR aerial photography collected on February 11, 2005. Here, the entire vegetation was classified into five major vegetation types/groups considering the histogram clustering pattern from GIS spatial analyst (Figure 7-3b) in order to simplify the calibration of *A* (Chapter 3). The initial *A*-values for major vegetation types were approximated based on the previous literature (DBEL, 2000; Sutron Corp., 2007; Min and Wise, 2010; Paudel et al., 2010). Because the field measured *n*-values or velocity data for specific habitat type/density were not available

for the STA2C2, calibration was used to determine the final values of *A*. During calibration process, *A* was carefully adjusted manually over a reasonable range to best-fit the spatio-temporal water levels. Previous work found *B* = -0.77 to be appropriate for most Everglades wetland plant communities (SFWMD, 2005a) and this value was used here for all vegetation types. The groundwater flow resistance was described by the hydraulic conductivity (k = 3.5 x 10-4 m s^{-1}, Harvey et al., 2000) which was applied uniformly for a single layer of 60 m thick surficial unconfined aquifer beneath the STA-2 (Reese and Wacker, 2009).

Model Calibration and Validation

The flow resistance coefficient, *A*, was calibrated to best-fit the measured stage data at six monitoring locations (B-west, B-east, E-west, E-east, G-west, G-east; see Figure 7-1 for the location) for the period from September 23, 2008 to September 30, 2009 (approximately 1 year) until the discrepancies between model generated values and observations were reduced to the smallest RMSE over six stations. Similarly, the seepage coefficient, K_s, that controls the seepage flow was adjusted by fitting the cumulative residuals of the water budget to make seepage close to the mass balance within STA2C2. The model was re-initialized with new stage data and subsequently performed validation simulations against the stage profiles at eight locations from October 1, 2009 to November 5, 2010.

The overall model performance was evaluated in terms of the ability of the model to simulate water levels in both calibration and validation periods. The established statistical measures of error and goodness-of-fit, such as RMSE, R^2, and CE were used (see Chapter 5 for the equations).

Simulation Scenarios

To evaluate the potential burning effects of emergent macrophytes on the flow regime of STA2C2, we divided emergent macrophytes dominated area into three zones, Z1, Z2, and Z3; Figure 7-3b). Changes in the depth and water levels were evaluated in both longitudinal (AA', BB') and transverse (EW1, EW2, and EW3) transects (see Figure 7-1 for the location). UNB scenario was designed to imitate the system operations and management applied from September 1, 2008 to November 30, 2010 (i.e., pre-burn condition). The next BZ1 scenario evaluated the burning effects of vegetation in Zone 1. Similarly, BZ1-2, and BZ1-3 evaluated the post-burn effects at Zone 1 and 2, and Zone 1 through Zone 3, respectively. These scenarios were expected to identify the potential benefits to reducing the flow resistance within the STA2C2 as a result of vegetation management approaches (thinning emergent macrophytes). Several peak-flow events (13 peaks) were identified from the time-series inflow data (Figure 7-4) and those periods were evaluated to assess the extent of deep water conditions. The area and the period where water depths were greater than 4 ft (1.22 m), and 3.5 ft (1.07 m), were determined.

Schaffranek et al. (2003) studied the burning (fire) of dense stand of emergent vegetation (Sawgrass; *Cladium jamaicense*) effects on the hydraulic resistance and surface-water flow behaviors in the Everglades National Park (ENP). They measured the vertical velocity profiles within 16 to 42 cm depths in nine different time periods after the burning took place (lightning ignited fire) in June 2, 2002; and found that the mean velocities at each sampling event ranged from 0.8 to 1.6 cm s^{-1}. In a similar unburned site (in terms of vegetation type and density), located in an area of dense stands of sawgrass at 280 m far from the burned site, they found that the mean velocities ranged

from 0.6 to 1.1 cm s^{-1}. Average velocities of all sampling events for unburned and burned sites were found to be 0.9 (± 0.2) cm s^{-1}, and 1.1 (± 0.2) cm s^{-1}, respectively. This indicates that the increase in average velocity in the burned site was approximately 22% greater than the unburned site. This study provided the opportunity for comparison of hydraulic resistance between pre–and–post burning conditions of STA2C2 occupied by dense emergent vegetation. It was assumed that STA2C2 had similar flow resistance behaviors to ENP site, considering the mean flow velocities. This assumption relies upon the consistent mean flow velocities observed during the pre-burning period of both systems (Cell 2; 0.5 ± 0.3 cm s^{-1}, ENP; 0.9 ± 0.2 cm s^{-1}). *A*-values of emergent macrophytes (primarily cattail, and sawgrass) of each burning zone were adjusted manually to achieve the 22% increase in the mean velocity from the pre-burn conditions. Twelve random points in each burning zone, which were consistent over space, were picked to calibrate the mean velocities.

Results and Discussion

Hydrodynamics

In general, model simulations of the water levels reproduced the features of the observed water levels in eight monitoring locations (Figure 7-5). Observed daily water levels were reasonably corresponded to the simulated water levels, as indicated by statistical metrics (Table 7-1). In addition, simulated outlet discharge was closely matched with observed discharges through G-332 spillway as well as cumulative outflow volume (Figure 7-6). Key model parameters used in the simulations are shown in the Table 7-2. *A*-values for different vegetation classes were estimated by calibration. Results show that *A*-value for the cattail (0.56) was the highest and lowest was with channels (0.05). Model validation simulations for the period from October 1, 2009 to

November 30, 2010 provided further confidence in the ability of the model to explain the field conditions outside the calibration boundaries. Results show that the validation performances were equally good as calibration performances; however, the model slightly over predicted at the F-3 location, and under predicted at G-east during the validation. A possible reason is that that the reconfigurations at the south-end of the STA2C2 (EAV to SAV) that was carried out during the model calibration period, may have affected water levels due to changes in flow paths. Keefe et al. (2010) noted that small changes in vegetation spatial distribution can have disproportionate impacts on hydraulic properties of the treatment wetland. Nevertheless, model results were encouraging to evaluate burning scenarios.

Sensitivity Analysis

Sensitivity of simulation results (water levels at 8 locations) for STA2C2 to flow resistance coefficient (*A*) were summarized in the Table 7-3. Results were expressed as sensitivity coefficients ($S_{wl,A}$), as described in Chapter 3. Coefficients were calculated for a ± 50% perturbation in *A*-values for each vegetation class. Results showed that simulated water levels were less sensitive to the changes in *A* (< 1%). At the back-end locations (G-west; G-east: and F-3) water levels had even lower sensitivity coefficients than at the front-end locations. Results indicated that sensitivity of water levels was generally declined with increasing distance from the inlet structures to changes in *A*-values of cattail and sawgrass. Simulated water levels at north-west region of the STA2C2, where open water with or without SAV and hydrilla vegetation class was dominant, were insensitive to the perturbation of *A*-values for all vegetation classes.

Vegetation Burning Effects

Cattail at the south-end of STA2C2 was reconfigured by applying herbicides in April 2009 in approximately 162 ha (400 acres) in order to convert into SAV (Germain and Pietro, 2011). During the model calibration period, slow growth of SAV was observed. As the SAV was not established in the area by the end of 2010 WY, a SAV inoculation was initiated in July 2010 to aid in the establishment process (Germain and Pietro, 2011). This indicates the evidence of considerable changes in the vegetation conditions. Also, the bottom layer contained dead and prostrate materials, and caused the flow slow until they were completely decomposed and settled (Kadlec and Wallace, 2008). After the vegetation die-off, flow resistance decreases as the drag exerted by vegetation stems and leaf reduces (Lee et al., 2004). Vegetation in the conversion area would cause gradually different flow resistance from thinning operations until the new vegetation established. In this respect, a separate hydraulic resistance parameter of the conversion area was determined through model calibration (A = 0.38).

The flow resistance parameter (A) was estimated for each designed burning zone by calibration. A-values were determined to be 0.24, 0.12, and 0.16 for Zone 1, Zone 2 and Zone 3, respectively, and applied for scenario simulations. Water levels along the transect BB' following the lowest and highest peak flow events, ranged from 3.81 to 4.24 m (difference; 0.43 m) for P7 and P11 at the front-end of the STA2C2, respectively; however, the difference in water levels at the back-end was 0.18 m (Figure 7-7a). Stage gradient changes were rapid for all peak flows at a distance approximately 4.3 to 4.8 km from the inlet (Figure 7-7b). Velocity distribution plots show that the flows deviated in an eastern direction at the south-end. These results indicate that stages at the front-end

are primarily controlled by inflows, and stages at the south-end of the wetland are primarily controlled by the outflow operations.

The burning of emergent macrophytes at different regions produced variations in the water levels. Here we demonstrated the simulation results for the highest peak flow event (P11; 37.9 $m^3 s^{-1}$) because the water level variation trends along transects for different peaks were similar.(Figure 7-8). Burning Zone 1 did not significantly influences the water levels within the STA2C2. At north-western region where frequent high water depths have been observed, had virtually no effects as a result of burning Zone 1 (Figure 7-8c). Burning Zone 1 and Zone 2 shows little effects at the front-end as indicated by approximately 5 cm difference in water levels between pre-burned and this scenario for P11; however, the effects at the south-end of the wetland is insignificant. Burning Zone 1 through 3 produced the difference in water levels greater than 10 cm around inlet areas to negligible at the south-end for P11.

Stage changes as a result of peak flow events for all 13 peaks and 4 scenarios were depicted in the Figure 7-8. Stage changes were gradually decreased with a distance from inlet structures to outlet. For a given location, higher inflow discharges generally resulted in a greater stage difference (exception to P3). P3 event was typically occurred following a long dry-up period of STA2C2. Figure 7-8 further supports our conclusion that the burning emergent macrophytes effects were more pronounced at inlet regions than at the south-end of the cell.

To identify the potential improvements over the plan to minimize deep water conditions, we estimated the duration (in days) and area (in km^2) with greater than 4 ft and 3.5 ft water depths (Table 7-4), recommended targets set as an operation plan for

STA-2 (Brown and Caldwell, 2010). These targets include avoiding 4 ft water depths for more than 3 consecutive days, and 3.5 ft for more than 10 consecutive days. By burning Zone 1 through 3, the highest improvement was achieved for P3; the cumulative area greater than 4 ft and 3.5 ft were reduced to 16.4 km^2 d from 29.2 km^2 d (43.8%), and 40.3 km^2 d to 32.2 km^2 d (20%), respectively. We picked four peak inflows events greater than 34 $m^3 s^{-1}$ (P1, P3, P8, P11) to demonstrate the duration, and areas (with percentage) with greater water depths (> 4 ft and 3.5 ft) for all four scenarios (Figure 7-10). Prolonged period of water depths were sustained when a peak flow event was followed by other peak flow events (e.g., P3). The higher improvement in minimizing deep water depths were with higher peak inflows for both recommended targets (Figure 7-11).

Summary

High water depths (greater than 4 ft) have been periodically observed in selected flow paths (typically at the north-west region) of STA2C2. Most of this wetland area was dominated by dense emergent macrophytes, which resulted in a greater flow resistance including high water depths. Most noticeably, these deep water conditions adversely influenced the emergent vegetation. Using a spatially distributed flow dynamic model, we evaluated the dynamics of the flow regime as a result of potential vegetation management considerations.

The model was constructed with fine resolution spatial topography and vegetation coverage data, and tested against 2-year stage data monitored at eight internal sampling locations. Flow resistance parameter (*A*) for major vegetation classes were estimated through model calibration, which ranged from 0.05 (channels) to 0.56 (cattail). Model simulations were extended to evaluate the burning effects of emergent

macrophytes on the variation of internal water levels. We concluded that thinning emergent macrophytes by burning or applying herbicide was not effective to minimize deep water depths within the wetland. Water depths greater than 4 ft (1.22 m) were contributed by peak flow events greater than 500 cfs (14.2 $m^3 s^{-1}$). Results indicated that stages at the front-end of the wetland were primarily controlled by inflow discharge. Similarly, stages at the south-end of the STA2C2 were influenced by outflow structure operations. Prolonged deep water depths were sustained when the peak inflow event was followed by consecutive peak inflow events. High water depths were primarily observed at the north-western area of the STA2C2 where the open water with or without SAV groups were dominant. A low sensitivity of simulated water levels for a ± 50% perturbation in *A*-values indicated that water level regime was less controlled by hydraulic resistance. It should be noted that the burning effects of vegetation on the flow regime was modeled by assuming the burning as a reduction in the hydraulic resistance. Therefore, burning emergent macrophytes had fewer impacts on the areas with deep water depths. Perhaps, the improvement in minimizing deep water areas achieved in this study could be attributed to the variation in the flow paths in burning zones. On the basis of this modeling study, thinning emergent macrophytes to minimize extended periods of water depths greater than 4 ft within STA2C2 may not be an effective management approach, depending on the magnitude of the inflow volumes and the antecedent water depths.

Table 7-1. Performance statistics of calibration and validation simulations.

Sampling location	Calibration			Validation		
	RMSE (m)	R^2	CE	RMSE (m)	R^2	CE
B-west	0.086	0.95	0.93	0.098	0.78	0.72
B-east	0.090	0.96	0.92	0.051	0.90	0.89
E-west	0.079	0.85	0.83	0.101	0.61	0.60
E-east	0.058	0.87	0.84	0.060	0.82	0.77
G-west	0.124	0.64	0.60	0.073	0.56	0.48
G-east	0.117	0.67	0.63	0.142	0.53	-0.60
D-3	-	-	-	0.059	0.88	0.70
F-3	-	-	-	0.133	0.74	-0.43

Table 7-2. Key parameters used in the model.

Symbol	Description	Value	Sources
A	Empirical constant of flow resistance, $m^{0.44}$ s		
	Cattail	0.56	Calibrated
	Sawgrass	0.42	Calibrated
	Open water with or without SAV	0.32	Calibrated
	Open channels	0.05	Calibrated
	Emergent macrophyte detritus at back-end conversion area	0.38	Calibrated
B	Empirical constant of flow resistance, unitless	-0.77	SFWMD (2005a)
K_{veg}	Vegetation reference crop potential ET correction coefficient, unitless (0-1)	1.0	Computed ET
k	Hydraulic conductivity, m s^{-1}	3.5×10^{-4}	Harvey et al. (2000)
K_S	Seepage coefficient, m^2 s^{-1}	0.007	Estimated from water budget (9/1/2008 - 1/30/2010)

Table 7-3. Sensitivity of modeled water level (*wl*) in the sampling locations to change in hydraulic resistance coefficient, *A* (± 50%).

Location	Calibration		50% Increase in *A*					50% Decrease in *A*				
	Avg. *wl*	± 1 SD (m)	vc1 (*A*=0.84)	vc2 (*A*=0.63)	vc3 (*A*=0.48)	v4 (*A*=0.08)	v5 (*A*=0.57)	vc1 (*A*=0.28)	vc2 (*A*=0.21)	vc3 (*A*=0.16)	v4 (*A*=0.03)	v5 (*A*=0.19)
			$S_{wl, A}$	$S_{wl, A}$	$S_{wl, A}$	$S_{wl, A}$	$S_{wl, A}$	$S_{wl, A}$	$S_{wl, A}$	$S_{wl, A}$	$S_{wl, A}$	$S_{wl, A}$
B-west	3.628	0.214	0.010	0.003	0.000	0.001	0.008	0.013	0.005	0.000	0.002	0.009
B-east	3.619	0.262	0.010	0.003	0.001	0.001	0.007	0.013	0.005	0.001	0.002	0.008
E-west	3.596	0.174	0.005	0.003	0.000	0.002	0.010	0.007	0.005	0.000	0.002	0.012
E-east	3.584	0.241	0.006	0.002	0.000	0.001	0.009	0.009	0.004	0.000	0.002	0.010
G-west	3.535	0.123	0.000	0.000	0.000	0.002	0.012	0.000	0.000	0.000	0.003	0.017
G-east	3.540	0.128	0.001	0.000	0.000	0.002	0.012	0.002	0.000	0.000	0.002	0.016
D-3	3.599	0.233	0.007	0.003	0.000	0.001	0.008	0.009	0.005	0.000	0.002	0.009
F-3	3.577	0.196	0.006	0.001	0.000	0.001	0.010	0.008	0.002	0.000	0.001	0.012

Sensitivity coefficient ($S_{wl, A}$) defined as the ratio of the change of approximately 2-year (September 23, 2008 to November 30, 2010) averaged *wl* to the change of hydraulic resistance coefficient, *A* for ± 50% change in the coefficient.
vc1 = cattail; vc2 = sawgrass; vc3 = open water with or without SAV+ open water with hydrilla; vc4 = channel; vc5 = reconfigured area vegetation after herbicide application (conversion area).

Table 7-4. Estimated duration and cumulative area of deep water conditions (water depths greater than 4 ft, and 3.5 ft) within the Stormwater Treatment Area 2 Cell 2.

ID	Inflows	Inflow rate	UNB				BZ1				BZ1-2				BZ1-3			
			WD >4'		WD >3.5'		WD >4'		WD >3.5'		WD >4'		WD >3.5'		WD >4'		WD >3.5'	
	date	(m^3/s)	(d)	A_c	(d)	A_c	(d)	A_c	(d)	A_c	(d)	A_c	(d)	A_c	(d)	A_c	(d)	A_c
P1	9/6/2008	34.9	7	7.2	10	13.7	7	7.2	10	13.4	5	6.7	9	12.4	5	5.5	8	9.6
P2	9/30/2008	33.0	8	8.2	11	14.6	8	8.0	11	14.2	7	6.5	10	13.3	4	3.1	9	10.3
P3	5/21/2009	35.5	23	29.2	27	40.3	23	29.2	27	40.0	22	26.9	26	36.9	21	16.4	25	32.2
P4	7/1/2009	28.5	5	6.7	7	9.8	5	6.7	7	9.6	5	6.1	7	8.7	4	4.1	6	7.2
P5	8/12/2009	28.7	4	3.6	9	10.2	4	3.6	9	10.2	4	2.3	8	8.9	1	0.4	7	5.7
P6	9/27/2009	22.7	1	0.8	5	4.8	1	0.8	5	4.7	1	0.4	4	4.0	0	0.0	3	2.0
P7	12/14/2009	11.2	0	0.0	0	0.0	0	0.0	0	0.0	0	0.0	0	0.0	0	0.0	0	0.0
P8	3/13/2010	34.5	4	5.3	8	9.5	4	5.3	8	9.4	4	5.0	7	8.0	4	3.0	5	6.1
P9	4/27/2010	27.2	2	1.5	5	5.6	2	1.4	5	5.5	1	0.9	4	4.6	1	0.2	4	2.7
P10	6/4/2010	29.7	5	6.1	7	9.9	5	6.1	7	9.7	5	5.5	7	8.8	4	4.1	5	7.1
P11	7/6/2010	37.9	5	5.3	8	8.8	5	5.2	8	8.6	4	4.5	6	8.0	4	3.0	5	6.4
P12	9/7/2010	29.1	8	7.7	11	12.9	8	7.7	11	12.9	6	6.2	9	11.8	4	3.3	8	9.8
P13	9/29/2010	16.8	0	0.0	3	2.0	0	0.0	3	2.0	0	0.0	3	1.1	0	0.0	0	0.0

WD represents the water depth, and A_c represents the cumulative area integrated over duration (km^2 d).

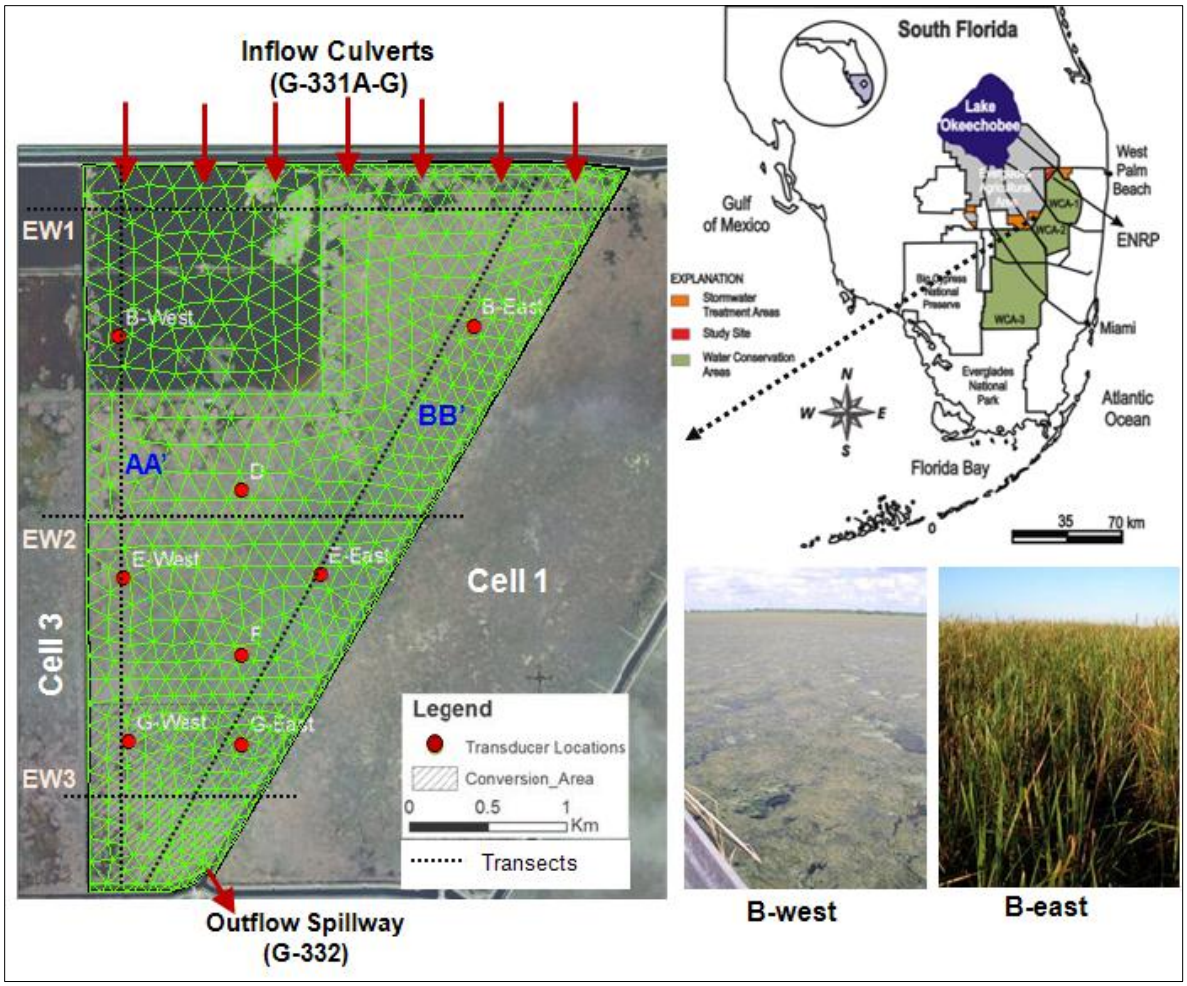

Figure 7-1. Location and plan view of study area, Stormwater Treatment Area 2 Cell 2 with inlet and outlet hydraulic structures (G-331A-G, G-332), sampling locations, transects and the computational model mesh.

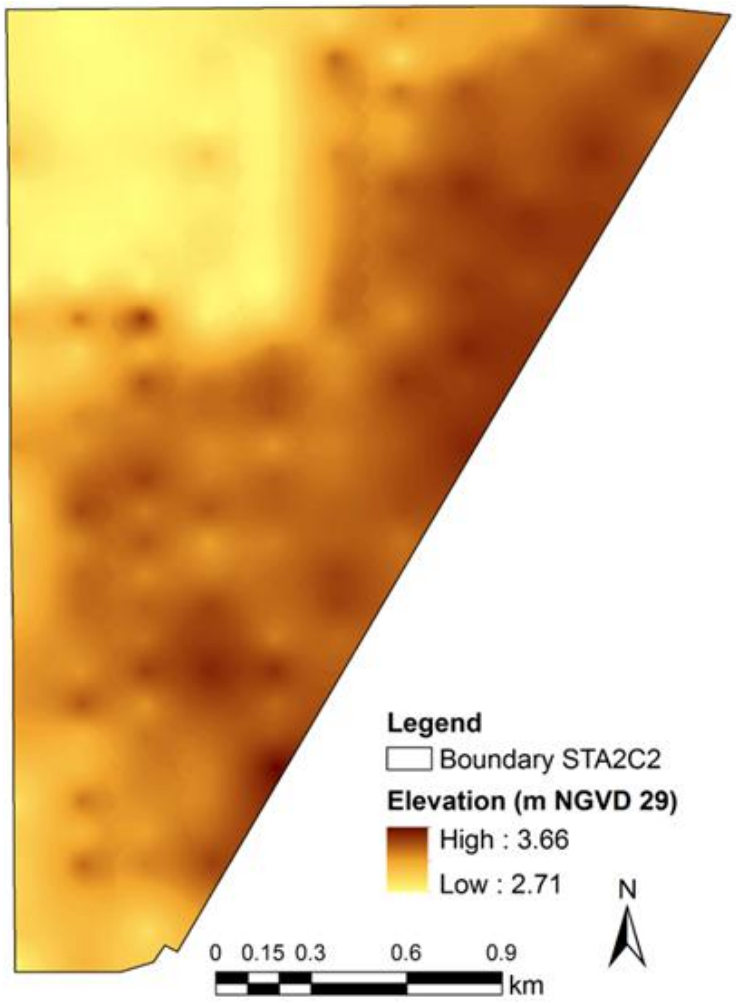

Figure 7-2. Bathymetry of Stormwater Treatment Area 2 Cell 2.

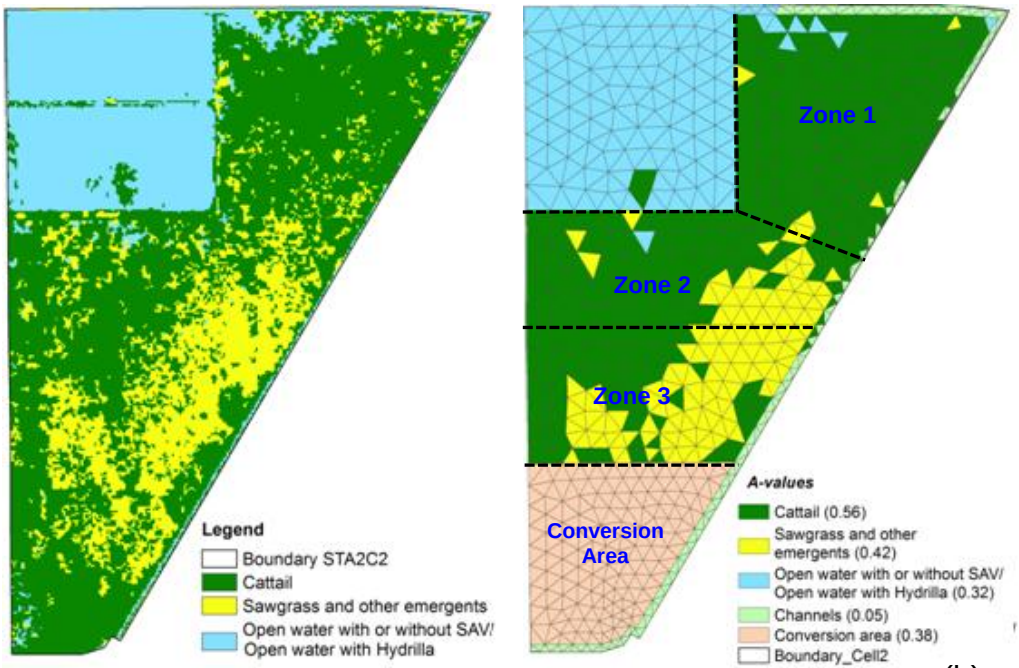

Figure 7-3. Vegetation distribution in Cell 2 of Stormwater Treatment Area 2: (a) reclassified major vegetation classes, (b) flow resistance coeficient (*A*) used in the model for different vegetation groups/classes, and zones used for model application.

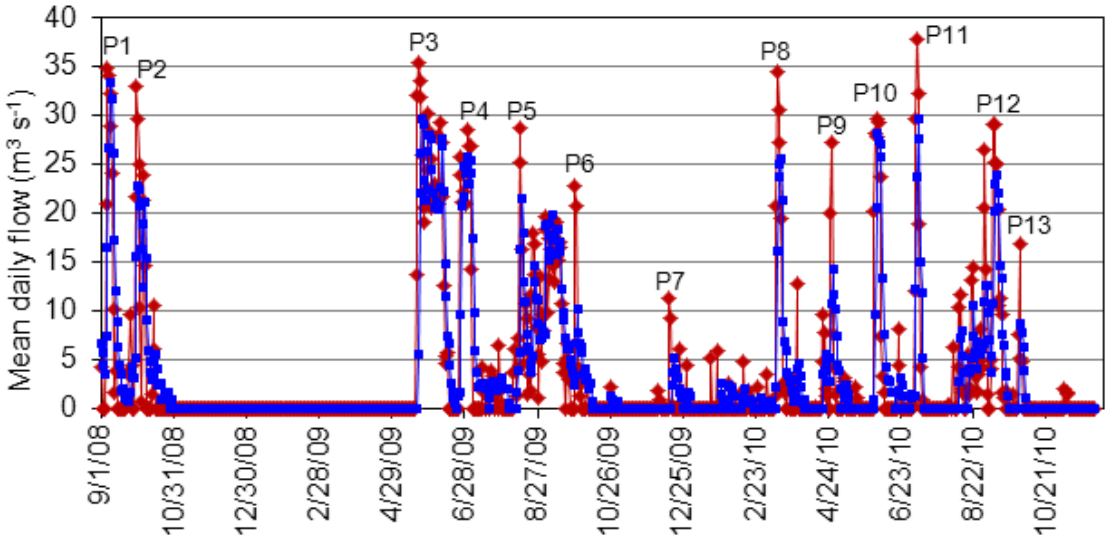

Figure 7-4. Measured daily averaged inflow (red line) and outflow (blue line) discharges with designated peak inflow events. Inflows represent the combined flows of all inflow culverts (G-331A to G-331G).

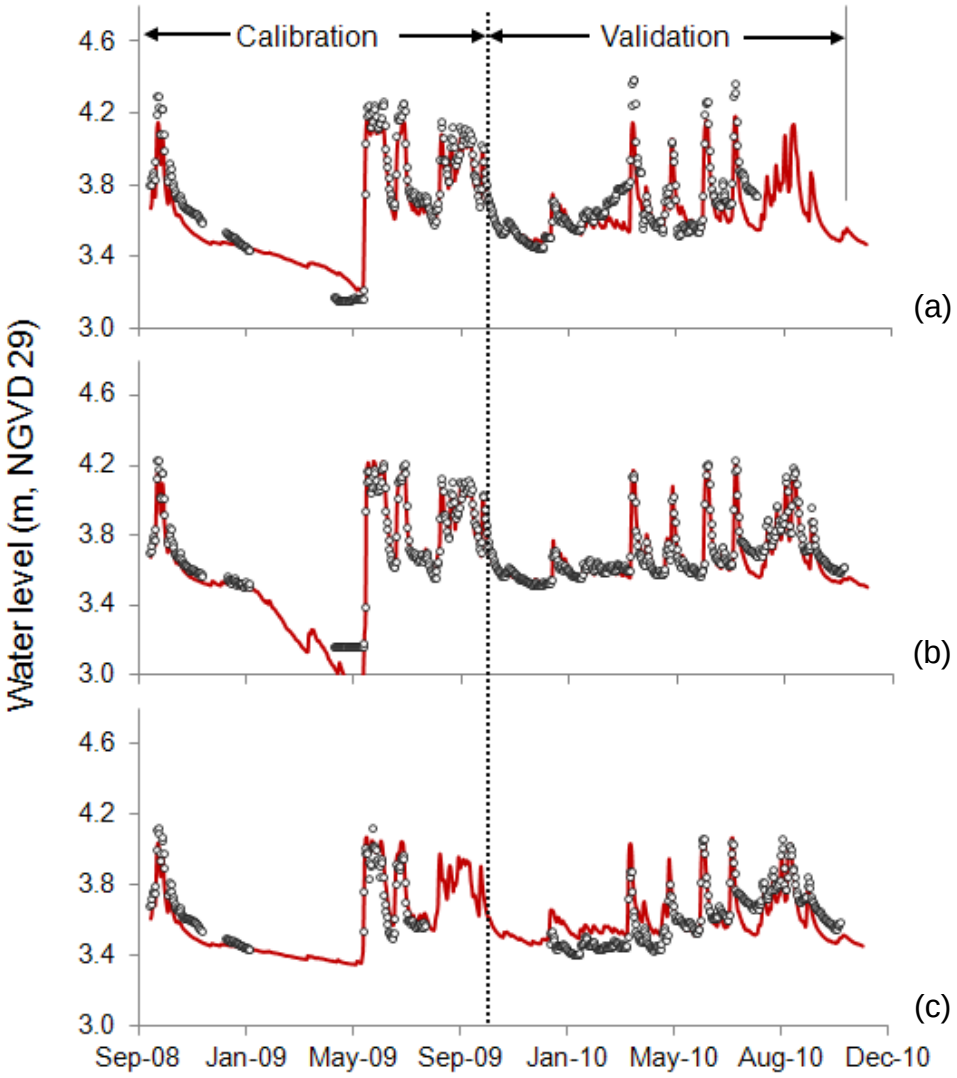

Figure 7-5. Observed daily average (circles) and modeled (red lines) water levels at eight sampling locations during the model calibration and validation periods: (a) B-west, (b) B-east, (c) E-west, (d) E-east, (e) G-west, (f) G-east, (g) D-3, and (h) F-3.

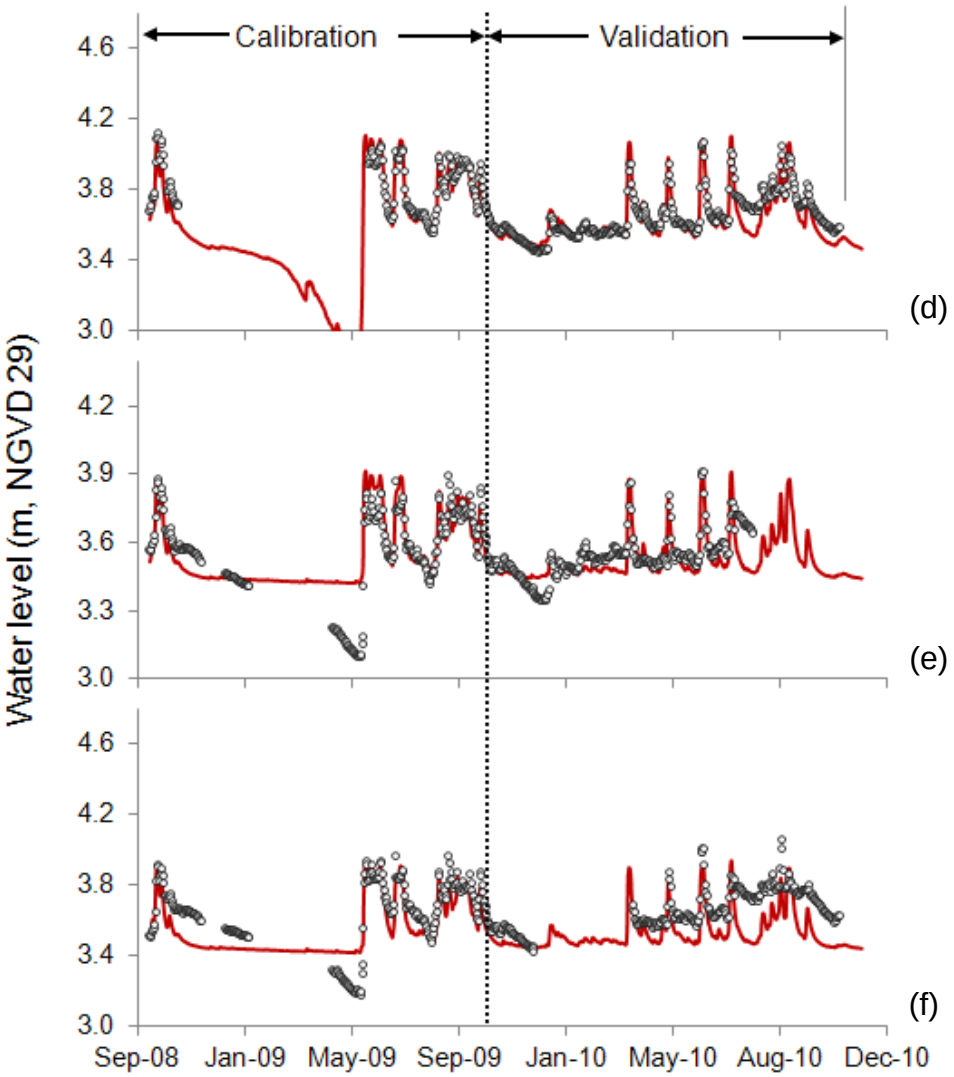

Figure 7-5. Continued.

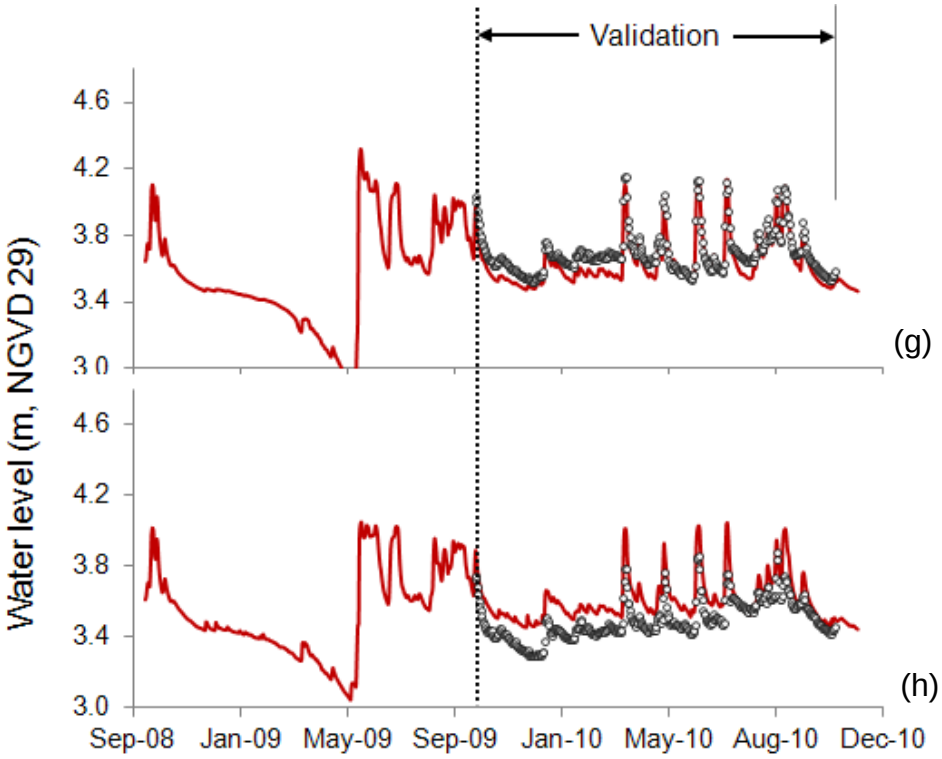

Figure 7-5. Continued.

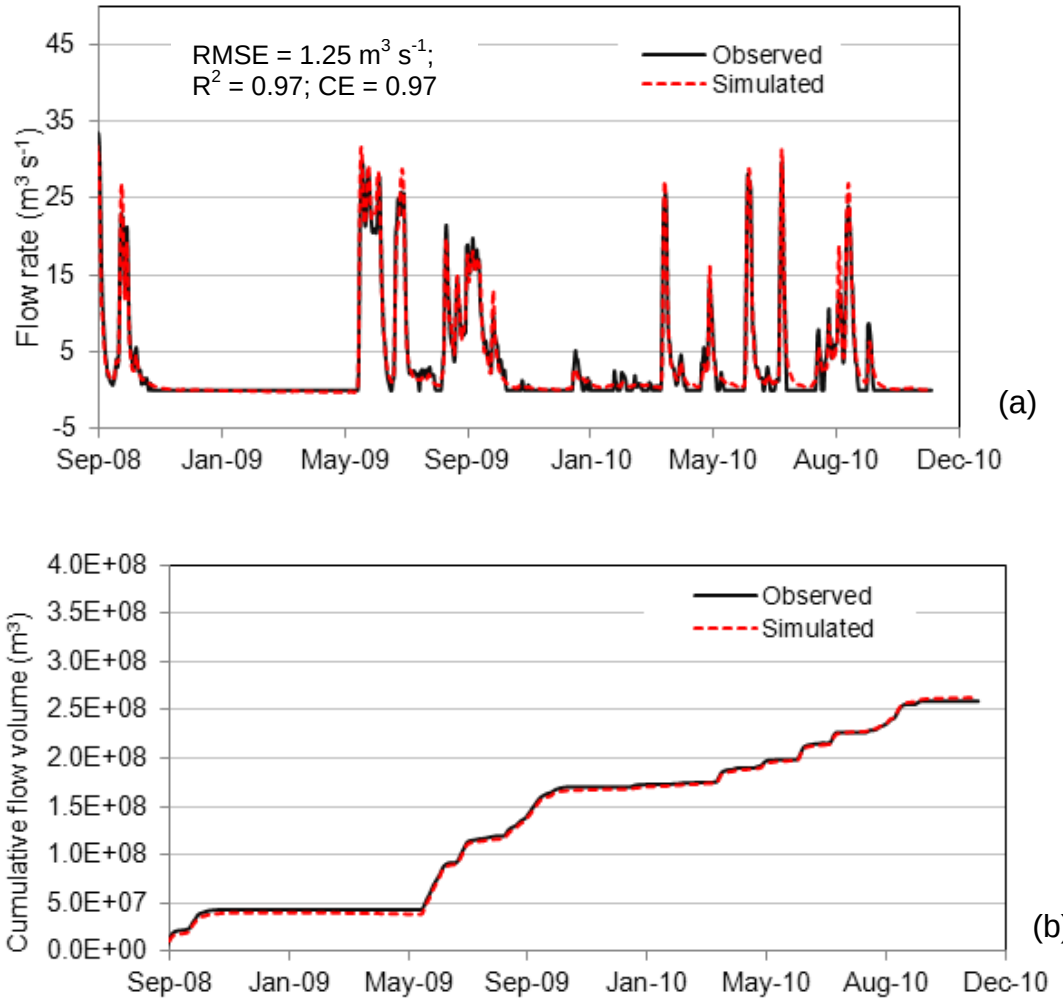

Figure 7-6. Comparison between measured and simulated values at G-332 hydraulic structure: (a) daily flows, and (b) cumulative flow volume for the simulation period (September 1, 2008 to November 30, 2010).

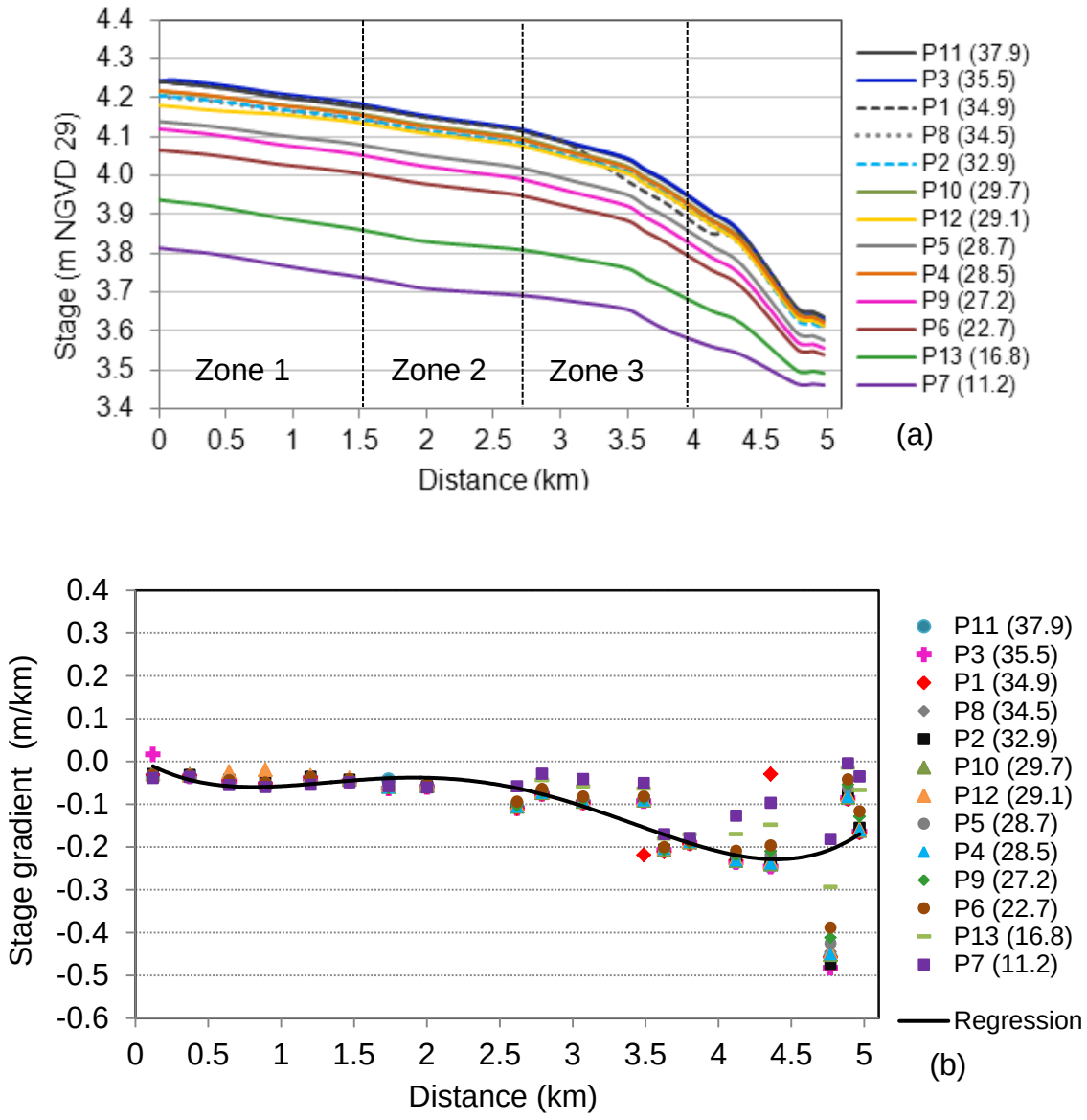

Figure 7-7. Simulated values along the BB' transect for 13 peak inflow events: (a) stage profile, and (b) stage gradient. Value in the parenthesis represents inflow discharge ($m^3 s^{-1}$). To calculate stage gradient, the difference in the stage between consecutive locations along transect BB' from the inlet divided by the distance between those locations.

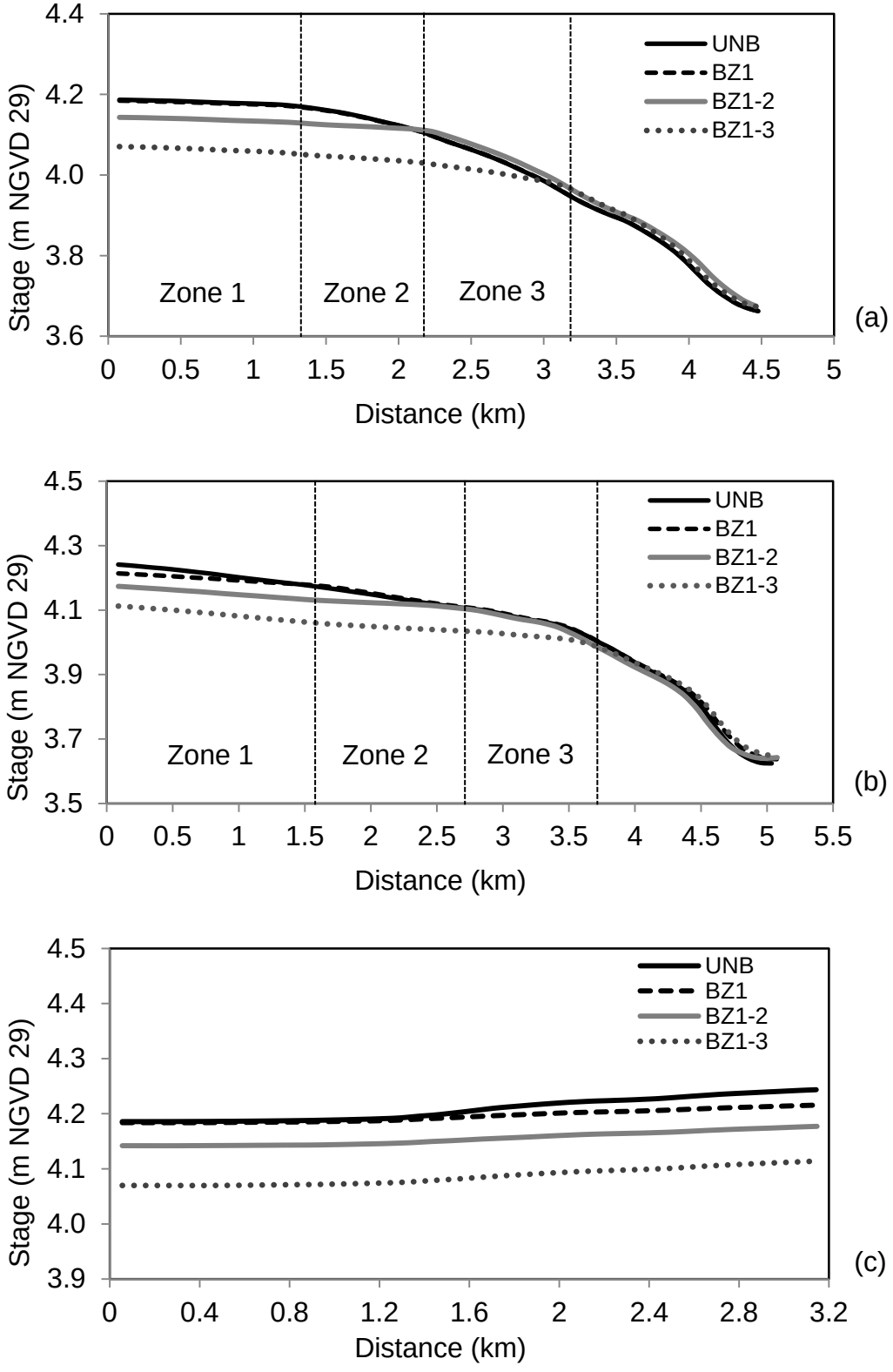

Figure 7-8. Simulated stage profiles along transects for P13: (a) AA', (b) BB', (c) EW1, (d) EW2, and (e) EW3. See Figure 7-1 for the location of transects.

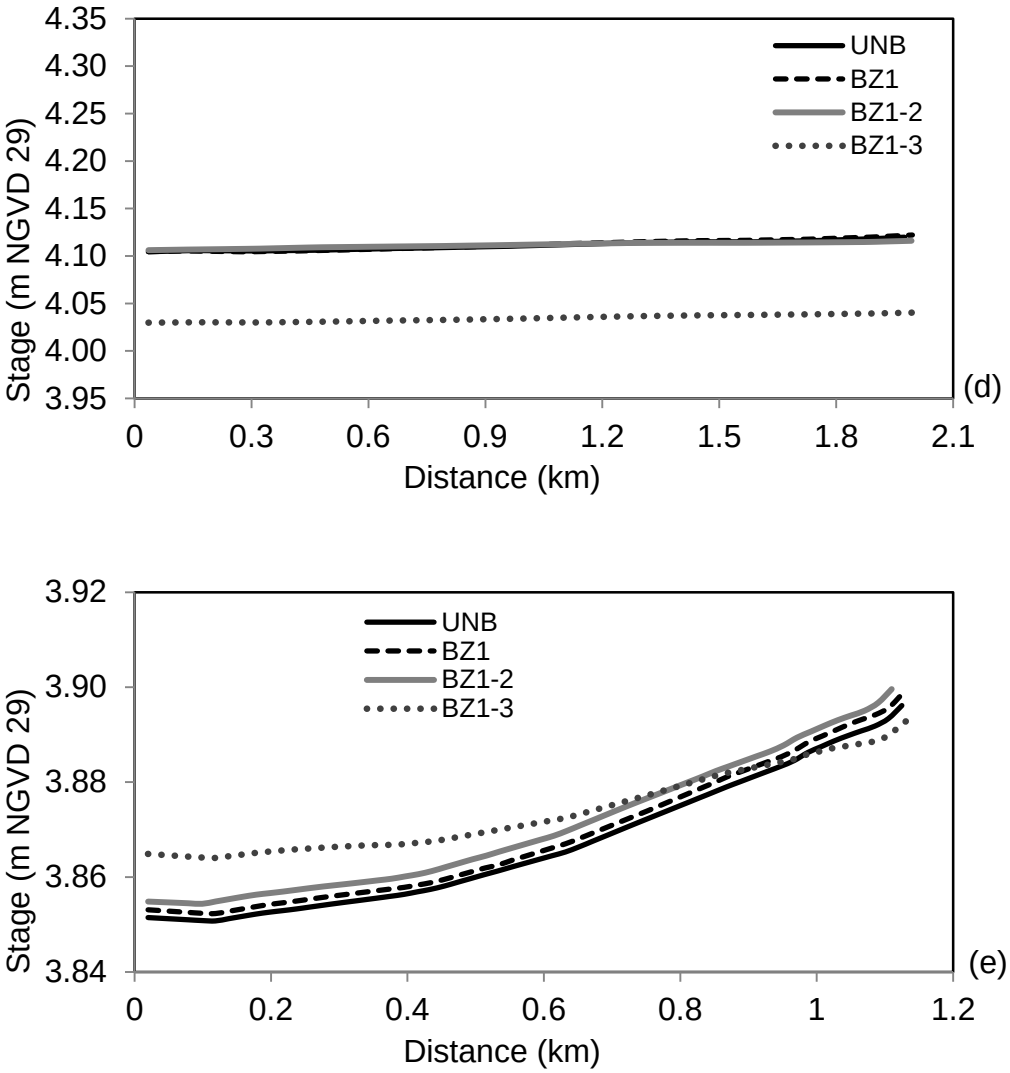

Figure 7-8. Continued.

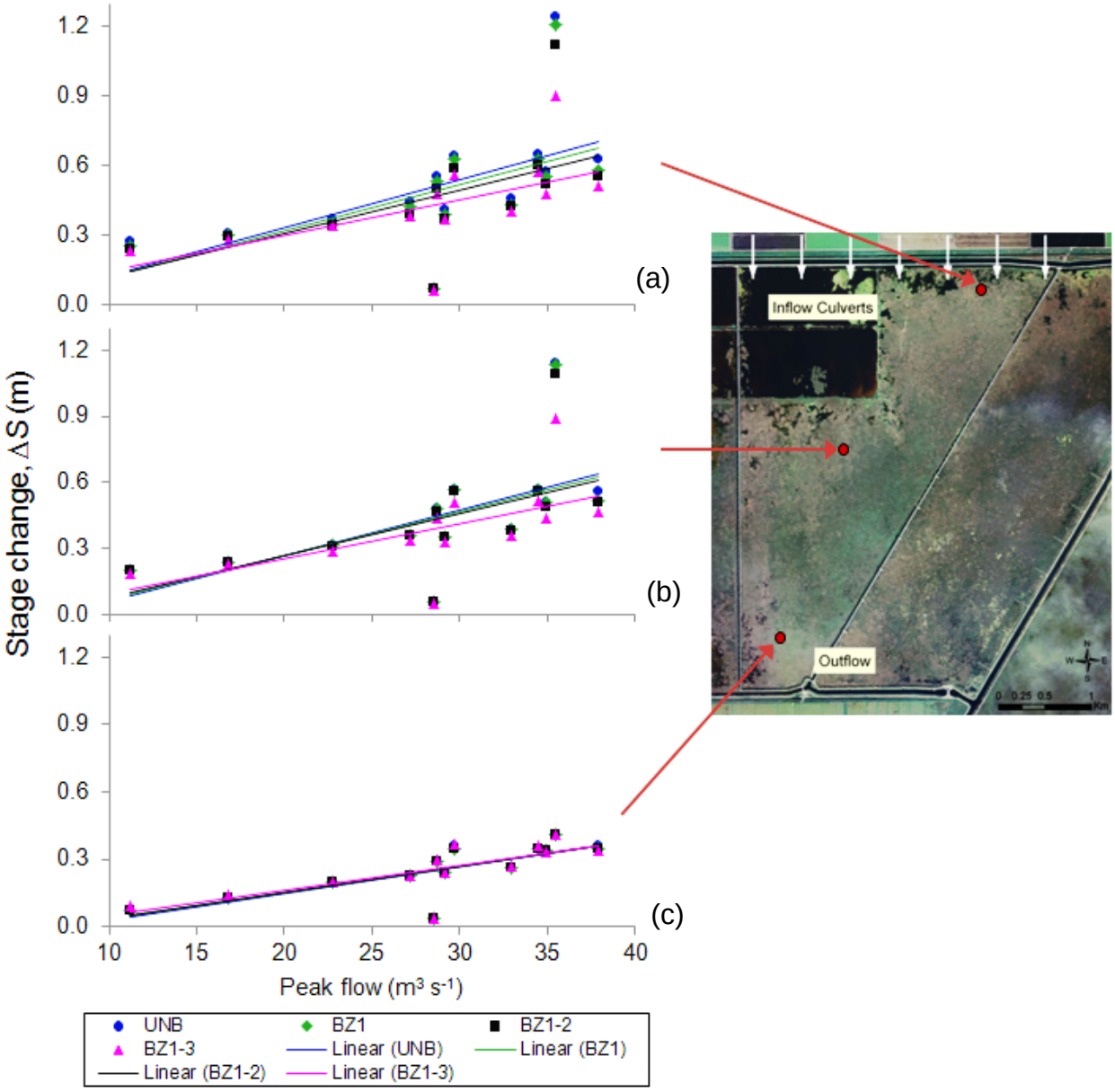

Figure 7-9. Simulated stage changes following 13 peak inflow events at (a) inlet region, (b) approximately middle, (c) outlet region.

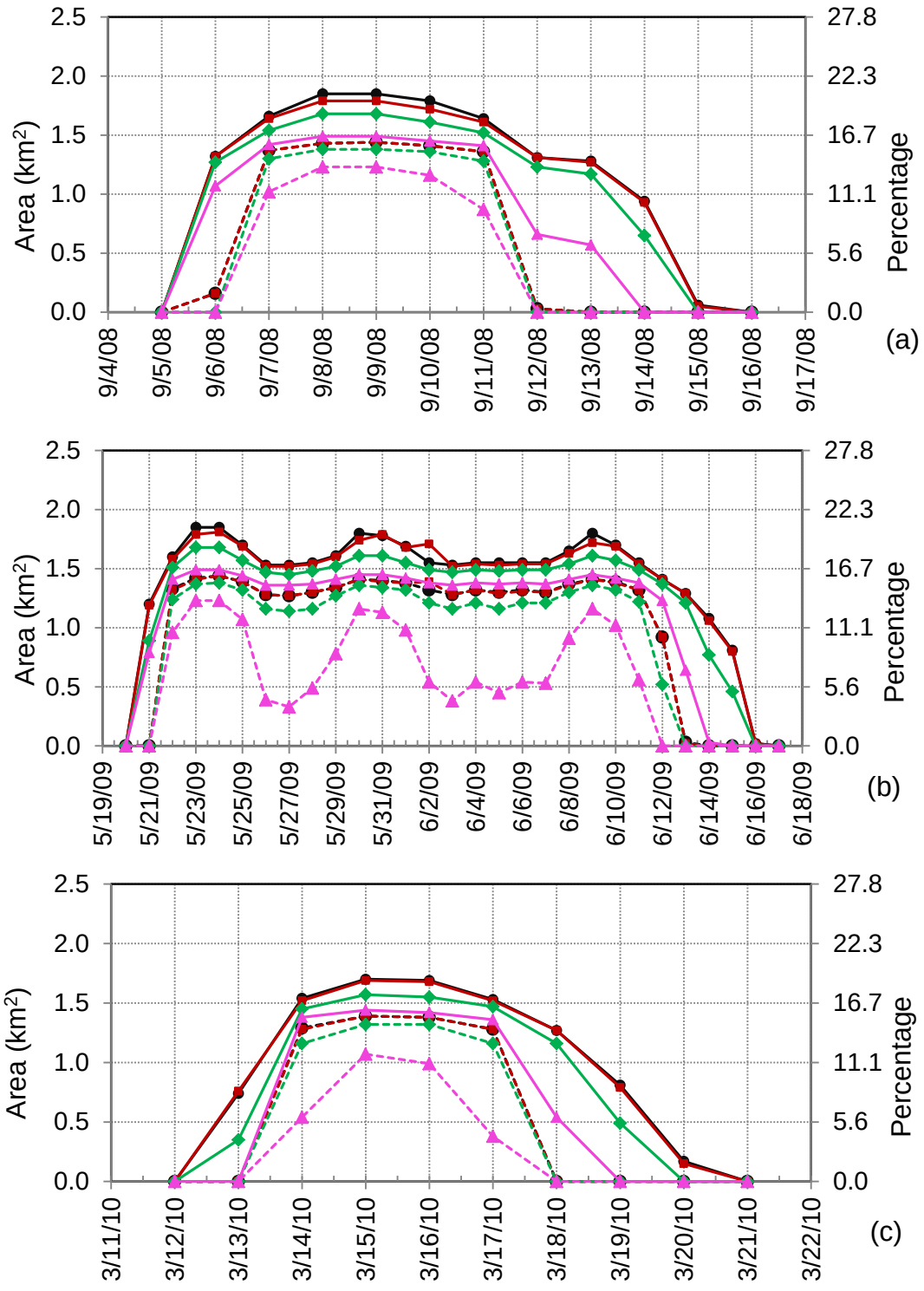

Figure 7-10. Cumulative area and percentage of total Stormwater Treatment Area 2 Cell 2 area in relation to the duration of water depths greater than 4 ft and 3.5 ft for four peak inflow events (greater than 34 $m^3 s^{-1}$) (a) P1, (b) P3, (c) P8, and (d) P11.

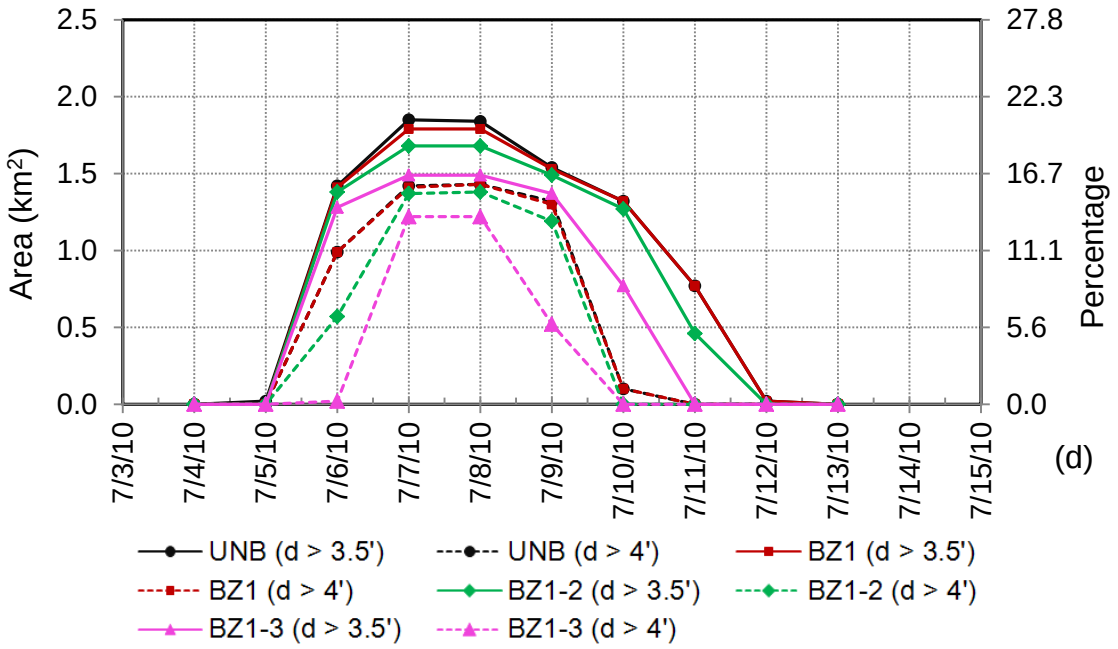

Figure 7-10. Continued.

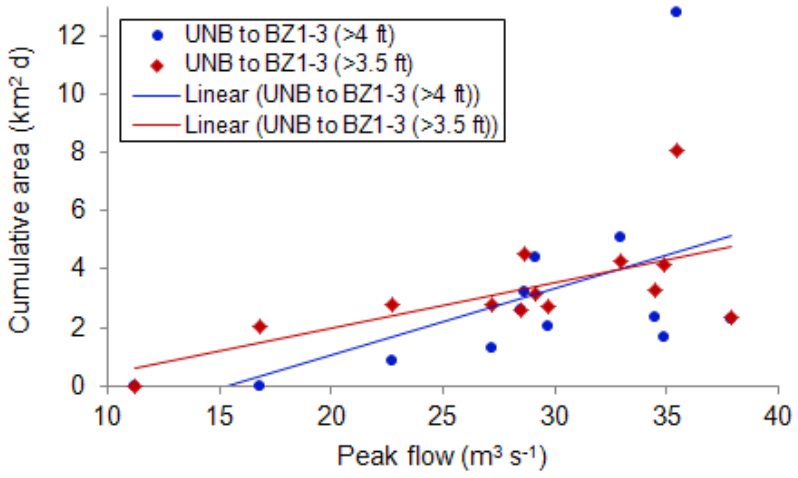

Figure 7-11. Improvement in the cumulative area (reduction in the area with water depths greater than 4 ft and 3.5 ft) during the post-burn simulation scenario (BZ1-3).

CHAPTER 8
CONCLUDING REMARKS

Conclusions and Recommendations

The Stormwater Treatment Areas (STAs) of the Florida Everglades have been found to be effective in reducing phosphorus concentrations in agricultural drainage waters. These large-scale constructed treatment wetlands are critical components of the Everglades restoration effort. Sustaining the effectiveness or optimizing the phosphorus removal performance of these wetlands has considerable significance to protect downstream Everglades by reducing phosphorus concentration levels in agricultural runoff before entering the Everglades. During over a decade of operational experience and data collection, water managers and environmental scientists are interesting in the development of mathematical models to synthesize and interpret field data, gain deeper understanding about the system dynamics, test research hypotheses, formulate management strategies, and forecast future conditions. Mathematical models often provide a ‘hands-on’ tool for water managers to evaluate the effectiveness of different approaches to optimize the STAs performance.

To assist the goal of protecting the Everglades ecosystem, this study investigated various research as well as management questions related to STA hydrology/hydraulics, and phosphorus biogeochemical cycling by using numerical simulation tools. Phosphorus biogeochemical models were developed in various dimensions (e.g., complexity levels, spatial scales, and time settings). Hydrologic Simulation Engine (HSE) of Regional Simulation Model (RSM) was used as a basic modeling framework to simulate coupled overland and groundwater flow, hydraulic structures, and levee seepage within STA systems. To simulate transport and

phosphorus transformation processes, a novel water quality model, Regional Simulation Model Water Quality (RSMWQ), was used. Both models were internally linked and simulated coupled hydrodynamic, transport and phosphorus biogeochemical cycling processes. The flexibility of the RSMWQ model platform enabled the reactions equations to be described in various model structural levels. Where the field data were not available to empirically derive physical parameters of models, parameters were calibrated against field measured data. Calibrated models were validated with data from beyond the calibration boundaries to gain additional confidence in the simulations. Subsequently, models were applied to explore various feasible research and management questions.

A two-dimensional (2-D), flow coupled phosphorus biogeochemical model of Cell 4 of Stormwater Treatment Area 1 West (STA-1W) was developed (Chapter 3). Cell 4 was one of the four treatment cells of Everglades Nutrient Removal project (ENRP), a prototype STA incorporated into STA-1W. To simulate more complex behavior of STAs, and complex geometries, this study provided new insights for simulation of added complexities. Internal hydrologic and transport processes were calibrated against measured tracer concentrations, and subsequently validated against outflow discharge and spatial chloride concentration data. Cycling of phosphorus was simulated as a first-order uptake and release process, with different uptake coefficients for open water/sparse submerged aquatic vegetation (SAV) areas (0.2 d^{-1}) and dense SAV areas (0.4 d^{-1}), and a much lower, uniform release coefficient (1.97×10^{-4} d^{-1}). The model was validated against the field data, and extended to simulate the effects of a suite of

feasible management alternatives on the long-term ability of the wetland to sustain total phosphorus (TP) removal.

We concluded that under simulated conditions of elimination of preferential channels, average annual TP treatment effectiveness increased by 25%. This finding highlights that the short-circuiting in STAs limits the wetland performance. Therefore, during the wetland construction, ditches/ channels should be filled, and low-relief uniform topography should be maintained. During operation, another feasible option is to plant macrophyte vegetation that increases the resistance to flow and reduces short-circuiting, and enhances the performance by biologically mediated phosphorus removal. Results showed that when inflow TP loads were assumed to be eliminated after 6 years of loading, the release of accumulated soil phosphorus sustained predicted annual average outlet concentrations above 6.7 μg L^{-1} for 18 years, decreasing at a rate of 0.16 μg L^{-1} yr^{-1}. This finding has implications to the long-term sustainability of treatment wetlands.

The analysis in Chapter 4 illustrated that increasing level of process-complexity in a biogeochemical model does not guarantee better simulation model to simulate TP dynamics, given the data and models under consideration. To conclude this, a suite of phosphorus biogeochemical models were developed to investigate prediction performances of models, and their ability to describe underlying physical phenomena in relation to the model complexity levels (modeling cost and effort). Although increased accuracy was observed when the level of process-complexity was increased in a sequence, the rate of improvement in the accuracy diminished towards the higher complexity spectrum. Model 6, the most complex model considered in this study, was

not necessarily the most ‘effective’ model to simulate the TP dynamics in Cell 4. Therefore, the process of developing a model of a complex and dynamic system, as in the case of the STAs, should require a robust way to evaluate the model with observations as well as an equally robust way to compare across differing levels of model complexity. This objective provided deeper insights about the suitable levels of model complexity in support of the STA performance optimization. In addition, this study addressed whether there is a benefit on increasing the levels of complexity with more and efforts, in relation to the prediction performance.

Next, we developed a phosphorus cycling model of a more complex system (a cell-network treatment wetland, STA-1W) in terms of geometry of the wetland, flow control structures, and spatial heterogeneity. In this study, four treatment cells (Cells 1 through 4) were considered, and these cells were connected by numerous hydraulic structures and separated by berms (levees). For this study, the model of Cell 4 (described in Chapter 3) provided deeper insights to simulate hydrodynamics and phosphorus cycling processes. The study in Chapter 5 illustrated that a hydrodynamic/transport model of a cell-network wetland adequately simulated the spatio-temporal dynamics of water levels, flow through the hydraulic structures, pump outflow, and the levee seepage. Results suggested that the model was capable of representing key physical conditions, and reasonably simulated the hydrologic/transport responses of STA-1W. The validated model was applied to explore water levels and velocity variations during the design maximum flow and due to the changes in vegetation management. Steady-state simulation results indicated that the design maximum inflow will be contained within the existing levee system. Also, there was not

a quantifiable improvement in the flow distribution across treatment cells—in terms of uniform flow—resulting from the changes in vegetation pattern in a sequential treatment trains (EAV cells followed by SAV cells), and .structural modifications.

The hydrodynamic/transport model described in Chapter 5 was used to simulate TP phosphorus biogeochemistry within four treatment cells of STA-1W (Chapter 6). The biogeochemical model variables were initially specified with spatial inputs (generated spatial maps based on observations), and primary model habitat-specific kinetic constants were determined through calibration. This helped characterize the spatial heterogeneity of different vegetation type/class and their responses to phosphorus biogeochemical cycling. In general, the model performed moderately well. In some locations, the model failed to capture the temporal dynamics. The stochastic nature of the observed phosphorus concentration profiles within monitoring locations, were not described by the model; thus, many instantaneous observations were not captured by the model in the calibration process. There could be a possibility on the existence of unknown processes, which were not considered in this modeling study. Nevertheless, the observed and the simulated cumulative phosphorus retention rates were similar, as calculated from the difference between inflow and outflow concentrations for each treatment cell, and were consistent with the overall phosphorus retention behavior. Results of this study, such as spatial distribution of soil TP levels over time can also be used to explore the potential cattail expansion areas that exceed a certain threshold of soil phosphorus levels.

Chapter 7 illustrated the type of research and management questions that can be addressed by using a spatially distributed numerical modeling tool. Using fine-resolution

spatial input data, a 2-D hydrodynamic model of Stormwater Treatment Area 2 Cell 2 (STA2C2) was developed, and extended simulations to investigate the effects of vegetation management alternatives on spatio-temporal flow dynamics. Vegetation management may include large-scale burning or herbicide application either for thinning dense emergent macrophytes or replacement by other plant species. High water depths (greater than 4 ft) were periodically observed in selected flow paths (typically at the north-west region) of STA2C2, which adversely impacted the emergent macrophytes. The goal of the study was to identify whether burning can provide potential benefits in reducing deep water depths. The hypothesis was that vegetation burning would reduce hydraulic resistance to flow and thus result in less deep submergence. On the basis of this modeling study, we concluded that burning or applying herbicide to minimize extended periods of water depths greater than 4 ft within STA2C2 may not be an effective management approach, depending on the magnitude of the inflow volumes and the antecedent water depths. Results indicated that water depths greater than 4 ft were primarily contributed by peak inflow events greater than 500 cfs (14.2 $m^3 s^{-1}$) and observed near the north-west inflow structures. Similarly, stages at the south-end of the STA2C2 were primarily influenced by the outflow structure operations. Water levels were insensitive to the variation in the flow resistance coefficient, a most-sensitive model parameter to water levels. Reducing peak inflows could be a best alternative to help reduce the deep water conditions within STA2C2.

Future Research

To increase confidence in these results and develop more specific recommendations, models require continuous refinement as additional data and knowledge/information about the system become available. The following topics are

suggested for future refinements and applications to specific management and research goals.

Model Validation

A model is an abstraction of the real system; therefore, it will not fully reflect the reality. It is the simplification or approximation of underlying behaviors of a dynamic system. A model is only a good tool if the assumptions in the model are good. Several assumptions have been made in these modeling studies. Although it is likely that simplifications in models are able to capture the overall/integrated response of the system, model validation of those assumptions with diverse physical conditions are required for a given modeling goal. In some cases, due to limited data, model variables are yet to be verified with detailed field measurements, such as soil TP and vegetation TP. Many parameters were determined through calibration. If parameters were empirically derived from detailed field measured data, it would enhance the model simulations; however, data were not available at this point. The stochastic nature of the data also complicated the calibration processes. Although a model cannot be truly validated in a dynamic natural system (Oreskes et al., 1994), model demonstrations are necessary to increase the credibility of the model with a wide range of conditions, for example, relaxation of the wetland after significant reduction in inflow TP concentrations, drought-induced recycling, and high and low inflow/outflow TP concentrations.

Kinetic Rate Constants

Although numerical modeling studies in wetlands have progressed recently, the wetland models with coupled flow/transport, with spatially characterized inputs and parameters are still in their infancy. First-order removal of nutrients or pollutants is a

common model assumption (Kadlec and Wallace, 2008). Capturing phosphorus behavior in space and time may be critical for heterogeneous wetlands under variable flow operations. The phosphorus cycling processes and associated rate constants are required to fit individually against observations to increase the robustness of the model. Field data are not yet sufficient to validate whether kinetic pathways (e.g., settling, recycle, burial, plant uptake) employed in this study follow the first-order process or second-order and so forth. In a heterogeneous wetland, these may be varied in space. Therefore, updating models upon available new data, deriving parameters from observations, and applying models to several “what-if” forcing functions may be necessary to add more credibility in these models.

Limitations

In this study, primary model parameters were determined through calibration by adjusting parameters manually using the trial and error method, and uncertainty analyses of model parameters and forcing functions were limited. As the models were computationally intensive because of spatially-distributed framework, it prohibited the use of formalized parameter estimation and uncertainty analysis techniques.

There are numerous sources of error in simulation model outputs, such as input errors, model errors and parameter errors. Input errors are mainly attributed to the error in measurement of data because the measurements are themselves subjected to error for some reasons and do not adequately reflect the real field conditions. Particularly, to match simulated and observed values of TP concentrations at internal locations was difficult because of the stochastic nature of concentration profiles and their random errors. Uncertainties in input information such as topographic features, vegetation, inflows, and boundary conditions may have impacted the calibration results. Model

errors are mainly associated with the structure of the model and numerical approximation techniques. These types of errors may arise due to invalid inadequate governing equations, invalid ranges, or improper discretization. To some degree model errors are inevitable because models were simplified in many aspects. Another major limitation is when phosphorus cycling parameters were aggregated to represent the combined effect of two or more biogeochemical processes between components. Therefore, such models cannot segregate the effects of individual processes that affect TP dynamics. For example, the models evaluated here cannot independently specify individual processes such as diffusion due to concentration gradient between water column and soil, resuspension of sediment TP, chemical precipitation, or particulate matter deposition. In this respect, model scenario simulation results have to be interpreted with caution when used in the management context or for any other modeling goals.

APPENDIX
SPATIAL DISTRIBUTION OF HYDRODYNAMIC VARIABLES IN STORMWATER TREATMENT AREA 2

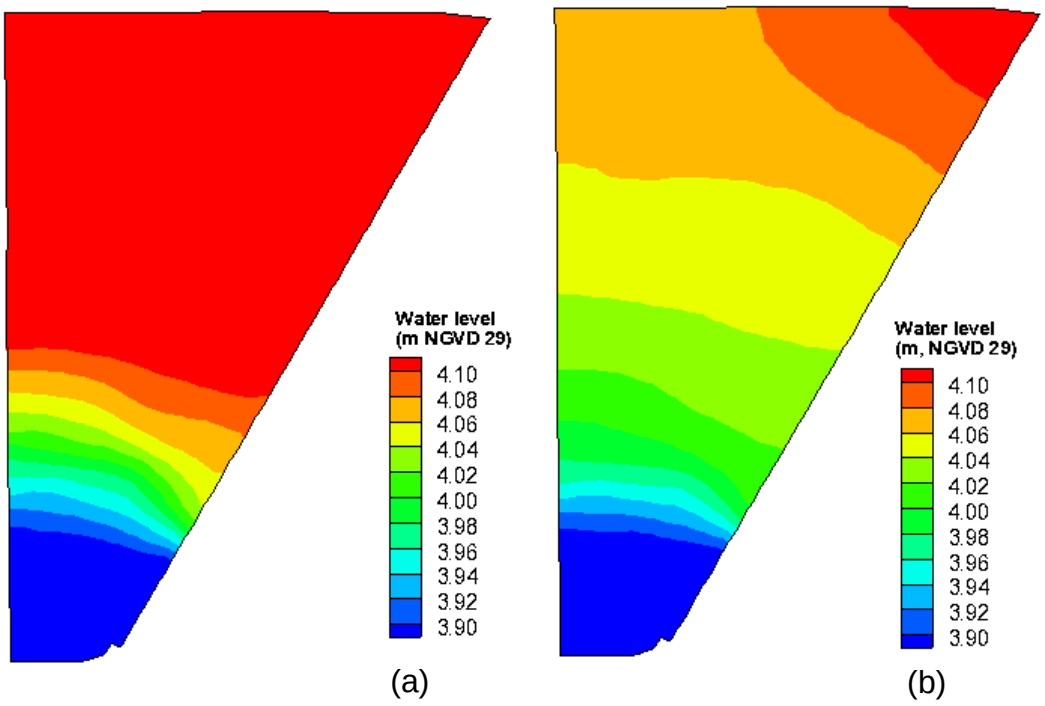

Figure A-1. Snapshot of surface water level following the highest peak flow event (P11; 37.9 $m^3 s^{-1}$) on July 8, 2010 (a) UNB scenario, (b) BZ1-3 scenario.

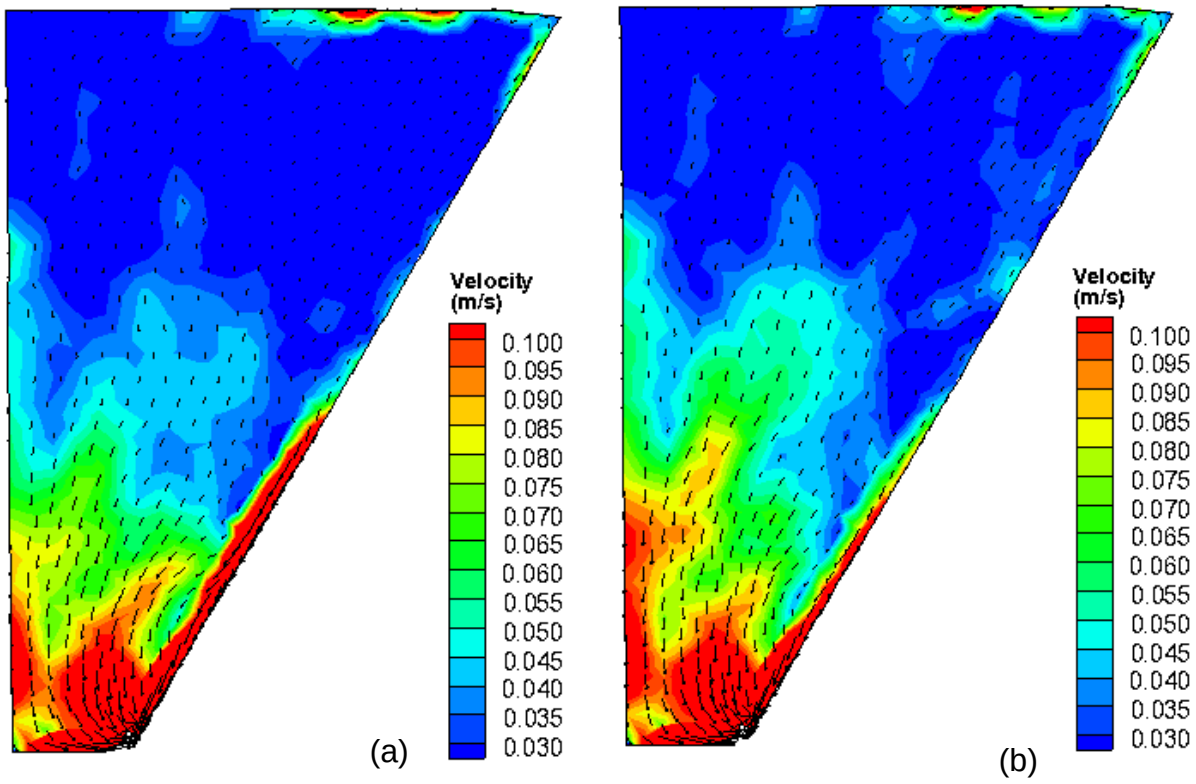

Figure A-2. Snapshot of velocity distribution following the highest peak flow event (P11; 37.9 $m^3 s^{-1}$) on July 8, 2010 (a) UNB scenario, (b) BZ1-3 scenario.

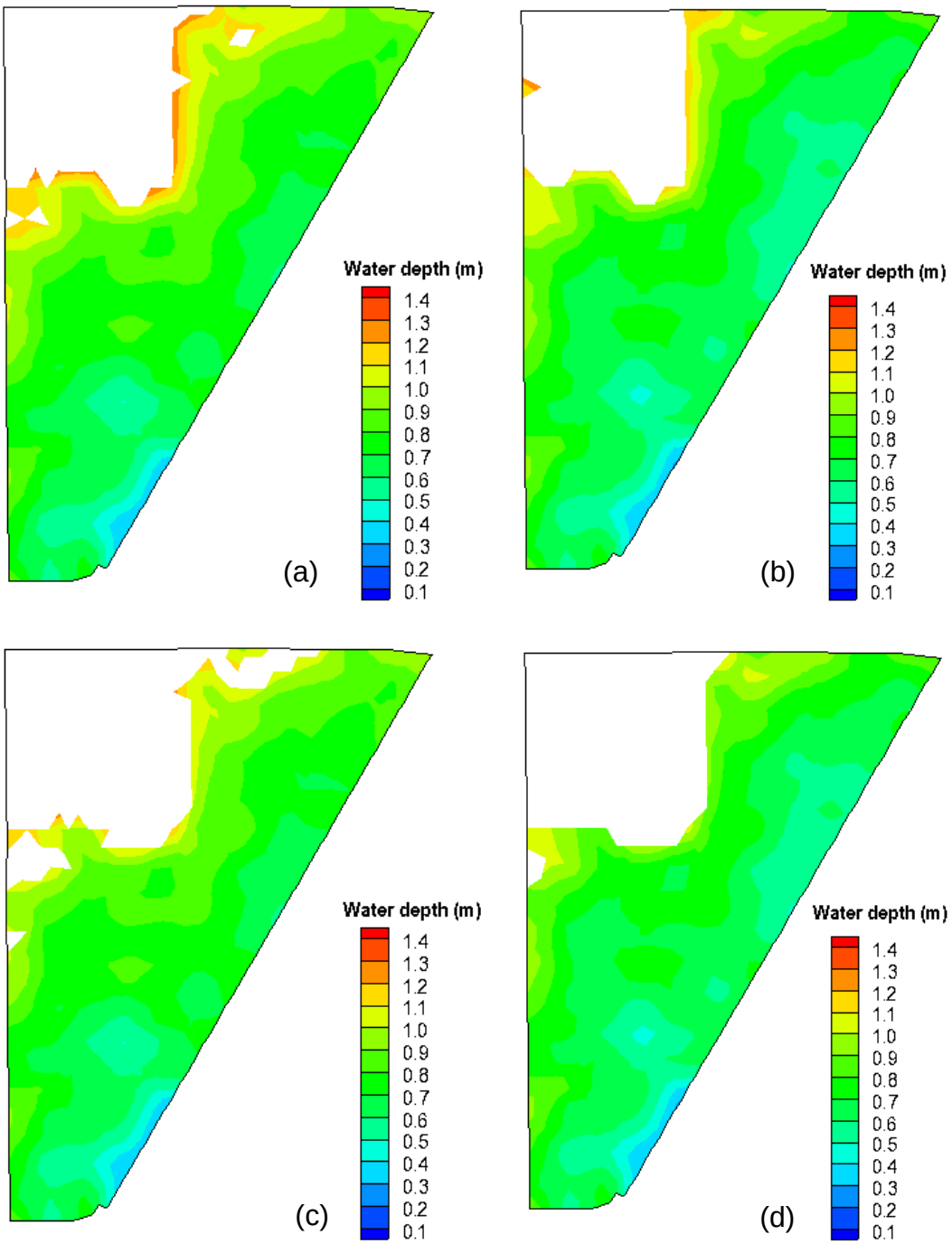

Figure A-3. Spatial distribution of water depths following peak inflow events (P3) on May 24, 2009. White color represents the areas with greater depths (a) P3 under UNB scenario, depth greater than 4ft, (b) P3 under BZ1-3 scenario, depths greater than 4 ft, (c) P3 under UNB scenario, water depths greater than 3.5 ft, (d) P3 under BZ1-3 scenario, water depths greater than 4 ft.

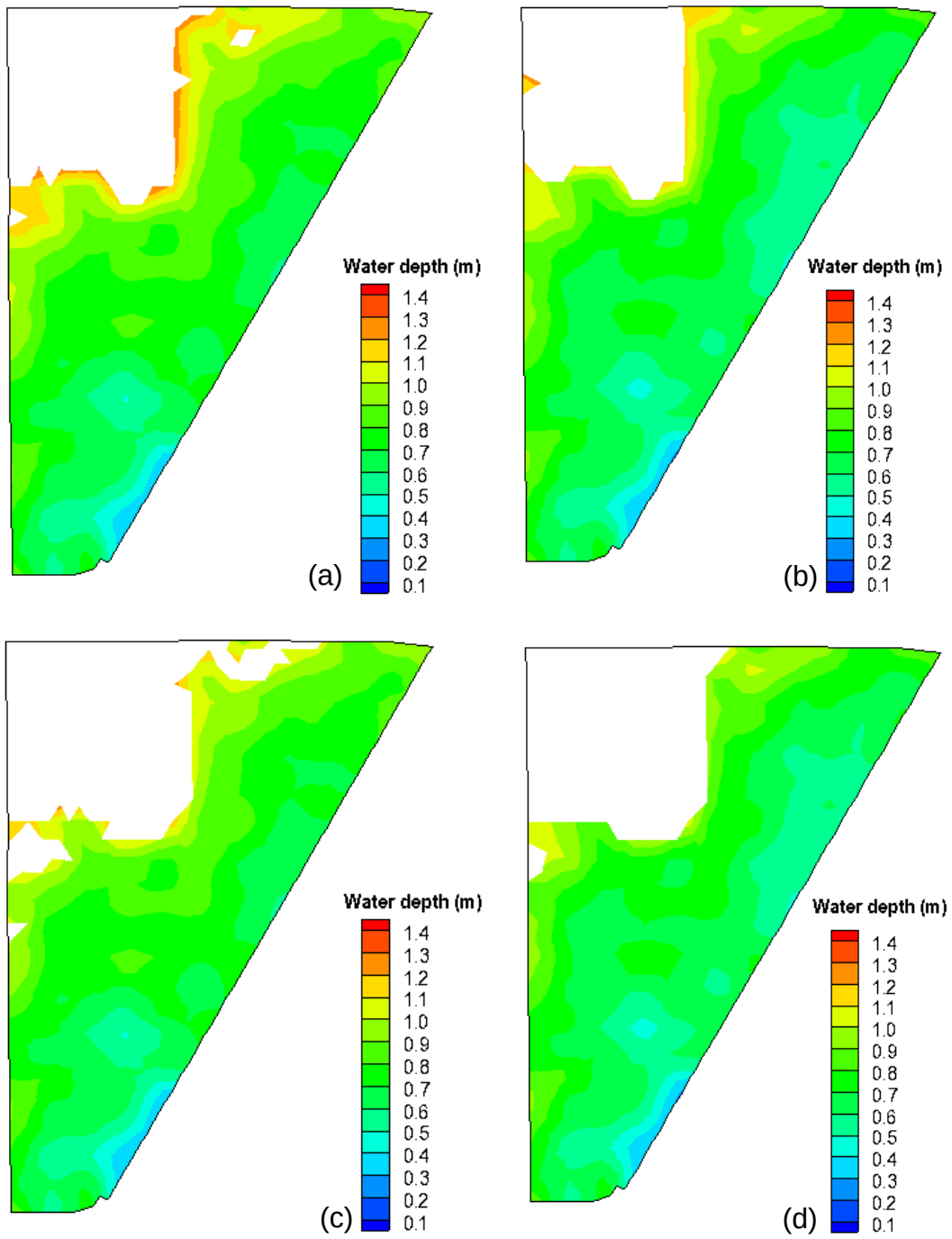

Figure A-4. Spatial distribution of water depths following peak inflow events (P11) on July 8, 2010. White color represents the areas with greater depths (a) P11 under UNB scenario, depth greater than 4ft, (b) P11 under BZ1-3 scenario, depths greater than 4 ft, (c) P11 under UNB scenario, water depths greater than 3.5 ft, (d) P11 under BZ1-3 scenario, water depths greater than 4 ft.

LIST OF REFERENCES

Abtew, W., 1996. Evapotranspiration measurements and modeling for three wetland systems in south Florida. Water Resources Bulletin 32, 465-473.

Abtew, W., Downey, D., 1998. Water budget analysis for the Everglades Nutrient. Removal Project. Technical Memorandum WRE–368. South Florida Water Management District, West Palm Beach, FL.

Abtew, W., Mullen, V., 1997. Water budget analysis for the Everglades Nutrient Removal Project (August 20, 1996 to August 19, 1997). Tech. Memo. WRE #354. South Florida Water Management District, West Palm Beach, FL.

Abtew, W., Obeysekera, J., 1995. Lysimeter study of evapotranspiration of cattails and comparison of 3 estimation methods. Transactions of the ASAE 38, 121-129.

Abtew, W., Obeysekera, J., Shih, G., 1995. Spatial variation of daily rainfall and network design. Transactions of the ASAE 38, 843-845.

Ahn, H., James, R.T., 2001. Variability, uncertainty, and sensitivity of phosphorus deposition load estimates in South Florida. Water Air and Soil Pollution 126, 37-51.

Akaike, H., 1973. Information theory and an extension of the maximum likelihood principle, Proceedings of the 2nd International Symposium on Information Theory Tsahkadsor, Armenian SSR, pp. 267–281.

Aldridge, B.B., Burke, J.M., Lauffenburger, D.A., Sorger, P.K., 2006. Physicochemical modelling of cell signalling pathways. Nature Cell Biology 8, 1195-1203.

Arhonditsis, G.B., Adams-VanHarn, B.A., Nielsen, L., Stow, C.A., Reckhow, K.H., 2006. Evaluation of the current state of mechanistic aquatic biogeochemical modeling: Citation analysis and future perspectives. Environmental Science & Technology 40, 6547-6554.

Arhonditsis, G.B., Brett, M.T., 2004. Evaluation of the current state of mechanistic aquatic biogeochemical modeling. Marine Ecology-Progress Series 271, 13-26.

Arnold, J.G., Allen, P.M., Morgan, D.S., 2001. Hydrologic model for design and constructed wetlands. Wetlands 21, 167-178.

Arnold, J.G., Williams, J.R., Srinivasan, R., King, K.W., Griggs, R.H., 1994. SWAT, Soil and water assessment tool, USDA Agricultural Research Service, Temple, TX.

Bal, K., Struyf, E., Vereecken, H., Viaene, P., De Doncker, L., de Deckere, E., Mostaert, F., Meire, P., 2011. How do macrophyte distribution patterns affect hydraulic resistances? Ecological Engineering 37, 529-533.

Beven, K., 2001. On explanatory depth and predictive power. Hydrological Processes 15, 3069-3072.

Bicknell, B.R., Imhoff, J.C., Kittle, J.L., Jr., Donigian, A.S., Jr., Johanson, R.C., 1997. Hydrological Simulation Program—Fortran, User's manual for version 11. US EPA, National Exposure Research Laboratory, Athens, GA., EPA/600/R-97/080.

Bingner, R.L., Theurer, F.D., 2009. AnnAGNPS technical processes documentation, version 5.00. Available at: <http://www.wsi.nrcs.usda.gov/products/w2q/h&h/tools_models/agnps/index.html. Accessed 12 Jan. 2010>

Black, C.A., Wise, W.R., 2003. Evaluation of past and potential phosphorus uptake at the Orlando Easterly Wetland. Ecological. Engineering 21, 277-290.

Boers, A.M., Zedler, J.B., 2008. Stabilized water levels and *Typha* invasiveness. Wetlands 28, 676-685.

Bolster, C.H., Saiers, J.E., 2002. Development and evaluation of a mathematical model for surface-water flow within the Shark River Slough of the Florida Everglades. Journal of Hydrology 259, 221-235.

Bouletreau, S., Izagirre, O., Garabetian, F., Sauvage, S., Elosegi, A., Sanchez-Perez, J., 2008. Identification of a minimal adequate model to describe the biomass dynamics of river epilithon. River Research and Applications 24, 36-53.

Box, G.E.P., Jenkins, G.M., 1970. Time series analysis: forecasting and control. Holden-Day, London.

Brigham Young University, 2004. The Department of Defense Groundwater Modeling System, GMS v5.1, Environmental Modeling Laboratory.

Brooks, R.J., Tobias, A.M., 1996. Choosing the best model: Level of detail, complexity, and model performance. Mathematical and Computer Modelling 24, 1-14.

Brown and Caldwell, 2010. Stormwater Treatment Area 2 operations plan. Report prepared for South Florida Water Management District, West Palm Beach, FL.

Burnham, K.P., Anderson, D.R., 2001. Kullback-Leibler information as a basis for strong inference in ecological studies. Wildlife Research 28, 111-119.

Burnham, K.P., Anderson, D.R., 2002. Model selection and multi-model inference: A practical information-theoretic approach, Springer.

Burns and McDonnell, 2000. Everglades Construction Project Stormwater Treatment Area-3/4 and East WCA-3A Hydropattern Restoration Task Report 5.3 Hydrodynamic Modeling. Report prepared for the South Florida Water Management District, West Palm Beach, FL.

Carleton, J.N., Grizzard, T.J., Godrej, A.N., Post, H.E., 2001. Factors affecting the performance of stormwater treatment wetlands. Water Research 35, 1552-1562.

Chavan, P.V., Dennett, K.E., 2008. Wetland simulation model for nitrogen, phosphorus, and sediments retention in constructed wetlands. Water Air and Soil Pollution 187, 109-118.

Chen, H., Zamorano, M.F., Ivanoff, D., 2010. Effect of flooding depth on growth, biomass, photosynthesis, and chlorophyll fluorescence of *typha domingensis*. Wetlands 30, 957-965.

Chen, X.J., Sheng, Y.P., 2005. Three-dimensional modeling of sediment and phosphorus dynamics in Lake Okeechobee, Florida: Spring 1989 simulation. Journal of Environmental Engineering-ASCE 131, 359-374.

Chimney, M.J., Goforth, G., 2006. History and description of the Everglades Nutrient Removal Project, a subtropical constructed wetland in south Florida (USA). Ecological Engineering 27, 268-278.

Chimney, M.J., Goforth, G., 2001. Environmental impacts to the Everglades ecosystem: a historical perspective and restoration strategies. Water Science and Technology 44, 93-100.

Chimney, M.J., Moustafa, M.Z., 1999. Effectiveness and optimization of stormwater treatment areas for phosphorus removal. Chapter 6, In: SFWMD, 1999 Everglades Interim Report, South Florida Water Management District, West Palm Beach, FL.

Chimney, M.J., Nungesser, M., Newman, J., Pietro, K., Germain, G., Lynch, T., Goforth, G., Moustafa, M.Z., 2000. Chapter 6: Stormwater Treatment Areas - Status of research and monitoring to optimize effectiveness of nutrient removal and annual report on operational compliance. In: SFWMD, 2000 Everglades Consolidated Report. South Florida Water Management District, West Palm Beach, FL, pp. 6-1–6-127.

Chimney, M.J., Pietro, K.C., 2006. Decomposition of macrophyte litter in a subtropical constructed wetland in south Florida (USA). Ecological Engineering 27, 301-321.

Choi, J., Harvey, J.W., 2000. Quantifying time-varying ground-water discharge and recharge in wetlands of the northern Florida Everglades. Wetlands 20, 500-511.

Christensen, N., Mitsch, W.J., Jorgensen, S.E., 1994. A first generation ecosystem model of the Des-Plaines River experimental wetlands. Ecological Engineering 3, 495-521.

Costanza, R., Sklar, F.H., 1985. Articulation, accuracy and effectiveness of mathematical-models - a review of fresh-water wetland applications. Ecological Modelling 27, 45-68.

Cox, G.M., Gibbons, J.M., Wood, A.T.A., Craigon, J., Ramsden, S.J., Crout, N.M.J., 2006. Towards the systematic simplification of mechanistic models. Ecological Modelling 198, 240-246.

Darley, W.M., 1982. Algal Biology: A Physiological Approach. Oxford Press, Oxford, UK.

Davis, S.M., 1991. Growth, decomposition, and nutrient retention of *Cladium-Jamaicense* Crantz and *Typha-Domingensis* Pers in the Florida Everglades. Aquatic Botany 40, 203-224.

Davis, S.M., 1994. Phosphorous inputs and vegetation sensitivity in the Everglades. In: Davis, S.M., Ogden, J.C. (Eds.), Everglades: the Ecosystem and its Restoration. St. Lucie Press, Delray Beach, FL, 357–378.

Dawson, C.W., Abrahart, R.J., See, L.M., 2007. HydroTest: A web-based toolbox of evaluation metrics for the standardised assessment of hydrological forecasts. Environmental Modelling & Software 22, 1034-1052.

DB Environmental Laboratories, Inc. (DBEL), 2000. STA-1W Cell 4 feasibility study report. Prepared for the South Florida Water Management District, West Palm Beach, FL and the Florida Department of Environmental Protection, Tallahassee, FL.

DB Environmental Laboratories, Inc. (DBEL), 2002. Submerged aquatic vegetation/limerock treatment system technology for removing phosphorus from Everglades Agricultural Area waters follow on study – Final Report. Prepared for the South Florida Water Management District, West Palm Beach, FL and the Florida Department of Environmental Protection, Tallahassee, FL.

DB Environmental Laboratories, Inc. (DBEL). 2004. Appendix 4B-4: Vegetation biomass and nutrient analysis for Stormwater Treatment Area 1 West (STA-1W). In: SFWMD, 2004 Everglades Consolidated Report. South Florida Water Management District, West Palm Beach, FL.

DB Environmental Laboratories, Inc. (DBEL) and MSA, 2006. Appendix 4-9: Baseline tracer studies: STA-2, Cell 3. In: SFWMD, 2006 Everglades Consolidated Report. South Florida Water Management District, West Palm Beach, FL.

DeBusk, W.F., Newman, S., Reddy, K.R., 2001. Spatio-temporal patterns of soil phosphorus enrichment in Everglades Water Conservation Area 2A. Journal of Environmental Quality 30, 1438-1446.

Dierberg, F.E., DeBusk, T.A., 2008. Particulate phosphorus transformations in south Florida stormwater treatment areas used for Everglades protection. Ecological Engineering 34, 100-115.

Dierberg, F.E., DeBusk, T.A., Jackson, S.D., Chimney, M.J., Pietro, K., 2002. Submerged aquatic vegetation-based treatment wetlands for removing phosphorus from agricultural runoff: response to hydraulic and nutrient loading. Water Research 36, 1409-1422.

Dierberg, F.E., Juston, J.J., DeBusk, T.A., Pietro, K., Gu, B.H., 2005. Relationship between hydraulic efficiency and phosphorus removal in a submerged aquatic vegetation-dominated treatment wetland. Ecological Engineering 25, 9-23.

Edmonds, B., 2000. Complexity and scientific modelling. Foundations of Science 5, 379-390.

Erwin, K.L., 1990. Freshwater marsh creation and restoration in the Southeast. In: Kusler, J.A., Kentula, M.E. (Eds.), Wetland Creation and Restoration: The Status of the Science. Island Press, Washington, D.C., pp. 233–265.

Feng, K., Molz, F.J., 1997. A 2-D, diffusion-based, wetland flow model. Journal of Hydrology 196, 230-250.

Fisher, M.M., Reddy, K.R., 2001. Phosphorus flux from wetland soils affected by long-term nutrient loading. Journal of Environmental Quality 30, 261-271.

Fitz, H.C., DeBellevue, E.B., Costanza, R., Boumans, R., Maxwell, T., Wainger, L., Sklar, F.H., 1996. Development of a general ecosystem model for a range of scales and ecosystems. Ecological Modelling 88, 263-295.

Fitz, H.C., Sklar, F.H., 1999. Ecosystem analysis of phosphorus impacts and altered hydrology in the Everglades: a landscape modeling approach. In: Reddy, K.R., O'Connor, G.A., Schelske, C.L. (Eds.), Phosphorus Biogeochemistry in Subtropical Ecosystems. Lewis Publishers, Boca Raton, FL, pp. 585–620.

Fitz, H.C., Sklar, F.H., Voinov, A.A., Waring, T., Costanza, R., and Maxwell, T., 2004. Development and application of the Everglades Landscape Model. In: Costanza, R., Voinov, A.A. (Eds.), Landscape simulation modeling: a spatially explicit, dynamic approach. Springer Verlag, New York, pp.143–171.

Fitz, H.C., Trimble, B., 2006. Documentation of the Everglades Landscape Model: ELM v2.5. Report from South Florida Water Management District, West Palm Beach, FL.

Flaig, E., VanZee, R., Lal, A.M.W., 2005. Hydrologic process modules of the regional simulation model: An overview. HSE White Paper. South Florida Water Management District, West Palm Beach, FL. <http://gwmftp.jacobs.com/Peer_Review/rsm_papers/RSM_HPM_whitepaper_060205_Draft.pdf#HPM_paper>.

Flynn, K.J., 2005. Castles built on sand: dysfunctionality in plankton models and the inadequacy of dialogue between biologists and modellers. Journal of Plankton Research 27, 1205-1210.

Friedrichs, M.A.M., Hood, R.R., Wiggert, J.D., 2006. Ecosystem model complexity versus physical forcing: Quantification of their relative impact with assimilated Arabian Sea data. Deep-Sea Research Part II-Topical Studies in Oceanography 53, 576-600.

Fulton, E.A., 2001. The effects of model structure and complexity on the behaviour and performance of marine ecosystem models. PhD thesis, School of Zoology, University of Tasmania, Hobart, Australia.

Fulton, E.A., Smith, A.D.M., Johnson, C.R., 2003. Effect of complexity on marine ecosystem models. Marine Ecology-Progress Series 253, 1-16.

Gan, T.Y., Dlamini, E.M., Biftu, G.F., 1997. Effects of model complexity and structure, data quality, and objective functions on hydrologic modeling. Journal of Hydrology 192, 81-103.

Germain, G., Pietro, K., 2011. Chapter 5: Performance and optimization of the Everglades Stormwater Treatment Areas. In: SFWMD, 2011 South Florida Environmental Report. South Florida Water Management District, West Palm Beach, FL. pp. 5-1–5-115.

Grace, J.B., 1989. Effects of water depth on *Typha Latifolia* and *Typha Domingensis*. American Journal of Botany 76, 762-768.

Grunwald, M., 2006. The Swamp: The Everglades, Florida, and the Politics of Paradise. Simon and Schuster, New York.

Gu, B., 2008. Phosphorus removal in small constructed wetlands dominated by submersed aquatic vegetation in South Florida, USA. Journal of Plant Ecology-Uk 1, 67-74.

Gu, B., Chimney, M.J., Newman, J., Nungesser, M.K., 2006. Limnological characteristics of a subtropical constructed wetland in south Florida (USA). Ecological Engineering 27, 345-360.

Gu, B., Dreschel, T., 2008. Effects of plant community and phosphorus loading rate on constructed wetland performance in Florida, USA. Wetlands 28, 81-91.

Gu, B., DeBusk, T.A., Dierberg, F.E., Chimney, M.J., Pietro, K.C., Aziz, T., 2001. Phosphorus removal from Everglades agricultural area runoff by submerged aquatic vegetation/limerock treatment technology: an overview of research. Water Science and Technology 44, 101-108.

Guardo, M., 1999. Hydrologic balance for a subtropical treatment wetland constructed for nutrient removal. Ecological Engineering 12, 315-337.

Guardo, M., Fink, L., Fontaine, T.D., Newman, S., Chimney, M., Bearzotti, R., Goforth, G., 1995. Large-Scale Constructed Wetlands for Nutrient Removal from Stormwater Runoff - an Everglades Restoration Project. Environmental Management 19, 879-889.

Guardo, M., Tomasello, R.S., 1995. Hydrodynamic simulations of a constructed wetland in south Florida. Water Resources Bulletin 31, 687–701.

Hammer, D.E., Kadlec, R.H., 1986. A model for wetland surface-water dynamics. Water Resources Research 22, 1951-1958.

Hannah, C., Vezina, A., St John, M., 2010. The case for marine ecosystem models of intermediate complexity. Progress in Oceanography 84, 121–128.

Haraldsson, H.V., Sverdrup, H.U., 2004. Finding simplicity in complexity in biogeochemical modelling. In: Wainwright, J., Mulligan, M. (Eds.), Environmental Modelling – Finding Simplicity in Complexity. John Wiley & Sons.

Harvey, J.W., Krupa, S.L., Gefvert, C., Choi, J., Mooney, R.H., Giddings, J.B., 2000. Interaction between ground water and surface water in the northern Everglades and relation to water budget and mercury cycling: Study methods and appendixes. U.S. Geological Survey Open-File Report, pp. 00–168.

Haws, N.W., Bouwer, E.J., Ball, W.P., 2006. The influence of biogeochemical conditions and level of model complexity when simulating cometabolic biodegradation in sorbent-water systems. Advances in Water Resources 29, 571–589.

Hecky, R.E., Kilham, P., 1988. Nutrient limitation of phytoplankton in fresh-water and marine environments - a review of recent-evidence on the effects of enrichment. Limnology and Oceanography 33, 796-822.

Ho, D.T., Engel, V.C., Variano, E.A., Schmieder, P.J., Condon, M.E., 2009. Tracer studies of sheet flow in the Florida Everglades. Geophysical Research Letters 36, L09401.

Horn, S.V., Adorisio, C., Bedregal, C., Gomez, J., Madden, J., Sievers, P., 2007. Chapter 4: Phosphorus sources controls for the basins tributary to the Everglades Protection Area. In: SFWMD, 2007 Everglades Consolidated Report. South Florida Water Management District, West Palm Beach, FL, pp. 4-1–4-75.

Huang, Y.H., Saiers, J.E., Harvey, J.W., Noe, G.B., Mylon, S., 2008. Advection, dispersion, and filtration of fine particles within emergent vegetation of the Florida Everglades. Water Resources Research 44, W04408.

Huber, W.C., and Dickinson, R.E., 1988. Storm Water Management Model User's Manual, v.4, EPA/600/3-88/001a, U.S. Environmental Protection Agency, Cincinnati, OH.

Huebner, R.S., 2008. Water budget analysis for Stormwater Treatment Area 2. Technical Publication SFWMD–103. South Florida Water Management District, West Palm Beach, FL.

Hughes, C.E., Binning, P., Willgoose, G.R., 1998. Characterisation of the hydrology of an estuarine wetland. Journal of Hydrology 211, 34–49.

Hurvich, C.M., Tsai, C.-L.,1989. Regression and time series model selection in small samples. Biometrika 76, 297–307.

HydroQual, Inc., 1997. SFWMD wetlands model: Calibration of the coupled periphyton/vegetation model to WCA2A, Project SFWMD0105, October 1997, West Palm Beach, FL.

Interstate Technology & Regulatory Council (ITRC), 2003. Technical and regulatory guidance document for constructed treatment wetlands. pp. 199.

Jadhav, R.S., Buchberger, S.G., 1995. Effects of vegetation on flow through free water surface wetlands. Ecological Engineering 5, 481-496.

James, A.I., Jawitz, J.W., 2007. Modeling two-dimensional reactive transport using a Godunov-mixed finite element method. Journal of Hydrology 338, 28-41.

James, A.I., Jawitz, J.W., Muñoz-Carpena, R., 2009. Development and implementation of a transport method for the Transport and Reaction Simulation Engine (TaRSE) based on the Godunov-Mixed Finite Element Method. USGS Scientific Investigations Report 2009-5034, pp. 40.

Jawitz, J.W., Muñoz-Carpena, R., Muller, S., Grace, K.A., James, A.I., 2008. Development, testing, and sensitivity and uncertainty analyses of a Transport and Reaction Simulation Engine (TaRSE) for spatially distributed modeling of phosphorus in South Florida peat marsh wetlands. USGS Scientific Investigations Report 2008-5029, pp. 109.

Janse, J.H., 1998. A model of ditch vegetation in relation to eutrophication. Water Science and Technology 37, 139-149.

Jansen, M.J.W., 1998. Prediction error through modelling concepts and uncertainty from basic data. Nutrient Cycling in Agroecosystems 50, 247-253.

Jorgensen, S.E., 1995. State-of-the-art of ecological modeling in limnology. Ecological Modelling 78, 101-115.

Jorgensen, S.E., 2002. Integration of ecosystem theories, Kluwer, Dordrecht.

Juston, J.M., DeBusk, T.A., 2011. Evidence and implications of the background phosphorus concentration of submerged aquatic vegetation wetlands in Stormwater Treatment Areas for Everglades restoration, Water Resources Research 47, W01511.

Kadlec, R.H., 1994. Detention and mixing in free-water wetlands. Ecological Engineering 3, 345-380.

Kadlec, R.H., 1997. An autobiotic wetland phosphorus model. Ecological Engineering 8, 145-172.

Kadlec, R.H., 2000. The inadequacy of first-order treatment wetland models. Ecological Engineering 15, 105-119.

Kadlec, R.H., Hammer, D.E., 1988. Modeling nutrient behavior in wetlands. Ecological Modelling 40, 37-66.

Kadlec, R.H., Knight, R.L., 1996. Treatment wetlands. Lewis Publishers, Boca Raton, FL, 893 pp.

Kadlec, R.H., Newman, S., 1992. Everglades protection Stormwater Treatment Area design support phosphorus removal in wetland treatment areas – Principles and data. DOR 106.

Kadlec, R.H., Wallace, S., 2008. Treatment wetlands, second ed. CRC Press, Boca Raton, FL, 952 pp.

Kalff, J., 2002. Limnology. Prentice Hall, Old Tappan, NJ.

Kazezyilmaz-Alhan, C.M., Medina, M.A., Jr., Richardson, C.J., 2007. A wetland hydrology and water quality model incorporating surface water/groundwater interactions. Water Resources Research 43, W04434.

Keefe, S.H., Barber, L.B., Runkel, R.L., Ryan, J.N., McKnight, D.M., Wass, R.D., 2004. Conservative and reactive solute transport in constructed wetlands. Water Resources Research 40, W01201.

Keefe, S.H., Daniels, J.S. (Thullen), Runkel, R.L., Wass, R.D., Stiles, E.A., Barber, L.B., 2010. Influence of hummocks and emergent vegetation on hydraulic performance in a surface flow wastewater treatment wetland. Water Resources Research 46, W11518.

Kirchner, J.W., 2006. Getting the right answers for the right reasons: Linking measurements, analyses, and models to advance the science of hydrology. Water Resources Research 42, W03S04.

Kirkman, L.K., 1995. Impacts of fires and hydrological regimes on vegetation in depression wetlands of southeastern USA. In: Cerulean, S.I.,Engstrom, R.T. (Eds.) Fire in wetlands: a management perspective. Proceedings of the Tall Timbers Fire Ecology Conference, No. 19. Tall Timbers Research Station, Tallahassee, FL.

Knight, R.L., Gu, B.H., Clarke, R.A., Newman, J.M., 2003. Long-term phosphorus removal in Florida aquatic systems dominated by submerged aquatic vegetation. Ecological Engineering 20, 45-63.

Knight, R.L., Ruble, R.W., Kadlec, R.H., Reed, S., 1994. Wetlands for wastewater treatment: Performance database. In: Moshiri, G.A. (Eds.), Constructed Wetlands for Water Quality Improvement. Lewis Publishers, Boca Raton.

Koch, M.S., Reddy, K.R., 1992. Distribution of soil and plant nutrients along a trophic gradient in the Florida Everglades. Soil Science Society of America Journal 56, 1492-1499.

Kusler, J.A., Kentula, M.E., 1990. Executive summary. In: Kusler, J.A., Kentula, M.E. (Eds.), Wetland Creation and Restoration: The status of the Science. Island Press, Washington, DC, USA.

Lal, A.M.W., 1998. Performance comparison of overland flow algorithms. Journal of Hydraulic Engineering- ASCE 124, 342-349.

Lal, A.M.W., 1998. Weighted implicit finite-volume model for overland flow. Journal of Hydraulic Engineering-ASCE 124, 941-950.

Lal, A.M.W., 2000. Numerical errors in groundwater and overland flow models. Water Resources Research 36, 1237-1247.

Lal, A.M.W., Van Zee, R., Belnap, M., 2005. Case study: Model to simulate regional flow in South Florida. Journal of Hydraulic Engineering- ASCE 131, 247-258.

Lee, J.K., Roig, L.C., Jenter, H.L., Visser, H.M., 2004. Drag coefficients for modeling flow through emergent vegetation in the Florida Everglades. Ecological Engineering 22, 237-248.

Legates, D.R., McCabe, G.J., 1999. Evaluating the use of "goodness-of-fit" measures in hydrologic and hydroclimatic model validation. Water Resources Research 35, 233-241.

Lightbody, A.F., Avener, M.E., Nepf, H.M., 2008. Observations of short-circuiting flow paths within a free-surface wetland in Augusta, Georgia, USA. Limnology and Oceanography 53, 1040-1053.

Lightbody, A.F., Nepf, H.M., 2006. Prediction of velocity profiles and longitudinal dispersion in emergent salt marsh vegetation. Limnology and Oceanography 51, 218-228.

Lindenschmidt, K.E., 2006. The effect of complexity on parameter sensitivity and model uncertainty in river water quality modelling. Ecological Modelling 190, 72-86.

Ljung, L., 1987. System Identification: Theory for the User, Prentice-Hall, Englewood Cliffs, NJ, USA. pp. 519.

Martin, J.L., McCutcheon, S.C., 1999. Hydrodynamics and transport for water quality modeling, CRC Press, Boca Raton, FL. pp. 794.

Martinez, C.J., Wise, W.R., 2003a. Analysis of constructed treatment wetland hydraulics with the transient storage model OTIS. Ecological Engineering 20, 211-222.

Martinez, C.J., Wise, W.R., 2003b. Hydraulic analysis of Orlando Easterly Wetland. Journal of Environmental Engineering-ASCE 129, 553-560.

McCormick, P.V., Newman, S., Miao, S., Gawlik, D.E., Marley, D., Reddy, K.R., Fontaine, T.D., 2002. Effects of anthropogenic phosphorus inputs on the Everglades. In: Porter, J.W., Porter, K.G. (Eds.), The Everglades, Florida Bay, and Coral Reefs of the Florida Keys – An Ecosystem Sourcebook. CRC Press, Boca Raton, FL, pp. 83–126.

McCormick, P.V., Newman, S., Payne, G., Miao, S., Fontaine, T.D., 2000. Chapter 3: Ecological effects of phosphorus enrichment of the Everglades. In: SFWMD, 2000 Everglades Consolidated Report. South Florida Water Management District, West Palm Beach, FL, pp. 3-1–3-72.

McCormick, P.V., Shuford,Robert B.E.,,III, Chimney, M.J., 2006. Periphyton as a potential phosphorus sink in the Everglades Nutrient Removal Project. Ecological Engineering 27, 279-289.

McDonald, C.P., Urban, N.R., 2010. Using a model selection criterion to identify appropriate complexity in aquatic biogeochemical models. Ecological. Modelling. 221, 428-432.

Meyers, M., Fitzpatrick, J., 2001. Predicted phosphorus removal in a stormwater treatment area using a wetland water quality model. In: Proceedings of the 2001 ASCE World Water Congress, Orlando, FL.

Miao, S., Edelstein, C., Carstenn, S., Gu, B., 2010. Immediate ecological impacts of a prescribed fire on a cattail-dominated wetland in Florida Everglades. Fundamental and Applied Limnology 176, 29-41.

Min, J., 2007. Two-dimensional (depth-averaged) modeling of flow and phosphorus dynamics in constructed wetlands. Ph.D. dissertation, University of Florida, Gainesville, FL.

Min, J., Paudel, R., Jawitz, J.W., 2010. Spatially distributed modeling of surface water flow dynamics in the Everglades ridge and slough landscape. Journal of Hydrology 390, 1-12.

Min, J., Paudel, R. Jawitz, J.W., 2011. Mechanistic biogeochemical model applications for Everglades restoration: A review of case studies and suggestions for future modeling needs. Critical Reviews in Environmental Science and Technology 41, 489-516.

Min, J., Wise, W.R., 2009. Simulating short-circuiting flow in a constructed wetland: the implications of bathymetry and vegetation effects. Hydrological Processes 23, 830-841.

Min, J., Wise, W.R., 2010. Depth-averaged, spatially distributed flow dynamic and solute transport modelling of a large-scaled, subtropical constructed wetland. Hydrological Processes 24, 2724-2737.

Mitsch, W.J., Cronk, J.K., Wu, X.Y., Nairn, R.W., Hey, D.L., 1995. Phosphorus Retention in Constructed Fresh-Water Riparian Marshes. Ecological Applications 5, 830-845.

Mitsch, W.J., Gosselink, J.G., 2000. Wetlands. New York: John Wiley & Sons, Inc., 3rd ed., 920 pp.

Mitsch, W.J., Reeder, B.C., 1991. Modeling Nutrient Retention of a Fresh-Water Coastal Wetland - Estimating the Roles of Primary Productivity, Sedimentation, Resuspension and Hydrology. Ecological Modelling 54, 151-187.

Moustafa, M.Z., 1998. Long-term equilibrium phosphorus concentrations in the everglades as predicted by a Vollenweider-type model. Journal of the American Water Resources Association 34, 135-147.

Moustafa, M.Z., 1999. Nutrient retention dynamics of the Everglades Nutrient Removal Project. Wetlands 19, 689-704.

Moustafa, M.Z., Fontaine, T.D., Guardo, M., James, R.T., 1998. The response of a freshwater wetland to long-term 'low level' nutrient loads: nutrients and water budget. Hydrobiologia 364, 41-53.

Moustafa, M.Z., Hamrick, J.M., 2000. Calibration of the wetland hydrodynamic model to the Everglades Nutrient Removal Project. Water Quality and Ecosystem Modeling 1, 141-168.

Mulligan, M., Wainwright, J., 2004. Modelling and model building. In Wainwright, J., Mulligan, M. (Eds.), Environmental Modelling: Finding Simplicity in Complexity. Wiley, Chichester, pp. 7–73.

Murray, A.B., 2007. Reducing model complexity for explanation and prediction. Geomorphology 90, 178-191.

Myung, J.I., Tang, Y., Pitt, M.A., 2009. Evaluation and Comparison of Computational Models. Methods in Enzymology: Computer Methods, 454, 287-304.

Nepf, H.M., 1999. Drag, turbulence, and diffusion in flow through emergent vegetation. Water Resources Research 35, 479-489.

Newman, J.M., Lynch, T., 2001. The Everglades Nutrient Removal Project test cells: STA optimization status of the research at the north site. Water Science and Technology 44, 117-122.

Noe, G.B., Childers, D.L., 2007. Phosphorus budgets in Everglades wetland ecosystems: the effects of hydrology and nutrient enrichment. Wetlands Ecology and Management 15, 189-205.

Noe, G.B., Childers, D.L., Jones, R.D., 2001. Phosphorus biogeochemistry and the impact of phosphorus enrichment: Why is the everglades so unique? Ecosystems 4, 603-624.

Nungesser, M.K., Chimney, M.J., 2001. Evaluation of phosphorus retention in a South Florida treatment wetland. Water Science and Technology 44, 109-115.

Nungesser, M.K., Chimney, M.J., 2006. A hydrologic assessment of the Everglades Nutrient Removal Project, a subtropical constructed wetland in south Florida (USA). Ecological Engineering 27, 331-344.

Oreskes, N., 2000. Why believe a computer? Models, measures, and meaning in the natural world. In: Schneiderman, J.S. (Eds.), The Earth Around Us. W.H. Freeman, San Francisco, CA.

Oreskes, N., Shraderfrechette, K., Belitz, K., 1994. Verification, Validation, and Confirmation of Numerical-Models in the Earth-Sciences. Science 263, 641-646.

Pant, H.K., Reddy, K.R., 2003. Potential internal loading of phosphorus in a wetland constructed in agricultural land. Water Research 37, 965-972.

Paudel, R., Min, J., Jawitz, J.W., 2010. Management scenario evaluation for a large treatment wetland using a spatio-temporal phosphorus transport and cycling model. Ecological Engineering 36, 1627-1638.

Perrin, C., Michel, C., Andreassian, V., 2001. Does a large number of parameters enhance model performance? Comparative assessment of common catchment model structures on 429 catchments. Journal of Hydrology 242, 275-301.

Persson, J., Somes, N.L.G., Wong, T.H.F., 1999. Hydraulics efficiency of constructed wetlands and ponds. Water Science and Technology 40, 291-300.

Persson, J., Wittgren, H.B., 2003. How hydrological and hydraulic conditions affect performance of ponds. Ecological Engineering 21, 259-269.

Piccone, T.T., 2003. Two-dimensional hydraulic analysis for Cell 5 of STA-1W, March 7 2003, South Florida Water Management District, West Palm Beach, FL.

Pietro, K., Bearzotti, R., Chimney, M., Germain, G., Iricanin, N., Piccone, T., and Samfilippo, K., 2006a. Chapter 4: STA performance, compliance and optimization. In: SFWMD, 2006 South Florida Environmental Report. South Florida Water Management District, West Palm Beach, FL, pp. 4-1–4-114.

Pietro, K., Bearzotti, R., Germain, G., Iricanin, N., 2009. Chapter 5: STA performance, compliance, and optimization. In: SFWMD, 2009 South Florida Environmental Report. South Florida Water Management District, West Palm Beach, FL, pp. 5-1–5-137.

Pietro, K.C., Chimney, M.J., Steinman, A.D., 2006b. Phosphorus removal by the Ceratophyllum/periphyton complex in a south Florida (USA) freshwater marsh. Ecological Engineering 27, 290-300.

Pietro, K., Germain, G., Bearzotti, R., Iricanin, N., 2010. Chapter 5: Performance, and optimization of the Everglades Stormwater Treatment Areas. In: SFWMD, 2010 South Florida Environmental Report. South Florida Water Management District, West Palm Beach, FL, pp. 5-1–5-158.

Pitt, M.A., Kim, W., Myung, I.J., 2003. Flexibility versus generalizability in model selection. Psychonomic Bulletin & Review 10, 29-44.

Pitt, M.A., Myung, I.J., 2002. When a good fit can be bad. Trends in Cognitive Sciences 6, 421-425.

Poeter, E., Anderson, D., 2005. Multimodel ranking and inference in ground water modeling. Ground Water 43, 597-605.

Porter, J.W., Porter, K.G., 2002. The Everglades, Florida Bay and Coral Reefs of the Florida Keys, CRC Press, New York.

Raghunathan, R., Slawecki, T., Fontaine, T.D., Chen, Z.Q., Dilks, D.W., Bierman, V.J., Wade, S., 2001. Exploring the dynamics and fate of total phosphorus in the Florida Everglades using a calibrated mass balance model. Ecological Modelling 142, 247-259.

Reckhow, K.H., 1999. Water quality prediction and probability network models. Canadian Journal of Fisheries and Aquatic Sciences 56, 1150-1158.

Reckhow, K.H., Chapra, S.C., 1999. Modeling excessive nutrient loading in the environment. Environmental Pollution 100, 197-207.

Reddy, K.R., 1991. Lake Okeechobee phosphorus dynamics study. Physico-chemical properties in the sediments. Report Prepared by University of Florida, Gainesville, for South Florida Water Management District, Contract No. C91-2393, 2, 1–235.

Reddy, K.R., Graetz, D.A., 1991. Phosphorus dynamics in the Everglades nutrient removal system. Final Report. Submitted to South Florida Water Management District, West Palm Beach, FL.

Reddy, K.R., Kadlec, R.H., Chimney, M.J., 2006. The Everglades Nutrient Removal Project. Ecological Engineering 27, 265-267.

Reed, S.C., Crites, R.W., Middlebrooks, E.J., 1995. Natural systems for waster management and treatment (2nd ed.), McGraw-Hill Inc., New York, NY, 433 pp.

Reese R.S., Wacker, M.A., 2009. Hydrogeologic and hydraulic characterization of the surficial aquifer system, and origin of high salinity groundwater, Palm Beach County, Florida. U.S. Geological Survey - Scientific Investigations Report 2009–5113, Reston, VA. pp. 92.

Refsgaard, J.C., Storm, B., 1995. MIKE SHE. In: Singh, V.P. (Eds.), Computer models of watershed hydrology. Water Resources Publications, Highlands Ranch, CO, 809–846.

Restrepo, J.I., Montoya, A.M., Obeysekera, J., 1998. A wetland simulation module for the MODFLOW ground water model. Ground Water 36, 764-770.

Robson, B.J., Hamilton, D.P., Webster, I.T., Chan, T., 2008. Ten steps applied to development and evaluation of process-based biogeochemical models of estuaries. Environmental Modelling & Software 23, 369-384.

Rohrer, K.P., 1999. Hydrogeological characterization and estimation of ground water seepage in the Everglades nutrient removal project. Technical Publication. WRE–372, South Florida Water Management District, West Palm Beach, FL.

Saiers, J.E., Harvey, J.W., Mylon, S.E., 2003. Surface-water transport of suspended matter through wetland vegetation of the Florida everglades. Geophysical Research Letters 30, 1987.

Schaffranek, R.W., Riscassi, A.L., Rybicki, N.B., Lombana, A.V., 2003. Fire effects on flow in vegetated wetlands of the Everglades. 2003 Greater Everglades Ecosystem Restoration Conference. <http://sofia.usgs.gov/geer/2003/posters/fireeffects/>

Schoups, G., Hopmans, J.W., 2006. Evaluation of model complexity and input uncertainty of field-scale water flow and salt transport. Vadose Zone Journal 5, 951-962.

SFWMD, 2001. Two dimensional hydraulic analysis for Cell 3 of STA-2, an SAV-dominated treatment cell, March 21, 2001.

SFWMD, 2005a. Documentation of the South Florida Water Management Model v5.5. SFWMD, West Palm Beach, FL, pp. 305.

SFWMD, 2005b. RSM theory manual – HSE v1.0. SFWMD, West Palm Beach, FL, pp. 308.

SFWMD, 2005c. RSM user manual – HSE v1.0. SFWMD, West Palm Beach, FL, pp. 286.

SFWMD, 2005d. STA-2 vegetation 2005. Assessed from GIS data catalogue on 10/8/2010. <http://my.sfwmd.gov/gisapps/sfwmdxwebdc/dataview.asp>

SFWMD, 2007. RSM technical reference manual – HSE theory manual v1.0. SFWMD, West Palm Beach, FL, pp. 44.

Sharma, P., Asaeda, T., Fujino, T., 2008. Effect of water depth on the rhizome dynamics of *Typha angustifolia*. Wetlands Ecology and Management 16, 43–49.

Sklar, F.H., Chimney, M.J., Newman, S., McCormick, P., Gawlik, D., Miao, S.L., McVoy, C., Said, W., Newman, J., Coronado, C., Crozier, G., Korvela, M., Rutchey, K., 2005. The ecological-societal underpinnings of Everglades restoration. Frontiers in Ecology and the Environment 3, 161-169.

Smith, D., Hornung, L., 2005. Optimization modeling of phosphorus removal in reservoir and Stormwater Treatment Areas. Florida Water Resources Journal 57, 68-76.

Snowling, S.D., Kramer, J.R., 2001. Evaluating modelling uncertainty for model selection. Ecological Modelling 138, 17-30.

Somes, N.L.G., Bishop, W.A., Wong, T.H.F., 1999. Numerical simulation of wetland hydrodynamics. Environment International 25, 773-779.

Squires, L., Vandervalk, A.G., 1992. Water-Depth Tolerances of the Dominant Emergent Macrophytes of the Delta Marsh, Manitoba. Canadian Journal of Botany-Revue Canadienne De Botanique 70, 1860-1867.

Sutron Corp., 2007. Updated STA-2 hydraulic analyses, Final report. SFWMD, West Palm Beach, FL, pp. 68.

Sutron Corp., 2005. STA-1W 2-D Hydraulic modeling, Final report. SFWMD, West Palm Beach, FL, pp. 136.

Swain, E.D., Wolfert, M.A., Bales, J.D., Goodwin, C.R., 2004. Two-dimensional hydrodynamic simulation of surface-water flow and transport to Florida Bay through the Southern Inland and Coastal Systems (SICS). U.S. Geological Survey Water-Resources Investigations Report 03-4287, pp. 56.

SWET, 2006. Watershed Assessment Model documentation and user's manual. Soil and Water Engineering Technology, Inc., Gainesville, FL.

Thompson, J.R., Sorenson, H.R., Gavin, H., Refsgaard, A., 2004. Application of the coupled MIKE SHE/MIKE 11 modelling system to a lowland wet grassland in southeast England. Journal of Hydrology 293, 151-179.

Thullen, J.S., Sartoris, J.J., Nelson, S.M., 2005. Managing vegetation in surface-flow wastewater-treatment wetlands for optimal treatment performance. Ecological Engineering 25, 583-593.

Tsanis, I.K., Prescott, K.L., Shen, H., 1998. Modelling of phosphorus and suspended solids in Cootes Paradise marsh. Ecological Modelling 114, 1-17.

van der Peijl, M.J., Verhoeven, J.T.A., 1999. A model of carbon, nitrogen and phosphorus dynamics and their interactions in river marginal wetlands. Ecological Modelling 118, 95-130.

Vollenweider, R.A., 1975. Input-output models with special reference to the phosphorus loading concept in limnology. Schweizerische Zeitschrift Hydrologie 37(1), 53–84.

von Zweck, P., Bushey, R., Neumeister, S., 2000. Hydraulic analyses of stormwater treatment areas in south Florida. In: Building Partnerships - 2000 Joint Conference on Water Resource Engineering and Water Resources Planning & Management.

Variano, E.A., Ho, D.T., Engel, V.C., Schmieder, P.J., Reid, M.C., 2009. Flow and mixing dynamics in a patterned wetland: Kilometer-scale tracer releases in the Everglades. Water Resources Research 45, W08422.

Wagenet, R., Rao, P., 1990. Modelling pesticide fate in soils, in pesticides in the soil environment: processes, impacts, and modelling. In: Cheng, H. (Ed.) Soil Science Society of America Book Series (No. 2), SSSA, Madison, WI, pp. 351–399.

Wainwright and Mulligan, 2004. In: Wainwright, J. (Eds.), Environmental Modelling: Finding Simplicity in Complexity, Wiley, London.

Walker, W.W., 1995. Design Basis for Everglades Stormwater Treatment Areas. Water Resources Bulletin 31, 671-685.

Walker, W.W., and Kadlec, R.H., 1996. A model for simulating phosphorus concentrations in waters and soils downstream of Everglades Stormwater Treatment Areas. Report prepared for U.S. Department of Interior. <http://www.wwwalker.net/epgm/>.

Walker, W.W., Kadlec, R.H., 2005. Dynamic model for Stormwater Treatment Areas. Model Version 2. <http://wwwalker.net/dmsta/index.htm>.

Walton, R., Chapman, R.S., Davis, J.E., 1996. Development and application of the wetlands dynamic water budget model. Wetlands 16, 347-357.

Wang, H., Jawitz, J.W., 2006. Hydraulic analysis of cell-network treatment wetlands. Journal of Hydrology 330, 721-734.

Wang, H.G., Jawitz, J.W., White, J.R., Martinez, C.J., Sees, M.D., 2006. Rejuvenating the largest municipal treatment wetland in Florida. Ecological Engineering 26, 132-146.

Wang, N.M., Mitsch, W.J., 2000. A detailed ecosystem model of phosphorus dynamics in created riparian wetlands. Ecological Modelling 126, 101-130.

Wetzel, R.G., 1994. Constructed wetlands: Scientific foundations are critical. In: Moshiri, G.A. (Eds.), Constructed Wetlands for Water Quality Improvement. Lewis Publishers, Boca Raton.

Werner, T.M., Kadlec, R.H., 2000. Wetland residence time distribution modeling. Ecological Engineering 15, 77-90.

Wong, T.H.F., Fletcher, T.D., Duncan, H.P., Jenkins, G.A., 2006. Modelling urban stormwater treatment—A unified approach. Ecological Engineering 27, 58-70.

Wong, T.H.F., Geiger, W.F., 1997. Adaptation of wastewater surface flow wetland formulae for application in constructed stormwater wetlands. Ecological Engineering 9, 187-202.

Worman, A., Kronnas, V., 2005. Effect of pond shape and vegetation heterogeneity on flow and treatment performance of constructed wetlands. Journal of Hydrology 301, 123-138.

BIOGRAPHICAL SKETCH

Rajendra Paudel was born in Raipur, Tanahun, Nepal. He received a Bachelor of Science degree in civil engineering at Tribhuvan University in October 1997. He held a civil engineering position in the GEOCE Consultants Pvt. Ltd., Nepal during 1997 to 2002. He got a Flemish Interuniversity Council Scholarship of Belgian Government to pursue Master of Science (MS) in water resources engineering for 2002-04 academic years, through an interuniversity program. He earned a MS degree in September 2004 from Katholieke Universitiet Leuven/Vrije Universitiet Brussels. He went back to Nepal in October 2004 and worked as a Senior Water Resources and Environmental Engineer in the Integrated Development Society-Nepal, a non-profit organization of Nepal. In August, he began his Ph.D. in soil and water science at the University of Florida, and eventually earned his doctorate in May 2011.

.